



Universiteit
Leiden
The Netherlands

Ventral striatal atrophy in Alzheimer's disease : exploring a potential new imaging marker for early dementia

Jong, L.W. de

Citation

Jong, L. W. de. (2018, December 11). *Ventral striatal atrophy in Alzheimer's disease : exploring a potential new imaging marker for early dementia*. Retrieved from <https://hdl.handle.net/1887/67427>

Version: Not Applicable (or Unknown)

License: [Licence agreement concerning inclusion of doctoral thesis in the Institutional Repository of the University of Leiden](#)

Downloaded from: <https://hdl.handle.net/1887/67427>

Note: To cite this publication please use the final published version (if applicable).

Cover Page



Universiteit Leiden

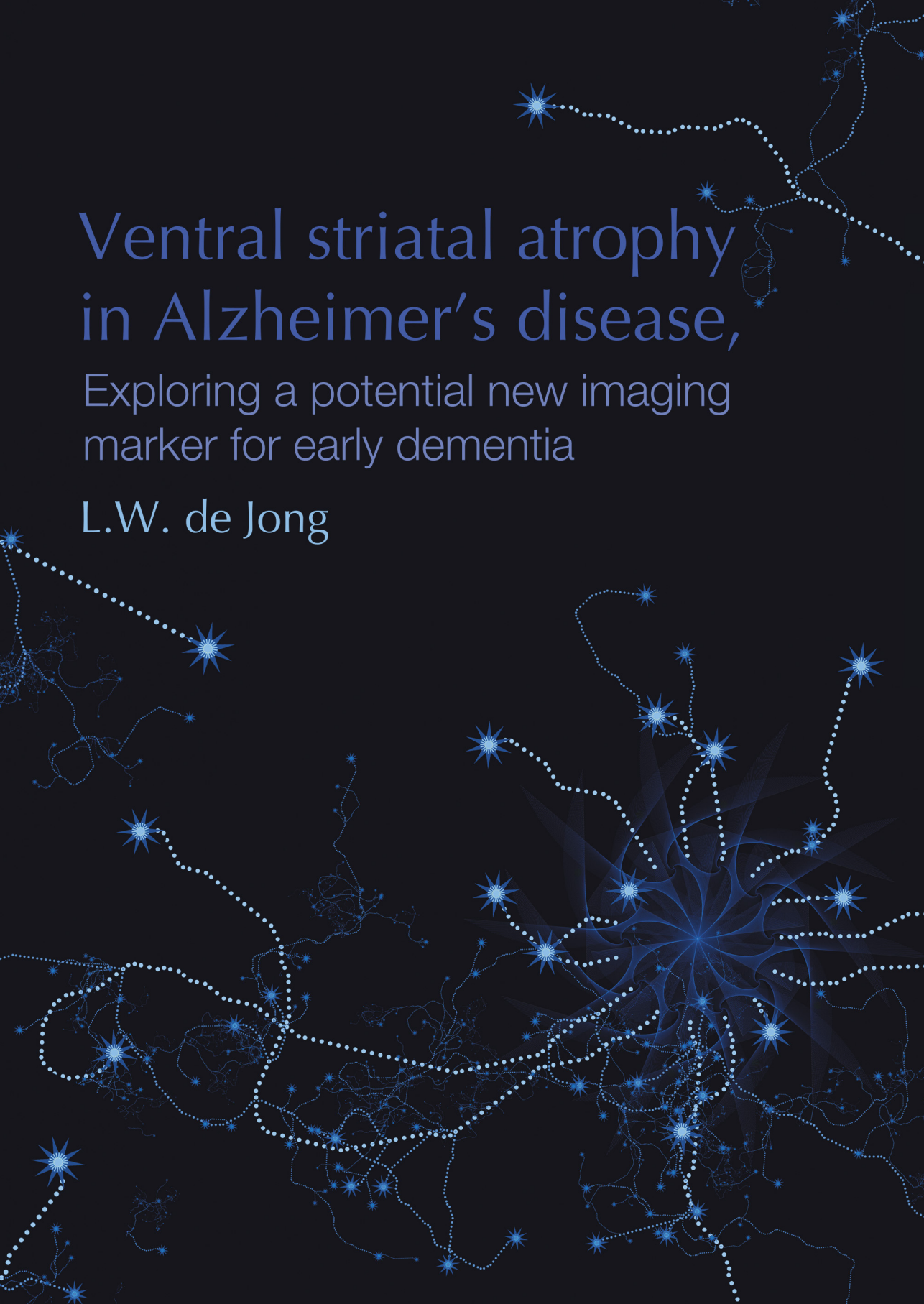


The handle <http://hdl.handle.net/1887/67427> holds various files of this Leiden University dissertation.

Author: Jong, L.W. de

Title: Ventral striatal atrophy in Alzheimer's disease : exploring a potential new imaging marker for early dementia

Issue Date: 2018-12-11



Ventral striatal atrophy in Alzheimer's disease,

Exploring a potential new imaging
marker for early dementia

L.W. de Jong

Ventral striatal atrophy in
Alzheimer's disease:
Exploring a potential new imaging
marker for early dementia

Laura de Jong

© Copyright L.W. de Jong, Leiden, The Netherlands, 2018. All rights reserved. The copyrights of the articles that have been published have been transferred to the respected journals. No part of this book may be reproduced, stored in a retrieval system, or transmitted in any form or by any means, without written permission of the author.

ISBN: 978-94-6361-199-2

Cover by L.W. de Jong designed with Context Free Art

Layout by L.W. de Jong and J.-S. Vidal composed with L^AT_EX

Printed by Optima Grafische Communicatie, Rotterdam

Ventral striatal atrophy in Alzheimer's disease:
Exploring a potential new imaging marker for early dementia

Proefschrift

ter verkrijging van de graad van Doctor aan de Universiteit Leiden,
op gezag van Rector Magnificus prof.mr. C.J.J.M. Stolker,

volgens besluit van het College voor Promoties

te verdedigen op dinsdag 11 december 2018

klokke 13:45 uur

door

Laura Willemijn de Jong

Geboren te Gouda in 1981

| | |
|-------------------|------------------------------------------------------------------------------------------------------------------------------------------------------------------------------------------------------------------------------------------------|
| Promotor | Prof. Dr. M.A. van Buchem |
| Copromotor | Dr. L.J. Launer, Laboratory of Epidemiology and Population Science, NIA/NIH, Bethesda, MD, VS |
| Promotiecommissie | Prof. Dr. Ir. M.J.P. Van Osch Prof. Dr. V. Gudnason, Icelandic Heart Association Prof. Dr. Ir. B.P.F. Lelieveldt Prof. Dr. G. Blauw Prof. Dr. W.M. van der Flier, VU Medisch Centrum Dr. M.W. Vernooij, Erasmus Medisch Centrum |

The research described in this thesis was conducted at the Department of Radiology of the Leiden University Medical Center (Leiden, the Netherlands), at the Icelandic Heart Institute (Kópavogur, Iceland), and at the Laboratory of Epidemiology and Population Science of the National Institutes of Health (Bethesda, Maryland USA).

The research described in this thesis was supported by the National Institutes of Health (Cooperative agreements 5U01AG017155-09 and 5U01AG019349-08, and Contracts N01-AG-1-2100 and N01-AG-4-2149), the Intramural Research Program of the National Institute on Aging, the Hjartavernd (Icelandic Heart Association), and the Althingi (Icelandic Parliament).

The author was supported by the Dutch Organisation for Health Research and Development (Zon Mw AGIKO grant number 92003536).

Aan mijn ouders en opa

Contents

| | | |
|-----------|-----------------------------------------------------------------|------------|
| 1 | General introduction | 9 |
| I | Ventral striatal atrophy in Alzheimer's disease | 27 |
| 2 | Reduced volumes putamen and thalamus in AD | 29 |
| 3 | Shape abnormalities of the striatum in AD | 49 |
| 4 | Ventral striatal volume and cognitive decline | 71 |
| 5 | Atrophy rates of MTL and BG and vascular risk factors | 89 |
| II | Allometric scaling in brain development and degeneration | 113 |
| 6 | Allometric scaling of brain structures | 115 |
| 7 | Bigger brains atrophy faster in later life | 145 |
| 8 | Summary and general discussion | 169 |
| | Appendix A Samenvatting | 183 |
| | Appendix B List of publications | 189 |
| | Appendix C Dankwoord | 191 |
| | Appendix D Curriculum vitae | 193 |

CHAPTER 1

General introduction

GENERAL INTRODUCTION

Brain & cognition: a spearhead on the Dutch research agenda

Cognitive problems are considered to have the biggest influence on the quality of life of older people compared to other chronic diseases that occur with ageing for example rheumatic, heart and vessels, diabetes and pulmonary complaints (Lavender 2008). In ageing populations, like in the Netherlands, the rise in incidence and prevalence of dementia is an important social and economic concern. Dementia will, most probably, become the number one cause of death in 2040 (The Dutch National Institute for Public Health and the Environment 2017). To prepare for the upcoming decades the Netherlands Organization for Scientific Research and the Royal Netherlands Academy of Arts and Sciences launched several initiatives between 2000-2017 that made brain and cognition the cornerstone of the Dutch research agenda (<https://www.hersenenencognitie.nl/publications/64>). Regarding dementia and cognitive decline, research was supported that could 1) improve our understanding of the pathophysiology of cognitive decline and dementia, 2) identify early markers of dementia, 3) identify modifiable risk factors that can counteract or delay the onset of cognitive decline, and 4) ultimately find a way of preventing or cure dementia. The research presented in this thesis was part of this larger movement and focused for one part on finding early markers of dementia on structural magnetic resonance imaging (MRI) and for another part on improving our knowledge on how to perform volumetric and morphometric studies of the human brain in face of neurodegenerative changes.

Theoretical concepts of Alzheimer's disease

In 1907, Alois Alzheimer presented a case of a woman of 51 years with progressive cognitive decline leading to the clinical description of a condition he named "pre-senile dementia" (Alzheimer 1907). Although asylum carers had been familiar with dementia in older people for centuries, the condition of Alzheimer's case had attracted his attention because of the rapid course of the disease and the relatively young age of the patient. He examined her brain after she died and found large quantities of neurofibrillary tangles and amyloid plaques. Nowadays, this form of dementia would perhaps be classified as a familial form of Alzheimer's disease (AD). This form of AD is relatively uncommon, constituting merely 3–5% of all AD cases (Fjell and Walhovd 2012). However, research throughout the 20th century showed that the most common form of dementia in older people is also characterized by accumulated amyloid- β ($A\beta$) plaques and neurofibrillary tangles (Ingelsson et al. 2004). This form of dementia is now known as

late onset sporadic AD. The current lifetime risk for a 65-year to develop this disease is estimated around 10.5% (Sperling et al. 2011). Definite diagnosis of AD is still made by postmortem analysis of the brain tissue. In clinical practice, however, people with suspected dementia are evaluated relative to the consensus NINCDS–ADRDA criteria (McKhann et al. 1984). The diagnosis of “probable AD” requires 1) progressive cognitive decline present in at least 2 areas of cognition in an individual between 40-90 years and 2) absence of other causes of the cognitive decline. These diagnostic criteria identify AD patients relatively late when the disease has already entered a full clinical stage. Researchers in the field, however, have an interest in selecting AD patients much earlier in their disease process. The update of the criteria in 2011 fulfilled this need to uniformly identify and stage patients in preclinical phases of AD by incorporating markers for $A\beta$ accumulation and markers for neuronal degeneration (Jack, Albert, et al. 2011). Although making the diagnosis has reached global standardization, the cause of AD is still unknown and widely debated. Our current understanding of the pathological process leading up to the clinical presentation of AD is encapsulated in two different theoretical models.

Cholinergic hypothesis of Alzheimer’s disease

The first model considers AD as the result of a reduction of the activity of the cholinergic system. This hypothesis was based on observations made in the late 60s and early 70s of the 20th century, of substantial neo-cortical deficits in choline acetyltransferase, an enzyme responsible for the synthesis of acetylcholine, reduced acetylcholine release, and loss of cholinergic cells in the nucleus basalis of Meynert in patients with AD. The cholinergic system is housed in the subcortical gray matter nuclei consisting of the striatum, basal nucleus of Meynert, other basal forebrain complex structures, and amygdala and has numerous downstream projections to cholinergic receptors on pyramidal neurons of allocortical and isocortical areas (Francis et al. 1999). There is no consensus on how cholinergic dysfunction influences the function of the cortex. It has been postulated that loss of cholinergic excitatory input to the pyramidal neurons may lead to hypoactivity with maintained inhibition by GABAergic neurons (Francis et al. 1999). However, others have postulated that low levels of acetylcholine may allow “runaway synaptic” modifications to form, leading to excitotoxicity of glutamatergic cortical neurons. This would be especially damaging for the medial temporal lobe, being one of the most constantly active structures in the brain due to its constant synapse formation supporting episodic memory (Hasselmo and Schnell 1994; Spitzer 1999). Regardless of the exact effect of acetylcholine on the cortex, this cholinergic model of AD considers the subcortical basal forebrain complex as the primary site of pathology leading to secondary neurodegen-

erative effects in the cortex exhibiting a localized vulnerability. In accordance with this model, the only validated treatment available today for AD patients in early phases of the clinical process is pharmacological inhibition of acetylcholinesterase. Acetylcholinesterase inhibitors have been shown to give moderate symptoms relieve in the early stages of the disease (JT O'Brien et al. 2017).

Amyloid cascade model

The second model considers AD as the result of accumulation of $A\beta$ plaques and the pathological events that follow from that. This model has focused on the finding of the abundance of neurofibrillary tangles and amyloid plaques in the cortex in post mortem brain specimens of patients with AD compared to those who were not suspected to have AD. Both are considered primary markers for establishing the definite diagnosis of AD, although neither is exclusively present in AD. Neurofibrillary tangles are also found in other taupathies diseases i.e., Parkinson's disease, Lewy body dementia (Iqbal and Grundke-Iqbal 2004) and amyloid plaques are also found in patients without signs of dementia before their death (Snowdon 2003; Latimer et al. 2017). Neurofibrillary tangles and amyloid plaques are not distributed in the same temporospatial way throughout the brain. An influential study published in 1991 described the spread of neurofibrillary tangles in a highly predictable temporospatial manner (H Braak and E Braak 1991). This temporospatial spreading pattern, known as the Braak and Braak stages, predicts the appearance of neurofibrillary tangles first in the transentorhinal and entorhinal cortices (stage I and II) after which they appear in the hippocampus (stages III and IV) and finally there is extensive neocortical involvement (stages V and VI). Neurofibrillary tangles are composed of aggregates of hyperphosphorylated tau protein and thought to represent remains of pyramidal neurons that have undergone a degenerative process. The stages of neurofibrillary tangle accumulation have shown to parallel the stages of brain atrophy in AD, which is encountered first in the medial temporal lobe, then in other limbic areas, and eventually affecting the whole brain (Dallaire-Th eroux et al. 2017). The accumulation of amyloid plaques occurs in a different manner. These are found throughout the cortex in early stages (Thal et al. 2002). The main constituent of amyloid plaques is $A\beta_{42}$, which is proteolytically derived from amyloid precursor protein (APP). The accumulation of $A\beta$ plaques has been attributed to inability of clearance of the insoluble $A\beta$ form. It has not been clarified why $A\beta$ plaques starts appearing in the brain, but it is suspected that genetic predisposition plays an important role, given that genetic mutations associated with familial AD are encoded on the APP gene (Fjell and Walhovd 2012). The formation of $A\beta$ plaques is thought to hamper the neuronal synaptic function and ultimately leads to neuronal death (Takahashi et al. 2002; Oakley et al. 2006). However, toxicity of

A β plaques is debated because about one third of elderly without cognitive or clinical symptoms is found to have plaques. This may suggest that the presence of A β plaques in the brain is not sufficient to cause AD. Contrary to the cholinergic hypothesis, the amyloid cascade model of AD considers AD a primarily cortical disease.

Regardless of the underlying model, AD is suspected to have a very long asymptomatic prodromal period of 1 or 2 decades before clinical symptoms appear (Amieva et al. 2008). Indeed accumulation of A β can be detected in 4% of adults in their 40s without symptoms (H Braak, Thal, et al. 2011). After failure of many attempts to find a therapy for AD in the clinical phase of the disease, research is starting to aim at preventive interventions in preclinical stages of the disease. Identifying early markers of the disease in this prodromal period is essential for this kind of research.

Relevance of neuroimaging studies in the assessment of AD

Today brain MRI is an established part in the assessment of patients with cognitive decline and suspected dementia (Sperling et al. 2011). The current role of structural brain MRI in clinical practice is twofold. First, MRI is used to exclude other (potentially treatable) causes of cognitive decline such as tumors or ischemic disease. And second, MRI is used to differentiate between different types of dementias. One way in which this done is by determining whether a typical pattern of cortical atrophy is present. For example, predominant atrophy of frontal and anterior temporal pole is suggestive of frontotemporal dementia, whereas predominant atrophy of the medial temporal lobe is suggestive of AD (Bocti et al. 2006). Also, other additional findings are supportive for certain diagnoses like cortical diffusion restriction is specific for Creutzfeldt–Jakob disease in the appropriate clinical context. However, clinical assessment of the patient is still the most important for establishing the eventual diagnosis. Abnormal cognitive test scores mark the beginning of the clinical disease, but the onset of this is influenced by the pre-morbid cognitive level of functioning and/or cognitive reserve (Stern 2012). Therefore, studies are conducted to explore extending the use of neuroimaging as a screening tool for AD especially for preclinical stages. Structural MRI as a screening method is most elegant, because of its widespread availability and noninvasive character. Global or focal loss of brain volume on structural MRI is thought to reflect loss of pyramidal neurons. Loss of medial temporal volume is considered the hallmark imaging marker for AD. In predicting change in cognitive functioning, neuroimaging markers have proven to be superior to CSF A β measurement (Walhovd et al. 2010; Da et al. 2014). Other imaging methods to evaluate those in preclinical stages of AD are amyloid and FDG PET scanning. Use of these methods is however limited, because they are expensive and invasive, and without perspective on adequate treatment they are not yet suitable

as a screening tool.

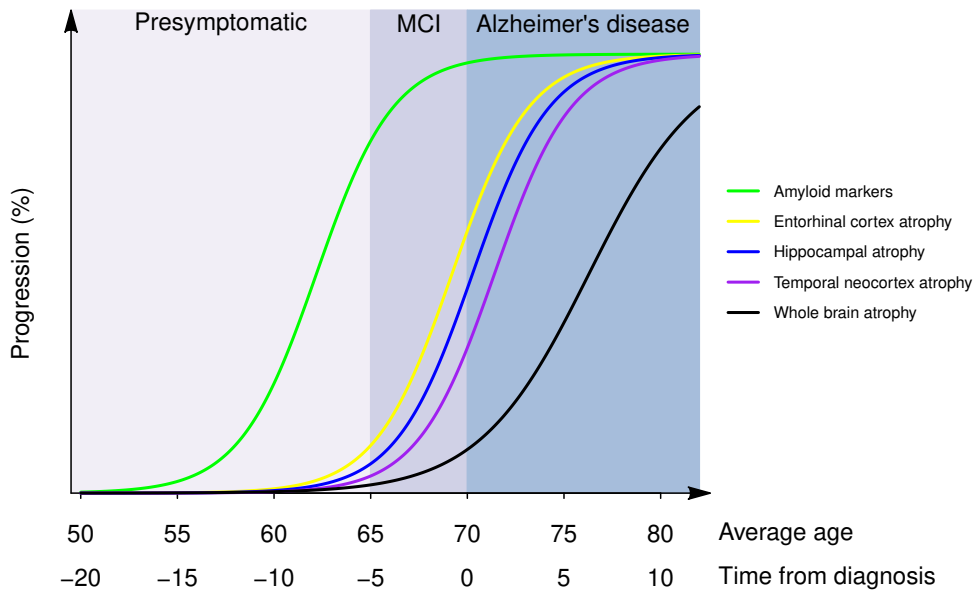
Hippocampal atrophy as imaging marker in AD

Medial temporal lobe volume loss is the most studied neurodegenerative marker of AD. It has been found to correlate with diagnosis of AD, to predict progression from mild cognitive impairment to AD, and to relate to disease severity (Jack, Petersen, PC O'Brien, et al. 1992; Fox et al. 1996; Jack, Petersen, Xu, et al. 2000; Schuff et al. 2009; Devanand et al. 2007). Medial temporal lobe atrophy is easily detected when visually inspecting the thickness of the hippocampus on MRI. Clinicians successfully integrated medial temporal lobe atrophy in daily clinical practice due to its high reproducibility, both when assessed semiquantitatively by visual scoring (Scheltens score) as when estimated quantitatively by manual or automated segmentation (Zandifar et al. 2017). Also, cognitive testing together with assessment of medial temporal lobe atrophy was shown to improve the accuracy of diagnosis as compared to cognitive testing alone (Da et al. 2014). Although medial temporal lobe volume loss was shown to correspond well with the accumulation of neurofibrillary tangles as predicted by the Braak and Braak stages and clinical progress of the disease, it is thought to occur relatively late in the disease process. The current dominating view within research on the relation of biomarkers and AD is captured in the dynamic biomarker model (figure 1). This model presumes that biomarkers reflecting levels of amyloid- β accumulation in the brain become abnormal long before hippocampal or whole brain atrophy and clinical symptoms occur (Jack, Knopman, et al. 2010). Based on the temporal relation of biomarkers and AD proposed by this model, use of medial temporal lobe atrophy is suited as a marker in secondary prevention trials in patients presenting with the earliest clinical stage of the disease or as an outcome measure (Cavedo et al. 2014). In the asymptomatic preclinical stages, however, medial temporal lobe atrophy may not be an adequate marker but amyloid markers may show more-substantial abnormalities (Frisoni et al. 2010). Thus, despite 3 decades of intensive neuroimaging research in AD, no accurate *preclinical* structural MRI marker for AD has been identified. Besides the study of atrophy of different structures of the medial temporal lobe, the allocortical cingulate gyrus and whole brain atrophy, there are some structures in the brain that have been given surprisingly little attention on structural MRI in AD. These are the subcortical structures that host the cholinergic system.

Why focus on the striatum when studying AD?

The first part of this thesis focused on volumetric and morphometric changes in the striatum in AD. There were three main arguments for studying the striatum in relation

Figure 1: Theoretical model of the progression of biological markers of AD



Adapted from Giovanni B. Frisoni, Nick C. Fox, Clifford R. Jack, Jr, Philip Scheltens, and Paul M. Thompson, The clinical use of structural MRI in Alzheimer's disease *Nature, Rev neurol* (2010).

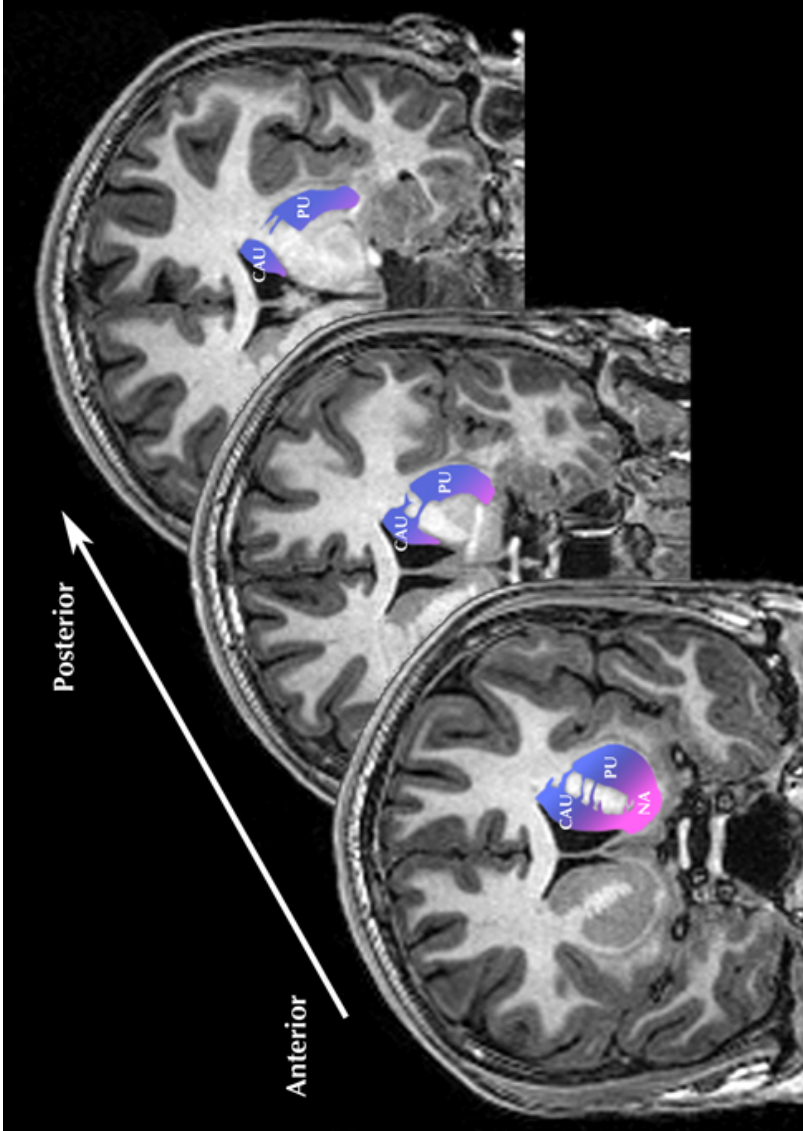
to AD and in particular as a candidate structure for being affected early in the disease process. First, the ventral striatum is an integrated part of the limbic system. The structure and function of all other limbic structures, i.e., entorhinal cortex, amygdala, hippocampus, basal forebrain, fornix, cingulate gyrus and medial prefrontal lobe, have been shown to be affected earlier in AD than neocortical structures (Mielke et al. 2012). The striatum forms the largest deep gray matter nucleus in the brain and consists of the caudate nucleus and putamen. The caudate nucleus and putamen are phylogenetically the same structure, which in the human brain, as opposed to for example rodent brains, is dispersed by the traversing internal capsule (Steiner and Tseng 2010). The function of the striatum is not fully understood. Historically, the striatum is thought to play a role in motor function, based on its association with neurodegenerative disorders affecting the control of movement, such as Parkinson's and Huntington's disease. However, the

last decades have shown the function of the striatum to be more complex mediating the full range of goal-directed behaviors, from motivation, reward and reinforcement based learning, decision making, to shaping final motor outcome (Haber 2016). The striatum receives input from nearly all areas of the cortex, the thalamus, and the dopaminergic cells of the brainstem in a roughly topographic organization (Haber 2016). The striatum projects GABAergic neurons to the internal segment of the globus pallidus and substantia nigra pars reticulata, termed the direct pathway, and to the external segment of the globus pallidus and subthalamic nucleus, termed the indirect pathway. From these projections arise via the thalamus back to mainly the frontal cortex (Shipp 2017). A distinction is made between the dorsal striatum and the ventral striatum. The ventral striatum occupies over 20% of the striatum (Haber 2011) and includes the nucleus accumbens, the medial and ventral portions of the caudate and putamen. There are no clear cytoarchitectonic borders between the ventral and the dorsal striatum but there is a gradual transition between areas with some differences in cellular composition (figure 2). The ventral striatum receives projections from the allocortical areas whereas the dorsal striatum receives projections from the neocortical areas (Gray 1999). The ventral striatum is considered part of the limbic system, projecting via the ventral pallidum and substantia nigra, subsequently the medial nucleus of the thalamus back to the ventral medial pre frontal cortex, the orbitofrontal cortex, dorsal anterior cingulate cortex and medial temporal lobe (Haber and McFarland 1999). Figure 3 schematically displays the main connections of the dorsal and ventral striatum with the rest of the brain. Given the central role of the ventral striatum in the limbic circuitry both receiving and projecting to other limbic structures, one of the focuses of the research presented in this thesis was to investigate whether the ventral striatum also showed stigmata of degeneration and in what stage of AD.

The second argument for investigating the striatum in AD was related to the known loss of cholinergic cells in AD. The largest concentrations of cholinergic cells in the brain are found in the basal forebrain complex and in the striatum (Havekes, Abel, and Van der Zee 2011). In AD a marked loss of the magnocellular cholinergic neurons is found in the basal nucleus of Meynert especially those areas that project to the medial temporal lobe, temporal pole and superior temporal lobe (Liu et al. 2015). Atrophy of the basal forebrain complex has been found to correlate with $A\beta$ burden (Kerbler et al. 2015). However, the striatum, rich of magnocellular cholinergic neurons, has not been studied extensively on brain MRI in relation to AD.

The last argument to study the striatum in relation to AD was related to recent findings of PiB PET amyloid imaging studies. In presenilin carriers associated with a familial form of AD, $A\beta$ deposition was shown to start in the striatum around the age of 45, when there was yet no proof of $A\beta$ deposition in the cortex or hippocampus

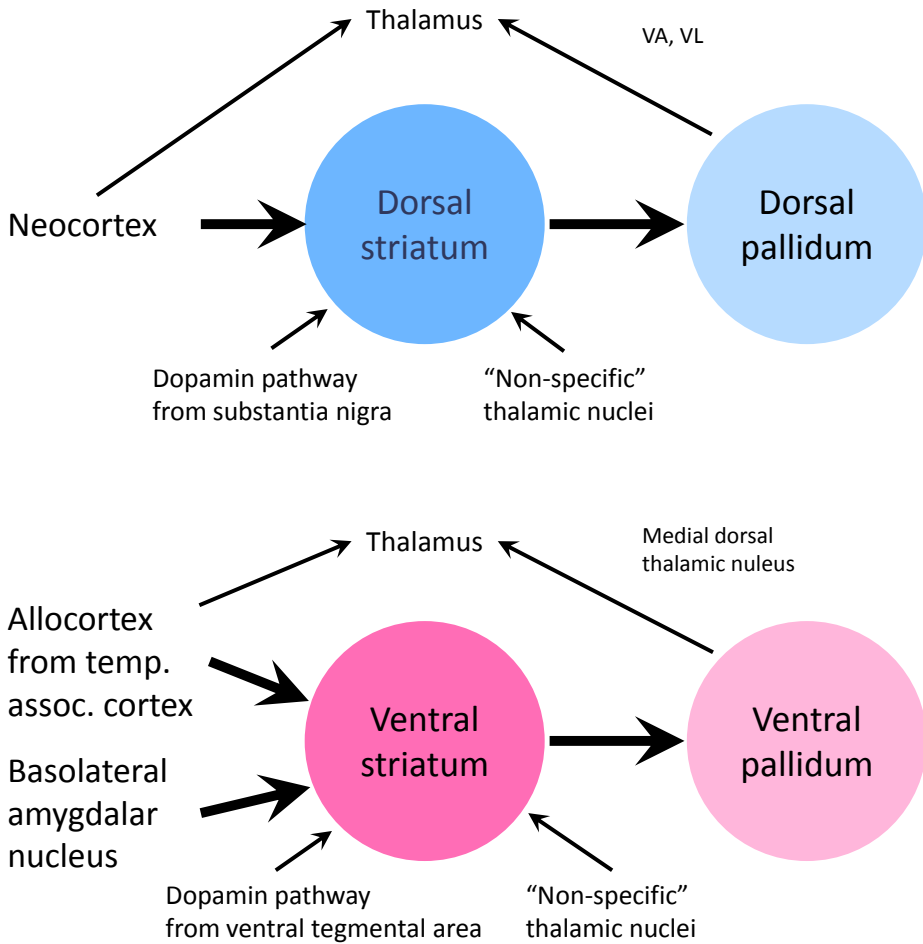
Figure 2: Striatum on coronal MRI



CAU, caudate nucleus; PU, putamen; NA, nucleus accumbens.

The color gradient represents the gradual transition from the ventral to dorsal striatum.

Figure 3: Schematic representation of the main connections of the ventral and dorsal striatum with the rest of the brain



Adapted from L Heimer and G van Hoesen (1979). Ventral Striatum. In: The Neostriatum. Ed. by I Divac and RGE Öberg. Oxford, UK: Pergamon, 147–158.

(Villemagne, Ataka, et al. 2009; Klunk et al. 2007). In mice studies, overexpression of $A\beta$ protein was associated with a reduction in striatal neurons (Richner, Bach, and West 2009). Although studies to late onset sporadic AD have not confirmed the presence of early striatal $A\beta$ depositions so far (Villemagne, Burnham, et al. 2013), the studies on familial AD suggest that the striatum is vulnerable to the presence of $A\beta$ even in small quantities.

Allometric scaling in brain development and atrophy

The second part of this thesis focused on how premorbid brain size influences brain structure and degeneration. Brain atrophy is widely studied, because it is assumed that loss of (regional) brain volume is a predictor for disease and goes hand in hand with functional decline of the brain (area). Manual segmentation of brain MRI is, however, time-consuming and limits the size of a study population. In the last two decades several software packages became freely available enabling automated estimation of intracranial volume (ICV) and total brain volume, and automated segmentation of different tissue classes of gray matter, white matter, and cerebrospinal fluid (FreeSurfer software (Freesurfer Software website; cortical Reconstruction and volumetric segmentation (Accessed July 1, 2018; <http://surfer.nmr.mgh.harvard.edu>)), SPM software (Accessed July 1, 2018; <http://www.fil.ion.ucl.ac.uk/spm/>)). This was followed in more recent years by the development of semiautomated brain segmentation tools dedicated to segmentation of the deep gray matter structures (FIRST website, (Accessed July 1, 2017; <https://fsl.fmrib.ox.ac.uk/fsl/fslwiki/FIRST>)). These automated segmentation techniques of brain MRI have led to a boom in comparative volumetric brain studies in clinical and epidemiological settings. Brain volumetric and morphometric studies are, however, met with criticism. On a group level, MRI-based measures of brain (substructure) volumes have proven their value by providing insight into the onset and spatial-temporal dynamics of cortical atrophy in normal ageing and neurodegenerative diseases such as AD. Nonetheless, results of brain comparative studies are not always useful for the individual patient because the predictive value of brain (structure) volumes for disease on individual patient level remains poor. The main reason for the poor predictability of brain volume for disease on individual level is the substantial variation in brain size in the general population. Brain volume or volume of its substructures cannot be studied directly, but are usually investigated relative to their maximal premorbid size. Head size or ICV are considered proxies for premorbid brain size and correction for either one of these in comparative brain studies is common practice (Barnes et al. 2010). One aspect in brain comparative studies that has not received enough attention is that some widely used methods of ICV adjustment are based on the assumption that brain substructures

scale linearly to ICV. For example, affine registration methods to align MR images of different individuals or the use of ratios of brain (substructure) volume to ICV, both assume that brains of different sizes are more or less linearly upscaled versions of each other. Although, this assumption is considerably influencing outcome measurements, it has not been tested sufficiently. As part of the efforts to improve accuracy and predictive value of brain volume for disease on a individual level, the second part of this thesis was dedicated to the study of scaling of sub-structures of the brain relative to ICV. Whether substructures of the brain scale isometrically to ICV was put to the test in a large population-based cohort. Furthermore, not only in brain development, but also current conceptions of degeneration of the brain and its influence on cognition are often based on assumptions of linearity. Therefore, in the last chapter the process of neurodegeneration, as reflected by several MRI markers of neurodegeneration, was studied relative to ICV in a population of older people spanning the spectrum from healthy cognitive ageing to dementia.

Aim of this thesis and brief outline

The aim of this thesis was first to investigate whether and to what extent the striatum undergoes degenerative changes in AD and whether striatal atrophy is related to cognitive decline in older people. The second aim of this thesis was to improve our knowledge on the physiological variability in brain structure and degeneration, which may result in a better understanding and identification of pathological atrophy patterns. Therefore this thesis is comprised of two complementary parts.

Part 1 investigated volumetric and morphometric changes of the striatum and its substructures in AD and its relation to cognitive decline. The central research question in **chapter 2** was whether the volumes of the striatum and its substructures were decreased in patients with AD compared to those who had healthy cognitive test scores. For this study brain MR images of a memory clinic population were investigated. In **chapter 3**, MR images of the same study population were further examined on the shape of the striatum. The question at stake was whether the striatum was losing volume in AD in a global manner or whether certain parts of the striatum were more affected than others. In particular it was investigated whether there was a difference between the ventral (limbic) and dorsal striatum. In **chapter 4**, the relation of the volume of the striatum and cognitive performance was studied with follow-up measurements of cognitive function spanning a decade. The relation of the volumes of the striatum (and its substructures) and global cognitive performance was compared with the relation of hippocampal volume and cognitive performance. Finally, since AD often co-occurs with large and/or small vessel disease, in **chapter 5**, it was examined whether change in striatal and hippocampal

volumes were influenced by the presence of cardiovascular risk factors.

Part two of the thesis investigated scaling of brain substructure volumes to ICV in a population based cohort of older adults. In **chapter 6** allometric scaling of substructures of the brain relative to ICV were investigated and the importance of scaling properties for adjustment methodologies in comparative brain volumetric studies discussed. In **chapter 7** the neurodegenerative process was studied relative to ICV in both cross-sectional and follow-up samples of older people spanning the spectrum from healthy cognition to dementia. More precisely, the influence of ICV on the amount of brain atrophy and white matter lesion load were studied, as well as the effect of ICV on the relation of these neurodegenerative markers and cognition.

Final **chapter 8** summarizes and provides a general interpretation of the results of the work presented in this thesis.

BIBLIOGRAPHY

- Alzheimer A (1907). "Über eine eigenartige Erkrankung der Hirnrinde". *Centralblatt für Nervenheilkunde und Psychiatrie* 30: 177–179.
- Amieva H, Le Goff M, Millet X, Orgogozo JM, Peres K, et al. (2008). "Prodromal Alzheimer's disease: successive emergence of the clinical symptoms". *Ann. Neurol.* 64 (5): 492–498. DOI: [10.1002/ana.21509](https://doi.org/10.1002/ana.21509).
- Barnes J, Ridgway GR, Bartlett J, Henley SM, Lehmann M, et al. (2010). "Head size, age and gender adjustment in MRI studies: a necessary nuisance?" *Neuroimage* 53 (4): 1244–1255. DOI: [10.1016/j.neuroimage.2010.06.025](https://doi.org/10.1016/j.neuroimage.2010.06.025).
- Bocti C, Rockel C, Roy P, Gao F, and Black SE (2006). "Topographical patterns of lobar atrophy in frontotemporal dementia and Alzheimer's disease". *Dement. Geriatr. Cogn. Disord.* 21 (5-6): 364–372. DOI: [10.1159/000091838](https://doi.org/10.1159/000091838).
- Braak H and Braak E (1991). "Alzheimer's disease affects limbic nuclei of the thalamus". *Acta Neuropathol.* 81 (3): 261–268. DOI: [10.1007/BF00305867](https://doi.org/10.1007/BF00305867).
- Braak H, Thal DR, Ghebremedhin E, and Del Tredici K (2011). "Stages of the pathologic process in Alzheimer disease: age categories from 1 to 100 years". *J. Neuropathol. Exp. Neurol.* 70 (11): 960–969. DOI: [10.1097/NEN.0b013e318232a379](https://doi.org/10.1097/NEN.0b013e318232a379).
- Cavedo E, Lista S, Khachaturian Z, Aisen P, Amouyel P, et al. (2014). "The Road Ahead to Cure Alzheimer's Disease: Development of Biological Markers and Neuroimaging Methods for Prevention Trials Across all Stages and Target Populations". *J. Prev. Alzheimers Dis.* 1 (3): 181–202. DOI: [10.14283/jpad.2014.32](https://doi.org/10.14283/jpad.2014.32).
- Da X, Toledo JB, Zee J, Wolk DA, Xie SX, et al. (2014). "Integration and relative value of biomarkers for prediction of MCI to AD progression: spatial patterns of brain atrophy,

- cognitive scores, APOE genotype and CSF biomarkers". *Neuroimage Clin.* 4: 164–173. DOI: [10.1016/j.nicl.2013.11.010](https://doi.org/10.1016/j.nicl.2013.11.010).
- Dallaire-Thérroux C, Callahan BL, Potvin O, Saikali S, and Duchesne S (2017). "Radiological-Pathological Correlation in Alzheimer's Disease: Systematic Review of Antemortem Magnetic Resonance Imaging Findings". *J. Alzheimers Dis.* 57 (2): 575–601. DOI: [10.3233/JAD-161028](https://doi.org/10.3233/JAD-161028).
- Devanand DP, Pradhaban G, Liu X, Khandji A, De Santi S, et al. (2007). "Hippocampal and entorhinal atrophy in mild cognitive impairment: prediction of Alzheimer disease". *Neurology* 68 (11): 828–836. DOI: [10.1212/01.wnl.0000256697.20968.d7](https://doi.org/10.1212/01.wnl.0000256697.20968.d7).
- Fjell AM and Walhovd KB (2012). "Neuroimaging results impose new views on Alzheimer's disease—the role of amyloid revised". *Mol. Neurobiol.* 45 (1): 153–172. DOI: [10.1007/s12035-011-8228-7](https://doi.org/10.1007/s12035-011-8228-7).
- Fox NC, Warrington EK, Freeborough PA, Hartikainen P, Kennedy AM, et al. (1996). "Presymptomatic hippocampal atrophy in Alzheimer's disease. A longitudinal MRI study". *Brain* 119 (Pt 6): 2001–2007. DOI: [10.1093/brain/119.6.2001](https://doi.org/10.1093/brain/119.6.2001).
- Francis PT, Palmer AM, Snape M, and Wilcock GK (1999). "The cholinergic hypothesis of Alzheimer's disease: a review of progress". *J. Neurol. Neurosurg. Psychiatr.* 66 (2): 137–147. DOI: [10.1136/jnnp.66.2.137](https://doi.org/10.1136/jnnp.66.2.137).
- Frisoni GB, Fox NC, Jack CR, Scheltens P, and Thompson PM (2010). "The clinical use of structural MRI in Alzheimer disease". *Nat. Rev. Neurol.* 6 (2): 67–77. DOI: [10.1038/nrneuro1.2009.215](https://doi.org/10.1038/nrneuro1.2009.215).
- Gray TS (1999). "Functional and anatomical relationships among the amygdala, basal forebrain, ventral striatum, and cortex. An integrative discussion". *Ann. N. Y. Acad. Sci.* 877: 439–444. DOI: [10.1111/j.1749-6632.1999.tb09281.x](https://doi.org/10.1111/j.1749-6632.1999.tb09281.x).
- Haber SN (2016). "Corticostriatal circuitry". *Dialogues Clin. Neurosci.* 18 (1): 7–21. (Visited on 09/10/2018). URL: <https://www.dialogues-cns.org/wp-content/uploads/issues/18/DialoguesClinNeurosci-18-7.pdf>.
- Haber SN and McFarland NR (1999). "The concept of the ventral striatum in nonhuman primates". *Ann. N. Y. Acad. Sci.* 877: 33–48. DOI: [10.1111/j.1749-6632.1999.tb09259.x](https://doi.org/10.1111/j.1749-6632.1999.tb09259.x).
- Haber SN (2011). *Neuroanatomy of Reward: A View from the Ventral Striatum*. In: *Neurobiology of sensation and reward*. Ed. by JA Gottfried. Boca Raton, FL: CRC Press.
- Hasselmo ME and Schnell E (1994). "Laminar selectivity of the cholinergic suppression of synaptic transmission in rat hippocampal region CA1: computational modeling and brain slice physiology". *J. Neurosci.* 14 (6): 3898–3914. URL: <http://www.jneurosci.org/content/14/6/3898> (visited on 09/10/2018).
- Havekes R, Abel T, and Van der Zee EA (2011). "The cholinergic system and neostriatal memory functions". *Behav. Brain Res.* 221 (2): 412–423. DOI: [10.1016/j.bbr.2010.11.047](https://doi.org/10.1016/j.bbr.2010.11.047).

- Heimer L and Hoesen G van (1979). "Ventral Striatum". In: *The Neostriatum*. Ed. by I Divac and RGE Öberg. Oxford, UK: Pergamon, 147–158. DOI: [10.1016/B978-0-08-023174-7.50013-8](https://doi.org/10.1016/B978-0-08-023174-7.50013-8).
- Ingelsson M, Fukumoto H, Newell KL, Growdon JH, Hedley-Whyte ET, et al. (2004). "Early A β accumulation and progressive synaptic loss, gliosis, and tangle formation in AD brain". *Neurology* 62 (6): 925–931. DOI: [10.1212/01.WNL.0000115115.98960.37](https://doi.org/10.1212/01.WNL.0000115115.98960.37).
- Iqbal K and Grundke-Iqbal I (2004). "Inhibition of neurofibrillary degeneration: a promising approach to Alzheimer's disease and other tauopathies". *Curr. Drug. Targets* 5 (6): 495–502. DOI: [10.2174/1389450043345254](https://doi.org/10.2174/1389450043345254).
- Jack CR, Albert MS, Knopman DS, McKhann GM, Sperling RA, et al. (2011). "Introduction to the recommendations from the National Institute on Aging-Alzheimer's Association workgroups on diagnostic guidelines for Alzheimer's disease". *Alzheimers Dement.* 7 (3): 257–262. DOI: [10.1016/j.jalz.2011.03.004](https://doi.org/10.1016/j.jalz.2011.03.004).
- Jack CR, Knopman DS, Jagust WJ, Shaw LM, Aisen PS, et al. (2010). "Hypothetical model of dynamic biomarkers of the Alzheimer's pathological cascade". *Lancet Neurol.* 9 (1): 119–128. DOI: [10.1016/S1474-4422\(09\)70299-6](https://doi.org/10.1016/S1474-4422(09)70299-6).
- Jack CR, Petersen RC, O'Brien PC, and Tangalos EG (1992). "MR-based hippocampal volumetry in the diagnosis of Alzheimer's disease". *Neurology* 42 (1): 183–188. DOI: [10.1212/WNL.42.1.183](https://doi.org/10.1212/WNL.42.1.183).
- Jack CR, Petersen RC, Xu Y, O'Brien PC, Smith GE, et al. (2000). "Rates of hippocampal atrophy correlate with change in clinical status in aging and AD". *Neurology* 55 (4): 484–489. DOI: [10.1212/WNL.55.4.484](https://doi.org/10.1212/WNL.55.4.484).
- Kerbler GM, Fripp J, Rowe CC, Villemagne VL, Salvado O, et al. (2015). "Basal forebrain atrophy correlates with amyloid β burden in Alzheimer's disease". *Neuroimage Clin.* 7: 105–113. DOI: [10.1016/j.nicl.2014.11.015](https://doi.org/10.1016/j.nicl.2014.11.015).
- Klunk WE, Price JC, Mathis CA, Tsopelas ND, Lopresti BJ, et al. (2007). "Amyloid deposition begins in the striatum of presenilin-1 mutation carriers from two unrelated pedigrees". *J. Neurosci.* 27 (23): 6174–6184. DOI: [10.1523/JNEUROSCI.0730-07.2007](https://doi.org/10.1523/JNEUROSCI.0730-07.2007).
- Latimer CS, Keene CD, Flanagan ME, Hemmy LS, Lim KO, et al. (2017). "Resistance to Alzheimer disease neuropathologic changes and apparent cognitive resilience in the Nun and Honolulu-Asia Aging Studies". *J. Neuropathol. Exp. Neurol.* 76 (6): 458–466. DOI: [10.1093/jnen/nlx030](https://doi.org/10.1093/jnen/nlx030).
- Lavender T (2008). "Doemdenken over vergrijzing onterecht". *NEMO Kennislink*. (Visited on 09/10/2018). URL: www.nemokennislink.nl/publicaties/doemdenken-over-vergrijzing-onterecht/.
- Liu AK, Chang RC, Pearce RK, and Gentleman SM (2015). "Nucleus basalis of Meynert revisited: anatomy, history and differential involvement in Alzheimer's and Parkinson's disease". *Acta Neuropathol.* 129 (4): 527–540. DOI: [10.1007/s00401-015-1392-5](https://doi.org/10.1007/s00401-015-1392-5).

- McKhann G, Drachman D, Folstein M, Katzman R, Price D, and Stadlan EM (1984). "Clinical diagnosis of Alzheimer's disease: report of the NINCDS-ADRDA Work Group under the auspices of Department of Health and Human Services Task Force on Alzheimer's Disease". *Neurology* 34 (7): 939–944. DOI: [10.1212/WNL.34.7.939](https://doi.org/10.1212/WNL.34.7.939).
- Mielke MM, Okonkwo OC, Oishi K, Mori S, Tighe S, et al. (2012). "Fornix integrity and hippocampal volume predict memory decline and progression to Alzheimer's disease". *Alzheimers Dement.* 8 (2): 105–113. DOI: [10.1016/j.jalz.2011.05.2416](https://doi.org/10.1016/j.jalz.2011.05.2416).
- O'Brien JT, Holmes C, Jones M, Jones R, Livingston G, et al. (2017). "Clinical practice with anti-dementia drugs: A revised (third) consensus statement from the British Association for Psychopharmacology". *J. Psychopharmacol. (Oxford)* 31 (2): 147–168. DOI: [10.1177/0269881116680924](https://doi.org/10.1177/0269881116680924).
- Oakley H, Cole SL, Logan S, Maus E, Shao P, et al. (2006). "Intraneuronal β -amyloid aggregates, neurodegeneration, and neuron loss in transgenic mice with five familial Alzheimer's disease mutations: potential factors in amyloid plaque formation". *J. Neurosci.* 26 (40): 10129–10140. DOI: [10.1523/JNEUROSCI.1202-06.2006](https://doi.org/10.1523/JNEUROSCI.1202-06.2006).
- Richner M, Bach G, and West MJ (2009). "Over expression of amyloid β -protein reduces the number of neurons in the striatum of APP^{swe}/PS1 Δ E9". *Brain Res.* 1266: 87–92. DOI: [10.1016/j.brainres.2009.02.025](https://doi.org/10.1016/j.brainres.2009.02.025).
- Schuff N, Woerner N, Boreta L, Kornfield T, Shaw LM, et al. (2009). "MRI of hippocampal volume loss in early Alzheimer's disease in relation to ApoE genotype and biomarkers". *Brain* 132 (Pt 4): 1067–1077. DOI: [10.1093/brain/awp007](https://doi.org/10.1093/brain/awp007).
- Shipp S (2017). "The functional logic of corticostriatal connections". *Brain Struct. Funct.* 222 (2): 669–706. DOI: [10.1007/s00429-016-1250-9](https://doi.org/10.1007/s00429-016-1250-9).
- Snowdon DA (2003). "Healthy aging and dementia: findings from the Nun Study". *Ann. Intern. Med.* 139 (5 Pt 2): 450–454. DOI: [10.7326/0003-4819-139-5_Part_2-200309021-00014](https://doi.org/10.7326/0003-4819-139-5_Part_2-200309021-00014).
- Sperling RA, Aisen PS, Beckett LA, Bennett DA, Craft S, et al. (2011). "Toward defining the preclinical stages of Alzheimer's disease: recommendations from the National Institute on Aging-Alzheimer's Association workgroups on diagnostic guidelines for Alzheimer's disease". *Alzheimers Dement.* 7 (3): 280–292. DOI: [10.1016/j.jalz.2011.03.003](https://doi.org/10.1016/j.jalz.2011.03.003).
- Spitzer M (1999). *The mind within the net: Models of learning, thinking, and acting*. Cambridge, MA: The Mit Press.
- Steiner H and Tseng KY (2010). *Handbook of Basal Ganglia Structure and function*. London: Academic Press.
- Stern Y (2012). "Cognitive reserve in ageing and Alzheimer's disease". *Lancet Neurol.* 11 (11): 1006–1012. DOI: [10.1016/S1474-4422\(12\)70191-6](https://doi.org/10.1016/S1474-4422(12)70191-6).
- Takahashi RH, Milner TA, Li F, Nam EE, Edgar MA, et al. (2002). "Intraneuronal Alzheimer $a\beta$ 42 accumulates in multivesicular bodies and is associated with synaptic pathology". *Am. J. Pathol.* 161 (5): 1869–1879. DOI: [10.1016/S0002-9440\(10\)64463-X](https://doi.org/10.1016/S0002-9440(10)64463-X).

- Thal DR, Rub U, Orantes M, and Braak H (2002). "Phases of A β -deposition in the human brain and its relevance for the development of AD". *Neurology* 58 (12): 1791–1800. DOI: [10.1212/WNL.58.12.1791](https://doi.org/10.1212/WNL.58.12.1791).
- The Dutch National Institute for Public Health and the Environment (2017). "Trend scenario PHF-2018 identifies societal challenges for the future". URL: http://www.rivm.nl/en/Documents_and_publications/Common_and_Present/Newsmessages/2017/Trend_scenario_PHF_2018_identifies_societal_challenges_for_the_future (visited on 09/10/2018).
- Villemagne VL, Ataka S, Mizuno T, Brooks WS, Wada Y, et al. (2009). "High striatal amyloid β -peptide deposition across different autosomal Alzheimer disease mutation types". *Arch. Neurol.* 66 (12): 1537–1544. DOI: [10.1001/archneurol.2009.285](https://doi.org/10.1001/archneurol.2009.285).
- Villemagne VL, Burnham S, Bourgeat P, Brown B, Ellis KA, et al. (2013). "Amyloid- β deposition, neurodegeneration, and cognitive decline in sporadic Alzheimer's disease: a prospective cohort study". *Lancet Neurol.* 12 (4): 357–367. DOI: [10.1016/S1474-4422\(13\)70044-9](https://doi.org/10.1016/S1474-4422(13)70044-9).
- Walhovd KB, Fjell AM, Brewer J, McEvoy LK, Fennema-Notestine C, et al. (2010). "Combining MR imaging, positron-emission tomography, and CSF biomarkers in the diagnosis and prognosis of Alzheimer disease". *AJNR Am. J. Neuroradiol.* 31 (2): 347–354. DOI: [10.3174/ajnr.A1809](https://doi.org/10.3174/ajnr.A1809).
- Zandifar A, Fonov V, Coupe P, Pruessner J, and Collins DL (2017). "A comparison of accurate automatic hippocampal segmentation methods". *Neuroimage* 155: 383–393. DOI: [10.1016/j.neuroimage.2017.04.018](https://doi.org/10.1016/j.neuroimage.2017.04.018).

PART I

Ventral striatal atrophy in Alzheimer's
disease

CHAPTER 2

Reduced volumes of putamen and thalamus in Alzheimer's disease: an MRI study

Laura W de Jong

Karin van der Hiele

Ilya M Veer

Jeanine J Houwing

Rudi GJ Westendorp

Edward LEM Bollen

Paul W de Bruin

Huub AM Middelkoop

Mark A van Buchem

Jeroen van der Grond

ABSTRACT

Background Atrophy is regarded a sensitive marker of neurodegenerative pathology. In addition to confirming the well-known presence of decreased global gray matter and hippocampal volumes in Alzheimer's disease (AD), this study investigated whether deep gray matter structures also suffer atrophy in AD, and whether such degeneration is associated with impaired cognitive function.

Methods In this cross sectional correlation study, two groups were compared on volumes of 7 subcortical regions: 70 memory complainers and 69 subjects diagnosed with probable AD. Using 3T 3D T1 MR images, volumes of nucleus accumbens, amygdala, caudate nucleus, hippocampus, pallidum, putamen and thalamus were automatically calculated by the FIRST-algorithm (FMRIB's Software Library). Subsequently, the volumes of the different regions were correlated with cognitive test results.

Results In addition to finding the expected association between cognitive decline and hippocampal atrophy in AD, volumes of putamen and thalamus were significantly reduced in patients diagnosed with probable AD. We also found that the decrease in volume correlated linearly with impaired global cognitive performance.

Interpretation These findings suggest that, beside neocortical and hippocampal atrophy, the deep gray matter structures in AD suffer atrophy as well and that degenerative processes in the putamen and thalamus may contribute to cognitive decline in AD.

INTRODUCTION

Characteristic degenerative pathology in Alzheimer's disease (AD) consists of atrophy and the increased presence of neurofibrillary tangles and amyloid plaques. This degenerative pathology gradually accumulates over a period of years, long before clinical symptoms become manifest (Jack et al. 1999; CD Smith et al. 2007). Herein, atrophy is considered a better marker for impaired functioning of brain regions than the deposits of insoluble proteins in plaques and tangles, since only a small portion of neurons contains tangles and the number of neurons that die, exceeds by far the number that contains tangles (AD Smith 2002). Description of cerebral atrophy patterns in the process of AD is considered important, because it may provide information on the pathogenesis of AD and on the contribution of various brain structures to cognitive decline.

Structural imaging studies have already identified several diagnostic markers of AD related to atrophy: hippocampal atrophy (de Leon, Convit, et al. 1995), amygdalar atrophy (Horinek, Varjassyova, and Hort 2007), medial temporal lobe atrophy (de Leon, Golomb, et al. 1993; Scheltens et al. 1992), precuneus atrophy (G Karas et al. 2007), and global gray matter atrophy (GB Karas et al. 2004). Most studies have focused on the cortex, and especially the hippocampus, regarding their crucial roles in higher cognitive functions and memory processes respectively, whereas the basal nuclei and thalamus have received less attention. There are, however, many reasons to assume that degeneration of deep gray matter structures, besides the hippocampus and the amygdala, may also occur in the process of AD and may contribute to cognitive deterioration. In 1990, Braak et al. noted the presence of amyloid depositions in the striatum in AD patients. Klunk et al. (2007) found that amyloid depositions appear in the striatum in very early stages of the disease in PS1 mutation carriers. Both studies indicated that the striatum is prone to AD pathology. Regarding subcortical atrophy and AD, Ferrarini et al. (2006) reported the changes in shape of the ventricle system in areas adjacent to the amygdala, thalamus, and caudate nucleus in patients with AD, indicating atrophic changes in those regions. Direct measurement of the caudate nucleus in AD patients revealed diminished volumes of this structure, although proportionate to whole brain atrophy (Almeida et al. 2003). Direct measurement of subcortical structures in Parkinson's disease, another neurodegenerative disorder accompanied in advanced stages by dementia, also showed decreased volumes of putamen and pallidum (Geng, Li, and Zee 2006). The impaired functioning of the basal nuclei has previously been related to cognitive dysfunction, since neurodegenerative extrapyramidal syndromes commonly show symptoms of cognitive dysfunction such as visuospatial deficits, depression, anxiety, and, in progressed stages, clinical dementia syndrome (Borroni et al. 2008). Atrophy of the thalamus has also been associated with cognitive decline in neurodegenerative disorders other than AD such as

multiple sclerosis, Huntington's disease, and Lewy body disease (Houtchens et al. 2007; Kassubek et al. 2005; Barber et al. 2002). Although little is known about the specific role that subcortical and thalamic structures have in cognitive processes, it is well recognized that the thalamus is essential for generating attention (Newman 1995) and its anterior and medial nuclei are involved in declarative memory functioning (Van der Werf et al. 2000). In spite of all these data, direct measurement of volumes of all large subcortical structures in AD patients, compared to those without cognitive impairment has not been assessed before; similarly, the correlation between the decrease of their volume and cognitive functioning has never been reported in the literature.

In this study we used FMRIB's Integrated Registration and Segmentation Tool (FIRST) (Patenaude et al. 2007b) to automatically measure the volumes of amygdala, hippocampus, nucleus accumbens, caudate nucleus, putamen, pallidum, and thalamus in patients visiting the outpatient memory clinic of our hospital. The aim of this study was to assess whether differences exist between volumes of the basal nuclei and the thalamus of subjects with AD compared to elderly subjects without cognitive impairment. We hypothesized that smaller volumes of the basal nuclei and thalamus exist in AD patients due to more severe atrophic changes in those regions, compared to the volume loss accompanying "normal ageing" in elderly subjects in whom no cognitive impairment can be objectified. We also hypothesized that smaller volumes of the deep gray matter structures, when corrected for age, gender, years of education, head size, and neocortical gray matter volume, correlate with poorer cognitive test results.

METHODS

Study design

Two hundred and nineteen consecutive patients, who visited the outpatient's clinic for memory deficits of the geriatric department of the Leiden University Medical Center (LUMC) between January 1, 2006 and October 1, 2007 were recruited for this study. All subjects who visited the clinic complained of memory loss and were examined according to a standardized protocol, which included whole brain MRI, neuropsychological screening, and a general medical and neurological examination by a neurologist or geriatrician. Cognitive testing took place prior or after MRI testing with a maximal interval of 14 days. The eventual diagnosis was determined in a multidisciplinary consensus meeting which employed the National Institute of Neurological and Communicative Disorders and Stroke and Alzheimer's Disease and Related Disorders Association (NINCDS-ADRDA) criteria for diagnosing probable AD (McKhann et al. 1984). This cross-sectional case-control study was approved by the local ethics committee. Written informed consent

was obtained from all subjects or from a close relative if a patient was demented.

Subjects

Subjects visited the memory clinic for a variety of indications, mostly memory complaints experienced by the patient or notified by people in his or her environment. In a multidisciplinary meeting, patients were categorized as having possible or probable AD, mild cognitive impairment, or a neurological or psychiatric disorder. The remaining patients, by whom objectively no memory deficits could be detected, were classified as memory complainers (MC). Attention was given to factors that might contribute to memory complaints in this heterogeneous group. Part of the memory complainers suffered mild depressions (Geriatric Depression Scale (GDS) (Yesavage and Sheikh 1986) < 10 ($n = 12$)), while in another part memory was declined due to psychosocial factors such as the loss of a family member or problems at work ($n = 17$). For over half of the memory complainers no clear explanation for subjectively experienced memory decline was found. Part of them might have had a very early stage of dementia, undetectable by our present means. For our study we included 139 subjects, for whom complete datasets were available. Seventy of them were classified as memory complainers and 69 as probable AD patients.

In total 80 subjects were excluded. Among them were subjects who did have cognitive impairment detected during neuropsychological testing but did not meet the criteria for probable AD ($n = 33$), or were diagnosed with other forms of dementia (frontotemporal dementia $n = 3$, Lewy body disease $n = 1$, vascular dementia $n = 3$, Parkinson's dementia $n = 2$). Other exclusion criteria for this study included; other neurological disorders ($n = 14$) e.g., normal pressure hydrocephalus, intracranial tumors, stroke etc.; severe mood disorders with GDS ≥ 10 ($n = 10$); alcohol abuse ($n = 8$); insufficient scan quality ($n = 2$); and reexamination of the subject neuropsychologically ($n = 4$).

Neuropsychological assessment

The cognitive functioning of all subjects was assessed using a standardized neuropsychological test battery, including the Cambridge Cognitive Examination-Revised (CAMCOG-R) (Roth et al. 1988) incorporating the Mini Mental State Examination (MMSE) (MF Folstein, SE Folstein, and McHugh 1975). Furthermore, all subjects were examined for signs of depression using the GDS to rule out severe depression as contributory factor to memory loss or cognitive decline.

MR data acquisition

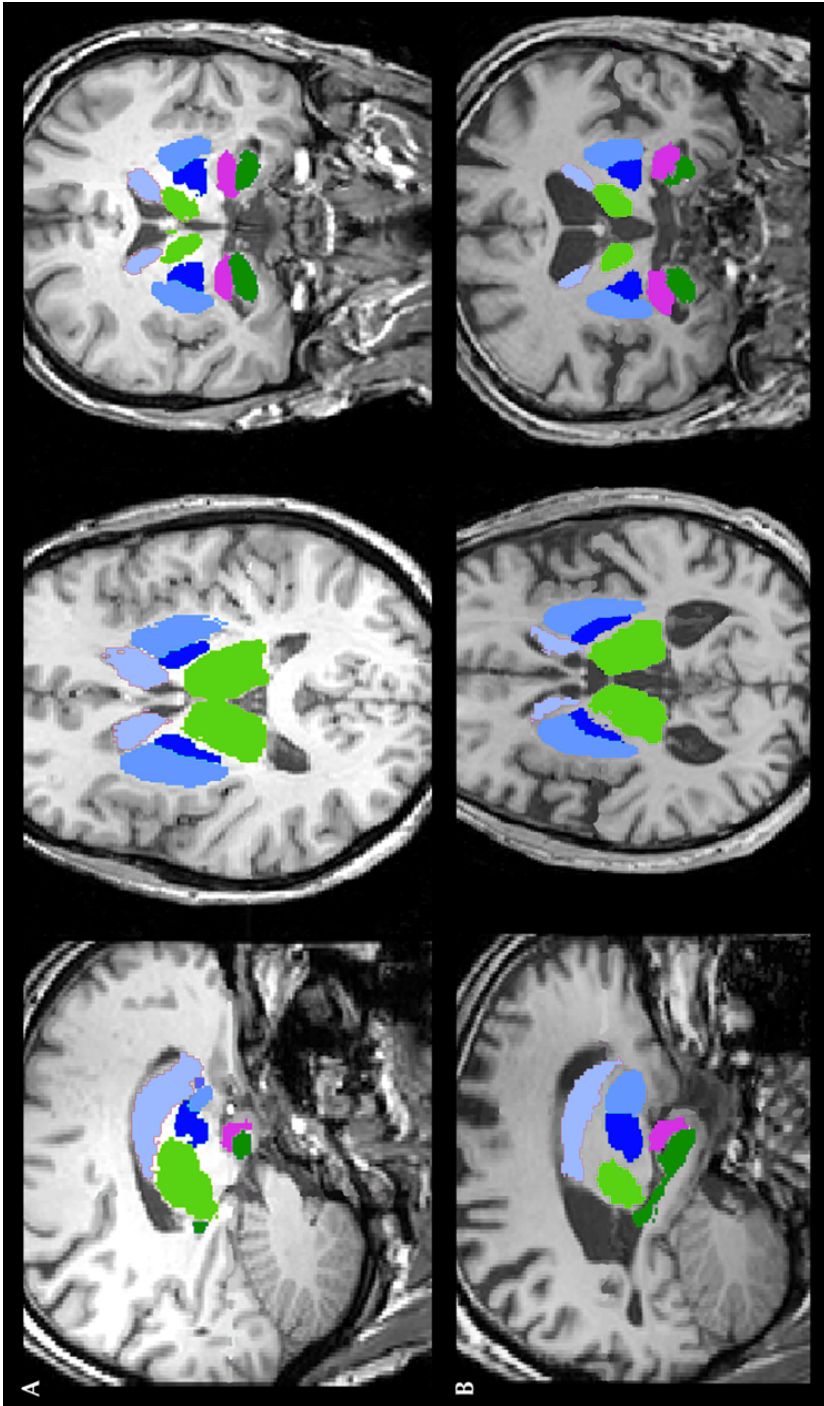
MRI was performed using a 3.0 Tesla whole body MRI scanner (Philips Medical Systems, Best, The Netherlands). Volume measurements of the basal nuclei and the thalamus were performed on 3D-T1-weighted MR images (acquisition parameters were as follows: TR = 9.8 ms; TE = 4.6 ms; flip angle = 8°; section thickness = 1.2 mm; number of sections = 120; no section gap; whole brain coverage; FOV = 224 mm; matrix = 192, reconstruction matrix = 256). Routine T2 weighted MRI and FLAIR were performed to rule out a mass lesion as contributory factor to memory loss or cognitive decline.

Measurement of volumes of deep gray matter structures

The algorithm FIRST (FMRIB's Integrated Registration and Segmentation Tool), was applied to separately estimate left and right volumes of seven subcortical regions; amygdala, hippocampus, nucleus accumbens, caudate nucleus, putamen, pallidum, and thalamus. FIRST is part of FSL (FMRIB's Software Library) and performs both registration and segmentation of the mentioned subcortical regions (Patenaude et al. 2007b; SM Smith, Jenkinson, et al. 2004). During registration, the input data (3D T1 images) are transformed to the MNI (Montreal Neurological Institute) 152 standard space, by means of affine transformations based on 12 degrees of freedom (i.e., 3 translations, 3 rotations, 3 scalings, and 3 skews). After subcortical registration, a subcortical mask is applied, to locate the different subcortical structures, followed by segmentation based on voxel intensities. Absolute volumes of subcortical structures are calculated, taking into account the transformations made in the first stage (Patenaude et al. 2007a). Finally a boundary correction is used to determine with what certainty the boundary voxels belong to the structure or not. In this study a z-value of 3 was used, corresponding to a 99.998% certainty that the voxel belonged to the subcortical structure. After registration and segmentation of all 139 MR scans, all segmented subcortical regions were visually checked for errors in registration and segmentation. None were found. Examples of subcortical segmentation, after boundary correction, of a subject classified as memory complainer and of a subject diagnosed with probable AD, are presented in respectively figure 1A and 1B.

Brain tissue volume, normalized for subject head size, was estimated with SIENAX (SM Smith, De Stefano, et al. 2001; SM Smith, Zhang, et al. 2002), part of FSL (SM Smith, Jenkinson, et al. 2004). SIENAX starts by extracting brain and skull images from the single whole-head input data (SM Smith, Zhang, et al. 2002). The brain image is then affine-registered to MNI152 space (Jenkinson and S Smith 2001; Jenkinson, Bannister, et al. 2002) (using the skull image to determine the registration scaling); this

Figure 1: FIRST-segmentation: A memory complainer, B Alzheimer's disease



is primarily in order to obtain the volumetric scaling factor, to be used as a normalization for head size. Next, tissue-type segmentation with partial volume estimation is carried out (Zhang, Brady, and S Smith 2001) in order to calculate total volume of brain tissue (including separate estimates of volumes of grey matter, white matter, peripheral grey matter and ventricular CSF). For this study we used the absolute volumes generated by the algorithm. To obtain neocortical gray matter volume independent from the deep gray matter structures of interest, we subtracted the volumes of the hippocampus and amygdala from the peripheral gray matter volume as given by SIENAX. The volumetric scaling factor was used as an estimate for head size.

Statistical analysis

SPSS v 14.0 for Windows was used for data analysis. The memory complainers were compared on age and educational level (in years of education including primary school) with those diagnosed with probable AD by one-way independent ANOVA, and compared on gender by a χ^2 test. The analysis consisted of two parts. The first part was designed to assess whether the means of cortical and deep gray matter volumes (FIRST and SIENAX-output) in probable AD were decreased compared to individuals without cognitive impairment. For each deep gray matter, a general linear model was used in which the volume of the deep gray matter structure was included as dependent factor and diagnosis as independent variable. Adjustments were made for age, sex, and head size. The beta coefficients and p -values between MC and probable AD were calculated. A p -value ≤ 0.05 was considered significant. Furthermore, Pearson correlation coefficients were calculated between the neocortical gray matter and the different deep gray matter structures, total brain volume, and total white matter volume.

In the second part, correlations between neuropsychological test results (CAMCOG-R score, executive subtest of CAMCOG-R, and MMSE score) and deep gray matter volumes were assessed for memory complainers and subjects with probable AD separately. For each deep gray matter structure, the relation of structure volume and cognitive test score was assessed in a linear model in which the cognitive test score was included as the dependent variable and the volume of the deep gray matter structure as the independent variable. Age, gender, years of education, head size, and neo cortical gray matter volume were also added as independent variables in these models, because of their expected influence on cognitive test scores. A collinearity test was performed to rule out multicollinearity between the independent variables, in which a R^2 above 64% was considered being a strong correlation.

RESULTS

Group demographic features are presented in table 1. Memory complainers differed significantly from probable AD subjects in age ($F = 38.1$, $p < 0.001$) and in years of education ($F = 9.97$, $p = 0.002$) but not in gender ($\chi^2 = 2.68$, $p = 0.10$). Although the male-female ratio was not significantly different between the memory complainers and probable Alzheimer's disease patients, it was incorporated as independent factor in the statistical analyses because of the relatively large number of female probable AD subjects and the known existence of different brain tissue volumes between the sexes.

Table 1: Demographics & group characteristics

| Mean (SD) | Memory Complainers | | | Probable Alzheimer's disease | | |
|--------------------|--------------------|----------|----------|------------------------------|-----------|-----------|
| | Male | Female | Total | Male | Female | Total |
| N | 35 | 35 | 70 | 25 | 44 | 69 |
| Age in years | 65 (13) | 67 (12) | 66 (13) | 76 (5.8) | 77 (8.2) | 77 (7.4) |
| Education in years | 12 (3.9) | 12 (3.5) | 12 (3.7) | 11 (4.5) | 8.9 (3.5) | 9.8 (4.0) |
| CAMCOG-R | 90 (7.0) | 90 (7.3) | 90 (7.1) | 69 (15) | 61 (14) | 64 (15) |
| CAMCOG-R exe | 15 (2.6) | 15 (3.1) | 15 (2.9) | 9.6 (3.6) | 9.2 (3.5) | 9.4 (3.5) |
| MMSE | 28 (1.6) | 27 (2.7) | 27 (2.3) | 20 (5.0) | 17 (4.4) | 18 (4.7) |

CAMCOG-R: CAMbridge COGnition examination Revised; CAMCOG-R exe: CAMbridge COGnition examination Revised executive functioning; MMSE: mini mental state examination.

Memory complainers and probable AD significantly differed in age (one-way ANOVA: $F = 38.1$, $p < 0.001$) and years of education (one-way ANOVA; $F = 9.97$, $p = 0.002$) but not in gender ($\chi^2 = 2.68$, $p = 0.10$).

Decreased volumes of putamen and thalamus in AD subjects

Mean volumes of deep gray matter structures in memory complainers and probable AD are shown in table 2 separately for men and women. All structures, except the right amygdala in women, the left and right caudate nucleus and total white matter in men, were smaller in probable AD compared to memory complainers. After correction for age, gender, and head size, both left and right hippocampus, putamen, and thalamus in probable AD remained significantly smaller compared to memory complainers (as shown in table 2). Also total brain volume and neocortical gray matter volume were significantly smaller in probable AD. Table 2 also shows the Pearson correlation coefficients between neocortical gray matter volume and the volumes of the deep gray matter structures, and their corresponding p -values. Both left and right nucleus accumbens, hippocampus, putamen, and thalamus were significantly correlated with the volume of the neocortical

gray matter in men and women. In men the right globus pallidus also correlated significantly with neocortical gray matter volume, and in women the right amygdala correlated significantly with neocortical gray matter volume.

Left putamen and thalamus volumes correlate with cognition

No multicollinearity between the selected variables, age, years of educations, head size, neocortical gray matter volume, and volumes of the deep gray matter structures, was found (all R^2 were found below 0.52). Therefore, all were entered in the linear regression model which was set up for each deep gray matter structure separately. β -regression coefficients of the correlations between volumes of deep gray matter structures and the main cognitive tests scores (the CAMCOG-R, a subtest on executive function of the CAMCOG-R, and the MMSE) of memory complainers and subjects with probable AD, are displayed in table 3. The corresponding p -values are displayed between parentheses. This table shows that volumes of the left hippocampus, left putamen, and left thalamus in probable AD subjects correlated significantly with all three cognitive test scores. Also, the right thalamus showed a significant correlation in probable AD subjects with the MMSE score. The remaining correlations between right hippocampus, right putamen, and right thalamus and cognitive test scores were stronger compared to the correlations of the other deep gray matter structures, but were not significant. In all the regression models between the hippocampus, putamen, and thalamus and the cognitive test scores of probable AD subjects, the volume of the deep gray matter structure constantly formed the strongest predictor of cognitive outcome compared to age, gender, years of education, head size, and neocortical gray matter volume.

In the linear regression models for memory complainers the left hippocampus, both the volume of the left and right nucleus accumbens, and the right thalamus correlated significantly with the CAMCOG-R score. The volume of the left hippocampus also correlated significantly with the MMSE score. In all regression models of the memory complainers, however, the correlation between educational level and cognitive test score exceeded in strength the correlation between volume of the deep gray matter and the cognitive test score, with all p -values < 0.01 .

The volumes of the caudate nucleus, amygdala, and the pallidum did not show any significant correlations with any of the cognitive test scores, in any of the groups.

DISCUSSION

First, in addition to the expected finding of reduced hippocampal and neocortical gray matter volumes in AD, the current study revealed significantly reduced volumes of both

Table 2: Mean volumes of deep gray matter structures in cm³ per diagnosis and gender)

| | Memory Complainers | | Probable Alzheimer's disease | | β^a in cm ³ | Pearson corr | |
|--------------------|--------------------------------------|-------------|--------------------------------------|-------------|---------------------------------|--------------|--------|
| | Mean volumes in cm ³ (SD) | | Mean volumes in cm ³ (SD) | | | NeoCor GM | |
| | Male | Female | Male | Female | Male | Female | |
| Amygdala | L 1.66 (0.28) | 1.44 (0.22) | 1.62 (0.35) | 1.36 (0.27) | -0.030 | 0.13 | 0.06 |
| Amygdala | R 1.72 (0.28) | 1.47 (0.26) | 1.57 (0.32) | 1.48 (0.37) | -0.054 | 0.23 | 0.33** |
| Hippocampus | L 4.20 (0.60) | 3.83 (0.74) | 3.73 (0.67) | 3.43 (0.69) | -0.244* | 0.58** | 0.33** |
| Hippocampus | R 4.21 (0.71) | 3.97 (0.72) | 3.57 (0.78) | 3.32 (0.65) | -0.295* | 0.61** | 0.39** |
| Accumbens | L 0.64 (0.16) | 0.51 (0.16) | 0.48 (0.19) | 0.42 (0.14) | -0.049 | 0.42** | 0.45** |
| Accumbens | R 0.47 (0.17) | 0.36 (0.15) | 0.35 (0.15) | 0.27 (0.10) | -0.035 | 0.32* | 0.40** |
| Caudate nucleus | L 4.41 (1.00) | 4.09 (0.81) | 4.49 (0.90) | 3.77 (0.82) | 0.027 | 0.18 | 0.21 |
| Caudate nucleus | R 4.96 (0.90) | 4.49 (0.60) | 5.01 (0.98) | 4.09 (0.78) | -0.188 | 0.08 | -0.02 |
| Putamen | L 5.90 (0.77) | 5.24 (0.61) | 5.25 (0.62) | 4.53 (0.83) | -0.381** | 0.53** | 0.37** |
| Putamen | R 6.47 (0.86) | 5.56 (0.75) | 5.80 (0.81) | 5.05 (0.78) | -0.285* | 0.45** | 0.34** |
| Globus pallidus | L 2.36 (0.99) | 2.26 (0.73) | 2.11 (0.55) | 1.97 (0.64) | -0.029 | 0.22 | -0.12 |
| Globus pallidus | R 2.39 (0.88) | 2.16 (0.73) | 2.03 (0.51) | 1.83 (0.67) | -0.234 | 0.32 | 0.07 |
| Thalamus | L 7.63 (1.07) | 7.40 (1.03) | 7.20 (0.87) | 6.18 (1.12) | -0.362* | 0.52** | 0.51** |
| Thalamus | R 7.68 (0.95) | 7.21 (0.92) | 6.88 (0.73) | 6.17 (1.08) | -0.409** | 0.61** | 0.46** |
| Brain ^b | 1204 (107) | 1085 (123) | 1113 (101) | 974 (77) | -41.7** | 0.64** | 0.63** |
| White matter | 506 (66) | 458 (58) | 522 (94) | 448 (61) | 6.4 | -0.17 | 0.09 |
| NeoCor GM | 511 (78) | 463 (73) | 412 (93) | 395 (87) | -39.3** | - | - |

a General linear model applied for estimating group differences (adjusted for age, gender, and head size); * $p \leq 0.05$; ** $p \leq 0.01$.

L: left; R: right; NeoCor GM: neocortical gray matter minus volumes of hippocampus and amygdala.

b Total of white and gray matter volume including deep gray matter structures.

Table 3: Relation of volume of deep gray matter structures and cognition

| | | CAMCOG-R | | CAMCOG-R exe | | MMSE | |
|-----------------|---|-----------------|------------------|-----------------|------------------|-----------------|------------------|
| | | MC ^a | pAD ^a | MC ^a | pAD ^a | MC ^a | pAD ^a |
| Amygdala | L | -0.02 | 0.13 | -0.02 | 0.13 | 0.07 | 0.20 |
| Amygdala | R | 0.05 | 0.20 | -0.04 | 0.15 | 0.09 | 0.08 |
| Hippocampus | L | 0.29** | 0.28* | 0.12 | 0.33* | 0.30* | 0.28* |
| Hippocampus | R | 0.16 | 0.18 | 0.11 | 0.22 | 0.29 | 0.20 |
| N. accumbens | L | 0.34** | 0.04 | 0.08 | 0.13 | 0.23 | 0.11 |
| N. accumbens | R | 0.31* | 0.17 | 0.12 | 0.26 | 0.19 | 0.14 |
| Caudate | L | -0.04 | 0.24 | -0.09 | 0.26 | -0.09 | 0.17 |
| Caudate | R | -0.12 | 0.07 | -0.07 | 0.14 | 0.03 | 0.14 |
| Putamen | L | 0.19 | 0.50** | -0.06 | 0.52** | 0.18 | 0.50** |
| Putamen | R | 0.20 | 0.25 | -0.09 | 0.14 | 0.17 | 0.19 |
| Globus pallidus | L | 0.07 | -0.09 | 0.11 | -0.16 | -0.08 | -0.13 |
| Globus pallidus | R | 0.02 | -0.08 | 0.03 | 0.02 | -0.08 | -0.09 |
| Thalamus | L | 0.07 | 0.37** | 0.001 | 0.43** | -0.16 | 0.37* |
| Thalamus | R | 0.39** | 0.21 | 0.08 | 0.18 | 0.27 | 0.31* |

CAMCOG-R: CAMbridge COGnition examination Revised; CAMCOG-R exe: CAMbridge COGnition examination Revised executive functioning; MC: memory complainers; pAD: probable Alzheimer's disease; MMSE: Mini Mental State Examination; L: left; R: right.

^a Linear regression analysis; β -coefficients of associations between volumes of deep gray matter regions and main cognitive test results (adjusted for age, gender, years of education, head size, and neocortical gray matter volume; * $p \leq 0.05$, ** $p \leq 0.01$)

left and right putamen and thalamus in patients diagnosed with probable AD compared to memory complainers. This volume reduction was found independent of age, gender, and head size. Second, we also found, that reduced volumes of the putamen and the thalamus independently correlated with impaired cognitive functioning in elderly subjects, when controlled for age, gender, educational level, head size, and neocortical gray matter volume. To the best of our knowledge, this is the first study that explicitly associates smaller volumes of putamen and thalamus with AD, and reveals their relation with cognitive functioning.

The finding of smaller volumes of hippocampus, putamen, and thalamus in patients diagnosed with probable AD suggests that degenerative pathology affects these struc-

tures more or earlier in the process of AD than other deep gray matter structures. Volumes of brain structures, especially gray matter volume, have been said to be of protective value in AD (Wolf et al. 2004). Our analysis supports this idea as well, since the smaller the volumes of hippocampus, putamen, and thalamus, the lower the cognitive test results were. In fact, in the AD group, especially the left volumes of the hippocampus, putamen, and thalamus formed the strongest predictors for cognitive performance. Hippocampal atrophy and its contribution to memory decline in the process of AD has been previously described and is widely accepted (Laakso et al. 1995; de Leon, Convit, et al. 1995). Putaminal and thalamic volume reduction in AD and their relations to cognitive decline, however, have not been reported before, and these findings seem to open a new perspective on AD. The basal nuclei and thalamus are known to participate in many different neuronal pathways, with functions that are not just restricted to motor behavior, but are also related to emotional, motivational, associative and cognitive abilities (Herrero, Barcia, and Navarro 2002). Strength of our study was the availability of cognitive data for all study participants. Our data showed that volume reduction of the left putamen and left thalamus were both significantly associated with global cognitive decline in elderly subjects visiting a memory clinic and exceeded in strength the correlation of left hippocampal and cognitive performance. To interpret this, data from other studies are needed. The putamen has been correlated with AD, since amyloid deposits are present early in the disease process (H Braak and E Braak 1990). At the moment however, very little is known on the putaminal role in cognition. Recent literature shows that as part of the striatum, the putamen is found active in probabilistic learning tasks (Graybiel 2005; Bellebaum et al. 2008) and working memory tasks (Dahlin et al. 2008). Furthermore, the putamen has been correlated with the emergence of dementia in other neurodegenerative disorders, like Parkinson's disease, due to dopaminergic or other neurochemical deficits (Emre 2003), indicating once more that its effect on cognitive impairment might be greater than previously assumed. Whether the putamen in the process of AD influences cognition due to impaired putaminal primary cognitive functions, inadequate neurochemical functioning, or discontinuing the cortico-thalamic projections, could not be answered in this study, and is an interesting topic for further research. In contrast to the putamen, slightly more is known on the thalamus and its relation to cognition. The thalamus consists of multiple nuclei and is classically metaphorized as an active relay center. The thalamus serves both sensory and motor mechanisms (Herrero, Barcia, and Navarro 2002). Cognitively it is involved in directing attention and suppressing irrelevant sensory input (Newman 1995) and its anterior, medial-dorsal, intralaminar, and midline nuclei are important for memory functions (Van der Werf et al. 2000). Thalamic atrophy has been related to cognitive performance in other neurodegenerative disorders, like Huntington's disease (Kassubek et al. 2005) and

multiple sclerosis (Houtchens et al. 2007), and herein affected mostly the executive functioning of patients. As part of the limbic system, atrophy of the anterior part of the thalamus in AD has been described. Callen et al. (2001) reported that the anterior part of the thalamus is significantly smaller in AD patients than in healthy controls. However, the size reduction of the thalamus in our study cannot entirely be explained by reduction of the anterior nuclei alone and suggests that other nuclei of the thalamus are also prone to atrophy in AD, in which the large medial-dorsal nucleus is an important candidate. Supportive to this thought is the finding of Braak et al. in 1991, that in all limbic nuclei of the thalamus extracellular amyloid deposits and neurofibrillary tangles occur, although the most severe involvement was found in the medial-dorsal nucleus. In summary, we found a clear reduction in size of the putamen and thalamus in probable AD patients compared to controls without memory deficits. This is in addition to the previously found presence of neurofibrillary tangles and amyloid plaques in the striatum and thalamus early in the disease process of AD. Moreover, the reduction in size of the putamen and thalamus, especially the left side, was correlated to global cognitive decline. At present no clear explanation can be given on the difference in correlational strength between left and right side of the putamen and thalamus. Part might be due to the dominant presence of the right-handedness among subjects in this population. Another explanation might be that the tested cognitive functions are more prominent on the left side. Whether shrinkage of the putamen and thalamus is a primary or a secondary phenomenon in the pathology of AD, also remains to be elucidated.

The presented data suggest that in AD some structures are affected by atrophy (i.e., the neocortical gray matter and hippocampus, putamen, and thalamus) whereas others are relatively preserved (i.e., the amygdala, nucleus accumbens, caudate nucleus, pallidum, and white matter). In previous studies it has been shown, however, that atrophy of the amygdala and caudate nucleus is also associated with AD; our data did not confirm this, though. The volumetric data showed that the amygdala was smaller in the probable AD group compared to the memory complainers, but this reduction in size was not significant when controlled for age, gender, and head size. We applied a strict analysis to assess significance between memory complainers and probable AD subjects, therefore possible shrinkage of the amygdala could have lost its significance. Another explanation might be that amygdala is affected later in the disease process of AD than the hippocampus, putamen, and thalamus, and therefore not prominent in MR imaging of patients who attended the memory clinic for the first time. The caudate nucleus was also not significantly smaller in memory complainers than in probable AD patients, nor were the nucleus accumbens, pallidum, and white matter volumes. None of these volumes showed a significant correlation with any of the cognitive test scores except for the nucleus accumbens which was significantly correlated with the CAMCOG-R score

in memory complainers, but not in probable AD subjects. Our study did not show a significant reduction in size of the nucleus accumbens in probable AD subjects compared to memory complainers, but found it was significantly correlated to the neocortical gray matter volume. A possible explanation for this relation to neocortical gray matter volume and cognitive decline in memory complainers is that the nucleus accumbens is affected in old age, but not specifically in AD. Another explanation is that the structure is just too small, relative to the other deep gray matter structures, to obtain sensitive data with our method.

One limitation of our study could be the use of memory complainers as control group instead of a cognitively healthy control group. Several studies have already revealed the presence of smaller left hippocampal volumes and decreased gray matter volumes among memory complainers, suggesting that this condition for some subjects forms a preclinical condition to AD (van der Flier et al. 2004; Saykin et al. 2006). However the memory complainers form a relevant control group, since if AD pathology is present; it is in a very early stage and very likely to be less pronounced than in clinical stages of AD.

Another limitation of our study could be the relative novelty of the software adopted from FSL. However, we did not detect any significant mismatches in segmentation of the subcortical structures performed by the algorithm (figure 1A and 1B are a 2D-representations of segmented subcortical structures by FIRST). Furthermore, our method of automated volume measurement has clear advantages compared to voxel based morphometry (VBM) and manual segmentation. VBM has shown its value in comparing groups of subjects in patterns of atrophy, but is prone to registration artifacts in the deep gray matter and not suitable for analysis of pattern of atrophy in an individual subject (Bookstein 2001; Frisoni and Whitwell 2008). Our method of semi-automatic volumetry can be used to measure volumes of different regions in individual patients and gives an indication of the actual amount of atrophy that occurs. Therefore, it is more patient specific and can be used as marker for disease progression on an individual level. Compared to manual segmentation, the method used has the advantage that its segmentation is based on voxel intensities, while in manual segmentation the contrast differences can be difficult to detect visually. Furthermore, since our method is automated, researcher bias in segmentation is absent.

A last limitation of our study was that because of the cross-sectional nature of the study, it could not be determined whether shrinkage of the thalamus, nucleus accumbens, and putamen was a primary or secondary phenomenon to hippocampal or neo cortical loss.

In conclusion, the present study demonstrates that besides global atrophy of the neocortex and atrophy of the medial temporal lobe, parts of the striatum and thalamus also show atrophy in Alzheimer's disease. Furthermore, our study suggests that putaminal

and thalamic atrophy play important roles in cognitive decline in patients with AD.

BIBLIOGRAPHY

- Almeida OP, Burton EJ, McKeith I, Gholkar A, Burn D, and O'Brien JT (2003). "MRI study of caudate nucleus volume in Parkinson's disease with and without dementia with Lewy bodies and Alzheimer's disease". *Dement. Geriatr. Cogn. Disord.* 16 (2): 57–63. DOI: [10.1159/000070676](https://doi.org/10.1159/000070676).
- Barber R, McKeith I, Ballard C, and O'Brien J (2002). "Volumetric MRI study of the caudate nucleus in patients with dementia with Lewy bodies, Alzheimer's disease, and vascular dementia". *J. Neurol. Neurosurg. Psychiatr.* 72 (3): 406–407. DOI: [10.1136/jnnp.72.3.406](https://doi.org/10.1136/jnnp.72.3.406).
- Bellebaum C, Koch B, Schwarz M, and Daum I (2008). "Focal basal ganglia lesions are associated with impairments in reward-based reversal learning". *Brain* 131 (3): 829–841. DOI: [10.1093/brain/awn011](https://doi.org/10.1093/brain/awn011).
- Bookstein FL (2001). "'Voxel-based morphometry' should not be used with imperfectly registered images". *Neuroimage* 14 (6): 1454–1462. DOI: [10.1006/nimg.2001.0770](https://doi.org/10.1006/nimg.2001.0770).
- Borroni B, Turla M, Bertasi V, Agosti C, Gilberti N, and Padovani A (2008). "Cognitive and behavioral assessment in the early stages of neurodegenerative extrapyramidal syndromes". *Arch. Gerontol. Geriatr.* 47 (1): 53–61. DOI: [10.1016/j.archger.2007.07.005](https://doi.org/10.1016/j.archger.2007.07.005).
- Braak H and Braak E (1990). "Alzheimer's disease: striatal amyloid deposits and neurofibrillary changes". *J. Neuropathol. Exp. Neurol.* 49 (3): 215–224. DOI: [10.1097/00005072-199005000-00003](https://doi.org/10.1097/00005072-199005000-00003).
- Braak H and Braak E (1991). "Alzheimer's disease affects limbic nuclei of the thalamus". *Acta Neuropathol.* 81 (3): 261–268. DOI: [10.1007/BF00305867](https://doi.org/10.1007/BF00305867).
- Callen DJ, Black SE, Gao F, Caldwell CB, and Szalai JP (2001). "Beyond the hippocampus: MRI volumetry confirms widespread limbic atrophy in AD". *Neurology* 57 (9): 1669–1674. DOI: [10.1212/WNL.57.9.1669](https://doi.org/10.1212/WNL.57.9.1669).
- Dahlin E, Neely AS, Larsson A, Backman L, and Nyberg L (2008). "Transfer of learning after updating training mediated by the striatum". *Science* 320 (5882): 1510–1512. DOI: [10.1126/science.1155466](https://doi.org/10.1126/science.1155466).
- de Leon MJ, Convit A, DeSanti S, Golomb J, Tarshish C, et al. (1995). "The hippocampus in aging and Alzheimer's disease". *Neuroimaging Clin. N. Am.* 5 (1): 1–17.
- de Leon MJ, Golomb J, Convit A, DeSanti S, McRae TD, and George AE (1993). "Measurement of medial temporal lobe atrophy in diagnosis of Alzheimer's disease". *Lancet* 341 (8837): 125–126. DOI: [10.1016/0140-6736\(93\)92610-6](https://doi.org/10.1016/0140-6736(93)92610-6).
- Emre M (2003). "What causes mental dysfunction in Parkinson's disease?" *Mov. Disord.* 18 Suppl 6: 63–71. DOI: [10.1002/mds.10565](https://doi.org/10.1002/mds.10565).

- Ferrarini L, Palm WM, Olofsen H, van Buchem MA, Reiber JH, and Admiraal-Behloul F (2006). "Shape differences of the brain ventricles in Alzheimer's disease". *Neuroimage* 32 (3): 1060–1069. DOI: [10.1016/j.neuroimage.2006.05.048](https://doi.org/10.1016/j.neuroimage.2006.05.048).
- Folstein MF, Folstein SE, and McHugh PR (1975). "'Mini-mental state'. A practical method for grading the cognitive state of patients for the clinician". *J. Psychiatr. Res.* 12 (3): 189–198. DOI: [10.1016/0022-3956\(75\)90026-6](https://doi.org/10.1016/0022-3956(75)90026-6).
- Frisoni GB and Whitwell JL (2008). "How fast will it go, doc? New tools for an old question from patients with Alzheimer disease". *Neurology* 70 (23): 2194–2195. DOI: [10.1212/01.wnl.0000313844.18381.a9](https://doi.org/10.1212/01.wnl.0000313844.18381.a9).
- Geng DY, Li YX, and Zee CS (2006). "Magnetic resonance imaging-based volumetric analysis of basal ganglia nuclei and substantia nigra in patients with Parkinson's disease". *Neurosurgery* 58 (2): 256–262. DOI: [10.1227/01.NEU.0000194845.19462.7B](https://doi.org/10.1227/01.NEU.0000194845.19462.7B).
- Graybiel AM (2005). "The basal ganglia: learning new tricks and loving it". *Curr. Opin. Neurobiol.* 15 (6): 638–644. DOI: [10.1016/j.conb.2005.10.006](https://doi.org/10.1016/j.conb.2005.10.006).
- Herrero MT, Barcia C, and Navarro JM (2002). "Functional anatomy of thalamus and basal ganglia". *Childs Nerv. Syst.* 18 (8): 386–404. DOI: [10.1007/s00381-002-0604-1](https://doi.org/10.1007/s00381-002-0604-1).
- Horinek D, Varjassyova A, and Hort J (2007). "Magnetic resonance analysis of amygdalar volume in Alzheimer's disease". *Curr. Opin. Psychiatry* 20 (3): 273–277. DOI: [10.1097/YC0.0b013e3280ebb613](https://doi.org/10.1097/YC0.0b013e3280ebb613).
- Houtchens MK, Benedict RH, Killiany R, Sharma J, Jaisani Z, et al. (2007). "Thalamic atrophy and cognition in multiple sclerosis". *Neurology* 69 (12): 1213–1223. DOI: [10.1212/01.wnl.0000276992.17011.b5](https://doi.org/10.1212/01.wnl.0000276992.17011.b5).
- Jack CR, Petersen RC, Xu YC, O'Brien PC, Smith GE, et al. (1999). "Prediction of AD with MRI-based hippocampal volume in mild cognitive impairment". *Neurology* 52 (7): 1397–1403. DOI: [10.1212/WNL.52.7.1397](https://doi.org/10.1212/WNL.52.7.1397).
- Jenkinson M, Bannister P, Brady M, and Smith S (2002). "Improved optimization for the robust and accurate linear registration and motion correction of brain images". *Neuroimage* 17 (2): 825–841.
- Jenkinson M and Smith S (2001). "A global optimisation method for robust affine registration of brain images". *Med Image Anal* 5 (2): 143–156.
- Karas GB, Scheltens P, Rombouts SA, Visser PJ, van Schijndel RA, et al. (2004). "Global and local gray matter loss in mild cognitive impairment and Alzheimer's disease". *Neuroimage* 23 (2): 708–716. DOI: [10.1016/j.neuroimage.2004.07.006](https://doi.org/10.1016/j.neuroimage.2004.07.006).
- Karas G, Scheltens P, Rombouts S, van Schijndel R, Klein M, et al. (2007). "Precuneus atrophy in early-onset Alzheimer's disease: a morphometric structural MRI study". *Neuroradiology* 49 (12): 967–976. DOI: [10.1007/s00234-007-0269-2](https://doi.org/10.1007/s00234-007-0269-2).

- Kassubek J, Juengling FD, Ecker D, and Landwehrmeyer GB (2005). "Thalamic atrophy in Huntington's disease co-varies with cognitive performance: a morphometric MRI analysis". *Cereb. Cortex* 15 (6): 846–853. DOI: [10.1093/cercor/bhh185](https://doi.org/10.1093/cercor/bhh185).
- Klunk WE, Price JC, Mathis CA, Tsopelas ND, Lopresti BJ, et al. (2007). "Amyloid deposition begins in the striatum of presenilin-1 mutation carriers from two unrelated pedigrees". *J. Neurosci.* 27 (23): 6174–6184. DOI: [10.1523/JNEUROSCI.0730-07.2007](https://doi.org/10.1523/JNEUROSCI.0730-07.2007).
- Laakso MP, Soininen H, Partanen K, Helkala EL, Hartikainen P, et al. (1995). "Volumes of hippocampus, amygdala and frontal lobes in the MRI-based diagnosis of early Alzheimer's disease: correlation with memory functions". *J. Neural Transm.-Park. Dis. Dement. Sect.* 9 (1): 73–86. DOI: [10.1007/BF02252964](https://doi.org/10.1007/BF02252964).
- McKhann G, Drachman D, Folstein M, Katzman R, Price D, and Stadlan EM (1984). "Clinical diagnosis of Alzheimer's disease: report of the NINCDS-ADRDA Work Group under the auspices of Department of Health and Human Services Task Force on Alzheimer's Disease". *Neurology* 34 (7): 939–944. DOI: [10.1212/WNL.34.7.939](https://doi.org/10.1212/WNL.34.7.939).
- Newman J (1995). "Thalamic contributions to attention and consciousness". *Conscious. Cogn.* 4 (2): 172–193. DOI: [10.1006/ccog.1995.1024](https://doi.org/10.1006/ccog.1995.1024).
- Patenaude B, Smith SM, Kennedy DN, and Jenkinson M (2007a). *Bayesian shape and appearance models, FMRIB technical report TR07BP1*. London. URL: <https://www.fmrib.ox.ac.uk/datasets/techrep/tr07bp1/tr07bp1.pdf> (visited on 09/10/2018).
- Patenaude B, Smith SM, Kennedy DN, and Jenkinson M (2007b). "FIRST-FMRIB's integrated registration and segmentation tool". In: *Human Brain Mapping Conference*, 420–428.
- Roth M, Huppert FA, Mountjoy CQ, and Tym E (1988). *CAMDEX-R the Cambridge examination for mental disorders of the elderly*. Cambridge, UK: Cambridge University Press.
- Saykin AJ, Wishart HA, Rabin LA, Santulli RB, Flashman LA, et al. (2006). "Older adults with cognitive complaints show brain atrophy similar to that of amnesic MCI". *Neurology* 67 (5): 834–842. DOI: [10.1212/01.wnl.0000234032.77541.a2](https://doi.org/10.1212/01.wnl.0000234032.77541.a2).
- Scheltens P, Leys D, Barkhof F, Huglo D, Weinstein HC, et al. (1992). "Atrophy of medial temporal lobes on MRI in 'probable' Alzheimer's disease and normal ageing: diagnostic value and neuropsychological correlates". *J. Neurol. Neurosurg. Psychiatr.* 55 (10): 967–972. DOI: [10.1136/jnnp.55.10.967](https://doi.org/10.1136/jnnp.55.10.967).
- Smith AD (2002). "Imaging the progression of Alzheimer pathology through the brain". *Proc. Natl. Acad. Sci. U.S.A.* 99 (7): 4135–4137. DOI: [10.1073/pnas.082107399](https://doi.org/10.1073/pnas.082107399).
- Smith CD, Chebrolu H, Wekstein DR, Schmitt FA, Jicha GA, et al. (2007). "Brain structural alterations before mild cognitive impairment". *Neurology* 68 (16): 1268–1273. DOI: [10.1212/01.wnl.0000259542.54830.34](https://doi.org/10.1212/01.wnl.0000259542.54830.34).
- Smith SM, De Stefano N, Jenkinson M, and Matthews PM (2001). "Normalized accurate measurement of longitudinal brain change". *J. Comput. Assist. Tomogr.* 25 (3): 466–475. URL: http://journals.lww.com/jcat/Fulltext/2001/05000/Normalized_Accurate_Measurement_of_Longitudinal.22.aspx (visited on 09/10/2018).

- Smith SM, Jenkinson M, Woolrich MW, Beckmann CF, Behrens TE, et al. (2004). "Advances in functional and structural MR image analysis and implementation as FSL". *Neuroimage* 23 Suppl 1: S208–219. DOI: [10.1016/j.neuroimage.2004.07.051](https://doi.org/10.1016/j.neuroimage.2004.07.051).
- Smith SM, Zhang Y, Jenkinson M, Chen J, Matthews PM, et al. (2002). "Accurate, robust, and automated longitudinal and cross-sectional brain change analysis". *Neuroimage* 17 (1): 479–489. DOI: [10.1006/nimg.2002.1040](https://doi.org/10.1006/nimg.2002.1040).
- van der Flier WM, van Buchem MA, Weverling-Rijnsburger AW, Mutsaers ER, Bollen EL, et al. (2004). "Memory complaints in patients with normal cognition are associated with smaller hippocampal volumes". *J. Neurol.* 251 (6): 671–675. DOI: [10.1007/s00415-004-0390-7](https://doi.org/10.1007/s00415-004-0390-7).
- Van der Werf YD, Witter MP, Uylings HB, and Jolles J (2000). "Neuropsychology of infarctions in the thalamus: a review". *Neuropsychologia* 38 (5): 613–627. DOI: [10.1016/S0028-3932\(99\)00104-9](https://doi.org/10.1016/S0028-3932(99)00104-9).
- Wolf H, Julin P, Gertz HJ, Winblad B, and Wahlund LO (2004). "Intracranial volume in mild cognitive impairment, Alzheimer's disease and vascular dementia: evidence for brain reserve?" *Int. J. Geriatr. Psychiatr.* 19 (10): 995–1007. DOI: [10.1002/gps.1205](https://doi.org/10.1002/gps.1205).
- Yesavage JA and Sheikh JI (1986). "Geriatric depression scale (GDS) recent evidence and development of a shorter version". *Clin. Gerontol.* 5 (1-2): 165–173. DOI: [10.1300/J018v05n01_09](https://doi.org/10.1300/J018v05n01_09).
- Zhang Y, Brady M, and Smith S (2001). "Segmentation of brain MR images through a hidden Markov random field model and the expectation-maximization algorithm". *IEEE Trans. Med. Imaging* 20 (1): 45–57. DOI: [10.1109/42.906424](https://doi.org/10.1109/42.906424).

CHAPTER 3

Shape abnormalities of the striatum in AD

Laura W de Jong

Luca Ferrarini

Jeroen van der Grond

Julien R Milles

Johan HC Reiber

Rudi GJ Westendorp

Edward LEM Bollen

Huub AM Middelkoop

Mark A van Buchem

Adapted from J Alzheimers Dis. 2011;23(1):49-59. doi: [10.3233/JAD-2010-101026](https://doi.org/10.3233/JAD-2010-101026).

ABSTRACT

Post mortem studies show pathological changes in the striatum in Alzheimer's disease (AD). Here, we examine the surface of the striatum in AD and assess whether changes of the surface are associated with impaired cognitive functioning. The shape of the striatum (nucleus accumbens, caudate nucleus, and putamen) was compared between 35 AD patients and 35 individuals without cognitive impairment. The striatum was automatically segmented from 3D T1 magnetic resonance images and automatic shape modeling tools (Growing Adaptive Meshes) were applied for morphometric analysis. Repeated permutation tests were used to identify locations of consistent shape deformities of the striatal surface in AD. Linear regression models, corrected for age, gender, educational level, head size, and total brain parenchymal volume were used to assess the relation between cognitive performance and local surface deformities. In AD patients, differences of shape were observed on the medial head of the caudate nucleus and on the ventral lateral putamen, but not on the accumbens. The head of the caudate nucleus and ventral lateral putamen are characterized by extensive connections with the orbitofrontal and medial temporal cortices. Severity of cognitive impairment was associated with the degree of deformity of the surfaces of the accumbens, rostral medial caudate nucleus, and ventral lateral putamen. These findings provide further evidence for the hypothesis that in AD primarily associative and limbic cerebral networks are affected.

INTRODUCTION

Histological studies have demonstrated pathological changes in the striatum of Alzheimer's disease (AD) patients. These changes comprise the presence of diffuse plaques throughout the striatum (Gearing, Levey, and Mirra 1997) and the presence of neurofibrillary tangles in mainly large striatal nerve cells (Oyanagi et al. 1991; Oyanagi et al. 1987). In *in vivo* studies, using magnetic resonance imaging (MRI), atrophy has been observed in the caudate nucleus (Karas et al. 2003) and putamen (de Jong et al. 2008) of AD patients. Furthermore, evidence for the occurrence of striatal degeneration early in the development of AD is accumulating. In a structural MRI study, atrophy of the basal forebrain, including the ventral striatum, has been found to precede the development of dementia (Hall et al. 2008). In a Pittsburgh compound B positron emission tomography study of a familial form of AD, amyloid depositions have been observed well before the onset of cognitive symptoms (Klunk et al. 2007) and . It is not known, however, whether striatal atrophy is a diffuse process or limited to parts of the striatum and whether it relates to impaired performance on certain cognitive tasks.

The human striatum comprises the nucleus accumbens, caudate nucleus, and putamen and is regarded as the major input nucleus of the basal ganglia, receiving afferents from the entire cortex, thalamus, and substantia nigra. Efferents from the striatum run to the internal and external parts of the globus pallidus, subthalamic nucleus, and substantia nigra pars reticulata, and from these structures output pathways arise to the thalamus, superior colliculus and pedunculopontine tegmental nucleus (Gerfen 1992). Via the thalamus feedback is given to the striatum and cortex, predominantly the frontal cortex (Herrero, Barcia, and Navarro 2002). The striatum contains limbic, associative, and sensorimotor subregions, a division derived from the connections with functionally different cortical areas. This functional subdivision does not follow the anatomical boundaries such as those between caudate and putamen, but exerts a ventromedial to dorsolateral gradient (Voorn et al. 2004).

Knowledge on the functions of the basal ganglia is also based on observations in pathological conditions and experimental animal studies. Basal ganglia diseases lead to profound motor and cognitive disorders; for instance dyskinesia in Huntington's disease, diminished motor function and initiation of motor tasks in Parkinson's disease, tics in Tourette's syndrome, and recurrent obsessions and compulsions in obsessive compulsive disorders (Utter and Basso 2008). Lesions in the striatum give rise to diverse motor and cognitive disturbances, most commonly dystonia and abulia (Bhatia and Marsden 1994). Based on these clinical observations, the striatum is believed to play an important role in choosing and switching between competing behaviors (Parkinson et al. 2000), reinforcement learning processes (Poldrack and Packard 2003), procedural memory and

habit formation (Graybiel 2008), and working memory (Landau et al. 2009). Due to the variety of networks the striatum takes part in and due to the variety of functions of different parts of the striatum, the location of pathological changes within the striatum may determine the symptoms that arise. A region-specific approach is therefore critical when studying the striatum. Volumetric analyses are limited to a crude division of the striatum along anatomical landmarks, which disregards the functional heterogeneity of the structure. Furthermore, contrast differences on MRI within the striatum are insufficient to identify different functional parts. Shape analysis, however, captures details on locations of atrophy and allows a regional assessment of areas related to cognitive symptoms along the surface of the structure.

Here, we further investigated the involvement of the striatum in AD and possible association with cognitive performance. The striatal shapes of 35 AD patients to those of 35 memory complainers (MCs) with normal cognitive test scores were compared. First, the locations of consistent significant shape changes in AD were assessed. Secondly, the degree of local surface deformities was related to performance on the Cambridge Cognitive Examination-Revised (CAMCOG-R). We postulate that especially the ventral striatal areas, anatomically connected to functional networks mostly affected in AD, i.e., the limbic and associative cortices, would show atrophy in AD. In addition, we postulated that shape abnormalities in these same areas related to impaired cognitive performance.

METHODS

Subjects and study design

Study and control subjects were recruited from the population who visited the outpatient's memory clinic of our institution between January 1, 2006 and May 1, 2008. Each subject was examined according to a standardized protocol, including a whole brain MRI examination, neuropsychological screening (including the CAMCOG-R (Roth et al. 1988), a screening test for cognitive performance, and Geriatric Depression Scale (GDS) (Yesavage and Sheikh 1986), and a general medical and neurological examination by a geriatrician and neurologist respectively. Per subject, all tests took place within a 2-week span. In a multidisciplinary meeting, patients with abnormal test results were diagnosed with possible or probable AD, other types of dementia, mild cognitive impairment (MCI), or a neurological or psychiatric disorder. The National Institute of Neurological and Communicative Disorders and Stroke and Alzheimer's Disease and Related Disorders Association (NINCDS-ADRDA) criteria were applied for diagnosing probable AD (pAD) (McKhann et al. 1984). Subjects with normal results on all cognitive tests were classified as memory complainers (MCs). Identified reasons for subjective memory

impairment experienced by the memory complainers included mild or severe depressions, and emotional psychosocial events such as the loss of a family member or problems at work. For over half of the memory complainers no explanation for the experienced memory decline was identified. For the current study, we excluded the following subjects from the entire population ($n = 399$): left-handed subjects ($n = 35$), people with cognitive deficits who did not meet the criteria for probable AD, including the category of MCI ($n = 141$); other forms of dementia ($n = 11$) e.g., frontotemporal dementia, Lewy body disease, vascular dementia, Parkinson's dementia; other neurological/psychiatric disorders ($n = 35$), e.g., normal pressure hydrocephalus, intracranial tumors, stroke etc.; severe mood disorders with GDS > 10 ; alcohol abuse ($n=8$); insufficient scan quality ($n = 4$). In order to minimize confounding effects in the shape analysis we selected from the remaining population ($n = 165$) two complete data sets of 35 probable AD patients and 35 MCs that matched in age, gender and years of education. The institutional review board of the Leiden University Medical Center approved this cross-sectional case-control study.

Magnetic Resonance data acquisition

MRI was performed using a 3.0 Tesla whole body MRI scanner (Philips Medical Systems, Best, The Netherlands) with a Sense HEAD 8 channel coil. 3D T1-weighted MR images were coronally acquired with voxel dimensions: 0.875 mm (left-right) \times 0.875 mm (feet-head) \times 1.4 mm (anterior-posterior). Phase encoding directions were anterior-posterior and left-right, and frequency encoding direction was feet-head. Remaining settings were: TR = 9.8 ms; TE = 4.6 ms; flip angle = 8°; section thickness = 1.2 mm; number of sections = 120; no section gap; whole brain coverage; FOV = 224 mm; matrix = 192, reconstruction matrix = 256 \times 256. CLEAR inhomogeneity correction was applied. Routine T2-weighted and fluid attenuated inversion recovery (FLAIR) weighted scans were performed to identify out large infarcts and mass lesions.

Automated segmentation of the striatum

Automated segmentation and volume estimation of the nucleus accumbens, caudate nucleus, putamen, and globus pallidus was performed using FIRST (FMRIB's Integrated Registration and Segmentation Tool) (Patenaude et al. 2007), part of FMRIB's Software Library (FSL) (SM Smith, Jenkinson, et al. 2004). We used the *run_first_all* script with default options, followed by a boundary correction with $z=3$. The segmentations of nucleus accumbens, caudate nucleus, and putamen were combined to form the striatum. All segmentations of our study sample were visually inspected for errors,

but none were found. SIENAX (Structural Image Evaluation, using Normalization, of Atrophy, X-sectional), also part of FSL, was used to estimate global brain tissue volumes (SM Smith, De Stefano, et al. 2001; SM Smith, Zhang, et al. 2002) and a scaling factor, used for normalization for head size.

Assessment of the relation of striatal volumes and cognitive performance

R 2.10.1 was used for data analysis (R Core Team 2009). Differences in mean age, gender, education in years, head size normalization factor, brain parenchymal volume (BPV), CAMCOG-R scores, and striatal volumes were tested by a two sample unpaired *t*-test. Relations of striatal volumes, normalized for head size, with cognition were also estimated. First corrections for age, gender, educational level, and BPV were made by means of linear regression analysis: expected values of CAMCOG-R score were calculated from regression of CAMCOG-R score on age, gender, education in years. Subsequently, residuals were correlated to normalized volumes of total striatum, caudate, putamen and nucleus accumbens. A *p*-value ≤ 0.05 was considered statistically significant.

Morphometric analysis of the striatum

Comparison of striatal shapes of AD and MC

Shape modeling The striatal segmentations by FIRST, registered to MNI (Montreal Neurological Institute) 152 standard space by means of affine transformation with 12 degrees of freedom, were used for quantitative analysis of local shape changes. Growing and Adaptive MESHes (GAMEs) method was adopted, which has been described previously and discussed here in essence (Ferrarini, Olofsen, et al. 2007). Left and right striatal hemisphere were separately analyzed, each formed by combining the caudate nucleus, putamen, and nucleus accumbens segmentations of that hemisphere.

In the growing phase of GAMEs a reference mesh for both left and right striatum was generated. First, a voxel-wise spatial probability map of the segmentation masks of the MC group was generated, by voxel counting at each voxel location. Voxels labeled as striatum in more than 20% of the MC masks formed the average segmentation volume, which formed the basis on which a mesh was grown. This threshold was chosen based on visual comparison of different meshes built with different thresholds (ranging from 10%–90%). We found thresholds above 60% to loose shape characteristics of the striatum, and thresholds below 15% needed exponentially more nodes to form the reference mesh. We assumed that a relatively large reference model would represent the “healthy” shape of the striatum, least affected by degenerative processes accompanying age. Therefore, a low threshold (20%) was chosen to create a relatively large reference model, but for

which approximately an average amount of nodes was needed to form the model (i.e., 605 for the left striatum and 645 for the right striatum). Accuracy for the mesh was set at 2 mm isotropic per node: considering that T1 structural images were normalized to 1 mm isotropic, higher resolutions would approach the voxel resolution, thus being meaningless. This reference mesh topology was frozen to keep the number of nodes and edges constant in the following steps.

In phase two of GAMES, the reference mesh was adapted to all striatal segmentation masks of both 35 MCs and 35 AD patients, thus 70 meshes for each striatal hemisphere were generated. The adaptation was based on the topology-preserving Kohonen self-organizing map algorithm (1990). The outcome of GAMES was a set of comparable meshes, also defined as a 3D Point Distribution Model (PDM). In this model each node (i.e., location) of the mesh had corresponding nodes through all other instances and therefore the meshes were locally comparable. Previous work has shown that corresponding nodes of meshes generated with GAMES are indeed representative of similar anatomical locations (Ferrarini, Palm, et al. 2008).

Statistical analysis of local shape differences between MCs and AD-patients Local shape differences between the MCs and AD patients were assessed using non-parametric repeated permutation tests and a bootstrapping technique (Ferrarini, Palm, et al. 2008). The advantage of repeated tests on bootstrapped subsamples is to reduce the bias of the results to the particular subjects included in the analysis. This leads to statistically more robust results, since only those locations are identified that are systematically different for different subsamples of the MC and AD group. Bootstrapping was set to 60% of the study sample, i.e., the entire set of 35 + 35 subjects was randomly subsampled to 21 + 21 subjects, and this was repeated 25 times ($N^{iter} = 25$).

Permutation tests were performed for each subsampled set (with the number of permutations set at 10,000). Each node in the 3D PDM was surrounded by two 3D clouds of 21 points (one cloud per study group). Non-parametric permutation tests were applied in case part of nodes was surrounded by clouds of points that were not normally distributed. Hotelling's T^2 statistic (HT^2) was used (1931), which is a simple generalization to multidimensional data of the Student's t -test. First, the average location and covariance matrix of each cloud were evaluated, from which the HT^2 statistic for the two groups was estimated ($HT_{original}^2$). Subsequently, the groups were randomly mixed 10,000 times, and for each time the corresponding Hotelling's (HT^2) statistic was calculated (HT_i^2 , $i = 1.10000$). The distribution of the HT_i^2 respects the null hypothesis for the two clouds to come from the same distribution. The percentage of HT_i^2 values higher than ($HT_{original}^2$) was considered the p -value for the given node. Repeating this procedure for each node resulted in a p -value map, in which each mesh node was given a

p -value for the null hypothesis that the two groups had similar local shape distributions in space. Given the entire set of 25 p -maps, the median p -value per node was evaluated. A p -value ≤ 0.05 for a node was considered significant. Moreover, a consistency index (CI) per node was assessed, representing the frequency a given node was found significantly different over the 25 iterations. The direction and length of the displacement vectors, needed to deform the average shape of the striatum of the MC population into the average shape of striatum of the AD population, were also estimated.

To ascertain that surface deformity was due to the pathology investigated and not to shifting of the whole structure, the centers of gravity between the groups were compared. Differences in center of gravity were nonsignificant and within the width of one voxel.

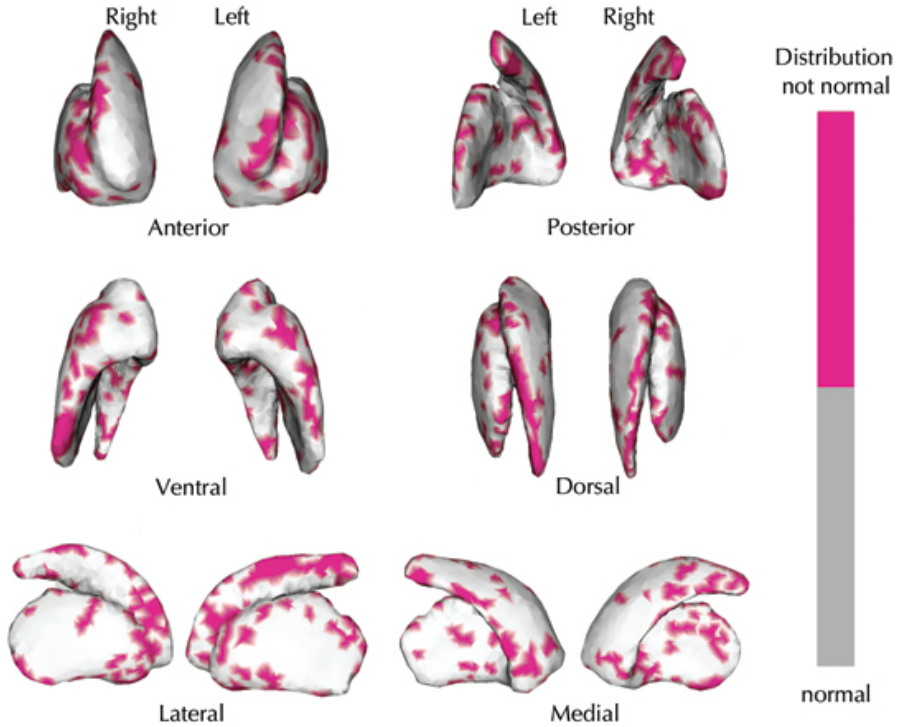
Assessment of the relation of striatal surface deformity with cognitive performance For each node location, the principal component of the associated cloud of points, consisting of 35 points for AD and 35 for MCs, was estimated. Subsequently, each point of the cloud was projected along the main eigenvector, with positive projections (with respect to the reference node on the reference mesh) pointing inwardly. The projection lengths around the reference nodes were tested on normality with the Lilliefors test (Lilliefors 1967). For each striatal hemisphere, approximately 25% of the nodes were not normally distributed ($p < 0.05$), however locations of not normally distributed point clouds were dispersed over the surface (figure 1) and applying false discovery rate corrections proved all the p -values to be nonsignificant. We therefore proceeded with a linear regression analysis. First, the CAMCOG-R score was regressed against age, gender, educational level, and BPV in a linear model. The residuals from these models were then linearly regressed against the projection lengths around each striatal surface node. Note that the projection lengths were calculated in standard space and thus normalized for head size. The direction, positive or negative, of the association of surface deformity with cognitive score was determined, together with r^2 and p -values of the model. A $p \leq 0.05$ was considered significant.

RESULTS

Group characteristics

Successful matching of the study groups MCs and AD was verified; no significant differences in age, gender, educational level, and scaling factor for head size normalization were found (table 1). Groupwise differences existed in total CAMCOG-R score and all subscores ($t = 8.4$, $df = 39$, $p < 0.001$), BPV ($t = 2.2$, $df = 68$, $p = 0.03$), total volumes of left ($t = 2.0$, $df = 61$, $p = 0.048$) and right striatum ($t = 2.2$, $df = 68$,

Figure 1: Normality of the point distributions surrounding the striatal surface nodes



The distributions of the point clouds surrounding each node on the surface of the striatum that were not normally distributed are colored red. Normality was tested with the Lilliefors test. 25% of the point clouds of the left striatum were not normally distributed and 24% of the right striatum (p -value < 0.05). Applying false discovery rate corrections proved all p -values to be not significant.

$p = 0.03$), and volume of left putamen ($t = 2.9$, $df = 63$, $p = 0.004$). Mean volumes of left and right caudate, right putamen, and left and right accumbens were smaller in AD, but did not reach statistical difference.

Table 1: Demographics & group characteristics

| | MCs ($n = 35$) Mean (SE) | AD ($n = 25$) Mean (SE) | Two-sample unpaired t -test t -value (df) | Cohen's d Effect size |
|-----------------------------|-------------------------------|------------------------------|------------------------------------------------------|----------------------------|
| Age in years | 72.4 (1.4) | 73.1 (1.4) | 0.31 (68) | 0.07 |
| Sex (Male : Female) | 15:20 | 15:20 | 0 (68) | 0.00 |
| Education | 11.2 (0.6) | 10.0 (0.7) | -1.20 (64) | -0.29 |
| Scaling factor ^a | 1.33 (0.02) | 1.34 (0.02) | -0.21 (67) | -0.05 |
| CAMCOG-R | 89.1 (0.9) | 62.7 (2.8) | -8.36 (38)*** | -1.44 |
| Subscores: | | | | |
| Orientation | 9.1 (0.1) | 6.5 (0.4) | -5.55 (40)*** | -1.11 |
| Language | 26.5 (0.3) | 21.3 (0.7) | -5.92 (44)*** | -1.17 |
| Memory | 21.1 (0.4) | 12.3 (1.0) | -7.60 (43)*** | -1.34 |
| Attention | 6.3 (0.1) | 3.8 (0.4) | -5.59 (40)*** | -1.13 |
| Visuo | 5.1 (0.1) | 2.8 (0.3) | -7.15 (46)*** | -1.33 |
| Executive | 14.5 (0.4) | 8.0 (0.7) | -7.71 (53)*** | -1.38 |
| Brain parenchyma | 1449 (16.1) | 1397 (17.0) | -2.23 (68)* | -0.52 |
| Striatum L | 13.2 (0.2) | 12.4 (0.3) | -2.01 (61)* | -0.47 |
| Striatum R | 14.3 (0.2) | 13.5 (0.2) | -2.20 (68)* | -0.51 |
| Caudate nucleus L | 5.5 (0.2) | 5.4 (0.2) | -0.34 (65) | -0.08 |
| Caudate nucleus R | 6.3 (0.2) | 5.9 (0.2) | -1.66 (68) | -0.39 |
| Putamen L | 7.0 (0.1) | 6.4 (0.2) | -2.94 (63)** | -0.67 |
| Putamen R | 7.5 (0.1) | 7.2 (0.2) | -1.49 (65) | -0.35 |
| N accumbens L | 0.68 (0.04) | 0.61 (0.03) | -1.44 (65) | -0.34 |
| N accumbens R | 0.49 (0.03) | 0.43 (0.03) | -1.20 (68) | -0.29 |

MCs, memory complainers; AD, Alzheimer patients; CAMCOG-R: Cambridge cognition examination Revised; BPV, total brain parenchymal volume; Striatum, consists of caudate nucleus, putamen, and nucleus accumbens; L, Left; R, Right

^a Scaling factor, used to normalize for head size

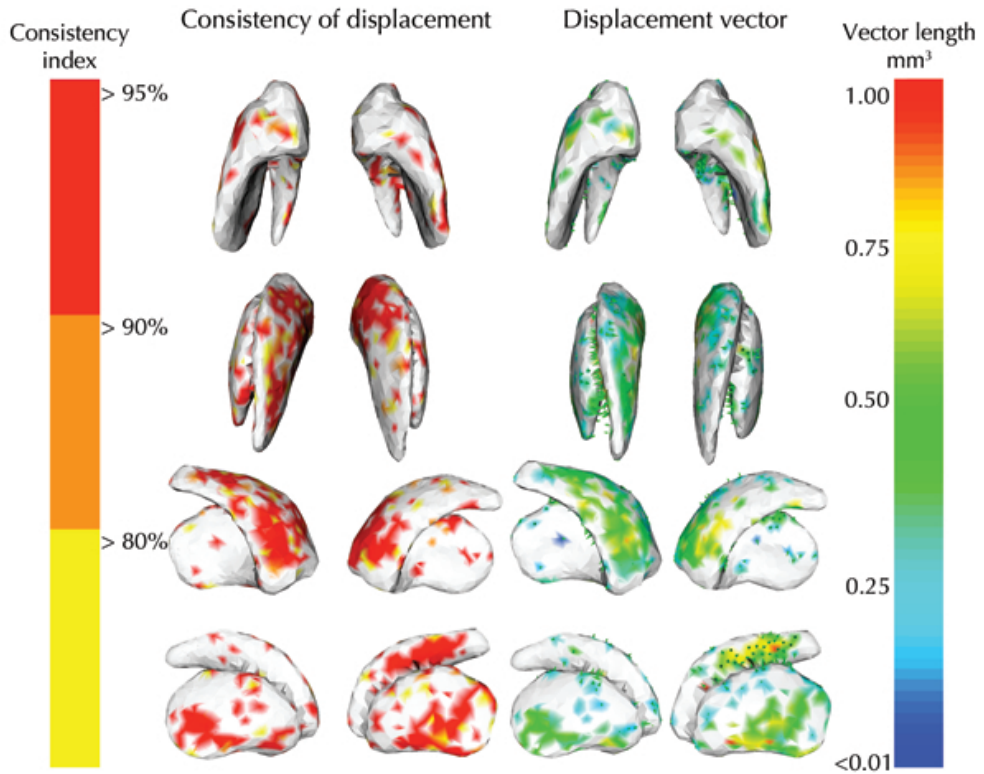
All volumes are in cm^3 and normalized for head size;

*** p -value < 0.0005; ** p -value < 0.005; * p -value < 0.05.

Local atrophy of the striatum in AD patients

Figure 2 summarizes the results of shape comparison between MCs and AD patients. Red colored areas were significantly different ($p < 0.05$) in > 95% of the repeated permutation tests, orange areas in > 90% of the tests, and yellow areas in > 80% of the tests. Symmetrical locations of significant consistent shape differences appeared in

Figure 2: Areas of significant striatal surface change in AD compared to MC



Consistency of displacement: the colored surface areas were significantly ($p < 0.05$) deformed in AD patients compared to MCs. Red areas were significantly different in more than 95% of the 25 iterations of the permutation tests, orange in more than 90%, and yellow in more than 80%.

Displacement vector: the length of the displacement vectors, needed to deform the surface of MC to AD, was color coded with red indicating a length of ≤ 1.00 mm to dark blue indicating < 0.01 mm. Outwardly directed displacement vectors were represented by green arrows on the surface. The displacement vectors of the lateral putamen and medial caudate were directed inwards.

both striatal hemispheres, i.e., the rostral medial caudate nucleus and ventral lateral putamen. Shape deformity in the left striatal hemisphere, however was more extended, i.e., 30.4% of total surface compared to 21.1% of the right hemisphere. On the left

striatum, areas of shape deformity on the caudate nucleus covered the medial wall with the largest confluent area on the ventral half of the caudate head and a smaller area on the lateral side of the caudate body. The left putamen showed areas of shape difference on the lateral side of the putamen, with the largest confluent areas on the ventral half. On the right striatum confluent areas of difference were found on the medial caudate head and ventral half of the lateral putamen. In both hemispheres, the medial sides of the putamen and the accumbens areas were virtually devoid of significant shape difference between the groups. Outward directions of the vector displacement of the surface nodes were displayed in green arrows. All areas of shape deformity were inwardly directed, except a small area on the left lateral caudate nucleus with outwardly directed arrows. The length of the displacement vectors were color coded showing the largest shape deformity in the ventral parts of the lateral putamen and in the caudate head between MCs and AD.

Table 2: Correlation of striatal volumes with CAMCOG-R score

| | | All subjects (n=70) | | MC (n=35) | | AD (n=35) | |
|-----------------|---|------------------------|----------------|----------------|----------------|----------------|----------------|
| | | R ^a | R ^b | R ^a | R ^b | R ^a | R ^b |
| Striatum | L | 0.41*** | 0.28* | 0.03 | -0.18 | 0.40* | 0.24 |
| | R | 0.25* | 0.13 | -0.12 | -0.27 | 0.10 | -0.04 |
| Caudate nucleus | L | 0.18 | 0.08 | -0.02 | -0.09 | 0.21 | 0.06 |
| | R | 0.10 | 0.02 | -0.15 | -0.17 | -0.13 | -0.23 |
| Putamen | L | 0.52*** | 0.41** | 0.06 | -0.18 | 0.51*** | 0.38* |
| | R | 0.27* | 0.19 | -0.10 | -0.29 | 0.24 | 0.16 |
| Accumbens | L | 0.18 | 0.09 | 0.06 | -0.17 | 0.07 | -0.02 |
| | R | 0.21 | 0.13 | 0.23 | -0.01 | 0.20 | 0.11 |

CAMCOG-R score, Cambridge cognition examination revised; L, Left; R, Right

^a Adjusted for age, gender, education in years, and head size.

^b Adjusted for age, gender, education in years, head size, and BPV.

*** p -value < 0.0005; ** p -value < 0.005; * p -value < 0.05.

Relation of striatal volumes and cognition

In the total sample CAMCOG-R score significantly decreased with decreasing volumes of total left striatum ($r = 0.41$, $p < 0.001$), total right striatum ($r = 0.25$, $p = 0.04$), left putamen ($r = 0.52$, $p < 0.001$), and right putamen ($r = 0.27$, $p = 0.03$). These associations were adjusted for age, gender, years of education, and head size. After additional correction for BPV decreasing CAMCOG-R score remained significantly related

to decreasing volumes of total left striatum ($r = 0.28$, $p = 0.02$) and left putamen ($r = 0.41$, $p < 0.001$). Performing the analysis separately for each group, associations of cognitive score with volume of the total left striatum ($r = 0.40$, $p = 0.02$) and left putamen ($r = 0.51$, $p = 0.003$) were found in the AD group, but no significant associations in the MC group (see table 2).

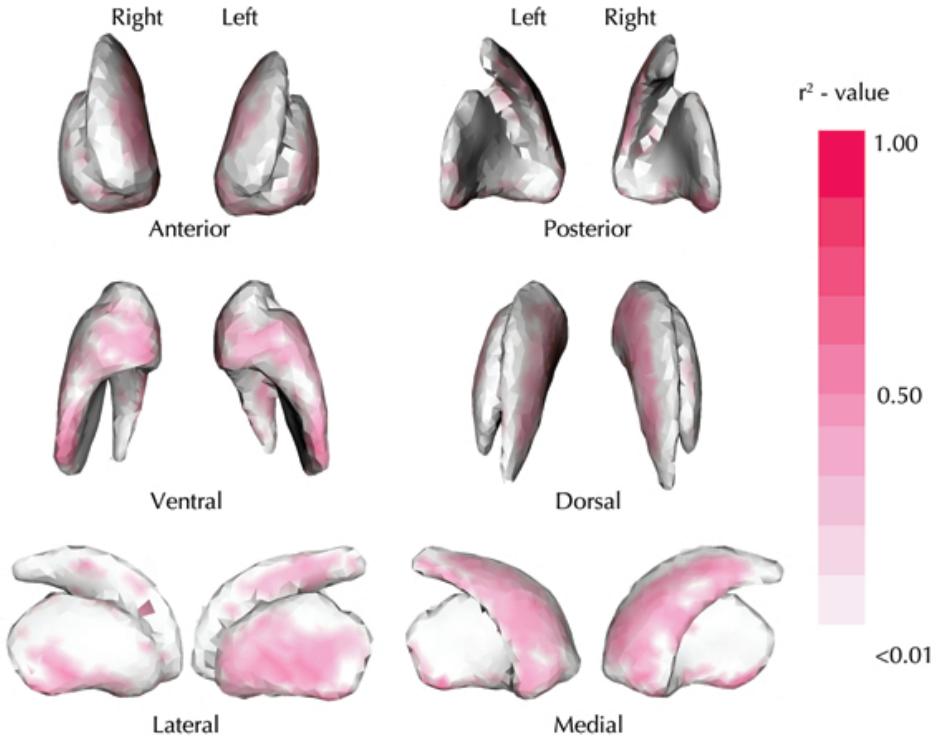
Relation of striatal shape and cognitive

Similar locations of surface deformity that associated with cognitive performance existed in both striatal hemispheres, after corrections for age, gender, years of education, BPV, and head size. The areas were, however, more extended on the left side with 40.1% of the total surface relating significantly to cognitive performance compared to 29.1% of the right striatal surface (figure 3). CAMCOG-R score in this study population positively related to surface deformity on the medial ventral caudate, lateral putamen, and accumbens areas. Strongest correlations were found on the left side with r^2 ranging from 0.05 to 0.30 and on the right with r^2 ranging from 0.05 to 0.27. The dorsal areas of the caudate and putamen, and the medial putamen did not significantly relate to CAMCOG-R score.

DISCUSSION

In this combined volumetric and morphometric analysis, shape abnormalities were observed in AD patients in the rostral medial caudate head and the ventral and lateral putamen when compared to memory complainers with normal cognitive test scores. This suggests that AD pathology predominantly affects the limbic and associative areas of the striatum. Furthermore, cognitive impairment related to the degree of surface deformity in the ventral areas of the caudate and putamen, and the accumbens area, but not to the dorsal areas. This association may be based on degenerative process in cognitively functional parts of the striatum or based on the disruption of the networks in which the striatum takes part. Atrophy of the striatum in AD has been described before, however, here we report on the occurrence of shape abnormalities selectively occurring in the ventral parts of the striatum and its relation to cognition. Our results are in agreement with multiple studies showing manifestation of AD pathology preferentially in the limbic and associative areas of the cerebrum (H Braak and E Braak 1991; Savioz et al. 2009). The present study design, however, is not suitable to dissociate an independent effect of striatal atrophy on cognitive symptoms in AD. Future studies are needed to assess whether striatal deformation is an early or late phenomenon in the development

Figure 3: Locations of striatal shape deformity related to cognitive performance



Surface areas of the striatum of which deformity significantly associated with CAMCOG-R score were colored red. All associations observed were negatively directed, meaning an increasing inward shape deformity in these areas related to a decreasing cognitive score. The r -value, estimated from a linear model corrected for age, gender, education in years, head size, and BPV for each surface node, was color coded with different shadings of red. Peak r^2 for the left striatum was 0.30 and for the right striatum 0.27. Forty percent of the left striatal surface associated significantly with CAMCOG-R score and 29% of the right striatum.

of AD and whether markers for striatal degeneration can improve risk prediction for AD in older people.

Selective degeneration of the striatum in AD is likely to underlie regional shape deformity found in the ventral caudate and putaminal areas. In histological studies on AD, a loss of the large cholinergic neurons was predominantly observed in the ventral stria-

tum. Neurofibrillary tangles were observed in the remaining cholinergic cells throughout the striatum (Oyanagi et al. 1987). The cholinergic interneuron network has extended arborizations and is tonically active (Wilson, Chang, and Kitai 1990). Moreover, it has been proposed that this network influences the activity of the entire striatum (Graybiel et al. 1994). The large cholinergic interneurons, however, are only a minority (1–2%) of all striatal cell types (Bolam, Wainer, and AD Smith 1984) and consequently, selective loss of these cells may not fully explain the significant surface deformity observed in this study. Another possible explanation for the observed shape deformity in the striatum in AD may be the presence of amyloid plaques triggering increased neural cell death in the striatum. Accumulation of amyloid in the striatum has been observed across different autosomal Alzheimer disease mutation types (Klunk et al. 2007; Villemagne et al. 2009) and related to loss of medium size spiny neurons in 12-month old APP^{swe}/PS1 Δ E9 transgenic mice compared to their wild type peers (Richner, Bach, and West 2009). Shape deformity could also be due to Wallerian degeneration following damage in other regions of the brain that are structurally connected to the striatum. Supportive for this hypothesis is a post mortem analysis of 20 cases observing that the occurrence of striatal changes paralleled the occurrence of neuritic plaques in the neocortex (Wolf et al. 1999).

Significant associations with cognitive decline were observed in the rostral medial caudate, ventral lateral putamen, but also in the nucleus accumbens. Previous studies have assigned reward and reinforcement learning tasks to the ventral striatum (Graybiel 2008; Haber and McFarland 1999) and together with the basolateral and extended amygdala the ventral striatum seems to be essential for stimulus associations to rewarding consequences of behavior (Gray 1999). Also, evidence is accumulating for anatomical substrates of incentive learning and habit formation in the rostral ventral parts of the caudate and putamen (Haber, Kim, et al. 2006). Atrophy of the putamen and the caudate nucleus has been related to the occurrence of neuropsychiatric symptoms in AD by others (Mega et al. 2000; Bruen et al. 2008). Our study shows that the areas of which deformity relates to cognitive impairment and AD are confined to the ventral parts of the putamen and caudate. Although, both volumetric and morphometric analysis were performed with corrections for global brain tissue volume, cognitive symptoms may still arise due to dysfunction elsewhere in the limbic and associative circuits in which the striatum takes part. The medial rostral part of the caudate nucleus and the rostral ventral putamen receive projections from the ventral medial prefrontal, orbitofrontal, and dorsal anterior cingulate cortices (Haber 2003), areas that are more affected in AD than other parts of the brain (Callen et al. 2001). Results of both volumetric and morphometric analyses show shape deformity and volume loss of the putamen in AD. The area of the ventral striatum caudal to the anterior commissure has not been studied extensively,

but a study on primates observed that this region is also part of the limbic striatum with afferents from the amygdala and a similar histochemical and cellular organization as the anterior ventral striatum (Fudge and Haber 2002). Also, part of the posterior ventral putamen, is regarded as the “visual striatum” forming a closed loop with the TE visual area of the inferotemporal lobe (Middleton and Strick 1996).

Another interesting finding of our study was the larger area of shape deformity and association with cognitive impairment in the left striatum, compared to the right. This is in agreement with several studies that described hemispherical asymmetrical findings for the hippocampus and orbitofrontal lobes in AD (Barnes et al. 2005; Raji et al. 2008). Also, our study included only right-handed persons, which may have increased the hemispherical dissimilarity.

We hypothesized that the entire limbic ventral striatum atrophies in AD, however, no difference of shape between AD and MC of the nucleus accumbens, which is part of the ventral striatum, was found. The nucleus accumbens is an essential part of the limbic striatum, receiving afferents from the ventral medial prefrontal cortex, amygdala, and hippocampus and integrating the information from these cortices (Gruber, Hussain, and O'Donnell 2009). We did find a relation of deformity of the accumbens with cognitive impairment. Shape deformity of the accumbens in AD cannot be excluded, based on these results only. There is evidence that part of the memory complainers have early stages of AD and may suffer striatal atrophy to a degree that diminishes the differences between the studied groups. Also, it may be that not all AD patients suffer shape abnormalities in the area of the accumbens or that our method is not sensitive enough for detection of shape deformity in this area.

Our results demonstrate the additional value of morphometric analysis as compared to a volumetric analysis in assessing changes in the striatum in AD patients. With volumetric analysis only, associations with cognitive decline were limited to the putamen. The morphological data also showed 1) shape deformity in the caudate nucleus, which associated with cognitive impairment and 2) localized shape deformity in especially the ventral half of the right putamen.

Lastly, some methodological limitations are of note. First, we used cross-sectional data for our determination of shape abnormalities in the striatum. Longitudinal data are needed to determine whether the shape deformity in the basal ganglia is a late or early phenomenon in the development AD and reflecting volume loss. Longitudinal data would also help assessing whether atrophy of the basal ganglia is primary or secondary to atrophy in other (limbic) brain regions, such as the hippocampus. The second important limitation of our study is that our control group consisted of memory complainers. Several studies revealed the presence of smaller left hippocampal volumes and decreased gray matter volumes among memory complainers, suggesting that this condition is an

early stage of AD in some patients (van der Flier et al. 2004; Saykin et al. 2006). However, the memory complainers form a relevant control group from a clinical perspective, since AD subjects need to be distinguished from MC and MCI cases. Also, if AD pathology is present, it is likely to be less pronounced than in demented patients, and the extent of striatal deformity may have been underestimated. A third limitation is that the CAMCOG-R score is a screening test for cognitive impairment and is not specifically aimed at detecting basal ganglia dysfunction. Future studies are needed to assess whether a specific cognitive function is affected by striatal atrophy in AD.

In conclusion, morphometric analysis of the striatum shows the occurrence of shape deformity in AD predominantly in the rostral medial part of the caudate nucleus and ventral lateral putamen in AD patients. These areas are known to participate in circuits with the medial temporal lobe and prefrontal cortex and were associated with cognitive impairment. Shape deformity of the accumbens was also associated with cognitive impairment, but was not significantly different between MCs and AD patients.

BIBLIOGRAPHY

- Barnes J, Scahill RI, Schott JM, Frost C, Rossor MN, and Fox NC (2005). "Does Alzheimer's disease affect hippocampal asymmetry? Evidence from a cross-sectional and longitudinal volumetric MRI study". *Dement. Geriatr. Cogn. Disord.* 19 (5-6): 338–344. DOI: [10.1159/000084560](https://doi.org/10.1159/000084560).
- Bhatia KP and Marsden CD (1994). "The behavioural and motor consequences of focal lesions of the basal ganglia in man". *Brain* 117 (4): 859–876. DOI: [10.1093/brain/117.4.859](https://doi.org/10.1093/brain/117.4.859).
- Bolam JP, Wainer BH, and Smith AD (1984). "Characterization of cholinergic neurons in the rat neostriatum. A combination of choline acetyltransferase immunocytochemistry, Golgi-impregnation and electron microscopy". *Neuroscience* 12 (3): 711–718. DOI: [10.1016/0306-4522\(84\)90165-9](https://doi.org/10.1016/0306-4522(84)90165-9).
- Braak H and Braak E (1991). "Alzheimer's disease affects limbic nuclei of the thalamus". *Acta Neuropathol.* 81 (3): 261–268. DOI: [10.1007/BF00305867](https://doi.org/10.1007/BF00305867).
- Bruen PD, McGeown WJ, Shanks MF, and Venneri A (2008). "Neuroanatomical correlates of neuropsychiatric symptoms in Alzheimer's disease". *Brain* 131 (9): 2455–2463. DOI: [10.1093/brain/awn151](https://doi.org/10.1093/brain/awn151).
- Callen DJ, Black SE, Gao F, Caldwell CB, and Szalai JP (2001). "Beyond the hippocampus: MRI volumetry confirms widespread limbic atrophy in AD". *Neurology* 57 (9): 1669–1674. DOI: [10.1212/WNL.57.9.1669](https://doi.org/10.1212/WNL.57.9.1669).
- de Jong LW, van der Hiele K, Veer IM, Houwing JJ, Westendorp RG, et al. (2008). "Strongly reduced volumes of putamen and thalamus in Alzheimer's disease: an MRI study". *Brain* 131 (12): 3277–3285. DOI: [10.1093/brain/awn278](https://doi.org/10.1093/brain/awn278).

- Ferrarini L, Olofsen H, Palm WM, van Buchem MA, Reiber JH, and Admiraal-Behloul F (2007). "GAMES: growing and adaptive meshes for fully automatic shape modeling and analysis". *Med. Image Anal.* 11 (3): 302–314. DOI: [10.1016/j.media.2007.03.006](https://doi.org/10.1016/j.media.2007.03.006).
- Ferrarini L, Palm WM, Olofsen H, van der Landen R, van Buchem MA, et al. (2008). "Ventricular shape biomarkers for Alzheimer's disease in clinical MR images". *Magn. Reson. Med.* 59 (2): 260–267. DOI: [10.1002/mrm.21471](https://doi.org/10.1002/mrm.21471).
- Fudge JL and Haber SN (2002). "Defining the caudal ventral striatum in primates: cellular and histochemical features". *J. Neurosci.* 22 (23): 10078–10082. URL: <http://www.jneurosci.org/content/22/23/10078> (visited on 09/10/2018).
- Gearing M, Levey AI, and Mirra SS (1997). "Diffuse plaques in the striatum in Alzheimer disease (AD): relationship to the striatal mosaic and selected neuropeptide markers". *J. Neuropathol. Exp. Neurol.* 56 (12): 1363–1370. DOI: [10.1097/00005072-199712000-00011](https://doi.org/10.1097/00005072-199712000-00011).
- Gerfen CR (1992). "The neostriatal mosaic: multiple levels of compartmental organization in the basal ganglia". *Annu. Rev. Neurosci.* 15: 285–320. DOI: [10.1146/annurev.ne.15.030192.001441](https://doi.org/10.1146/annurev.ne.15.030192.001441).
- Gray TS (1999). "Functional and anatomical relationships among the amygdala, basal forebrain, ventral striatum, and cortex. An integrative discussion". *Ann. N. Y. Acad. Sci.* 877: 439–444. DOI: [10.1111/j.1749-6632.1999.tb09281.x](https://doi.org/10.1111/j.1749-6632.1999.tb09281.x).
- Graybiel AM (2008). "Habits, rituals, and the evaluative brain". *Annu. Rev. Neurosci.* 31: 359–387. DOI: [10.1146/annurev.neuro.29.051605.112851](https://doi.org/10.1146/annurev.neuro.29.051605.112851).
- Graybiel AM, Aosaki T, Flaherty AW, and Kimura M (1994). "The basal ganglia and adaptive motor control". *Science* 265 (5180): 1826–1831. DOI: [10.1126/science.8091209](https://doi.org/10.1126/science.8091209).
- Gruber AJ, Hussain RJ, and O'Donnell P (2009). "The nucleus accumbens: a switchboard for goal-directed behaviors". *PLoS ONE* 4 (4): e5062. DOI: [10.1371/journal.pone.0005062](https://doi.org/10.1371/journal.pone.0005062).
- Haber SN (2003). "The primate basal ganglia: parallel and integrative networks". *J. Chem. Neuroanat.* 26 (4): 317–330. DOI: [10.1016/j.jchemneu.2003.10.003](https://doi.org/10.1016/j.jchemneu.2003.10.003).
- Haber SN, Kim KS, Maily P, and Calzavara R (2006). "Reward-related cortical inputs define a large striatal region in primates that interface with associative cortical connections, providing a substrate for incentive-based learning". *J. Neurosci.* 26 (32): 8368–8376. DOI: [10.1523/JNEUROSCI.0271-06.2006](https://doi.org/10.1523/JNEUROSCI.0271-06.2006).
- Haber SN and McFarland NR (1999). "The concept of the ventral striatum in nonhuman primates". *Ann. N. Y. Acad. Sci.* 877: 33–48. DOI: [10.1111/j.1749-6632.1999.tb09259.x](https://doi.org/10.1111/j.1749-6632.1999.tb09259.x).
- Hall AM, Moore RY, Lopez OL, Kuller L, and Becker JT (2008). "Basal forebrain atrophy is a presymptomatic marker for Alzheimer's disease". *Alzheimers. Dement.* 4 (4): 271–279. DOI: [10.1016/j.jalz.2008.04.005](https://doi.org/10.1016/j.jalz.2008.04.005).

- Herrero MT, Barcia C, and Navarro JM (2002). "Functional anatomy of thalamus and basal ganglia". *Childs Nerv. Syst.* 18 (8): 386–404. DOI: [10.1007/s00381-002-0604-1](https://doi.org/10.1007/s00381-002-0604-1).
- Hotelling H (1931). "The generalization of 'Student's' ratio." *Ann. Math. Statist.* 2 (3): 360–378. DOI: [10.1214/aoms/1177732979](https://doi.org/10.1214/aoms/1177732979).
- Karas GB, Burton EJ, Rombouts SA, van Schijndel RA, O'Brien JT, et al. (2003). "A comprehensive study of gray matter loss in patients with Alzheimer's disease using optimized voxel-based morphometry". *Neuroimage* 18 (4): 895–907. DOI: [10.1016/S1053-8119\(03\)00041-7](https://doi.org/10.1016/S1053-8119(03)00041-7).
- Klunk WE, Price JC, Mathis CA, Tsopelas ND, Lopresti BJ, et al. (2007). "Amyloid deposition begins in the striatum of presenilin-1 mutation carriers from two unrelated pedigrees". *J. Neurosci.* 27 (23): 6174–6184. DOI: [10.1523/JNEUROSCI.0730-07.2007](https://doi.org/10.1523/JNEUROSCI.0730-07.2007).
- Kohonen T (1990). "The self-organizing map". *Proc. IEEE* 78 (9): 1464–1480. DOI: [10.1109/5.58325](https://doi.org/10.1109/5.58325).
- Landau SM, Lal R, O'Neil JP, Baker S, and Jagust WJ (2009). "Striatal dopamine and working memory". *Cereb. Cortex* 19 (2): 445–454. DOI: [10.1093/cercor/bhn095](https://doi.org/10.1093/cercor/bhn095).
- Lilliefors HW (1967). "On the Kolmogorov-Smirnov test for normality with mean and variance unknown". *J. Am. Stat. Assoc.* 62 (318): 399–402. DOI: [10.2307/2283970](https://doi.org/10.2307/2283970).
- McKhann G, Drachman D, Folstein M, Katzman R, Price D, and Stadlan EM (1984). "Clinical diagnosis of Alzheimer's disease: report of the NINCDS-ADRDA Work Group under the auspices of Department of Health and Human Services Task Force on Alzheimer's Disease". *Neurology* 34 (7): 939–944. DOI: [10.1212/WNL.34.7.939](https://doi.org/10.1212/WNL.34.7.939).
- Mega MS, Lee L, Dinov ID, Mishkin F, Toga AW, and Cummings JL (2000). "Cerebral correlates of psychotic symptoms in Alzheimer's disease". *J. Neurol. Neurosurg. Psychiatr.* 69 (2): 167–171. DOI: [10.1136/jnmp.69.2.167](https://doi.org/10.1136/jnmp.69.2.167).
- Middleton FA and Strick PL (1996). "The temporal lobe is a target of output from the basal ganglia". *Proc. Natl. Acad. Sci. U.S.A.* 93 (16): 8683–8687. URL: <http://www.pnas.org/content/pnas/93/16/8683.full.pdf> (visited on 09/10/2018).
- Oyanagi K, Takahashi H, Wakabayashi K, and Ikuta F (1987). "Selective involvement of large neurons in the neostriatum of Alzheimer's disease and senile dementia: a morphometric investigation". *Brain Res.* 411 (2): 205–211. DOI: [10.1016/0006-8993\(87\)91071-7](https://doi.org/10.1016/0006-8993(87)91071-7).
- Oyanagi K, Takahashi H, Wakabayashi K, and Ikuta F (1991). "Large neurons in the neostriatum in Alzheimer's disease and progressive supranuclear palsy: a topographic, histologic and ultrastructural investigation". *Brain Res.* 544 (2): 221–226. DOI: [10.1016/0006-8993\(91\)90057-3](https://doi.org/10.1016/0006-8993(91)90057-3).
- Parkinson J, Fudge J, Hurd Y, Pennartz C, and Peoples L (2000). "Finding motivation at Seabrook Island: the ventral striatum, learning and plasticity". *Trends Neurosci.* 23 (9): 383–384. DOI: [10.1016/S0166-2236\(00\)01644-1](https://doi.org/10.1016/S0166-2236(00)01644-1).

- Patenaude B, Smith SM, Kennedy DN, and Jenkinson M (2007). *Bayesian shape and appearance models, FMRIB technical report TR07BP1*. London. URL: <https://www.fmrib.ox.ac.uk/datasets/techrep/tr07bp1/tr07bp1.pdf> (visited on 09/10/2018).
- Poldrack RA and Packard MG (2003). "Competition among multiple memory systems: converging evidence from animal and human brain studies". *Neuropsychologia* 41 (3): 245–251. DOI: [10.1016/S0028-3932\(02\)00157-4](https://doi.org/10.1016/S0028-3932(02)00157-4).
- R Core Team (2009). *R: A Language and Environment for Statistical Computing*. R Foundation for Statistical Computing. Vienna, Austria. URL: <http://www.R-project.org/>.
- Raji CA, Becker JT, Tsopelas ND, Price JC, Mathis CA, et al. (2008). "Characterizing regional correlation, laterality and symmetry of amyloid deposition in mild cognitive impairment and Alzheimer's disease with Pittsburgh Compound B". *J. Neurosci. Methods* 172 (2): 277–282. DOI: [10.1016/j.jneumeth.2008.05.005](https://doi.org/10.1016/j.jneumeth.2008.05.005).
- Richner M, Bach G, and West MJ (2009). "Over expression of amyloid β -protein reduces the number of neurons in the striatum of APPswe/PS1 Δ E9". *Brain Res.* 1266: 87–92. DOI: [10.1016/j.brainres.2009.02.025](https://doi.org/10.1016/j.brainres.2009.02.025).
- Roth M, Huppert FA, Mountjoy CQ, and Tym E (1988). *CAMDEX-R the Cambridge examination for mental disorders of the elderly*. Cambridge, UK: Cambridge University Press.
- Savioz A, Leuba G, Vallet PG, and Walzer C (2009). "Contribution of neural networks to Alzheimer disease's progression". *Brain Res. Bull.* 80 (4-5): 309–314. DOI: [10.1016/j.brainresbull.2009.06.006](https://doi.org/10.1016/j.brainresbull.2009.06.006).
- Saykin AJ, Wishart HA, Rabin LA, Santulli RB, Flashman LA, et al. (2006). "Older adults with cognitive complaints show brain atrophy similar to that of amnesic MCI". *Neurology* 67 (5): 834–842. DOI: [10.1212/01.wnl.0000234032.77541.a2](https://doi.org/10.1212/01.wnl.0000234032.77541.a2).
- Smith SM, De Stefano N, Jenkinson M, and Matthews PM (2001). "Normalized accurate measurement of longitudinal brain change". *J. Comput. Assist. Tomogr.* 25 (3): 466–475. URL: http://journals.lww.com/jcat/Fulltext/2001/05000/Normalized_Accurate_Measurement_of_Longitudinal.22.aspx (visited on 09/10/2018).
- Smith SM, Jenkinson M, Woolrich MW, Beckmann CF, Behrens TE, et al. (2004). "Advances in functional and structural MR image analysis and implementation as FSL". *Neuroimage* 23 Suppl 1: S208–219. DOI: [10.1016/j.neuroimage.2004.07.051](https://doi.org/10.1016/j.neuroimage.2004.07.051).
- Smith SM, Zhang Y, Jenkinson M, Chen J, Matthews PM, et al. (2002). "Accurate, robust, and automated longitudinal and cross-sectional brain change analysis". *Neuroimage* 17 (1): 479–489. DOI: [10.1006/nimg.2002.1040](https://doi.org/10.1006/nimg.2002.1040).
- Utter AA and Basso MA (2008). "The basal ganglia: an overview of circuits and function". *Neurosci. Biobehav. Rev.* 32 (3): 333–342. DOI: [10.1016/j.neubiorev.2006.11.003](https://doi.org/10.1016/j.neubiorev.2006.11.003).
- van der Flier WM, van Buchem MA, Weverling-Rijnsburger AW, Mutsaers ER, Bollen EL, et al. (2004). "Memory complaints in patients with normal cognition are associated with smaller hippocampal volumes". *J. Neurol.* 251 (6): 671–675. DOI: [10.1007/s00415-004-0390-7](https://doi.org/10.1007/s00415-004-0390-7).

- Villemagne VL, Ataka S, Mizuno T, Brooks WS, Wada Y, et al. (2009). "High striatal amyloid β -peptide deposition across different autosomal Alzheimer disease mutation types". *Arch. Neurol.* 66 (12): 1537–1544. DOI: [10.1001/archneurol.2009.285](https://doi.org/10.1001/archneurol.2009.285).
- Voorn P, Vanderschuren LJ, Groenewegen HJ, Robbins TW, and Pennartz CM (2004). "Putting a spin on the dorsal-ventral divide of the striatum". *Trends Neurosci.* 27 (8): 468–474. DOI: [10.1016/j.tins.2004.06.006](https://doi.org/10.1016/j.tins.2004.06.006).
- Wilson CJ, Chang HT, and Kitai ST (1990). "Firing patterns and synaptic potentials of identified giant aspiny interneurons in the rat neostriatum". *J. Neurosci.* 10 (2): 508–519. URL: <http://www.jneurosci.org/content/10/2/508> (visited on 09/10/2018).
- Wolf DS, Gearing M, Snowdon DA, Mori H, Markesbery WR, and Mirra SS (1999). "Progression of regional neuropathology in Alzheimer disease and normal elderly: findings from the Nun study". *Alzheimer Dis. Assoc. Disord.* 13 (4): 226–231. URL: http://journals.lww.com/alzheimerjournal/Fulltext/1999/10000/Progression_of_Regional_Neuropathology_in.9.aspx (visited on 09/10/2018).
- Yesavage JA and Sheikh JI (1986). "Geriatric depression scale (GDS) recent evidence and development of a shorter version". *Clin. Gerontol.* 5 (1-2): 165–173. DOI: [10.1300/J018v05n01_09](https://doi.org/10.1300/J018v05n01_09).

CHAPTER 4

Ventral striatal volume is associated with cognitive decline in older people: a population based MR-study

Laura W de Jong

Y Wang

Lon R White

Bingbing Yu

Mark A van Buchem

Lenore J Launer

Adapted from *Neurobiol Aging*. 2012 Feb;33(2):424.e1-10. doi: [10.1016/j.neurobiolaging.2010.09.027](https://doi.org/10.1016/j.neurobiolaging.2010.09.027).

ABSTRACT

Striatal degeneration may contribute to cognitive impairment in older people. Here, we examine the relation of atrophy of the striatum and its substructures to cognitive decline and dementia in study participants ranging from normal cognition to dementia. Data were from the prospective community-based Honolulu Asia Aging Study of Japanese American men born 1900–1919. Brain MRI (1.5T) was acquired on a stratified subsample ($n = 477$) that included four groups defined by cognitive status relative to the scan date: subjects without dementia ($n = 347$), subjects identified as demented 2–3 years prior to brain scanning ($n = 30$), at the time of scanning ($n = 58$), and 3–5 years after scanning ($n = 42$). Volumes of the striatum, including the accumbens, putamen, and caudate nucleus were automatically estimated from T1 MR images. Global cognitive function was measured with the CASI, at four exams spanning an 8-year interval. Trajectories of cognitive decline were estimated for each quartile of striatal volume using mixed models, controlling for demographic variables, measures of cerebrovascular damage, global brain atrophy, and hippocampal volume. Diagnosis of dementia before, during, and after brain scanning was associated with smaller volumes of nucleus accumbens and putamen, but not with caudate nucleus volume. Subjects in the lowest quartile of nucleus accumbens volume, both in the total sample and in the subjects not diagnosed with dementia during the study, had a significantly ($p < 0.0001$) steeper decline in cognitive performance compared to those in the highest quartile. In conclusion, volumes of the nucleus accumbens and putamen are closely associated with the occurrence of dementia and nucleus accumbens volume predicts cognitive decline in older people. These associations were found independent of the magnitude of other pivotal markers of cognitive decline, i.e., cerebrovascular damage and hippocampal volume. The present study suggests a role for the ventral striatum in the development of clinical dementia.

INTRODUCTION

The effects on cognition of degenerative changes in the medial temporal lobe have been widely studied. However, other structures atrophy with age as well and may also contribute significantly to late-life cognitive impairment. The striatum is of particular interest because it is part of two systems prone to degeneration in older people, the limbic and the fronto-striatal system. The striatum, is anatomically divided by the capsula interna into the caudate nucleus, putamen, and nucleus accumbens. The caudate nucleus and putamen are histologically similar and their functions are thought to be congruous with their somato-topographical connections to the neocortex. The caudate nucleus is part of circuits to the dorsolateral prefrontal cortex, lateral orbital prefrontal cortex, and posterior parietal cortex. The putamen is part of circuits with the motor cortex and the somatosensory cortex (Utter and Basso 2008). The nucleus accumbens, located ventro-anterior, differs histologically and functionally from the caudate nucleus and putamen. Its cells have smaller dimensions and are organized into subnuclei (Brockhaus 1942). The nucleus accumbens projects to, and receives input from, several limbic regions including the medial temporal lobe and anterior cingulate cortex. Functionally, the ventral striatum (nucleus accumbens and fundi of the caudate and putamen) participates in processing limbic information and the dorsal striatum (caudate nucleus and putamen) in sensorimotor information (Voorn et al. 2004).

The role of the striatum in cognitive processes has been studied in specific basal ganglia disorders and as part of basal forebrain atrophy in Alzheimer's disease (AD). In Huntington's disease (HD), atrophy of the caudate nucleus is associated with impaired executive functioning (Peinemann et al. 2005), bicaudate ratio with impaired language learning (De Diego-Balaguer et al. 2008), and smaller volumes of the putamen with worse psychomotor function (Jurgens et al. 2008). Apart from classical basal ganglia diseases, in a recent volumetric study it was observed that AD cases had significantly decreased volumes of the putamen compared to memory complainers (de Jong et al. 2008). Also, basal forebrain atrophy, including parts of the ventral striatum, was observed as long as 4.5 years before the development of clinical symptoms (Hall et al. 2008; Teipel et al. 2005). Despite the data on striatal volumes in dementia and basal ganglia diseases, little is known on the relation between striatal volume and cognitive decline in older people, varying from cognitively "normal" to impaired. Also not known is, whether other predictors of cognitive impairment, such as cerebrovascular damage, global brain atrophy, or hippocampal volume, mediate this relation or whether striatal volumes can improve our ability to predict cognitive decline in older people.

Here, we examine the relation of striatal volume to dementia and global cognitive function and decline, in the entire spectrum from cognitively healthy to demented older

subjects. We account for the presence and extent of several pivotal cerebrovascular damage parameters, hippocampal volume, and global brain atrophy. Subjects are from the well-characterized population based cohort of the Honolulu-Asia Aging Study (HAAS), who participated in an MRI substudy.

METHODS

Subjects and study design

Study subjects were older Japanese-American men, born between 1900–1919, who participated in the HAAS, an expansion of the Honolulu-Heart Program. A detailed description of the HAAS can be found elsewhere (White et al. 1996). In short, subjects were examined in 1991–1993 (baseline exam 4), and in three follow-up exams in 1994–1996 (exam 5), 1997–1999 (exam 6), and 1999–2000 (exam 7). The study was approved by the institutional review board of the Kuakini Medical Center and all respondents signed informed consent forms, except those who were demented, for whom an informed caretaker signed the consent

Assessment of cognitive function and dementia

During each exam all subjects were evaluated on cognitive performance and dementia cases were ascertained using a multistep procedure described elsewhere (White et al. 1996). Briefly, all subjects were screened with the Cognitive Ability Screening Instrument (CASI), which ranges in score from 0–100 (Teng et al. 1994). If subjects were screened positive, they were further evaluated with neuropsychological tests based on the CERAD (Consortium to Establish a Registry for Alzheimer’s Disease) battery (Morris et al. 1989), a neurologic exam, a proxy interview, and a diagnostic brain scan. Diagnoses were made in a consensus meeting in which the DSM-III-R (American Psychiatric Association 1987) was applied for dementia, the NINCDS-ADRDA criteria (McKhann et al. 1984) for AD, and the CADDTC (California Alzheimer’s Disease Diagnostic and Treatment Centers) criteria were applied for vascular dementia (VaD) (Chui et al. 1992). Depressive symptomology was measured in the first exam, using the Center for Epidemiologic Studies-Depression scale (CES-D) (Radloff 1977).

During the first follow-up examination (exam 5 1994–1996), whole brain Magnetic Resonance Imaging (MRI) was obtained on a stratified subsample of the total cohort. This subsample included a random sample of approximately 10% of the cognitively unimpaired participants and a selected over-sample of subjects with prevalent dementia (exam 4), subjects who scored poorly on cognitive testing but did not meet the criteria

for clinical dementia, subjects who possessed the apolipoprotein E type $\epsilon 4$ (APOE $\epsilon 4$ positive), and subjects with clinical stroke (Scher et al. 2007). Successful brain MR images were obtained from 575 subjects.

MRI acquisition and readings

Magnetic Resonance Imaging (MRI) was performed using a 1.5 Tesla MRI system (GE Signa Advantage) in the Kuakini Medical Center in Honolulu. The protocol has been described (Scher et al. 2007) elsewhere. Standardized MR readings were performed by readers at the John Hopkins Reading Center, blinded to the subject's medical history or health status at the time of scanning. The number of cerebral infarcts, lacunar infarcts, subcortical infarcts, and white matter lesions was evaluated according to Cardiovascular Health Study protocols (Longstreth et al. 1998). lacunar infarcts were defined having a maximal diameter of 3.0–20 mm. For this analysis, subjects were grouped according to the number of lacunar infarcts identified (0 = no lacunar infarct, 1 = 1–2, and 2 = 3–5 lacunar infarcts). White matter hyperintensities (WMH) on proton density images were scored on a scale from 0–9 (0 = no white matter hyperintensities and 9 = all white matter involved), and for the analyses grouped as follows: 1 = 1–3, 2 = 4–6, and 3 = 7–9. As an indicator of global brain atrophy, bi-frontal distance was measured, defined on T1 weighted axial slices as the largest right-left distance between the lateral borders of the right and left frontal horns. Inner table distance, the right-left dimension between the inner tables of the skull, was measured at the same level of the bi-frontal distance, and used to correct the bi-frontal distance for intracranial volume (Korf et al. 2004). Manually measured intracranial volume (ICV) and hippocampal volume were acquired using a protocol described previously (Korf et al. 2004).

Segmentation of cortical and deep gray matter structures

The algorithm FIRST (FMRIB's Integrated Registration and Segmentation Tool), of the FSL package (Smith et al. 2004) was used for automated segmentation of left and right nucleus accumbens, caudate nucleus, and putamen (Patenaude et al. 2007). This software package has been evaluated relative to manual tracing methods and other automated segmentation tools and an average Dice coefficient for the striatum of 0.81 was estimated (Babalola et al. 2009; Morey et al. 2009). We used the *run_first_all*-script with default options, followed by a boundary correction with a z-score of 3. The output of FIRST consisted of non-normalized striatal volumes. Total striatal volume was calculated by adding up the volumes of the caudate nucleus, putamen, and nucleus accumbens.

Statistical analysis

Analytical sample

There were 549 scanned subjects with successfully processed ICV and hippocampal volume (Korf et al. 2006). For the present study we excluded subjects whose scans could not be successfully processed by FIRST ($n = 18$), those with subcortical infarcts > 20 mm ($n = 20$), which may cause large errors in the computed volumes, and those who were diagnosed with or developed types of dementia other than AD, VaD, or mixed type of AD/VaD dementia ($n = 34$). Our final study sample included 477 subjects. In general, the sample of prevalent and incident dementia cases in this analysis tended to be of mild severity and to have a slower rate of functional decline than cases who were not scanned. Of those who were not diagnosed with dementia during the study about 30% did not survive the total 8-year follow-up time.

Relation of striatal volumes and time of dementia diagnosis

Each striatal structure volume was normally distributed across the total study sample of 477 subjects. To assess whether the striatal volumes are smaller in subjects with dementia or will be diagnosed with dementia in the future, we assigned each subject to one of 4 exhaustive and mutually exclusive categories; 1) those who had been identified as demented at the first HAAS examination 4 (baseline prevalent dementia cases: $n = 30$), 2) those who were identified as demented at the first follow-up examination 5 (incident dementia cases when scanned $n = 59$), 3) those who were identified as demented in follow-up exams 6 or 7 ($n = 42$), and 4) all others ($n = 347$). For descriptive purposes, we will refer to these groups as: prevalent dementia, incident dementia, future dementia, and no dementia. The groups were compared on age, ICV, years of education, CASI-score, CES-D score, bi-frontal distance (corrected for inner table distance), hippocampal volume, and striatal volumes by one-way ANOVA, and compared on cerebral and lacunar infarcts, WMH, and presence of APOE $\epsilon 4$ allele (yes = 34 and 44, no = all other genotypes) (Hixson and Powers 1991) by a Pearson's χ^2 test. Tests for linear association and pairwise comparison of striatal volumes between the study groups were performed.

Association of striatal volume and cognitive decline

For the longitudinal analyses the total sample was divided by quartile of volume of the striatum and substructures. Slopes from quartiles 1–3 were, separately, compared to the slope of the 4th quartile (highest volume quartile). For this, a mixed model approach was used, with random intercepts and age at each of the four HAAS exams as the

time line. The mixed model accounted for varying time intervals between the exams of different subjects, differences in the number of measurements per subject (unbalanced data), and differences in age at baseline exam. Whether or not slopes differed across quartiles and over time, was tested with an interaction term of age (the time scale) and quartile of volume, compared with the 4th quartile. We adjusted for age at baseline exam, educational level, ICV, CES-D, lacunar infarcts, cerebral infarcts, WMH, bifrontal distance, presence of APOE ϵ 4 allele, and quartile of hippocampal volume. To check whether potential associations were not due to overrepresentation of demented subjects in the lower quartiles of volume, we reran the mixed model analysis on the no dementia group only ($n = 347$). Furthermore, we tested non-linearity in the cognitive trajectories by adding a quadratic term into the model. This term was not significant, and the linear model was more parsimonious without sacrificing the model fit (table 1), so we proceeded with the linear model.

Table 1: Test of linear vs. quadratic cognitive deterioration by quartile of striatal volume

| Structure | Quartile | Full sample ($n = 477$) | | | No dementia sample ($n = 347$) | | |
|-------------------|----------|---------------------------|---------------|------------------|----------------------------------|---------------|------------------|
| | | p | AIC linear | AIC quadratic | p | AIC linear | AIC quadratic |
| Striatum | | | | | | | |
| | I | 0.83 | 2524 | 2530 | 0.03 | 1704 | 1706 |
| | II | 0.55 | 2744 | 2750 | 0.14 | 2254 | 2258 |
| | III | 0.07 | 2787 | 2789 | < 0.01 | 2347 | 2347 |
| | IV | < 0.01 | 2617 | 2616 | < 0.01 | 2261 | 2257 |
| Nucleus accumbens | | | | | | | |
| | I | 0.93 | 2337 | 2343 | 0.02 | 1311 | 1311 |
| | II | 0.21 | 2766 | 2771 | 0.08 | 2338 | 2341 |
| | III | 0.30 | 2626 | 2631 | 0.52 | 2312 | 2318 |
| | IV | 0.52 | 2747 | 2753 | 0.29 | 2520 | 2525 |
| Putamen | | | | | | | |
| | I | 0.15 | 2519 | 2523 | 0.26 | 1662 | 1667 |
| | II | 0.23 | 2718 | 2722 | 0.28 | 2246 | 2251 |
| | III | 0.91 | 2811 | 2817 | 0.96 | 2241 | 2248 |
| | IV | 0.01 | 2616 | 2615 | < 0.01 | 2375 | 2372 |
| Caudate nucleus | | | | | | | |
| | I | 0.12 | 2550 | 2554 | 0.03 | 2055 | 2057 |
| | II | 0.91 | 2808 | 2814 | 0.87 | 2088 | 2094 |
| | III | 0.62 | 2673 | 2679 | 0.47 | 2142 | 2148 |
| | IV | 0.71 | 2621 | 2627 | 0.31 | 2235 | 2240 |

AIC, Akaike's information criterion

RESULTS

Dementia and smaller striatal volumes

The dementia study groups differ in age ($p = 0.008$), CASI-score ($p < 0.0001$), volumes of the striatum ($p = 0.0004$), putamen and accumbens volume ($p < 0.0001$), all three indicators of cerebrovascular damage, i.e., cerebral and lacunar infarcts and WMH ($p < 0.0001$), bi-frontal distance ($p < 0.0001$), and hippocampal volume ($p < 0.0001$) (Table 2). Pairwise comparison between no dementia group and each of the three dementia groups shows significantly smaller volumes of the total striatum, nucleus accumbens, and putamen in the prevalent (all $p < 0.001$) and incident dementia ($p = 0.002$ for total striatum, $p < 0.001$ for nucleus accumbens, $p = 0.002$ for putamen) groups, and also smaller volumes of the accumbens in the future dementia group ($p = 0.003$). Comparison of prevalent dementia with future dementia shows larger volumes of the striatum ($p = 0.03$), putamen ($p = 0.01$), and accumbens ($p = 0.001$) in future dementia and comparison of prevalent dementia with incident dementia shows a larger volume of the accumbens ($p = 0.01$) in incident dementia.

Striatal volume and prediction of cognitive decline

Figure 1 summarizes the results of the longitudinal analysis, showing the predicted decline in CASI scores over time per quartile of striatal volume; spaghetti plots of a random sample of 10 subjects of each quartile are also included in the figure. There was a significant difference in decline of CASI score in quartile IV compared to quartile I for the nucleus accumbens (slope Δ (SE) = -1.39 (0.21), $p < 0.0001$). There were no significant differences between quartile IV and I for the putamen (slope Δ (SE) = -0.33 (0.22), $p = 0.13$), caudate nucleus (slope Δ (SE) = -0.01 (0.22), $p = 0.98$), or total striatal volume (slope Δ (SE) = -0.34 (0.21), $p = 0.11$).

A summary of the longitudinal analysis with the no-dementia group only ($n=347$) is shown in Figure 2. Similar to the analysis on the total sample, a significant slope difference between quartile IV and I for the nucleus accumbens was seen (slope Δ (SE) = -1.39 (0.21), $p < 0.0001$), but not for the putamen (slope Δ (SE) = 0.14 (0.15), $p = 0.47$), caudate nucleus (slope Δ (SE) = 0.07 (0.19), $p = 0.71$), or striatum (slope Δ (SE) = -0.03 (0.19), $p = 0.89$).

The overall significance of the models estimating the cognitive change slope by quartile of striatal volume are shown in Table 3; results were adjusted for age, education in years, gender, ICV, CES-D score, cerebral infarcts, lacunar infarcts, WMH, bi-frontal distance, and the presence of APOE $\epsilon 4$ allele. For comparison we show similar analyses

Table 2: Group characteristics according to identification of dementia relative to MRI: HAAS MRI subsample

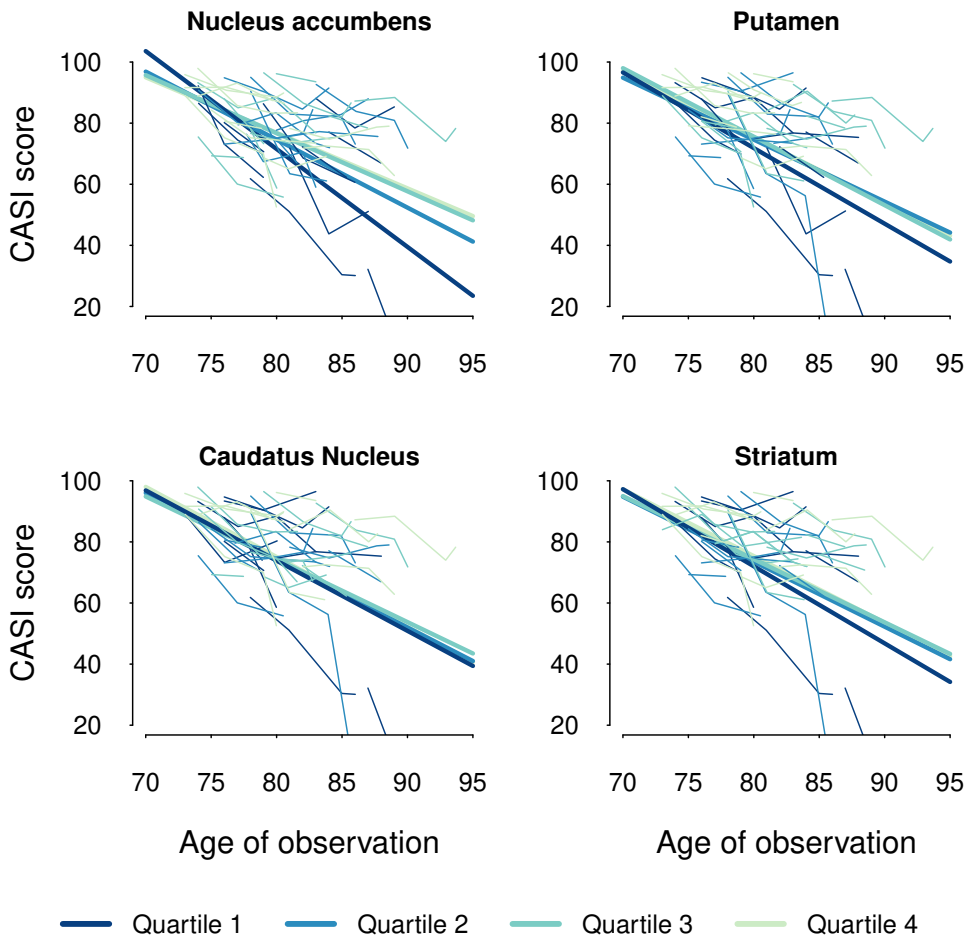
| Mean (SD) or % | No dementia (<i>n</i> = 347) | Future dementia (<i>n</i> = 42) | Incident dementia (<i>n</i> = 58) | Prevalent dementia (<i>n</i> = 30) | <i>p</i> ANOVA or χ^2 |
|-----------------------------|-------------------------------------|----------------------------------------|------------------------------------------|-------------------------------------------|----------------------------------|
| Age ^a | 81.3 (5.0) | 82.7 (5.1) | 82.2 (4.9) | 84.2 (5.1) | 0.008 |
| ICV | 1436 (110) | 1429 (116) | 1440 (107) | 1442 (100) | 0.95 |
| Education ^a | 10.4 (3.0) | 10.2 (3.1) | 9.9 3(.2) | 9.4 (2.6) | 0.23 |
| CASI-score | 79.8 (9.8) | 72.5 (8.5) | 60.3 (16.2) | 44.8 (19.8) | <.0001 |
| CES-D score | 3.7 (3.5) | 4.5 (4.5) | 4.3 (2.2) | 3.0 (2.2) | 0.32 |
| Bi-frontal dist. | 0.34 (0.03) | 0.34 (0.04) | 0.36 (0.03) | 0.36 (0.03) | <.0001 |
| Striatum | 20.0 (2.3) | 19.7 (2.6) | 18.9 (3.3) | 18.5 (2.0) | <.0004 |
| Accumbens | 1.38 (0.24) | 1.26 (0.23) | 1.21 (0.28) | 1.08 (0.18) | <.0001 |
| Putamen | 9.7 (1.2) | 9.4 (1.4) | 9.1 (1.7) | 8.7 (1.1) | <.0001 |
| Caudate | 8.9 (1.3) | 9.0 (1.3) | 8.6 (1.7) | 8.7 (1.6) | 0.30 |
| Hippocampus | 5.6 (0.8) | 5.2 (0.7) | 4.9 (0.9) | 4.3 (0.9) | <.0001 |
| APOE ϵ 4 | 37 | 29 | 26 | 30 | <.0001 |
| Cerebral infarcts | | | | | |
| 0 | 93 | 93 | 88 | 81 | |
| 1 | 6 | 7 | 7 | 15 | <.0001 |
| ≥ 2 | 1 | 0 | 5 | 4 | |
| Lacunar infarcts | | | | | |
| 0 | 58 | 61 | 47 | 46 | |
| 1–2 | 31 | 34 | 32 | 35 | <.0001 |
| 3–5 | 10 | 5 | 21 | 19 | |
| White Matter Hyperintensity | | | | | |
| 0–3 | 75 | 71 | 60 | 46 | |
| 4–6 | 20 | 24 | 29 | 35 | <.0001 |
| 7–9 | 4 | 5 | 10 | 7 | |

CASI, Cognitive Ability Screening Instrument; CES-D, Center for Epidemiologic Studies Depression.

a in years

for the hippocampus. We found the slope of the cognitive decline to significantly differ among the quartiles of hippocampal volume. Adjusting for the hippocampus quartiles, as well as other markers of brain pathology and cardiovascular disease risk factors, we found there was still a significant difference among quartiles of the nucleus accumbens ($p < 0.0001$). As shown in Figures 1 and 2, this largely reflected the steeper slope in decline of the 4th quartile relative to the first quartiles. Volumes of the total striatum, caudate nucleus, and putamen, were not associated with cognitive decline.

Figure 1: Predicted CASI-score over time per quartile of striatal volume



CASI Score, predicted mean CASI (Cognitive Ability Screening Instrument) score over 8-year interval, adjusted for age, age at baseline, educational level, ICV, CES-D score, lacunar infarcts, cerebral infarcts, WMH, bi-frontal distance/inner table distance, APOE $\epsilon 4$ allele, hippocampal volume quartiles.

DISCUSSION

The present study assessed the relation of the volume of the striatum and its substructures and global cognitive performance in the entire spectrum of cognitively healthy to

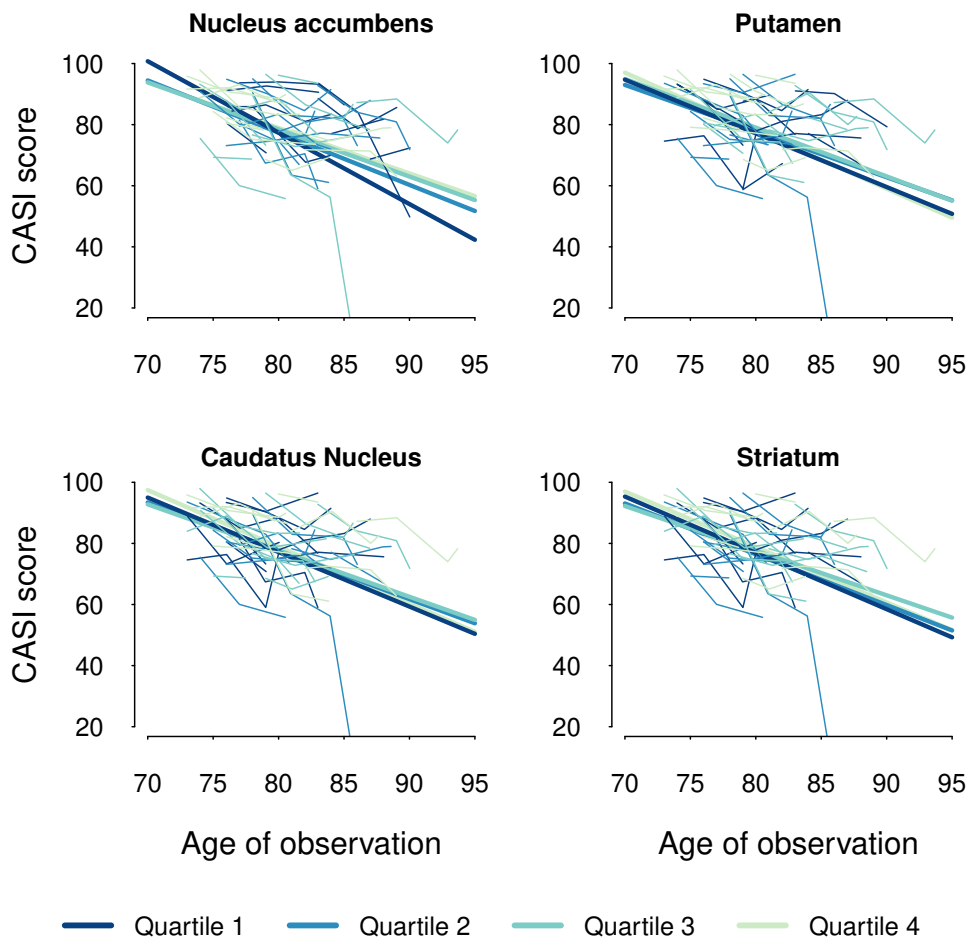
Table 3: Volume of striatum and hippocampus in predicting cognitive decline

| Model | Effects ^a | Full sample (<i>n</i> = 477) | | No dementia sample (<i>n</i> = 347) | |
|--------------------------|----------------------|----------------------------------|-----------------|-----------------------------------------|-----------------|
| | | <i>F</i> -value | <i>p</i> -value | <i>F</i> -value | <i>p</i> -value |
| Hippocampus (Hipp) | | | | | |
| | Hipp quartiles | 9.8 | <.0001 | 5.4 | 0.001 |
| | Age × Hipp quartiles | 12.8 | <.0001 | 6.4 | 0.0003 |
| Nucleus accumbens (NAcc) | | | | | |
| | NAcc quartiles | 14.9 | <.0001 | 6.5 | 0.0002 |
| | Hipp quartiles | 12.7 | <.0001 | 2.9 | 0.04 |
| | Age × NAcc quartiles | 17.1 | <.0001 | 7.3 | <.0001 |
| Caudate nucleus (CN) | | | | | |
| | CN quartiles | 0.6 | 0.65 | 1.5 | 0.22 |
| | Hipp quartiles | 19.5 | <.0001 | 3.8 | 0.01 |
| | Age × CN quartiles | 0.5 | 0.65 | 1.5 | 0.22 |
| Putamen (Put) | | | | | |
| | Put quartiles | 1.1 | 0.36 | 1.6 | 0.19 |
| | Hipp quartiles | 15.8 | <.0001 | 3.7 | 0.01 |
| | Age × Put quartiles | 1.4 | 0.25 | 1.7 | 0.16 |
| Striatum (Str) | | | | | |
| | Str quartiles | 1.4 | 0.23 | 1.7 | 0.16 |
| | Hipp quartiles | 16.2 | <.0001 | 3.2 | 0.02 |
| | Age × Str quartiles | 1.7 | 0.16 | 1.7 | 0.16 |

^a Separate effects of age, education in years, gender, ICV, CES-D score, cerebral infarcts, lacunar infarcts, WMH, bi-frontal distance, and presence of APOE ϵ 4 allele are not displayed.

demented older people. We found volumes of the nucleus accumbens (as they were at the time of scanning) to be lower in subjects diagnosed with dementia 2–3 years prior to, at the time of, and 3–5 years after, the brain MR-scan was acquired. Total volumes of the striatum, and separately the putamen were smaller in subjects diagnosed with dementia prior to and at the time of scanning. Furthermore, we found that quartiles of nucleus accumbens volume significantly differed in the rate of cognitive decline both in the total sample and the sample of subjects who were not identified with dementia during the course of the study. Specifically, subjects in the lowest quartile of accumbens volume had a significantly steeper slope of cognitive decline measured over an 8-year period, independent of global brain atrophy, hippocampal volume, presence of APOE ϵ 4 allele, or the amount of cerebrovascular damage. Thus, our findings suggest, the ventro-anterior striatal substructure, the nucleus accumbens, is a significant indicator for cognitive decline. Prospective studies of people who are not demented at baseline are

Figure 2: Predicted CASI-score over time per quartile of striatal volume (non-demented people only)



CASI Score, Predicted mean CASI (Cognitive Ability Screening Instrument) score over 8-year interval, adjusted for age, age at baseline, educational level, ICV, CES-D score, lacunar infarcts, cerebral infarcts, WMH, bi-frontal distance/inner table distance, APOE $\epsilon 4$ allele, hippocampal volume quartiles.

needed to investigate whether atrophy in the accumbens is a marker for some specific cognitive trajectories, such as a fast or steep decline.

These findings contribute to our understanding of the stages of cognitive decline.

The striatum is the largest structure of the basal ganglia, both hemispheres together measuring approximately 20 cm³, and is regarded as an input nucleus for cortical projections (Utter and Basso 2008). Several studies have described the topographical arrangement of the human striatum in distinct, sometimes partially overlapping, circuits serving motor and cognitive functions (Alexander, DeLong, and Strick 1986; Draganski et al. 2008; Leh et al. 2007; Middleton and Strick 2000). Of interest here is the anterior cingulate loop described by Alexander (Grahn, Parkinson, and Owen 2008). This loop includes the ventral striatum, which receives input from the anterior cingulate cortex, hippocampal cortex, entorhinal cortex, and the superior and inferior temporal gyri. The ventral striatum consists of the nucleus accumbens, fundi of the caudate and putamen, and olfactory stria (Brockhaus 1942). Since the accumbens is part of the limbic circuit, we had postulated that it shared the limbic circuits' vulnerability to degenerate during the dementing process. In our study the nucleus accumbens was significantly smaller in subjects with dementia and subjects who were going to become demented. Volume of the accumbens contributed independently to the model explaining cognitive decline in older people. This contribution was independent of more generally used indicators of cognitive decline hippocampal volume, global brain atrophy, and cerebrovascular damage parameters. The results were similar in the sample not diagnosed with dementia during the 8-year follow-up period.

Pathological studies of the striatum in AD have shown that in particular, the cholinergic interneurons contain neurofibrillary tangles and are lost in the ventral striatum, which may be a potential explanation for our findings (Lehéricy et al. 1989; Selden, Mesulam, and Geula 1994). Studies are needed to determine the processes leading to smaller accumbens volumes in older (demented) subjects, as well as the temporal relation with other neurodegenerative changes in the brain. It has been postulated that the nucleus accumbens plays a pivotal role in memory and learning processes (Goldenberg et al. 1999; Gonzalez-Burgos and Feria-Velasco 2008; Graybiel 2008), possibly explaining the association of smaller volumes with more rapid cognitive decline. However, the nucleus accumbens is part of the intricate basal forebrain system and detailed knowledge of how this system facilitates cognitive functioning is still lacking, as is our understanding of the precise role of the nucleus accumbens (Alheid and Heimer 1988).

We also found associations between the volume of the putamen and diagnosis of dementia, although not with cognitive decline. Previously, smaller volumes of the putamen were observed in people with dementia (de Jong et al. 2008). It is possible that decrease in the volume of the putamen becomes evident in more progressed stages of dementia and not in preclinical stages, which may explain the association with dementia but not with prediction of cognitive decline. Contrary to expectation, the caudate nucleus was not associated with dementia or cognitive decline in our study, whereas other studies

have pointed out the occurrence of degeneration of the head of the caudate nucleus in AD (Frisoni et al. 2002; Karas et al. 2003; Rombouts et al. 2000). Possibly, this inconsistency reflects differences in where the borders were placed between the nucleus accumbens and the caudate nucleus, but it may also be that the volume differences for the caudate nucleus are too small to detect by our method.

A major advantage of our study was the highly reproducible separate segmentation of caudate, putamen, and nucleus accumbens, and that we were able to study these substructures in association with longitudinal changes in cognition and dementia status. However, the limitations in the extent to which the “borders” between the striatal substructures can be identified, need to be taken into account when interpreting the data. The borders of these structures are better viewed as transition zones with overlapping functions. Currently, it is not possible to delineate substructures based on a functional division, because of overlapping functional zones and low contrast within the neostriatal structure on MR. Finally, the striatal volume calculations were based on the delineation of the surface or boundary voxels, which does not account for within structure changes, including lacunar infarcts, iron accumulation, and enlarged Virchow Robin spaces in the deep gray matter. This may lead to a potential overestimation of striatal volume. To minimize this effect we excluded subjects with large infarcts (> 20mm) in the deep gray matter region, and controlled for the presence of lacunar infarcts.

CONCLUSION

The present study shows that the volume of the nucleus accumbens is closely associated with cognitive performance in older subjects, independent of other common brain changes in older persons. Additional studies are needed to further determine the clinical significance of atrophy in the striatum in community-based individuals

BIBLIOGRAPHY

- Alexander GE, DeLong MR, and Strick PL (1986). “Parallel organization of functionally segregated circuits linking basal ganglia and cortex”. *Annu. Rev. Neurosci.* 9: 357–381. DOI: [10.1146/annurev.ne.09.030186.002041](https://doi.org/10.1146/annurev.ne.09.030186.002041).
- Alheid GF and Heimer L (1988). “New perspectives in basal forebrain organization of special relevance for neuropsychiatric disorders: the striatopallidal, amygdaloid, and corticopetal components of substantia innominata”. *Neuroscience* 27 (1): 1–39. DOI: [10.1016/0306-4522\(88\)90217-5](https://doi.org/10.1016/0306-4522(88)90217-5).
- American Psychiatric Association (1987). *Diagnostic and statistical manual of mental disorders DSM-III-R (3rd ed. revised)*. Washington, DC: Authors.

- Babalola KO, Patenaude B, Aljabar P, Schnabel J, Kennedy D, et al. (2009). "An evaluation of four automatic methods of segmenting the subcortical structures in the brain". *Neuroimage* 47 (4): 1435–1447. DOI: [10.1016/j.neuroimage.2009.05.029](https://doi.org/10.1016/j.neuroimage.2009.05.029).
- Brockhaus H (1942). "Zur feineren anatomie des septum und des striatum". *Journal für Psychologie und Neurologie* 5 (1): 56. URL: http://www.thehumanbrain.info/database/db_literature/brockhaus_striatum1942d.pdf (visited on 09/10/2018).
- Chui HC, Victoroff JI, Margolin D, Jagust W, Shankle R, and Katzman R (1992). "Criteria for the diagnosis of ischemic vascular dementia proposed by the State of California Alzheimer's Disease Diagnostic and Treatment Centers". *Neurology* 42 (3): 473–480. DOI: [10.1212/WNL.42.3.473](https://doi.org/10.1212/WNL.42.3.473).
- De Diego-Balaguer R, Couette M, Dolbeau G, Durr A, Youssov K, and Bachoud-Levi AC (2008). "Striatal degeneration impairs language learning: evidence from Huntington's disease". *Brain* 131 (11): 2870–2881. DOI: [10.1093/brain/awn242](https://doi.org/10.1093/brain/awn242).
- de Jong LW, van der Hiele K, Veer IM, Houwing JJ, Westendorp RG, et al. (2008). "Strongly reduced volumes of putamen and thalamus in Alzheimer's disease: an MRI study". *Brain* 131 (12): 3277–3285. DOI: [10.1093/brain/awn278](https://doi.org/10.1093/brain/awn278).
- Draganski B, Kherif F, Klöppel S, Cook PA, Alexander DC, et al. (2008). "Evidence for segregated and integrative connectivity patterns in the human Basal Ganglia". *J. Neurosci.* 28 (28): 7143–7152. DOI: [10.1523/JNEUROSCI.1486-08.2008](https://doi.org/10.1523/JNEUROSCI.1486-08.2008).
- Frisoni GB, Testa C, Zorzan A, Sabattoli F, Beltramello A, et al. (2002). "Detection of grey matter loss in mild Alzheimer's disease with voxel based morphometry". *J. Neurol. Neurosurg. Psychiatr.* 73 (6): 657–664. DOI: [10.1136/jnnp.73.6.657](https://doi.org/10.1136/jnnp.73.6.657).
- Goldenberg G, Schuri U, Grömminger O, and Arnold U (1999). "Basal forebrain amnesia: does the nucleus accumbens contribute to human memory?" *J. Neurol. Neurosurg. Psychiatr.* 67 (2): 163–168. DOI: [10.1136/jnnp.67.2.163](https://doi.org/10.1136/jnnp.67.2.163).
- Gonzalez-Burgos I and Feria-Velasco A (2008). "Serotonin/dopamine interaction in memory formation". *Prog. Brain Res.* 172: 603–623. DOI: [10.1016/S0079-6123\(08\)00928-X](https://doi.org/10.1016/S0079-6123(08)00928-X).
- Grahn JA, Parkinson JA, and Owen AM (2008). "The cognitive functions of the caudate nucleus". *Prog. Neurobiol.* 86 (3): 141–155. DOI: [10.1016/j.pneurobio.2008.09.004](https://doi.org/10.1016/j.pneurobio.2008.09.004).
- Graybiel AM (2008). "Habits, rituals, and the evaluative brain". *Annu. Rev. Neurosci.* 31: 359–387. DOI: [10.1146/annurev.neuro.29.051605.112851](https://doi.org/10.1146/annurev.neuro.29.051605.112851).
- Hall AM, Moore RY, Lopez OL, Kuller L, and Becker JT (2008). "Basal forebrain atrophy is a presymptomatic marker for Alzheimer's disease". *Alzheimers. Dement.* 4 (4): 271–279. DOI: [10.1016/j.jalz.2008.04.005](https://doi.org/10.1016/j.jalz.2008.04.005).
- Hixson JE and Powers PK (1991). "Restriction isotyping of human apolipoprotein A-IV: rapid typing of known isoforms and detection of a new isoform that deletes a conserved repeat". *J. Lipid Res.* 32 (9): 1529–1535. URL: <http://www.jlr.org/content/32/9/1529.full.pdf> (visited on 09/10/2018).

- Jurgens CK, van de Wiel L, van Es AC, Grimbergen YM, Witjes-Ane MN, et al. (2008). "Basal ganglia volume and clinical correlates in 'preclinical' Huntington's disease". *J. Neurol.* 255 (11): 1785–1791. DOI: [10.1007/s00415-008-0050-4](https://doi.org/10.1007/s00415-008-0050-4).
- Karas GB, Burton EJ, Rombouts SA, van Schijndel RA, O'Brien JT, et al. (2003). "A comprehensive study of gray matter loss in patients with Alzheimer's disease using optimized voxel-based morphometry". *Neuroimage* 18 (4): 895–907. DOI: [10.1016/S1053-8119\(03\)00041-7](https://doi.org/10.1016/S1053-8119(03)00041-7).
- Korf ESC, White LR, Scheltens P, and Launer LJ (2004). "Midlife blood pressure and the risk of hippocampal atrophy: the Honolulu Asia Aging Study". *Hypertension* 44 (1): 29–34. DOI: [10.1161/01.HYP.0000132475.32317.bb](https://doi.org/10.1161/01.HYP.0000132475.32317.bb).
- Korf ESC, White LR, Scheltens P, and Launer LJ (2006). "Brain aging in very old men with type 2 diabetes: the Honolulu-Asia Aging Study". *Diabetes Care* 29 (10): 2268–2274. DOI: [10.2337/dc06-0243](https://doi.org/10.2337/dc06-0243).
- Leh SE, Ptito A, Chakravarty MM, and Strafella AP (2007). "Fronto-striatal connections in the human brain: a probabilistic diffusion tractography study". *Neurosci. Lett.* 419 (2): 113–118. DOI: [10.1016/j.neulet.2007.04.049](https://doi.org/10.1016/j.neulet.2007.04.049).
- Lehéry S, Hirsch EC, Cervera P, Hersh LB, Hauw JJ, et al. (1989). "Selective loss of cholinergic neurons in the ventral striatum of patients with Alzheimer disease". *Proc. Natl. Acad. Sci. U.S.A.* 86 (21): 8580–8584. URL: <http://www.pnas.org/content/pnas/86/21/8580.full.pdf> (visited on 09/10/2018).
- Longstreth WT, Bernick C, Manolio TA, Bryan N, Jungreis CA, and Price TR (1998). "Lacunar infarcts defined by magnetic resonance imaging of 3660 elderly people: the Cardiovascular Health Study". *Arch. Neurol.* 55 (9): 1217–1225. URL: <https://jamanetwork.com/journals/jamaneurology/fullarticle/774257> (visited on 09/10/2018).
- McKhann G, Drachman D, Folstein M, Katzman R, Price D, and Stadlan EM (1984). "Clinical diagnosis of Alzheimer's disease: report of the NINCDS-ADRDA Work Group under the auspices of Department of Health and Human Services Task Force on Alzheimer's Disease". *Neurology* 34 (7): 939–944. DOI: [10.1212/WNL.34.7.939](https://doi.org/10.1212/WNL.34.7.939).
- Middleton FA and Strick PL (2000). "Basal ganglia and cerebellar loops: motor and cognitive circuits". *Brain Res. Brain Res. Rev.* 31 (2-3): 236–250. DOI: [10.1016/S0165-0173\(99\)00040-5](https://doi.org/10.1016/S0165-0173(99)00040-5).
- Morey RA, Petty CM, Xu Y, Hayes JP, Wagner HR, et al. (2009). "A comparison of automated segmentation and manual tracing for quantifying hippocampal and amygdala volumes". *Neuroimage* 45 (3): 855–866. DOI: [10.1016/j.neuroimage.2008.12.033](https://doi.org/10.1016/j.neuroimage.2008.12.033).
- Morris JC, Heyman A, Mohs RC, Hughes JP, van Belle G, et al. (1989). "The Consortium to Establish a Registry for Alzheimer's Disease (CERAD). Part I. Clinical and neuropsychological assessment of Alzheimer's disease". *Neurology* 39 (9): 1159–1165. DOI: [10.1212/WNL.39.9.1159](https://doi.org/10.1212/WNL.39.9.1159).

- Patenaude B, Smith SM, Kennedy DN, and Jenkinson M (2007). *Bayesian shape and appearance models, FMRIB technical report TR07BP1*. London. URL: <https://www.fmrib.ox.ac.uk/datasets/techrep/tr07bp1/tr07bp1.pdf> (visited on 09/10/2018).
- Peinemann A, Schuller S, Pohl C, Jahn T, Weindl A, and Kassubek J (2005). "Executive dysfunction in early stages of Huntington's disease is associated with striatal and insular atrophy: a neuropsychological and voxel-based morphometric study". *J. Neurol. Sci.* 239 (1): 11–19. DOI: [10.1016/j.jns.2005.07.007](https://doi.org/10.1016/j.jns.2005.07.007).
- Radloff LS (1977). "The CES-D scale: A self-report depression scale for research in the general population". *Appl. Psychol. Meas.* 1 (3): 385–401. DOI: [10.1177/014662167700100306](https://doi.org/10.1177/014662167700100306).
- Rombouts SA, Barkhof F, Witter MP, and Scheltens P (2000). "Unbiased whole-brain analysis of gray matter loss in Alzheimer's disease". *Neurosci. Lett.* 285 (3): 231–233. DOI: [10.1016/S0304-3940\(00\)01067-3](https://doi.org/10.1016/S0304-3940(00)01067-3).
- Scher AI, Xu Y, Korf ESC, White LR, Scheltens P, et al. (2007). "Hippocampal shape analysis in Alzheimer's disease: a population-based study". *Neuroimage* 36 (1): 8–18. DOI: [10.1016/j.neuroimage.2006.12.036](https://doi.org/10.1016/j.neuroimage.2006.12.036).
- Selden N, Mesulam MM, and Geula C (1994). "Human striatum: the distribution of neurofibrillary tangles in Alzheimer's disease". *Brain Res.* 648 (2): 327–331. DOI: [10.1016/0006-8993\(94\)91136-3](https://doi.org/10.1016/0006-8993(94)91136-3).
- Smith SM, Jenkinson M, Woolrich MW, Beckmann CF, Behrens TE, et al. (2004). "Advances in functional and structural MR image analysis and implementation as FSL". *Neuroimage* 23 Suppl 1: S208–219. DOI: [10.1016/j.neuroimage.2004.07.051](https://doi.org/10.1016/j.neuroimage.2004.07.051).
- Teipel SJ, Flatz WH, Heinsen H, Bokde AL, Schoenberg SO, et al. (2005). "Measurement of basal forebrain atrophy in Alzheimer's disease using MRI". *Brain* 128 (11): 2626–2644. DOI: [10.1093/brain/awh589](https://doi.org/10.1093/brain/awh589).
- Teng EL, Hasegawa K, Homma A, Imai Y, Larson E, et al. (1994). "The Cognitive Abilities Screening Instrument (CASI): a practical test for cross-cultural epidemiological studies of dementia". *Int. Psychogeriatr.* 6 (1): 45–58. DOI: [10.1017/S1041610294001602](https://doi.org/10.1017/S1041610294001602).
- Utter AA and Basso MA (2008). "The basal ganglia: an overview of circuits and function". *Neurosci. Biobehav. Rev.* 32 (3): 333–342. DOI: [10.1016/j.neubiorev.2006.11.003](https://doi.org/10.1016/j.neubiorev.2006.11.003).
- Voorn P, Vanderschuren LJ, Groenewegen HJ, Robbins TW, and Pennartz CM (2004). "Putting a spin on the dorsal-ventral divide of the striatum". *Trends Neurosci.* 27 (8): 468–474. DOI: [10.1016/j.tins.2004.06.006](https://doi.org/10.1016/j.tins.2004.06.006).
- White L, Petrovitch H, Ross GW, Masaki KH, Abbott RD, et al. (1996). "Prevalence of dementia in older Japanese-American men in Hawaii: The Honolulu-Asia Aging Study". *JAMA-J. Am. Med. Assoc.* 276 (12): 955–960. DOI: [10.1001/jama.1996.03540120033030](https://doi.org/10.1001/jama.1996.03540120033030).

CHAPTER 5

Different susceptibility of medial temporal lobe and basal ganglia atrophy rates to vascular risk factors

Laura W de Jong

Lars E Forsberg

Jean-Sébastien Vidal

Sigurdur Sigurdsson

Alex P Zijdenbos

Melissa Garcia

Gudny Eiriksdottir

Vilmundur Gudnason

Mark A van Buchem

Lenore J Launer

Adapted from *Neurobiol Aging*. 2014 Jan;35(1):72-8. doi: [10.1016/j.neurobiolaging.2013.07.009](https://doi.org/10.1016/j.neurobiolaging.2013.07.009).

ABSTRACT

Atrophy of medial temporal lobe (MTL) and basal ganglia (BG) are characteristic of various neurodegenerative diseases in older people. In search of potentially modifiable factors that lead to atrophy in these structures, we studied the association of vascular risk factors to atrophy of MTL and BG in 368 non-demented men and women (born 1907–1935) who participated in the Age, Gene/Environment, Susceptibility-Reykjavik Study. A fully automated segmentation pipeline estimated volumes of MTL and BG from whole brain MRI performed at baseline and 2.4 years later. Linear regression models showed higher systolic and diastolic blood pressures and the presence of APOE ϵ 4 were independently associated with increased atrophy of MTL but no association of vascular risk factors with atrophy of BG was found. The different susceptibility of MTL and BG atrophy to the presence of vascular risk factors suggests the relatively preserved perfusion of BG when vascular risk factors are present.

INTRODUCTION

Several vascular risk factors are associated with the development of cognitive decline and Alzheimer's disease in the ageing population, among others obesity, high blood pressure, and high serum cholesterol (Debette et al. 2011; EL Kivipelto M.H et al. 2001; Tolppanen et al. 2012). A large body of literature is available that shows great overlap between these risk factors for cognitive decline and Alzheimer's disease on the one hand and risk factors for atrophy of brain structures on the other hand. Of particular interest are risk factors for pathological changes in the medial temporal lobe (MTL) and the basal ganglia and thalamus (BG), since pathological changes in these structures have been associated with an increased risk for Alzheimer's disease and cognitive decline in older people (Barnes et al. 2009; de Jong, van der Hiele, et al. 2008; de Jong, Wang, et al. 2012). Because of the growing ageing population, identification of potentially modifiable risk factors for atrophy of MTL and BG is important. Proper treatment may prevent or postpone the development of cognitive decline and therefore have a major public health impact.

Decreased volumes of MTL have been associated with untreated elevated midlife systolic and diastolic blood pressures (Korf, White, et al. 2004), type 2 diabetes (Korf, White, et al. 2006), high BMI at midlife (Debette et al. 2011), and the presence of APOE 4 allele (den Heijer, Oudkerk, et al. 2002). The APOE genotype is in particular relevant vascular risk factor, since it is involved in cholesterol metabolism and in repair of brain injury (Liu et al. 2013) and therefore may be related to MTL volume decline via multiple mechanisms. APOE ϵ 4 allele has also been associated with steeper rates of annual decline in hippocampal volume (Moffat et al. 2000). Although the associations of APOE ϵ 4 and midlife exposure to other vascular risk factors with decreased MTL volumes is supported by many reports, studies of associations of late life vascular risk factor exposure and MTL volume measurements tend to give mixed results or show no association (Gattringer et al. 2012). However, many of these studies are based on cross-sectional data and/or may not use direct measurements of MTL volume (Debette et al. 2011).

Although important in cognitive decline, less is known on vascular risk factors and volumetric changes in the BG. The striatum and thalamus are particularly susceptible to hypertensive cerebral small vessel disease (SVD), which on its turn is associated with cognitive decline (Prins et al. 2005; Smallwood et al. 2012). The striatum is supplied by perforating branches from the medial cerebral artery and the thalamus by perforating branches from the posterior cerebral artery, just shortly after both cerebral arteries have branched from the circle of Willis (Schmahmann 2003). This analogous irrigation may lead to similar effects of vascular risk factors in the striatum and thalamus. Man-

ifestations of SVD that are visible on magnetic resonance images (MRI), i.e., lacunar infarcts, microbleeds, and dilated Virchow Robin spaces, indeed frequently occur simultaneously in the striatum and the thalamus (Vermeer, Longstreth, and Koudstaal 2007; Zhu, Tzourio, et al. 2010; Zhu, Dufouil, et al. 2010). Besides macroscopically visible traits of SVD, microscopic pathology, such as micro infarcts or gliosis, may impact the structural integrity of the BG neural network as well (Gouw et al. 2011) and may lead to general atrophy of the structure. Since vascular risk factors have been related to the occurrence of SVD in the BG, we hypothesize that BG atrophy rates also increases in the presence of vascular risk factors.

In this follow-up brain MRI-study, we examined baseline and follow-up volumes of MTL and BG in relation to various vascular risk factors in late life. We hypothesized that those factors associated with cognitive decline are related to a higher atrophy rate of the MTL, but also a higher atrophy rate of the BG, in particular high blood pressure. Furthermore, we examined whether the effects of different vascular risk factors on the MTL and BG interacted with each other or exerted independent effects. We chose to combine volumes of the striatum (including caudate nucleus, putamen, and globus pallidus) with the thalamic volume, because of their analogous vascularization. For descriptive purposes we refer to these structures as BG. Participants were from the population based Age, Gene/Environment, Susceptibility-Reykjavik Study (AGES-Reykjavik), who took part in a midterm follow-up MR substudy.

METHODS

Study population

Data were from the well-characterized population-based AGES-Reykjavik study, (2002–2006) composed of men and women born between 1907–1935. The design of the study has been described elsewhere (Harris et al. 2007). Participants underwent extensive clinical evaluation, brain MRI, and cognitive testing. Cases of dementia were ascertained in a three-step process, as described previously (Harris et al. 2007), including a screening based on the Mini Mental State Examination and the Digit Symbol Substitution Test, a diagnostic neuropsychological test battery, an informant interview, and a neurological examination. A consensus diagnosis of dementia and MCI was made by a panel including a geriatrician, neurologist, neuropsychologist, and neuroradiologist. Dementia was classified according to Diagnostic and Statistical Manual of Mental Disorders, Fourth Edition, criteria (American Psychiatric Association 1994) A random sample of 410 participants was selected from the cohort that had successfully acquired MRI at baseline between 2004–2006 ($N = 4614$). From this sample we excluded those with missing or low quality

images that could not be adequately segmented ($n = 35$) and demented cases ($n = 3$). Because large areas of ischemic damage may affect the scan analysis, we also excluded those with hemispherical infarcts spanning 3 or more cortical lobes ($n = 2$), and those with parenchymal defects in the BG larger than 30 mm ($n = 2$). Our final study sample consisted of 368 non-demented people with successfully processed brain MR at both time points. This subsample underwent follow-up brain scanning, performed between June 2006 and March 2007, with an average interval of 2.4 (SD = 0.16) years from the first scan.

Protocol approvals, registrations, and patient consents

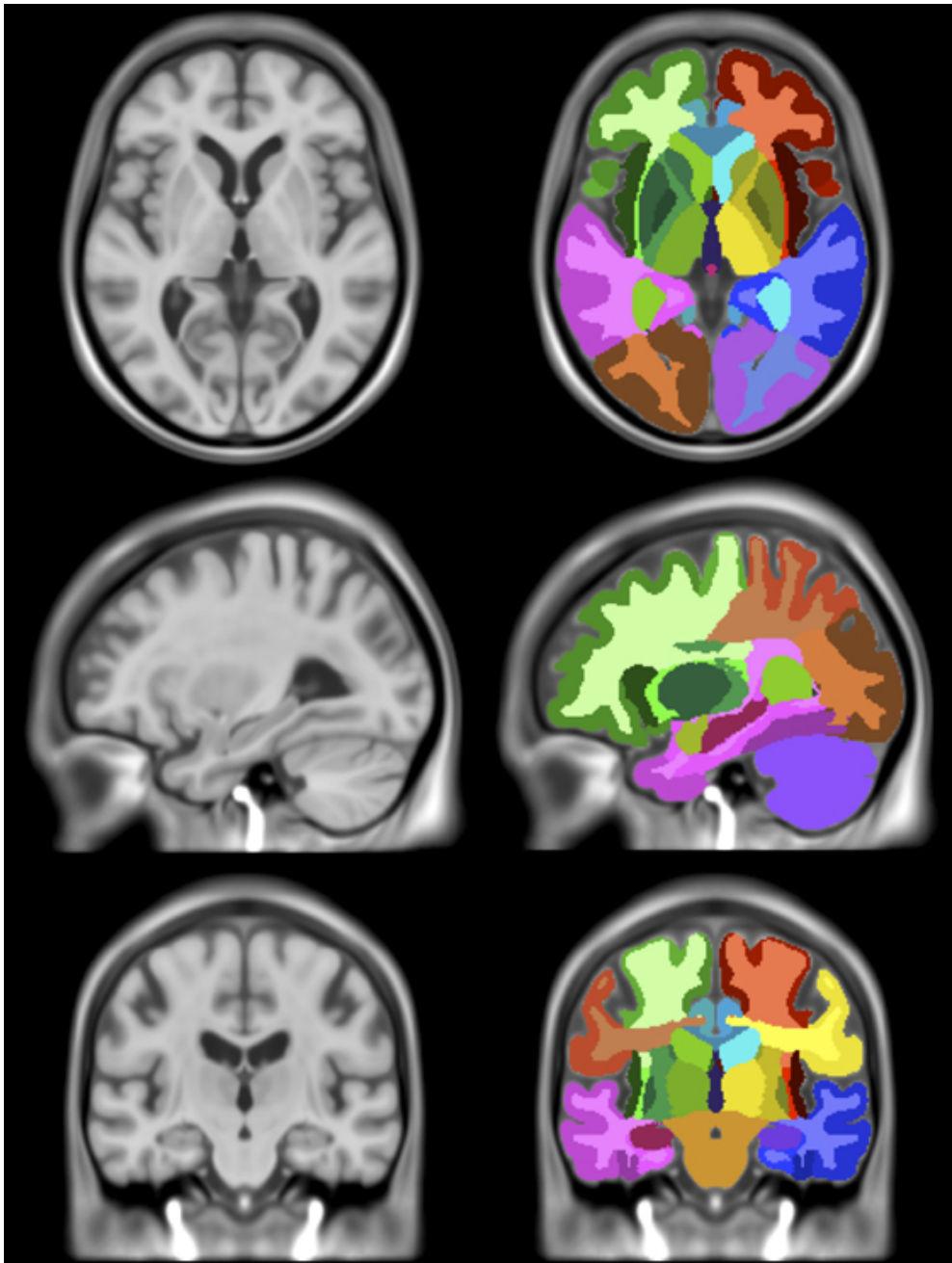
All participants signed an informed consent. The AGES-Reykjavik study was approved by the Intramural Research Program of the National Institute on Aging, the National Bioethics Committee in Iceland (VSN00-063), the Icelandic Data Protection Authority, and the institutional review board of the U.S. National Institute on Aging, National Institutes of Health.

Acquisition and post processing of MRI

MRI was performed in the Icelandic Heart Association Research Institute on a 1.5-T Signa Twinspeed system (General Electric Medical Systems) MRI scanner with 8-channel head coil (General Electric Medical Systems, Waukesha, WI). The image protocol, described previously (Sveinbjornsdottir et al. 2008), included whole brain axial T1-weighted 3-dimensional, FSE PD/T2, and FLAIR sequences, with the same acquisition parameters at both time points. Scans were processed with a fully automated segmentation pipeline described previously (Sigurdsson et al. 2012). Preprocessing of the images included inter slice intensity normalization, noise reduction, and correction for intensity nonuniformity. The pipeline combined the use of a regional probabilistic atlas (figure 1), created with a large sample of the AGES-Reykjavik study ($N = 314$), with a multispectral tissue segmentation method. The atlas was warped non-linearly to the T1-weighted images of each study participant, where the intersection of regional delineation by the atlas with the results from the tissue segmentation was used to calculate the volumes of the regions of interest. The manual segmentation protocols for MTL and BG, used to create the probabilistic atlas, are reported in the appendix.

Substructure volumes of MTL, i.e., amygdala and hippocampus, and substructures of BG, i.e., caudate nucleus, putamen, accumbens, globus pallidus, and thalamus were combined. By combining substructures we reduced the possibility that volume loss due to observational noise in one substructure became volume gain in the adjacent substructure.

Figure 1: Brain regions of the probabilistic atlas in the AGES-Reykjavik atlas



ICV was defined as the sum of CSF, total gray and white matter, and white matter lesion volume.

Validation

Performance of the automated segmentation pipeline of AGES-Reykjavik study was validated against four scans that were manually segmented into different brain regions. Dice-kappa scores were calculated for each region (caudate nucleus: 0.93, putamen: 0.87, accumbens: 0.69, pallidus: 0.66, thalamus: 0.92, hippocampus: 0.79, amygdala: 0.79).

Risk factors and covariates

All covariates and risk factors were measured at baseline. Education level (college or university education versus lower education), smoking history (never, former, or current smoker), and alcohol intake history (never, former or current drinker) were assessed by questionnaire. Body mass index (BMI) was calculated as current weight divided by squared midlife height (taken from data of the Reykjavik Study examination that occurred 25 years (SD = 4.2) earlier). Blood pressure was measured at baseline, 216 (59%) participants were using antihypertensive medication and 152 (41%) were unmedicated. Diabetes was defined as a history of physician diagnosed diabetes, use of glucose-modifying medication, or fasting blood glucose of ≥ 7.0 mmol/L. MRI infarct-like lesions were identified by trained radiographers as defects in the brain parenchyma with a maximal diameter of at least 4 mm and associated with hyperintensity on T2 and fluid-attenuated inversion recovery images. For lesions in the cerebellum and brain stem or lesions with cortical involvement, no size criterion was required. APOE genotype was successfully determined in 366 participants (Eiriksdottir et al. 2006). Participants were classified by genotype into 3 groups having either one or two APOE $\epsilon 2$ alleles (22, 23), two APOE $\epsilon 3$ alleles (33), or one or two APOE $\epsilon 4$ alleles (34, 44). Participants with one APOE $\epsilon 2$ allele and one APOE $\epsilon 4$ (24) were excluded from the analysis ($N = 5$).

Statistical analysis

Characteristics of the study sample were compared with characteristics of the rest of the AGES-Reykjavik sample that underwent MR scanning ($N = 4246$). The study sample was on average younger (mean 75.5 (SD = 5.3) [range 67–90 yo] vs. mean 76.5 (SD = 5.5) [range 66–98 yo], $p = 0.001$), had lower volume of WML (mean 18.7 (SD = 19.1) vs. mean 21.0 (SD = 21.1), $p = 0.03$) and higher MMSE score (median 28 (20th

percentile = 26, 80th percentile = 29) vs. median 27 (20th percentile = 24, 80th percentile = 29), $p < 0.0001$) (Table 1).

The change in volume of BG and MTL were calculated as annualized percent change as follows:

$$\frac{\text{Volume } Time_2 - \text{Volume } Time_1}{\text{Volume } Time_1 \times (Time_2 - Time_1)} \times 100$$

Mean baseline and follow-up BG and MTL volumes (unadjusted for ICV) and mean annualized percent change in BG and MTL volumes were calculated for the total sample and for women and men separately (table 2). Pearson correlations of baseline BG and MTL volumes with follow-up volumes and with annualized percent changes were also calculated (last two columns of table 2).

Differences in baseline volume and annualized percent change of BG and MTL among groups with different APOE genotype (33, and 34/44, and 23/22), smoking and alcohol status (never, former, current), presence of diabetes and MRI infarct-like lesions were assessed in a general linear model. Continuous variables, i.e., age, BMI, LDL, HDL, glucose, and blood pressure levels, were transformed into z-scores, so coefficients from the different risk factors could be compared. Furthermore, continuous variables were also dichotomized at the median value for age and WML or according to clinically relevant thresholds: BMI ≥ 25 kg/m², LDL ≥ 4.1 mmol/L, HDL < 1.03 mmol/L for men and < 1.30 mmol/L for women, glucose level > 5.6 mmol/L, systolic blood pressure ≥ 140 mmHg, diastolic blood pressure ≥ 90 mmHg. Relations between the continuous variables (z-scored) and dichotomized variables were assessed in a general linear model. Models with baseline BG or MTL volumes as dependent variable were adjusted for age (as a continuous variable), sex, and ICV. Since annualized percent change in MTL volume was significantly related to MTL volume at baseline (table 2), models with annualized percent change in BG or MTL as dependent variables were additionally adjusted for baseline volume of BG or MTL respectively. Models for associations with LDL and HDL level were also adjusted for the use of statins. Models for associations with systolic and diastolic blood pressure were also adjusted for the use of antihypertensive medication.

To assess whether the relations of blood pressure with baseline and percent change in MTL and BG volumes were altered by the use of antihypertensive medication, the interaction terms between blood pressure and use of hypertensive medication were evaluated in these models. Also, to assess whether the relations of blood pressure and different APOE genotypes with baseline volumes and percent changes of BG and MTL varied by age, the interaction terms between age and blood pressure and age and APOE genotype were evaluated in these models. Moreover, to see whether the relations of blood pressure with baseline and percent change of BG and MTL atrophy were potentially driven by APOE genotype, the interaction term between blood pres-

Table 1: Characteristics of AGES-Reykjavik and MRI follow-up samples

| Characteristics, Mean (SD) ^a | AGES Reykjavik (N = 4246) | Study sample (N = 368) | p ^b |
|-----------------------------------------|------------------------------|---------------------------|----------------|
| Age | 76.5 (5.5) | 75.5 (5.3) | 0.001 |
| Women, % (N) | 58 (2464) | 59 (216) | 0.85 |
| intracranial volume (cm ³) | 1501 (148) | 1501 (150) | 0.86 |
| Apo E genotype, % (N) | | | |
| 33 | 63 (2623) | 61 (223) | |
| 34/44 | 27 (1096) | 27 (98) | 0.67 |
| 22/23 | 10 (403) | 11 (40) | |
| High Education, % (N) | 11 (457) | 12 (43) | 0.65 |
| Dementia, % (N) | 5 (202) | 0 (0) | |
| MMSE score | 26.5 (3.1) | 27.5 (1.8) | <.0001 |
| Body mass index (kg/m ²) | 26.9 (4.4) | 27.1 (4.1) | 0.58 |
| Serum low-density lipoprotein (mmol/L) | 3.49 (1.04) | 3.59 (1.04) | 0.08 |
| Serum high-density lipoprotein (mmol/L) | 1.60 (0.45) | 1.60 (0.44) | 0.95 |
| Smoking status, % (N) | | | |
| Never | 43 (1824) | 46 (172) | |
| Former | 45 (1898) | 44 (163) | 0.12 |
| Current | 12 (521) | 9 (33) | |
| Alcohol intake, % (N) | | | |
| Never | 23 (955) | 21 (78) | |
| Former | 12 (523) | 9 (33) | 0.09 |
| Current | 65 (2728) | 69 (255) | |
| Diabetes, % (N) | 11 (475) | 11 (41) | 0.95 |
| Glucose | 5.75 (1.14) | 5.80 (1.36) | 0.56 |
| White matter lesions (cm ³) | 21.0 (21.1) | 18.7 (19.1) | 0.03 |
| MRI infarct-like lesions, % (N) | 31 (1320) | 30 (110) | 0.68 |
| Hypertension ^c | 52 (2222) | 54 (198) | 0.63 |
| Systolic blood pressure (mmHg) | 142.3 (20.5) | 143.1 (19.2) | 0.44 |
| Diastolic blood pressure (mmHg) | 73.8 (9.6) | 74.5 (9.8) | 0.15 |

a or percentage (N) if stated

b from *t*-test for continuous variables and χ^2 test for class variables

c defined as systolic blood pressure ≥ 140 and or diastolic blood pressure ≥ 90

Table 2: Descriptive statistics for BG and MTL baseline and follow-up volumes and annualized percent change

| Region of interest | Descriptive measures | | | Pearson's correlations between: | | |
|----------------------|------------------------------------|-------------------------------------|-----------|---------------------------------|----------------------------------|------------------------------|
| | Baseline volume in cm ³ | Follow-up volume in cm ³ | Mean (SD) | % change | Baseline volume follow-up volume | Baseline volume and % change |
| Basal ganglia | | | | | | |
| All | 35.4 (3.3) | 34.9 (3.3) | | -0.57 (0.85) | 0.98** | -0.038 |
| Women | 34.4 (2.9) | 34.0 (3.0) | | -0.48 (0.78) | 0.98** | 0.028 |
| Men | 36.9 (3.3) | 36.2 (3.3) | | -0.69 (0.92) | 0.97** | -0.014 |
| Medial temporal lobe | | | | | | |
| All | 10.6 (1.1) | 10.4 (1.2) | | -0.83 (1.03) | 0.98** | 0.14* |
| Women | 10.2 (1.0) | 10.0 (1.0) | | -0.78 (1.03) | 0.97** | 0.21* |
| Men | 11.2 (1.1) | 11.0 (1.1) | | -0.92 (1.04) | 0.97** | 0.18* |

Baseline volume and follow-up volume, raw volume unadjusted for intracranial volume; % change, annualized percent change computed with formula: $100 \times (\text{volume}_{\text{time}_2} - \text{volume}_{\text{time}_1}) / (\text{volume}_{\text{time}_1} \times (\text{time}_2 - \text{time}_1))$.

* $p < 0.05$; ** $p < 0.0005$.

sure and APOE genotype was tested. Lastly, we tested a three-way interaction term (*age* × *presence of high blood pressure* × *APOE genotype*). All interaction terms were found nonsignificant (all *p*-values > 0.32), therefore they were not included in the models of which the results are displayed in table 4 and table 3.

Finally, we tested the association of annualized percent change in BG and MTL volumes in two separate models with all covariates and risk factors variables (age, sex, APOE genotype, diabetes, smoking status, alcohol status, MRI infarct-like lesions, and z-scores of BMI, HDL, WML, and blood pressure) entered simultaneously. Because of collinearity, separate full risk factor models were made for systolic and diastolic blood pressure. Statistical analyses were conducted with R 2.11.1 (R Core Team 2010). A two-sided alpha level of 0.05 was considered significant.

RESULTS

The sample consisted of 368 participants with a mean age of 75.5 (SD = 5.3 years; range 67–90 years) and 58.7% were women. Mean baseline volume of the BG was 35.4 cm³ (SD = 3.3) and average annualized percent change in BG was –0.57% per year (–0.5 cm³/year). Mean baseline volume of the MTL was 10.6 cm³ (SD = 1.1) and average annualized percent change in MTL was –0.83%/year (–0.2 cm³/year). Men had a significantly larger decrease in BG compared to women (–0.69%/year vs. –0.48%/year, *p* = 0.02). Annualized percent change in MTL did not differ among men and women (Table 2).

Analysis of baseline volumes

Baseline volumes of BG and MTL were associated with few risk factors (Table 4): a smaller volume of BG was found among older participants, participants with BMI below 25 and participants with WML below median value. A smaller volume of MTL was associated with older participants, participants with BMI below 25, current smokers, participants without MRI infarct-like lesions and participants with fasting glucose level below 5.6 mmol/L. Neither BG nor MTL baseline volumes were associated with blood pressure levels or APOE genotype.

Table 3: Association of BG and MTL baseline volume with vascular risk factors

| Risk factors | N | Basal ganglia volume (cm ³) | | MTL volume (cm ³) | |
|-----------------------------|-----|-----------------------------------------|-------------------|-------------------------------|-------------------|
| | | Mean (SD) ^a | p ^b | Mean (SD) ^a | p ^b |
| Age continuous | | -0.62 (0.14) ^c | <.0001 | -0.22 (0.04) ^c | <.0001 |
| < 75 ^d years old | 169 | 35.9 (3.1) | 0.001 | 10.8 (1.0) | <.0001 |
| ≥ 75 years old | 199 | 35.0 (3.4) | | 10.5 (1.2) | |
| APOE | | | | | |
| 33 | 223 | 35.3 (3.5) | | 10.6 (1.2) | |
| 34/44 | 98 | 35.6 (3.0) | 0.7 | 10.7 (1.1) | 0.74 |
| 23/22 | 40 | 35.8 (3.0) | | 10.7 (1.2) | |
| Body mass index continuous | | 0.55 (0.14) ^c | <.0001 | 0.22 (0.04) ^c | <.0001 |
| < 25 kg/m ² | 141 | 34.5 (3.1) | 0.003 | 10.3 (1.1) | 0.0001 |
| ≥ 25 kg/m ² | 225 | 36.0 (3.3) | | 10.9 (1.1) | |
| LDL continuous | | -0.01 (0.17) ^{c,e} | 0.96 ^e | 0.05 (0.05) ^{c,e} | 0.34 ^e |
| < 4.1 mmol/L | 261 | 35.6 (3.3) | 0.56 ^e | 10.7 (1.2) | 0.40 ^e |
| ≥ 4.1 mmol/L | 107 | 35.0 (3.4) | | 10.5 (1.1) | |
| HDL continuous | | -0.19 (0.15) ^{c,e} | 0.20 ^e | -0.09 (0.05) ^{c,e} | 0.06 ^e |
| Low | 23 | 35.4 (3.3) | 0.21 ^e | 10.7 (1.2) | 0.95 ^e |
| High | 345 | 35.8 (3.5) | | 10.6 (1.0) | |
| Smoking | | | | | |
| Never | 172 | 35.1 (3.3) | | 10.6 (1.1) | |
| Former | 163 | 35.8 (3.2) | 0.3 | 10.7 (1.2) | 0.006 |
| Current | 33 | 34.8 (3.4) | | 10.4 (1.0) | |
| Alcohol intake | | | | | |
| Never | 78 | 34.7 (2.9) | | 10.3 (1.0) | |
| Former | 33 | 36.0 (2.8) | 0.54 | 10.9 (1.0) | 0.48 |
| Current | 255 | 35.5 (2.8) | | 10.7 (1.2) | |
| Diabetes | | | | | |
| No diabetes | 327 | 35.4 (3.3) | 0.45 | 10.6 (1.1) | 0.29 |
| Diabetes | 41 | 35.5 (3.0) | | 10.9 (1.1) | |

Continued on next page

LDL, serum low-density lipoprotein; HDL, serum high-density lipoprotein

a raw means (unadjusted for age, sex and ICV), or beta (standard error) if stated

b *p*-value from general linear model corrected for age, sex, ICV; for continuous variables z-scores were used

c beta (standard error) from general linear model corrected for age, sex, and ICV

d cut off at median value

e additionally adjusted for use of statins

Table 3 – continued from previous page

| Risk factors | N | Basal ganglia volume (cm ³) | | MTL volume (cm ³) | |
|-------------------------------------|-----|-----------------------------------------|-------------------|-------------------------------|-------------------|
| | | Mean (SD) ^a | p ^b | Mean (SD) ^a | p ^b |
| Fasting glucose continuous | | −0.12 (0.14) ^c | 0.41 | −0.002 (0.04) ^c | 0.96 |
| < 5.6 mg/dL | 192 | 35.1 (3.1) | 0.59 | 10.5 (1.1) | 0.04 |
| ≥ 5.6 mg/dL | 176 | 35.7 (3.5) | | 10.8 (1.2) | |
| WML continuous | | 0.34 (0.15) ^c | 0.02 | 0.06 (0.05) ^c | 0.19 |
| < 12.5 ^d cm ³ | 184 | 34.8 (3.2) | 0.0004 | 10.5 (1.1) | 0.49 |
| ≥ 12.5 cm ³ | 184 | 36.1 (3.3) | | 10.8 (1.2) | |
| MRI infarct-like lesions | | | | | |
| No | 258 | 35.4 (3.2) | 0.99 | 10.6 (1.1) | 0.007 |
| Yes | 110 | 35.4 (3.5) | | 10.8 (1.2) | |
| Systolic BP continuous | | 0.05 (0.14) ^{c,e} | 0.73 ^e | −0.01 (0.05) ^{c,e} | 0.75 ^e |
| < 140 mmHg | 171 | 35.2 (3.1) | 0.44 ^e | 10.6 (1.1) | 0.88 ^e |
| ≥ 140 mmHg | 197 | 35.6 (3.4) | | 10.7 (1.2) | |
| Diastolic BP continuous | | 0.28 (0.15) ^{c,e} | 0.06 ^e | −0.02 (0.05) ^{c,e} | 0.68 ^e |
| < 90 mmHg | 343 | 35.3 (3.3) | 0.07 ^e | 10.6 (1.1) | 0.99 ^e |
| ≥ 90 mmHg | 25 | 37.2 (3.4) | | 11.0 (1.5) | |

WML, white matter lesions; BP, blood pressure

a raw means (unadjusted for age, sex and ICV), or beta (standard error) if stated

b *p*-value from general linear model corrected for age, sex, ICV; for continuous variables z-scores were used

c beta (standard error) from general linear model corrected for age, sex, and ICV

d cut off at median value

e additionally adjusted for use of antihypertensive medication

Analysis of volume change over the 2.4 year period

Basal Ganglia

Annualized percent change in BG was not associated with age or any vascular risk factors except systolic blood pressure (Table 4). Participants with systolic blood pressure ≥ 140 mmHg had a steeper decline ($\Delta = -0.23\%/yr$, $p = 0.03$). However, in the full risk factor model, none of the risk factors showed a significant association with BG percent change.

Medial Temporal Lobe

Annualized percent change in MTL was linearly associated with age (β (SE) = -0.167 (0.052), $p < 0.001$) and was steeper in participants ≥ 75 years compared to younger

Table 4: Association of annualized percent change in BG and MTL volume with vascular risk factors

| Risk factors | N | Basal ganglia Mean (SD) | p ^a | Medial temporal lobe Mean (SD) | p ^a |
|---------------------------------------------|-----|-------------------------------|-------------------|-----------------------------------|-------------------|
| Age | | | | | |
| < 75 years old (median value) | 169 | -0.060 (0.045) ^b | 0.18 | -0.167 (0.052) ^b | 0.001 |
| ≥ 75 years old | 199 | -0.53 (0.79) | 0.65 | -0.65 (1.00) | 0.04 |
| Apo E genotype | | | | | |
| 33 | 223 | -0.54 (0.86) | 0.12 | -0.69 (0.88) | <0.0001 |
| 34 or 44 | 98 | -0.66 (0.80) | | -1.16 (1.23) | |
| 23 or 22 | 40 | -0.41 (0.88) | | -0.70 (0.91) | |
| Body mass index | | | | | |
| < 25 kg/m ² | 141 | 0.004 (0.046) ^b | 0.93 | 0.061 (0.054) ^b | 0.93 |
| ≥ 25 kg/m ² | 225 | -0.58 (0.79) | 0.58 | -0.98 (1.16) | 0.27 |
| | | -0.55 (0.88) | | -0.72 (0.92) | |
| Diabetes | | | | | |
| No diabetes | 327 | -0.55 (0.83) | 0.51 | -0.82 (1.06) | 0.67 |
| Diabetes | 41 | -0.69 (0.94) | | -0.89 (0.83) | |
| Serum low-density lipoprotein | | | | | |
| < 4.1 mmol/L | 261 | -0.025 (0.052) ^{b,c} | 0.63 ^c | 0.091 (0.059) ^{b,c} | 0.13 ^c |
| ≥ 4.1 mmol/L | 107 | -0.57 (0.89) | 0.94 ^c | -0.88 (1.08) | 0.34 ^c |
| | | -0.55 (0.73) | | -0.67 (0.89) | |
| Serum high-density lipoprotein ^d | | | | | |
| Low | 23 | -0.012 (0.046) ^{b,c} | 0.79 ^c | -0.043 (0.052) ^{b,c} | 0.42 ^c |
| High | 345 | -0.43 (0.80) | 0.45 ^c | -0.77 (1.20) | 0.86 ^c |
| | | -0.59 (0.85) | | -0.84 (1.01) | |

Continued on next page

a p from general linear model corrected for age, sex, ICV, baseline volume; b β (standard error) from general linear model corrected for age, sex, ICV, and baseline volume; c additionally adjusted for use of statins; d threshold for women low: HDL < 1.30 mmol/L and high: ≥ 1.30 mmol/L, for men low: < 1.03 mmol/L and high: ≥ 1.03 mmol/L.

Table 4 – continued from previous page

| Risk factors | N | Basal ganglia Mean (SD) | p ^a | Medial temporal lobe Mean (SD) | p ^a |
|---------------------------------------|-----|-------------------------------|-------------------|-----------------------------------|--------------------|
| Smoking status | | | | | |
| Never | 172 | -0.47 (0.83) | | -0.68 (0.95) | |
| Former | 163 | -0.64 (0.88) | 0.36 | -0.99 (1.06) | 0.13 |
| Current | 33 | -0.66 (0.86) | | -0.87 (1.19) | |
| Alcohol intake | | | | | |
| Never | 78 | -0.41 (0.82) | | -0.69 (1.13) | |
| Former | 33 | -0.54 (0.82) | 0.41 | -0.89 (0.90) | 0.48 |
| Current | 255 | -0.62 (0.86) | | -0.86 (1.02) | |
| Fasting glucose | | | | | |
| < 5.6 mg/dL | 192 | -0.081 (0.044) ^b | 0.06 | -0.056 (0.052) ^b | 0.25 |
| ≥ 5.6 mg/dL | 176 | -0.57 (0.79) | 0.55 | -0.91 (1.10) | 0.25 |
| White matter lesions volume | | | | | |
| < 12.5 cm ³ (median value) | 184 | -0.52 (0.72) | 0.88 | -0.67 (0.96) | 0.08 |
| ≥ 12.5 cm ³ | 184 | -0.61 (0.95) | | -0.99 (1.08) | |
| MRI infarct-like lesions | | | | | |
| No | 258 | -0.52 (0.82) | 0.28 | -0.78 (1.01) | 0.34 |
| Yes | 110 | -0.68 (0.89) | | -0.95 (1.09) | |
| Systolic blood pressure | | | | | |
| < 140 mmHg | 171 | -0.080 (0.045) ^{b,c} | 0.08 ^c | -0.155 (0.051) ^{b,c} | 0.003 ^c |
| ≥ 140 mmHg | 197 | -0.44 (0.78) | 0.03 ^c | -0.72 (0.98) | 0.16 ^c |
| Diastolic blood pressure | | | | | |
| < 90 mmHg | 343 | -0.015 (0.047) ^{b,c} | 0.74 ^c | -0.143 (0.053) ^{b,c} | 0.008 ^c |
| ≥ 90 mmHg | 25 | -0.55 (0.85) | 0.30 ^c | -0.81 (1.03) | 0.10 ^c |
| | | -0.77 (0.83) | | -1.15 (1.11) | |

a p from general linear model corrected for age, sex, ICV, baseline volume; b β (standard error) from general linear model corrected for age, sex, ICV, and baseline volume; c additionally adjusted for use of antihypertensive medication.

participants ($\Delta = -0.34\%/yr$, $p = 0.04$). There was significantly more annualized decline in MTL volumes in carriers of the APOE genotype 34/44 ($\Delta = -0.47\%/yr$, $p < 0.0001$) and a steeper decline in MTL volume with increasing systolic ($p = 0.003$) and diastolic ($p = 0.008$) blood pressure. Furthermore, in the full risk factor model for MTL volume change, APOE $\epsilon 4$ (β (SE) = -0.47 (0.11), $p < 0.0001$), systolic and diastolic blood pressure remained significantly associated with a steeper decrease in volume of MTL.

Interaction terms

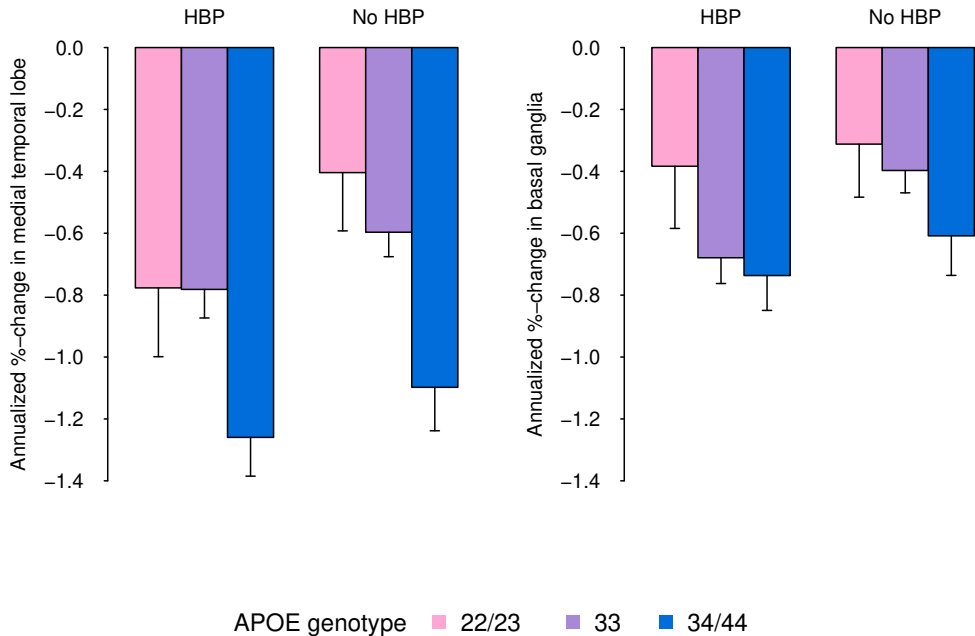
All potential relevant interaction terms, including all possible combinations between age, blood pressure and APOE genotype, were found nonsignificant (all p -values > 0.32). In figure 2 we show combined effects of high blood pressure and APOE genotype for mean values of annualized percent change in BG and MTL adjusted for age, sex, and ICV. Change in BG and MTL volumes were higher among hypertensive participants compared to non-hypertensive participants, however, we found no evidence for an interaction with APOE genotype.

DISCUSSION

In the present follow-up study we investigated the influence of late life exposure to vascular risk factors on MTL and BG atrophy rates. Neurodegeneration of MTL and BG are both associated with cognitive impairment with ageing, we therefore expected both structures to show increased atrophy rates in the presence of well-known vascular risk factors in this sample of non-demented older people. However, MTL and BG volume changes showed different susceptibility to vascular risk factors. MTL volume decline over 2.4 years was significantly steeper 1) as systolic and diastolic blood pressures increased and 2) in carriers of the APOE $\epsilon 4$ allele. In contrast, BG volume loss was slightly higher in participants with high systolic blood pressure, but was not associated with any of the other vascular risk factors that were investigated.

The association of higher blood pressure in late life with increased MTL atrophy rates is important. MTL atrophy may form (part of) the neuropathological basis leading to cognitive decline in older people, and the results of the present study suggest controlling high blood pressure in late life may limit MTL atrophy. Additionally, we showed that systolic and diastolic blood pressure and APOE $\epsilon 4$ independently increased MTL atrophy. Mechanisms linking high blood pressure and APOE $\epsilon 4$ to increased MTL atrophy are under investigation. High blood pressure has been associated with decreased perfusion in the brain in men (Waldstein et al. 2010), which may play a pathogenic role in brain

Figure 2: Combined effects of hypertension and Apo E genotype on MTL volume decline



atrophy. The APOE polymorphism in its turn is known to affect serum lipid levels, and to play a role in regeneration and re-myelination of axons (Mahley and Rall 2000). APOE $\epsilon 4$ carriers are assumed to be less effective in protecting neurons from excessive damage and have a reduced regenerative capacity.

Although some studies with cross-sectional design show diminished MTL volumes with high blood pressure (den Heijer, Launer, et al. 2005; Korf, Scheltens, et al. 2005; Lu et al. 2011), others failed to show this association, especially those that study late-life risk factor exposure (Gattringer et al. 2012). This discrepancy is also visible in our results. The cross-sectional analysis did not show any difference in baseline MTL volume with higher blood pressure or presence of APOE $\epsilon 4$ compared to the rest of the sample. Possibly this discrepancy is related to study sample composition. It is known that in preclinical dementia, blood pressure tends to go down while brain atrophy is already ongoing (Qiu et al. 2004). These effects may have distorted the cross-sectional analysis since populations of non-demented subjects consist of healthy and undiagnosed individuals (Tolppanen et al. 2012). One of the strengths of the present study was therefore the availability of follow-up data.

Although several reports have been written on the susceptibility of BG to hypertension-related SVD and arteriolosclerosis, in this study no consistent associations were found between vascular risk factors and changes in volume of the BG. We did find a trend of increased loss of BG volume with higher systolic blood pressure but this was only significant when systolic blood pressure was taken as a dichotomous variable. Possibly the weak association is due to slight increased atrophy of BG secondary to global brain atrophy. Men displayed a steeper decline in BG volume than women, which has also been reported in other studies, in particular for the putamen (Coffey et al. 1998; Nunnemann et al. 2009).

What might explain the contrast in vascular risk profile between the MTL and BG? Possibly this is related to the difference in vascular anatomy of the two regions. BG are supplied by the lenticulostriate and thalamic arteries, which are branching directly from the medial and posterior cerebral artery (Cho et al. 2008; Schmahmann 2003). As a consequence, the hydrostatic pressure in the circle of Willis is directly translated into the small, thin-walled arteries and arterioles of the BG. On the one hand, this makes these vessels vulnerable for hypertension-induced arteriolosclerosis that can give rise to hemorrhages and lacunar infarcts in the BG. On the other hand, due to the relatively high hydrostatic pressure, perfusion pressure in these vessels, even if affected by arteriolosclerosis, is maintained. This is different for the MTL, which is perfused by fine leptomeningeal vessels that arise after gradual branching from the posterior cerebral artery, anterior choroidal artery (to a lesser degree), and medial cerebral artery (amygdala) (Duvernoy 2005). The hydrostatic pressure in the leptomeningeal vessels is relatively low as a consequence of the gradual branching, making them relatively immune for the development of arteriolosclerosis. Excessive central pressure, however, has been associated with micro vascular remodeling that increases resting resistance and hyperemic reserve (Mitchell et al. 2005). It may be hypothesized that high blood pressure gives rise to hypoperfusion of MTL as a consequence of this remodeling, resulting in widespread atrophy and changes of the tissue composition. Moreover, hippocampus is known for its sensitivity to ischemia (Atlas 1996) and hypoperfusion may particularly affect the volume of this structure. More studies are needed to investigate the relation between higher blood pressure and effects on perfusion of cerebral regions.

Regarding the other vascular risk factors that were studied, we observed positive associations of baseline volumes of both BG and MTL with BMI, of WML with BG, and of MRI infarct-like lesions and blood glucose with MTL. These associations are not readily explained and may require further investigation. For BMI it has been shown that obesity in midlife is a risk factor for the development of AD (M Kivipelto et al. 2005), however, later in life similar age-related volumetric changes in the brain were found similar in obese vs. nonobese (Driscoll et al. 2012). Moreover, it is known that

individuals who are CSF $A\beta$ -positive, PiB-positive, or have an elevated tau/ $A\beta$ ratio have lower mean BMI than $A\beta$ -negative individuals (Vidoni et al. 2011). Therefore, as with the cross-sectional analysis of blood pressure and APOE genotype, these associations may be distorted by the presence of undiagnosed preclinical dementia in this non-demented sample.

A limitation of our study was the relatively short duration of follow-up and therefore we could not determine the effects of vascular risk factors on MTL and BG atrophy over a longer term. Yet, the observed significant associations with MTL volume change suggest the duration of the study was sufficient enough to detect unmistakably different effects of vascular risk factors on BG and MTL volume decline.

CONCLUSION

Higher systolic and diastolic blood pressures, and the presence of APOE $\epsilon 4$, were independently associated with a steeper decline in volume of MTL over 2.4 years in older people. In contrast, atrophy rate of BG was not associated with the vascular risk factors. Although BG are a site of frequent manifestations of SVD, their distinct vascularization possibly leads to relative preservation of perfusion in the presence of vascular risk factors.

BIBLIOGRAPHY

- American Psychiatric Association (1994). *Diagnostic and statistical manual of mental disorders DSM-IV (4th ed.)* Washington, DC: Authors.
- Atlas SW (1996). *Magnetic resonance imaging of the brain and spine*. Philadelphia, PA: Lippincott Williams & Wilkins.
- Barnes J, Bartlett JW, van de Pol LA, Loy CT, Scahill RI, et al. (2009). "A meta-analysis of hippocampal atrophy rates in Alzheimer's disease". *Neurobiol. Aging* 30(11): 1711–1723. DOI: [10.1016/j.neurobiolaging.2008.01.010](https://doi.org/10.1016/j.neurobiolaging.2008.01.010).
- Cho ZH, Kang CK, Han JY, Kim SH, Kim KN, et al. (2008). "Observation of the lenticulostriate arteries in the human brain in vivo using 7.0T MR angiography". *Stroke* 39(5): 1604–1606. DOI: [10.1161/STROKEAHA.107.508002](https://doi.org/10.1161/STROKEAHA.107.508002).
- Coffey CE, Lucke JF, Saxton JA, Ratcliff G, Unitas LJ, et al. (1998). "Sex differences in brain aging: a quantitative magnetic resonance imaging study". *Arch. Neurol.* 55(2): 169–179. DOI: [10.1001/archneur.55.2.169](https://doi.org/10.1001/archneur.55.2.169).
- de Jong LW, van der Hiele K, Veer IM, Houwing JJ, Westendorp RG, et al. (2008). "Strongly reduced volumes of putamen and thalamus in Alzheimer's disease: an MRI study". *Brain* 131(12): 3277–3285. DOI: [10.1093/brain/awn278](https://doi.org/10.1093/brain/awn278).

- de Jong LW, Wang Y, White LR, Yu B, van Buchem MA, and Launer LJ (2012). "Ventral striatal volume is associated with cognitive decline in older people: a population based MR-study". *Neurobiol. Aging* 33 (2): 1–10. DOI: [10.1016/j.neurobiolaging.2010.09.027](https://doi.org/10.1016/j.neurobiolaging.2010.09.027).
- Debette S, Seshadri S, Beiser A, Au R, Himali JJ, et al. (2011). "Midlife vascular risk factor exposure accelerates structural brain aging and cognitive decline". *Neurology* 77 (5): 461–468. DOI: [10.1212/WNL.0b013e318227b227](https://doi.org/10.1212/WNL.0b013e318227b227).
- den Heijer T, Launer LJ, Prins ND, van Dijk EJ, Vermeer SE, et al. (2005). "Association between blood pressure, white matter lesions, and atrophy of the medial temporal lobe". *Neurology* 64 (2): 263–267. DOI: [10.1212/01.WNL.0000149641.55751.2E](https://doi.org/10.1212/01.WNL.0000149641.55751.2E).
- den Heijer T, Oudkerk M, Launer LJ, van Duijn CM, Hofman A, and Breteler MM (2002). "Hippocampal, amygdalar, and global brain atrophy in different apolipoprotein E genotypes". *Neurology* 59 (5): 746–748. DOI: [10.1212/WNL.59.5.746](https://doi.org/10.1212/WNL.59.5.746).
- Driscoll I, Beydoun MA, An Y, Davatzikos C, Ferrucci L, et al. (2012). "Midlife obesity and trajectories of brain volume changes in older adults". *Hum. Brain Mapp.* 33 (9): 2204–2210. DOI: [10.1002/hbm.21353](https://doi.org/10.1002/hbm.21353).
- Duvernoy HM (2005). *The human hippocampus: functional anatomy, vascularization and serial sections with MRI*. Berlin: Springer-Verlag.
- Eiriksdottir G, Aspelund T, Bjarnadottir K, Olafsdottir E, Gudnason V, et al. (2006). "Apolipoprotein E genotype and statins affect CRP levels through independent and different mechanisms: AGES-Reykjavik Study". *Atherosclerosis* 186 (1): 222–224. DOI: [10.1016/j.atherosclerosis.2005.12.012](https://doi.org/10.1016/j.atherosclerosis.2005.12.012).
- Gattringer T, Enzinger C, Ropele S, Gorani F, Petrovic KE, et al. (2012). "Vascular risk factors, white matter hyperintensities and hippocampal volume in normal elderly individuals". *Dement. Geriatr. Cogn. Disord.* 33 (1): 29–34. DOI: [10.1159/000336052](https://doi.org/10.1159/000336052).
- Gouw AA, Seewann A, van der Flier WM, Barkhof F, Rozemuller AM, et al. (2011). "Heterogeneity of small vessel disease: a systematic review of MRI and histopathology correlations". *J. Neurol. Neurosurg. Psychiatr.* 82 (2): 126–135. DOI: [10.1136/jnnp.2009.204685](https://doi.org/10.1136/jnnp.2009.204685).
- Harris TB, Launer LJ, Eiriksdottir G, Kjartansson O, Jonsson PV, et al. (2007). "Age, Gene/Environment Susceptibility-Reykjavik Study: multidisciplinary applied phenomics". *Am. J. Epidemiol.* 165 (9): 1076–1087. DOI: [10.1093/aje/kwk115](https://doi.org/10.1093/aje/kwk115).
- Kivipelto M. and Helkala EL, Laakso MP, Hänninen T, Hallikainen M, Alhainen K, et al. (2001). "Midlife vascular risk factors and Alzheimer's disease in later life: longitudinal, population based study". *BMJ* 322 (7300): 1447–1451. DOI: [10.1136/bmj.322.7300.1447](https://doi.org/10.1136/bmj.322.7300.1447).
- Kivipelto M, Ngandu T, Fratiglioni L, Viitanen M, Kareholt I, et al. (2005). "Obesity and vascular risk factors at midlife and the risk of dementia and Alzheimer disease". *Arch. Neurol.* 62 (10): 1556–1560. DOI: [10.1001/archneur.62.10.1556](https://doi.org/10.1001/archneur.62.10.1556).
- Korf ESC, Scheltens P, Barkhof F, and de Leeuw FE (2005). "Blood pressure, white matter lesions and medial temporal lobe atrophy: closing the gap between vascular pathology and

- Alzheimer's disease?" *Dement. Geriatr. Cogn. Disord.* 20 (6): 331–337. DOI: [10.1159/000088464](https://doi.org/10.1159/000088464).
- Korf ESC, White LR, Scheltens P, and Launer LJ (2004). "Midlife blood pressure and the risk of hippocampal atrophy: the Honolulu Asia Aging Study". *Hypertension* 44 (1): 29–34. DOI: [10.1161/01.HYP.0000132475.32317.bb](https://doi.org/10.1161/01.HYP.0000132475.32317.bb).
- Korf ESC, White LR, Scheltens P, and Launer LJ (2006). "Brain aging in very old men with type 2 diabetes: the Honolulu-Asia Aging Study". *Diabetes Care* 29 (10): 2268–2274. DOI: [10.2337/dc06-0243](https://doi.org/10.2337/dc06-0243).
- Liu CC, Kanekiyo T, Xu H, and Bu G (2013). "Apolipoprotein E and Alzheimer disease: risk, mechanisms and therapy". *Nat. Rev. Neurol.* 9(2): 106–118. DOI: [10.1038/nrneuro1.2012.263](https://doi.org/10.1038/nrneuro1.2012.263).
- Lu PH, Thompson PM, Leow A, Lee GJ, Lee A, et al. (2011). "Apolipoprotein E genotype is associated with temporal and hippocampal atrophy rates in healthy elderly adults: a tensor-based morphometry study". *J. Alzheimers Dis.* 23 (3): 433–442. DOI: [10.3233/JAD-2010-101398](https://doi.org/10.3233/JAD-2010-101398).
- Mahley RW and Rall SC (2000). "Apolipoprotein E: far more than a lipid transport protein". *Annu. Rev. Genomics Hum. Genet.* 1: 507–537. DOI: [10.1146/annurev.genom.1.1.507](https://doi.org/10.1146/annurev.genom.1.1.507).
- Mitchell GF, Vita JA, Larson MG, Parise H, Keyes MJ, et al. (2005). "Cross-sectional relations of peripheral microvascular function, cardiovascular disease risk factors, and aortic stiffness: the Framingham Heart Study". *Circulation* 112 (24): 3722–3728. DOI: [10.1161/CIRCULATIONAHA.105.551168](https://doi.org/10.1161/CIRCULATIONAHA.105.551168).
- Moffat SD, Szekely CA, Zonderman AB, Kabani NJ, and Resnick SM (2000). "Longitudinal change in hippocampal volume as a function of apolipoprotein E genotype". *Neurology* 55 (1): 134–136. DOI: [10.1212/WNL.55.1.134](https://doi.org/10.1212/WNL.55.1.134).
- Nunnemann S, Wohlschlagel AM, Ilg R, Gaser C, Etgen T, et al. (2009). "Accelerated aging of the putamen in men but not in women". *Neurobiol. Aging* 30 (1): 147–151. DOI: [10.1016/j.neurobiolaging.2007.05.016](https://doi.org/10.1016/j.neurobiolaging.2007.05.016).
- Prins ND, van Dijk EJ, den Heijer T, Vermeer SE, Jolles J, et al. (2005). "Cerebral small-vessel disease and decline in information processing speed, executive function and memory". *Brain* 128 (9): 2034–2041. DOI: [10.1093/brain/awh553](https://doi.org/10.1093/brain/awh553).
- Qiu C, Strauss E von, Winblad B, and Fratiglioni L (2004). "Decline in blood pressure over time and risk of dementia: a longitudinal study from the Kungsholmen project". *Stroke* 35 (8): 1810–1815. DOI: [10.1161/01.STR.0000133128.42462.ef](https://doi.org/10.1161/01.STR.0000133128.42462.ef).
- R Core Team (2010). *R: A Language and Environment for Statistical Computing*. R Foundation for Statistical Computing. Vienna, Austria. URL: <http://www.R-project.org/>.
- Schmahmann JD (2003). "Vascular syndromes of the thalamus". *Stroke* 34 (9): 2264–2278. DOI: [10.1161/01.STR.0000087786.38997.9E](https://doi.org/10.1161/01.STR.0000087786.38997.9E).

- Sigurdsson S, Aspelund T, Forsberg L, Fredriksson J, Kjartansson O, et al. (2012). "Brain tissue volumes in the general population of the elderly: the AGES-Reykjavik study". *Neuroimage* 59 (4): 3862–3870. DOI: [10.1016/j.neuroimage.2011.11.024](https://doi.org/10.1016/j.neuroimage.2011.11.024).
- Smallwood A, Oulhaj A, Joachim C, Christie S, Sloan C, et al. (2012). "Cerebral subcortical small vessel disease and its relation to cognition in elderly subjects: a pathological study in the Oxford Project to Investigate Memory and Ageing (OPTIMA) cohort". *Neuropathol. Appl. Neurobiol.* 38 (4): 337–343. DOI: [10.1111/j.1365-2990.2011.01221.x](https://doi.org/10.1111/j.1365-2990.2011.01221.x).
- Sveinbjornsdottir S, Sigurdsson S, Aspelund T, Kjartansson O, Eiriksdottir G, et al. (2008). "Cerebral microbleeds in the population based AGES-Reykjavik study: prevalence and location". *J. Neurol. Neurosurg. Psychiatr.* 79 (9): 1002–1006. DOI: [10.1136/jnnp.2007.121913](https://doi.org/10.1136/jnnp.2007.121913).
- Tolppanen AM, Solomon A, Soininen H, and Kivipelto M (2012). "Midlife vascular risk factors and Alzheimer's disease: evidence from epidemiological studies". *J. Alzheimers Dis.* 32 (3): 531–540. DOI: [10.3233/JAD-2012-120802](https://doi.org/10.3233/JAD-2012-120802).
- Vermeer SE, Longstreth WT, and Koudstaal PJ (2007). "Silent brain infarcts: a systematic review". *Lancet Neurol.* 6 (7): 611–619. DOI: [10.1016/S1474-4422\(07\)70170-9](https://doi.org/10.1016/S1474-4422(07)70170-9).
- Vidoni ED, Townley RA, Honea RA, Burns JM, Weiner M, et al. (2011). "Alzheimer disease biomarkers are associated with body mass index". *Neurology* 77 (21): 1913–1920. DOI: [10.1212/WNL.0b013e318238eec1](https://doi.org/10.1212/WNL.0b013e318238eec1).
- Waldstein SR, Lefkowitz DM, Siegel EL, Rosenberger WF, Spencer RJ, et al. (2010). "Reduced cerebral blood flow in older men with higher levels of blood pressure". *J. Hypertens.* 28 (5): 993–998. DOI: [10.1097/HJH.0b013e328335c34f](https://doi.org/10.1097/HJH.0b013e328335c34f).
- Zhu YC, Dufouil C, Soumare A, Mazoyer B, Chabriat H, and Tzourio C (2010). "High degree of dilated Virchow-Robin spaces on MRI is associated with increased risk of dementia". *J. Alzheimers Dis.* 22 (2): 663–672. DOI: [10.3233/JAD-2010-100378](https://doi.org/10.3233/JAD-2010-100378).
- Zhu YC, Tzourio C, Soumare A, Mazoyer B, Dufouil C, and Chabriat H (2010). "Severity of dilated Virchow-Robin spaces is associated with age, blood pressure, and MRI markers of small vessel disease: a population-based study". *Stroke* 41 (11): 2483–2490. DOI: [10.1161/STROKEAHA.110.591586](https://doi.org/10.1161/STROKEAHA.110.591586).

APPENDIX

Manual segmentation protocol

The caudate nucleus, putamen, globus pallidus, and thalamus were delineated on axial T1-weighted 3-dimensional images (acquisition parameters: TR = 21.0 ms; TE = 8.0 ms; flip angle = 30°; section thickness = 1.5 mm; number of sections=110; no section gap; whole brain coverage; FOV = 240 mm; matrix = 256 × 256). Anatomical borders of the caudate were medial the lateral ventricle, lateral the internal capsule, inferior the nucleus accumbens and more posterior the internal capsule. The boundaries of the putamen were medial the internal capsule and globus pallidus, and lateral the external capsule (the claustrum was not separately labeled). The globus pallidus laterally bordered the putamen, and anteriorly and medially the internal capsule. The thalamus included the thalamus, pulvinar, subthalamic nucleus, and hypothalamus. The anterior border and lateral border were formed by the posterior limb of the internal capsule, the medial border by the lateral ventricle, and more caudally the septum pellucidum and superior colliculus, and the posterior border by the third ventricle and crus fornx. The nucleus accumbens was drawn in coronal plane as the gray matter connecting caudate nucleus and putamen. A line from the lower tip of the lateral ventricle to the lower tip of the internal capsule was considered the superior boundary. The septum pellucidum was regarded the medial border. The nucleus was delineated posteriorly until the anterior commissure was seen. The amygdala was identified in coronal plane, at the level of the anterior commissure and drawn superior to the top of the temporal horn of the lateral ventricle and hippocampus. Medial and lateral anatomical boundaries were the cerebrospinal fluid (CSF) of the uncal sulcus and white matter of the MTL. The inferior border was formed by the temporal horn of the lateral ventricle and more anteriorly by white matter of the entorhinal cortex. The hippocampus was identified on the coronal slice where the mamillary bodies were visible. Areas included were the CA-1 through CA-4 sections, dentate gyrus, and subiculum. A straight horizontal line from the top of the temporal horn of the lateral ventricle formed the superior border with amygdala and the gray-white matter junction between the subiculum and white matter of the parahippocampal gyrus formed the inferior border. CSF in the temporal horn formed the lateral border and CSF of hippocampal sulcus the medial border. Posteriorly, the structure was drawn until no longer seen, usually where the splenium and crus fornx were clearly visible. Both amygdala and hippocampus were reviewed in axial plane and modified if necessary along the described borders.

PART II

Allometric scaling in brain development and
degeneration

CHAPTER 6

Allometric scaling of brain structures to intracranial volume: an epidemiological MRI study

Laura W de Jong

Jean-Sébastien Vidal

Lars E Forsberg

Alex P Zijdenbos

Tad Haight

Alzheimer's Disease Neuroimaging Initiative

Sigurdur Sigurdsson

Vilmundur Gudnason

Mark A van Buchem

Lenore J Launer

Adapted from Hum Brain Mapp. 2017 Jan;38(1):151-164. doi: [10.1002/hbm.23351](https://doi.org/10.1002/hbm.23351).

ABSTRACT

There is growing evidence that substructures of the brain scale allometrically to total brain size, i.e., in a nonproportional and nonlinear way. Here, we examined scaling coefficients of different volumes of interest (VOI) to intracranial volume (ICV) and assessed whether they were allometric or isometric and whether they were significantly different from each other. Furthermore, reproducibility of allometric scaling across different age groups and study populations was investigated. Scaling of VOI to ICV was studied in samples of cognitively healthy adults from the community-based AGES-Reykjavik study ($N = 3883$), the Coronary Artery Risk Development in Young Adults Study (CARDIA) ($N = 709$), and the Alzheimer's Disease Neuroimaging Initiative (ADNI) ($N = 180$). Data encompassed participants with different age, ethnicity, risk factor profile, and ICV and VOI obtained with different automated MRI segmentation techniques. Our analysis showed that 1) allometric scaling is a trait of all parts of the brain, 2) scaling of neocortical white matter, neocortical gray matter, and deep gray matter structures including the cerebellum are significantly different from each other and 3) allometric scaling of brain structures cannot solely be explained by age-associated atrophy, sex, ethnicity, or a systematic bias from study-specific segmentation algorithm, but appears to be a true feature of brain geometry.

INTRODUCTION

Since the development of (semi-) automated segmentation techniques for brain MRI, a large body of literature has emerged comparing brain volumes of different groups of people in order to find measurable traits distinctive or predictive for certain diseases. Having a good understanding of the physiologic variation in brain geometry is indispensable to discover pathological patterns. Human brain size varies considerably and different adjustment methods are applied to reduce noise stemming from this variation. Despite widespread use of standardization techniques, adjusting for ICV or total brain volume (TBV) when analyzing VOI is complex and controversial. In volumetric studies, ratios of VOI to ICV or TBV, or linear regression-based methods are commonly used. However, a critical evaluation of these techniques showed that each of these adjustment method unmasks different types of relations and result in different magnitude of effects (O'Brien et al. 2011; Voevodskaya et al. 2014). In morphometric studies linear or nonlinear stereotaxic registration of brain MR images are often used. A critical evaluation of these techniques showed that spatial transformation of MR brain images may result in significant opposite group level differences or different proportionality of brain regions compared to those obtained in native space (Allen et al. 2008). Moreover, whether it is necessary to apply head-size adjustment in all types of comparative brain studies was evaluated in a study that investigated the effect of head size on several metrics of the brain, i.e., total brain volume, VOI, cortical thickness and voxel-based morphometry (VBM). It was concluded that head size adjustment should be considered in all volumetric and VBM studies, but not in cortical thickness studies (Barnes et al. 2010).

Probably, part of the inconsistencies in results obtained with different head/brain size adjustment methods can be explained by differences in underlying assumptions of these methods regarding preservation of proportionality of VOI to TBV across the total range of brain size variation in the population. Some techniques, such as ratio-based methods or linear registration, assume isometry of the brain, i.e., proportionality of VOI to TBV is preserved. Other techniques, such as linear regression-based methods or non-linear registration, allow for allometry to occur in case proportionality is not preserved. Although, these different theoretical underpinnings have been recognized (O'Brien et al. 2011) and caution is called when choosing the adjustment method, it is uncertain whether allometric scaling is true feature of brain geometry.

Some previous studies have provided evidence for allometric scaling of VOI to overall brain size. One study found larger proportions of cerebral WM and smaller proportions of GM in larger TBV compared to lower TBV (Lüders, Steinmetz, and Jancke 2002). Another study that focused on the necessity of head size, age and gender adjustment in MRI studies, found nonlinear relations of cortical GM, hippocampus and putamen to ICV with a power less than 1 (Barnes et al. 2010). Other neocortical metrics such as cortical thickness, total surface area, and sulcal depth have also been found to scale different from what would be predicted based on ICV in case of isometry (Im et al. 2008). Moreover, a recent study examined power law relations of deep GM structures and many regions of cortical GM and found most of them to have nonlinear relation with ICV. Some cortical areas had a power law larger than 1 and others smaller than 1. It was also tested whether prediction error of a statistical model would decrease when ICV correction was based on power-proportion method compared to the commonly used ANCOVA method. Prediction errors with use of power proportion method were slightly lower for structures that had strong nonlinear relations to ICV (Liu et al. 2014).

Although, nonlinearity and nonproportionality in scaling of some VOI to ICV have been reported, results are heterogeneous and little is known on scaling of especially deep GM regions (striatum and thalamus) and cerebellum. Also, it has not been investigated whether scaling coefficients of different brain structures are significantly different from each other. Here, scaling of volumes of frontal, parieto-occipital and temporal cortical GM, cortical WM, medial temporal lobe (MTL), striatum, thalamus, and cerebellum with ICV was studied using automatically segmented MRI brain scans of a large sample of community dwelling older adults ($N = 3883$) who participated in AGES-Reykjavik study. First, we investigated whether and to what extent VOI showed allometric scaling to ICV. Second, we estimated whether scaling coefficients of different VOI were significantly different from each other. Third, we studied whether scaling was similar in different age groups of our sample. Fourth, we set up an experiment to test whether the automated segmentation pipeline of AGES-Reykjavik study could give rise to allometric scaling. Fifth, because allometric scaling would have considerable influence on head/brain size adjustment methods, the fit of the allometric model on the volumetric data was compared to the linear model. And lastly, since the AGES-Reykjavik study population consisted of older Icelandic individuals, extrapolation of our results to groups of younger individuals and/ or different ethnicity was potentially limited. Therefore, supportive analyses were conducted in two other samples (CARDIA and ADNI) that differed in mean age, source population, and method of automated MR segmentation to estimate brain volumes.

METHODS

General design of the AGES-Reykjavik study

The general design and demographics of the AGES-Reykjavik study have been described elsewhere (Harris et al. 2007). The population-based sample of the AGES-Reykjavik study consisted of 5764 men and women, born between 1907–1935. Participants underwent extensive clinical evaluation, including cognitive function testing and brain MRI. All participants signed an informed consent. The AGES-Reykjavik study was approved by the Intramural Research Program of the National Institute on Aging, the National Bioethics Committee in Iceland (VSN00-063), the Icelandic Data Protection Authority, and the institutional review board of the U.S. National Institute on Aging, National Institutes of Health.

Acquisition and automated segmentation of MRI

MRI was performed at the Icelandic Heart Association on a single study dedicated 1.5T GE Signa Twinspeed EXCITE system MRI scanner. The image protocol, described previously (Sigurdsson et al. 2012), included a T1-weighted 3D spoiled gradient echo (TE 8 ms; TR 21 ms; FA 30°, FoV 240 mm; matrix 256 × 256; 110 slices; slice thickness 1.5 mm), a FSE PD/T2 (TE1 22 ms; TE2 90 ms; TR 3220 ms; echo train length 8; FA 90°, FoV 220 mm; matrix 256 × 256; slice thickness 3.0 mm), and a FLAIR (TE 100 ms; TR 8000 ms; inversion time 2000 ms; FA 90°, FoV 220 mm; matrix 256 × 256; slice thickness 3.0 mm).

A fully automated segmentation pipeline was developed based on the Montreal Neurological Institute processing pipeline (Sigurdsson et al. 2012; Zijdenbos, Forghani, and Evans 2002). The pipeline used a multispectral approach to segment voxels into global tissue classes (cerebrospinal fluid (CSF), GM, WM and white matter hyperintensities (WMH)). Following this, a regional parcellation pipeline –atlas-based segmentation method– was developed to obtain volumes of different substructures of the brain.

Determination of VOI

The regional tissue segmentation pipeline parcelled the brain in 56 different regions (figure 1 of chapter 5). However, for the present study, we combined regions into a limited amount of 8 VOI known to differ in gross cytoarchitectural features. We separately assessed scaling of neocortical GM and WM to investigate in further detail the previously reported proportional changes as function of TBV. Three regions of neocor-

tical GM were investigated, i.e., frontal (comprising of orbitofrontal and prefrontal GM, precentral gyrus, cingulated gyrus, insula and fornix), temporal (comprising of lateral temporal GM, parahippocampal and fusiform gyrus), and parieto-occipital GM. Cortical WM volume was studied in total and included all lobar WM, corpus callosum, internal and external capsule, and WMH. The medial temporal lobe (MTL), striatum, thalamus and cerebellum were separately studied because of their importance in many studies to neurodegenerative processes. MTL included amygdala and hippocampus (including CA regions I–IV, fimbria, and subiculum of the hippocampus). Striatum included the nucleus accumbens, caudate nucleus, putamen, and globus pallidus. The thalamus included also the hypothalamus. The cerebellum included cerebellar GM and WM. Left and right hemispheres of each structure were combined. Total brain volume (TBV) was calculated as the sum of the neocortical GM and WM, MTL, striatum, thalamus, brainstem and cerebellum. ICV was defined as the sum of TBV and CSF.

Quality control of MRI segmentation

The quality of the segmentation of the 8 composite VOI was mostly dependent on the performance of the global tissue segmentation into GM, WM, WMH, and CSF, and for a small part dependent on the definition of topographical borders by the regional tissue segmentation. Performance of both global tissue and regional tissue segmentation was evaluated. The quality control of global tissue classification consisted of 3 steps described in (Sigurdsson et al. 2012). In summary these were: 1) visual inspection of the segmentation of 14 a priori selected slices of each subject ($N = 4356$), which led to additional manual editing in 43 cases and rejection of 53 cases and 2) comparison of automated versus manual global tissue segmentation of 5 preselected slices across the brain (including a slice located at the junction of the thalamus and subthalamic structures for reviewing segmentation of the deep gray matter nuclei) in 20 randomly selected cases. Resulting dice similarity index scores (Zijdenbos, Dawant, and Margolin 1994) were 0.82, 0.82, and 0.83 for GM, WM, and CSF respectively. 3) Reproducibility of the entire process of MRI acquisition and post-processing was evaluated by repeated scanning and segmentation (4 times in total) of 32 participants. Excellent intraclass correlation for all global tissue was found ($r > 0.98$, for all). Because the present study relies for an important part on good quality of ICV segmentation, the performance of the automated pipeline was further evaluated specifically on ICV. ICV was manually segmented on the same 20 brain scans used for step 2 of the quality control. Two researchers with extensive neuroradiological experience and blinded for the results of the automated segmentation, segmented ICV on axial 3D T1 weighted images, with correction and editing in sagittal and coronal planes. Resulting ICV were correlated with

ICV obtained by the automated pipeline. Pearson's correlation was 0.97 (0.93–0.99) and Bland-Altman plot showed a small overestimation of ICV of 31 cm³ on average by the automated segmentation, but no proportional error (figure 1 and 2).

Performance of regional tissue classification was validated against four complete manually labeled scans. Dice similarity index scores per studied region were; frontal GM: 0.83, temporal GM: 0.83, parieto-occipital GM: 0.81, striatum: 0.83, MTL: 0.80, thalamus: 0.92, cerebellum: 0.92, white matter: 0.86.

Statistical analysis

All statistical analyses were performed with SAS v 9.13 (SAS Institute Inc., Cary, NC, USA) and all graphs were generated with R v 3.1.2 (R Core Team 2014).

Analytical sample of AGES-Reykjavik Study

MR scanning was performed on consenting MR eligible participants, between 2002 and 2006. From the total AGES-Reykjavik sample of 5764 participants, 4726 underwent successful MRI scanning. Global and regional segmentations were successful in 4613 MR scans. We excluded cases of dementia ($n = 202$) and MCI ($n = 422$), assumed to have higher rates of atrophy, and cases for which cognitive function had not been assessed ($n = 106$). Our final study sample consisted of 3883 people with successful brain MRI and segmentation of the images. Demographics and brain structure volumes of the AGES-Reykjavik study population were compared between women and men with t -tests for continuous variables and χ^2 tests for categorical variables. All VOI were normally distributed.

Estimation of scaling coefficients of different VOI

Allometric coefficients of VOI with ICV were calculated using the general equation of allometric analyses, $\log(y) = \log(b) + \alpha \times \log(x)$, where x is ICV, y VOI, $\log(b)$ intercept, and α represents the allometric coefficient (Harvey 1982), i.e., the slope of the regression between $\log(\text{ICV})$ and $\log(\text{VOI})$. A coefficient greater than 1.0 is considered a positive allometric coefficient, i.e., VOI increased with a power greater than 1 relative to ICV. A coefficient smaller than 1.0 is seen as a negative allometric coefficient, i.e., VOI increased with a power less than 1 relative to ICV. We chose ICV, instead of TBV, as measure of brain volume to avoid a possible bias towards isometry in estimating allometric coefficients of large VOI. Large structures occupy large volumes in TBV making the range of possible deviations from isometry smaller; this may produce an overestimate of coefficients towards 1 and reduce the ability to estimate allometric

Figure 1: Accuracy of automated segmentation pipeline; Pearson correlation manual versus automated segmentation of ICV

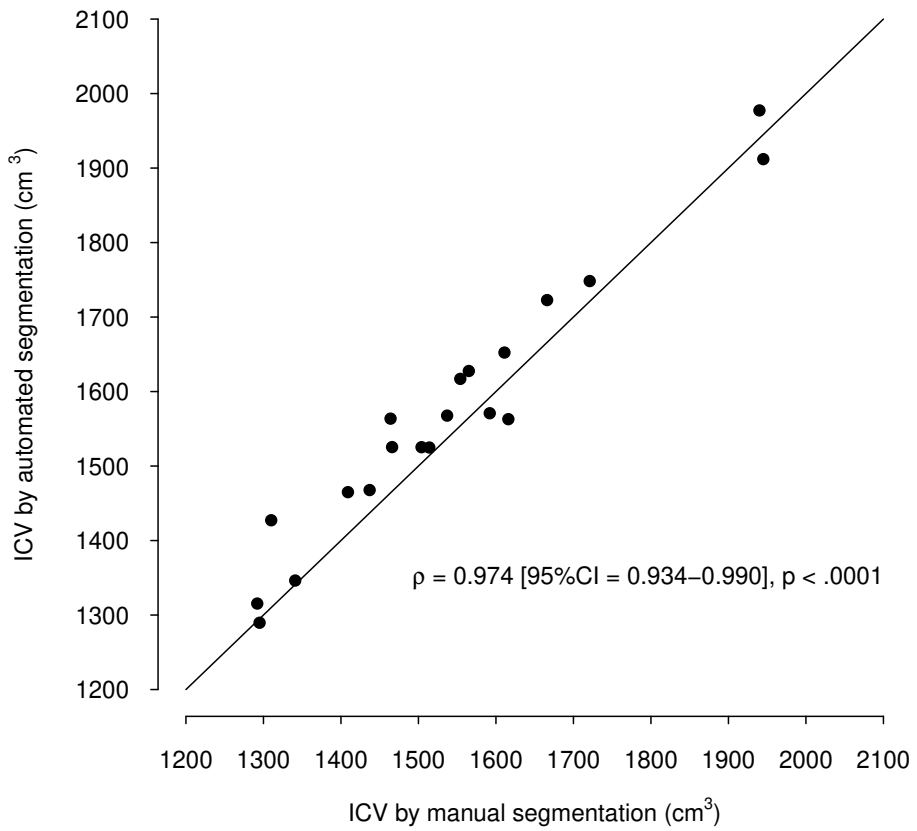
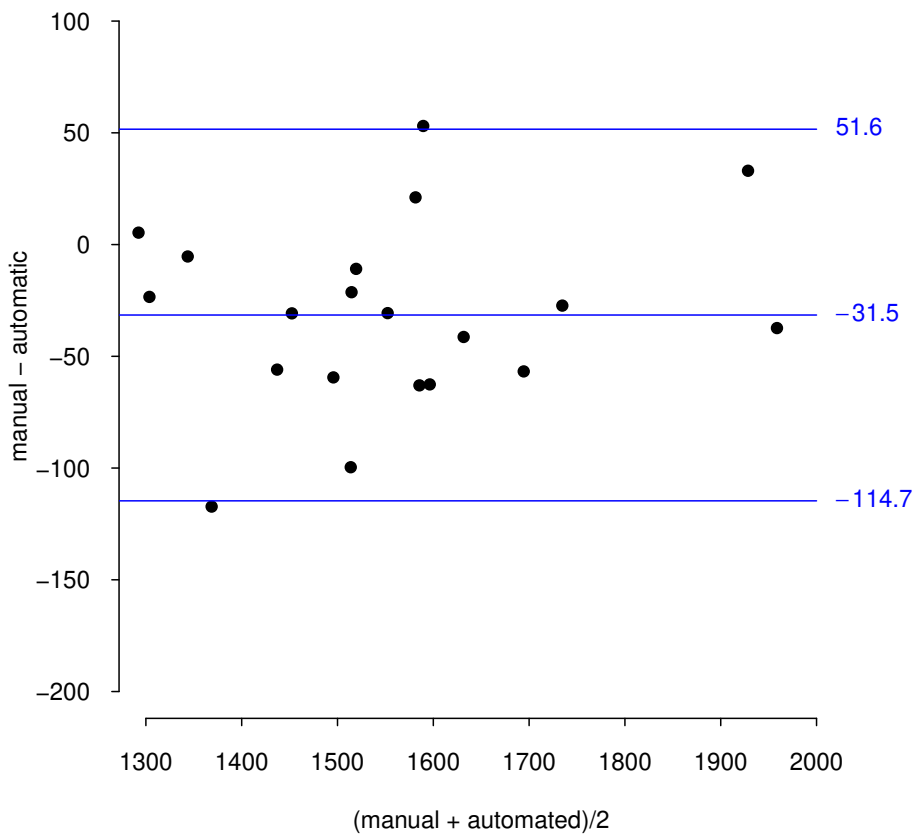


Figure 2: Accuracy of automated segmentation pipeline; Bland-Altman plot manual versus automated segmentation of ICV



coefficients deviant from 1 (Deacon 1990). With the use of ICV none of the structures studied comprised more than 24% (WM) of ICV. Another important reason was that ICV is regarded as a marker for brain volume at its maximum size and therefore a marker of “premorbid” brain size. At time of scanning, brains of most study participants experienced more or less atrophy due to ageing or pathological processes. These are factors we can largely control for in our statistical analyses, whereas it is more difficult to control for differences between current TBV and original TBV. Log-transformed VOI were plotted against log transformed ICV (figure 3). For each VOI, allometric coefficients with ICV were calculated adjusted for age and sex, ($\log(\text{VOI}) = \text{intercept} + \alpha \times \log(\text{ICV}) + \beta_{\text{age}} \times \text{age} + \beta_{\text{sex}} \times \text{sex}$) and tested against the isometric scaling law of 1:1.

Comparison of allometric scaling coefficients of different VOI

Allometric coefficients of the different VOI to ICV were compared using a marginal model (PROC MIXED SAS procedure (SAS Institute Inc., Cary, NC, USA) with repeated statement and unstructured correlation matrix), which takes into account the correlations between the VOI. The log transformed VOI were entered as dependent variables and log transformed ICV as independent variable. Interactions of $\log(\text{VOI})$ with $\log(\text{ICV})$ were entered in the model as a cross product together with $\log(\text{ICV})$, $\log(\text{VOI})$, age, and sex. The model was also run with additional independent variables (year of birth, height, achievement of higher education (high school diploma or above), presence of infarct(s), and contrast-to-noise ratio (CNR) between GM and WM and CNR between GM and cerebrospinal fluid), but these did not exert significant effects and were omitted to keep the model parsimonious. A Bonferroni correction was applied to adjust for multiple testing (number of comparisons between slopes in the 3 mixed models = 85) and a p -value < 0.00059 ($= 0.05/85$) was considered significant. The analysis was performed in the entire sample and repeated for women and men separately. The numerical results of the marginal model are reported in table 2.

Allometric scaling of VOI in different age groups

To assess whether age influenced scaling of VOI with ICV, scaling coefficients of VOI to ICV were calculated for each quartile of age; the age range of the youngest quartile being 66–71 years, and of subsequent quartiles being, 72–75, 76–79 and 80–95 years. The coefficients were compared among the quartiles by testing whether there was an interaction between the quartiles and ICV.

Testing the segmentation pipeline with artificially linearly scaled data

To test whether a potential systematic error in the automated segmentation pipeline could introduce allometry in the volumetric data of AGES-Reykjavik study, artificially linearly scaled brain scans were entered into the pipeline and the output was investigated for allometry. Scans of a relatively small (1402 cm³) and relatively large brain (1756 cm³) were skull stripped and linearly scaled by factors ranging from 0.75–1.25 of its original size with steps of 0.01. The resulting sets of scaled images were subsequently processed through the AGES-Reykjavik pipeline. Log transformed volumes of the global tissues GM, WM and CSF were plotted against log transformed ICV and α -coefficients were calculated.

Comparison of allometric model and linear regression model

The fit of the allometric model of the relation of each VOI to ICV on the data was compared to a linear regression model. The line of prediction from the allometric model and linear model were superimposed in the same graph and R^2 of each model was calculated. Both models were conducted with adjustments for age and sex.

Supportive analyses in datasets of CARDIA and ADNI

Supportive analyses were conducted in datasets of CARDIA and ADNI. In both samples the allometric coefficients of VOI with ICV were calculated, corrected for age and sex, and tested against the isometric scaling law of 1:1, similar to the first part of analysis conducted in the AGES-Reykjavik data.

The multicenter prospective cohort CARDIA study was designed to examine the development and determinants of clinical and subclinical cardiovascular disease and its risk factors. Between 1985–1986, 5115 black and white men and women (aged 16–30) were recruited from 4 urban sites across the United States and underwent 8 examination cycles (Friedman et al. 1988). All participants provided written informed consent at each exam, and institutional review boards from each study site and the coordinating center annually approved the study. In 2010–2011, 3498 (72%) of the surviving cohort attended a 25-year follow-up exam. As part of this exam, a subsample of the cohort participated in the CARDIA Brain substudy, designed to investigate the morphology, pathology, physiology and function of the brain with MRI. Exclusion criteria at the time of sample selection, or at the MRI site, were a contraindication to MRI or a body size that was too large for the MRI scanner. Of those who were eligible for the substudy, 719 individuals received whole brain MRI scans. Post-scan image processing was performed by the Section of Biomedical Image Analysis (BIA), Department of Radiology, University

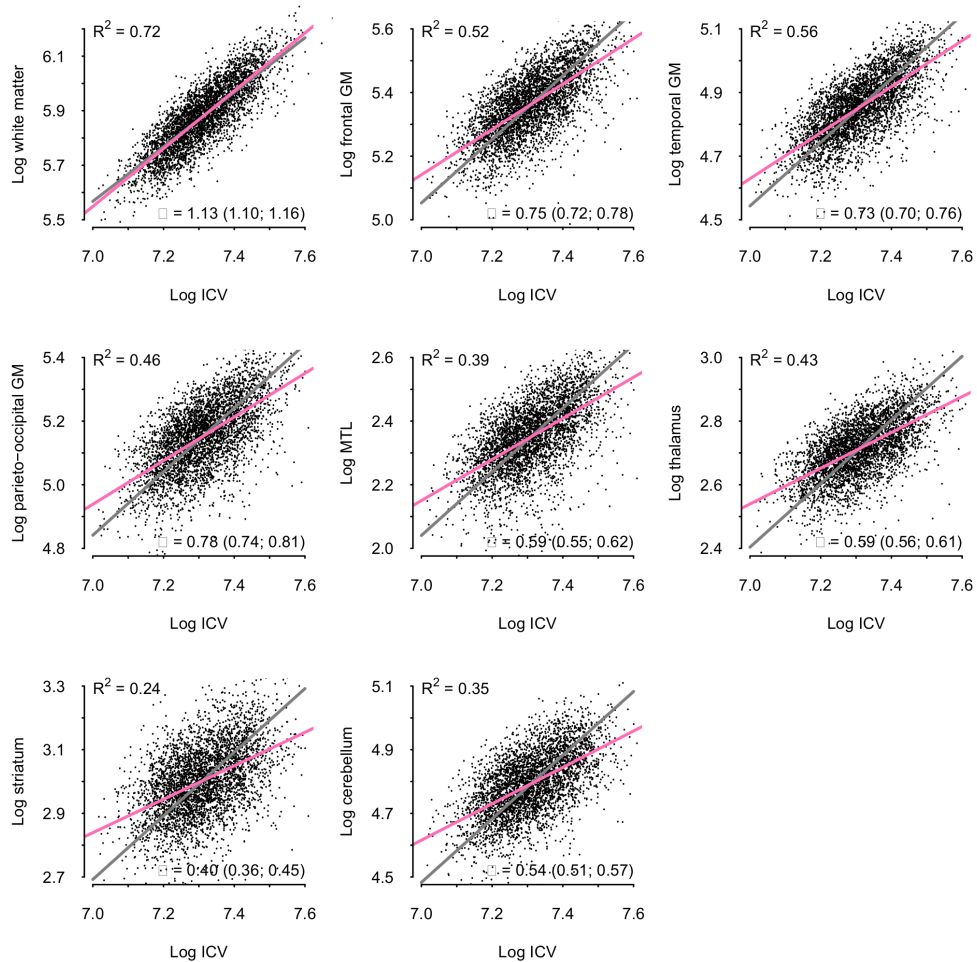
of Pennsylvania. MRI scans were inspected and passed through a quality control process. Based on previously described methods (Davatzikos, Tao, and Shen 2003; Goldszal et al. 1998; Lao et al. 2008; Shen et al. 2002; Zacharaki et al. 2008), an automated algorithm was used to segment MRI structural images of supratentorial brain tissue into GM, WM and cerebrospinal fluid. GM and WM were further characterized and segmented as 92 anatomic ROIs in each hemisphere, from which summary VOIs used in the current study were calculated. ICV was calculated as the sum of all supratentorial structures, but not infratentorial.

Some data used in the preparation of this article were obtained from the Alzheimer's Disease Neuroimaging Initiative (ADNI) database (Accessed July 1, 2017. <http://adni.loni.usc.edu>). The ADNI was launched in 2003 by the National Institute on Aging, the National Institute of Biomedical Imaging and Bioengineering, the Food and Drug Administration, private pharmaceutical companies and nonprofit organizations, as a \$60 million, 5-year public-private partnership. The primary goal of ADNI has been to test whether serial MRI, positron emission tomography, other biological markers, and clinical and neuropsychological assessment can be combined to measure the progression of MCI and early AD. Determination of sensitive and specific markers of very early AD progression is intended to aid researchers and clinicians to develop new treatments and monitor their effectiveness, as well as lessen the time and cost of clinical trials.

The Principal Investigator of this initiative is Michael W. Weiner, MD, VA Medical Center and University of California-San Francisco. ADNI is the result of efforts of many coinvestigators from a broad range of academic institutions and private corporations, and subjects have been recruited from over 50 sites across the U.S. and Canada. The initial goal of ADNI was to recruit 800 subjects but ADNI has been followed by ADNI-GO and ADNI-2. To date these three protocols have recruited over 1500 adults, ages 55 to 90, to participate in the research, consisting of cognitively normal older individuals, people with early or late MCI, and people with early AD. The follow-up duration of each group is specified in the protocols for ADNI-1, ADNI-2 and ADNI-GO. Subjects originally recruited for ADNI-1 and ADNI-GO had the option to be followed in ADNI-2. For up-to-date information, see <http://www.adni-info.org>.

For the supportive analysis of our study we used volumetric brain measures derived from the standardized 1.5 T MRI screening dataset in cognitively healthy subjects that was collected between August 2005 and October 2007 and processed using FreeSurfer software (Freesurfer Software website. Cortical Reconstruction and volumetric segmentation (Accessed July 1, 2017. <http://surfer.nmr.mgh.harvard.edu>).

Figure 3: Allometric coefficients of VOI with ICV



Gray line, isometry line; Red line, line of allometric log-log model between ICV and VOI.

RESULTS

Characteristics AGES-Reykjavik sample

The AGES-Reykjavik sample had a mean age of 75.7 (standard deviation = 5.2) years, of which 59.8% were women. ICV ranged from 1116–2162 cm³ in the total sample; from 1116–1868 cm³, in women and from 1232–2162 cm³ in men. Women had on average a lower educational level ($p < 0.0001$), higher BMI ($p = 0.003$), were diagnosed less often with diabetes ($p < 0.0001$), and had smoked ($p < 0.0001$) and drank alcohol ($p < 0.0001$) more sparingly compared to men. Women had lower means of ICV and all VOI compared to men ($p < 0.0001$) (table 1).

Allometric scaling coefficients of all VOI

All VOI scaled non-isometrically to ICV (figure 3). After correction for age and sex, a positive allometric coefficient of 1.14 (95% confident interval = 1.11–1.17) was estimated for WM volume and negative allometric coefficients were found for frontal GM (0.76 (0.73–0.79)), temporal GM (0.75 (0.72–0.78)), parieto-occipital GM (0.79 (0.76–0.83)), MTL (0.60 (0.56–0.64)), thalamus (0.59 (0.56–0.62)), striatum (0.41 (0.37–0.45)), and cerebellum (0.55 (0.52–0.59)). All were found significantly differently from 1 (1:1 scaling law to ICV ($p < 0.0001$)).

Significant scaling differences between VOI

Results from the marginal model showed that the α -coefficient of WM volume to ICV was significantly different from the α -coefficients of all GM VOI (table 2) in the entire sample, and in women and men separately. The α -coefficients of the different neocortical GM areas to ICV were not significantly different from each other in women and men separately. Also, the α -coefficients of MTL, thalamus, and cerebellum were not significantly different from each other in women and men separately. However, in the entire sample the α -coefficient of the MTL was not significantly different from the α -coefficient of the parieto-occipital GM, but was significantly different from the thalamus and the cerebellum. The α -coefficient of the striatum was significantly different from all other α -coefficients except for the α -coefficient of the thalamus and cerebellum in the entire sample, and the α -coefficient of the cerebellum in men only.

Table 1: General characteristics of the study sample

| Mean (SD) or % (N) | All N = 3883 | Women N = 2307 | Men N = 1576 | p^a |
|--------------------------|-----------------|-------------------|-----------------|--------|
| Age in years | 75.7 (5.2) | 75.6 (5.3) | 75.8 (5.1) | 0.27 |
| Higher education | 12.2 (473) | 6.52 (150) | 20.6 (323) | <.0001 |
| Smoking status | | | | |
| Never | 41.7 (1619) | 53.2 (1226) | 24.9 (393) | |
| Former | 44.5 (1728) | 34.8 (803) | 58.7 (925) | <.0001 |
| Current | 13.8 (534) | 12.0 (276) | 16.4 (258) | |
| Alcohol intake | | | | |
| Never | 21.5 (829) | 29.3 (671) | 10.1 (158) | |
| Former | 10.8 (418) | 7.78 (178) | 15.3 (240) | <.0001 |
| Current | 67.7 (2608) | 62.9 (1440) | 74.6 (1168) | |
| BMI (kg/m ²) | 27.0 (4.3) | 27.2 (4.7) | 26.8 (3.7) | 0.003 |
| Diabetes | 11.1 (430) | 8.76 (202) | 14.5 (228) | <.0001 |
| Stroke | 28.9 (1123) | 23.5 (541) | 36.9 (582) | <.0001 |
| Intracranial volume | 1503 (147) | 1423 (105) | 1619 (121) | <.0001 |
| Total brain volume | 1046 (98) | 1005 (80) | 1105 (91) | <.0001 |
| WM | 360 (45) | 342 (37) | 386 (42) | <.0001 |
| Neocortical gray matter | | | | |
| Frontal | 215 (22) | 207 (19) | 225 (22) | <.0001 |
| Temporal | 129 (13) | 124 (11) | 136 (13) | <.0001 |
| Parieto-occipital | 174 (19) | 169 (17) | 181 (19) | <.0001 |
| Thalamus | 15.1 (1.4) | 14.7 (1.2) | 15.8 (1.3) | <.0001 |
| Medial temporal lobe | 10.6 (1.1) | 10.2 (1.0) | 11.1 (1.1) | <.0001 |
| Striatum | 20.3 (2.3) | 19.5 (2.0) | 21.3 (2.2) | <.0001 |
| Cerebellum | 121.3 (12.0) | 117.4 (10.6) | 126.9 (11.7) | <.0001 |

BMI, body mass index; WM, sum of neocortical white matter; all volumes in cm³.

a t -test for continuous variables and χ^2 test for categorical variables.

Allometric scaling in different age groups

α -coefficients of VOI to ICV for each quartile of age are shown in table 3. α -coefficients of the both cortical and deep GM structures and cerebellum in the older quartiles appeared somewhat lower compared to the younger quartiles and the α -coefficient of WM appeared higher in the older quartiles. However, these differences were nonsignificant, except for temporal GM which was significantly lower in the older quartiles compared to the younger ($p = 0.004$).

Table 2: Comparison of α -coefficients of different VOI to ICV, random effects mixed model

| VOI | α -coefficient (95%CI) | White matter | | | | | p-values from comparison of α -coefficients | | | | |
|----------------|-------------------------------|--------------|--------------|--------------|-------------|--------|----------------------------------------------------|-------------|-------------|--------|-------------|
| | | White matter | Frontal | Temporal | Par-occ | MTL | Thalamus | Cerebellum | | | |
| All N = 3883 | | | | | | | | | | | |
| White matter | 1.09 (1.06-1.11) | | | | | | | | | | |
| Frontal | 0.740 (0.714-0.766) | <.0001 | | | | | | | | | |
| Temporal | 0.750 (0.724-0.774) | <.0001 | 0.34 | | | | | | | | |
| Par-occ | 0.712 (0.683-0.741) | <.0001 | 0.009 | 0.002 | | | | | | | |
| MTL | 0.672 (0.642-0.702) | <.0001 | <.0001 | <.0001 | 0.02 | | | | | | |
| Thalamus | 0.588 (0.563-0.613) | <.0001 | <.0001 | <.0001 | <.0001 | <.0001 | | | | | |
| Cerebellum | 0.598 (0.570-0.627) | <.0001 | <.0001 | <.0001 | <.0001 | <.0001 | 0.48 | | | | |
| Str | 0.552 (0.518-0.586) | <.0001 | <.0001 | <.0001 | <.0001 | <.0001 | <.0001 | 0.02 | | | 0.01 |
| Women N = 2307 | | | | | | | | | | | |
| White matter | 1.14 (1.11-1.18) | | | | | | | | | | |
| Frontal | 0.748 (0.709-0.787) | <.0001 | | | | | | | | | |
| Temporal | 0.724 (0.687-0.762) | <.0001 | 0.15 | | | | | | | | |
| Par-occ | 0.776 (0.732-0.819) | <.0001 | 0.12 | 0.01 | | | | | | | |
| MTL | 0.591 (0.543-0.639) | <.0001 | <.0001 | <.0001 | <.0001 | <.0001 | | | | | |
| Thalamus | 0.590 (0.553-0.627) | <.0001 | <.0001 | <.0001 | <.0001 | <.0001 | 0.97 | | | | |
| Cerebellum | 0.552 (0.508-0.596) | <.0001 | <.0001 | <.0001 | <.0001 | <.0001 | <.0001 | 0.18 | 0.11 | | |
| Striatum | 0.380 (0.325-0.434) | <.0001 | <.0001 | <.0001 | <.0001 | <.0001 | <.0001 | <.0001 | <.0001 | <.0001 | <.0001 |

Continued on next page

VOI, volume of interest; White Matter, sum of neo-cortical white matter; Frontal, frontal neo-cortical gray matter; Temporal, temporal neo-cortical gray matter; Par-occ, parietal and occipital neo-cortical gray matter; MTL, medial temporal lobe. p-value from log-log mixed model adjusted for age and sex. Bold figures represent non-significant P-values (> 0.00059) after Bonferroni correction.

Table 2 – continued from previous page

| VOI | α -coefficient (95%CI) | White matter | Frontal | Temporal | Par-occ | MTL | Thalamus | Cerebellum |
|----------------|-------------------------------|--------------|-------------|-------------|---------|-------------|-------------|-------------|
| Men $N = 1576$ | | | | | | | | |
| White matter | 1.11 (1.07-1.16) | | | | | | | |
| Frontal | 0.761 (0.713-0.809) | <.0001 | | | | | | |
| Temporal | 0.742 (0.696-0.787) | <.0001 | 0.33 | | | | | |
| Par-occ | 0.787 (0.731-0.843) | <.0001 | 0.24 | 0.07 | | | | |
| MTL | 0.589 (0.532-0.645) | <.0001 | <.0001 | <.0001 | <.0001 | | | |
| Thalamus | 0.582 (0.536-0.627) | <.0001 | 0.0004 | <.0001 | <.0001 | 0.81 | | |
| Cerebellum | 0.523 (0.469-0.577) | <.0001 | <.0001 | <.0001 | <.0001 | 0.07 | 0.04 | |
| Striatum | 0.431 (0.367-0.495) | <.0001 | <.0001 | <.0001 | <.0001 | <.0001 | <.0001 | 0.01 |

VOI, volume of interest; White matter, sum of neo-cortical white matter; Frontal, frontal neo-cortical gray matter; Temporal, temporal neo-cortical gray matter; Par-occ, parietal and occipital neo-cortical gray matter; MTL, medial temporal lobe.

p -value from log-log mixed model adjusted for age and sex.

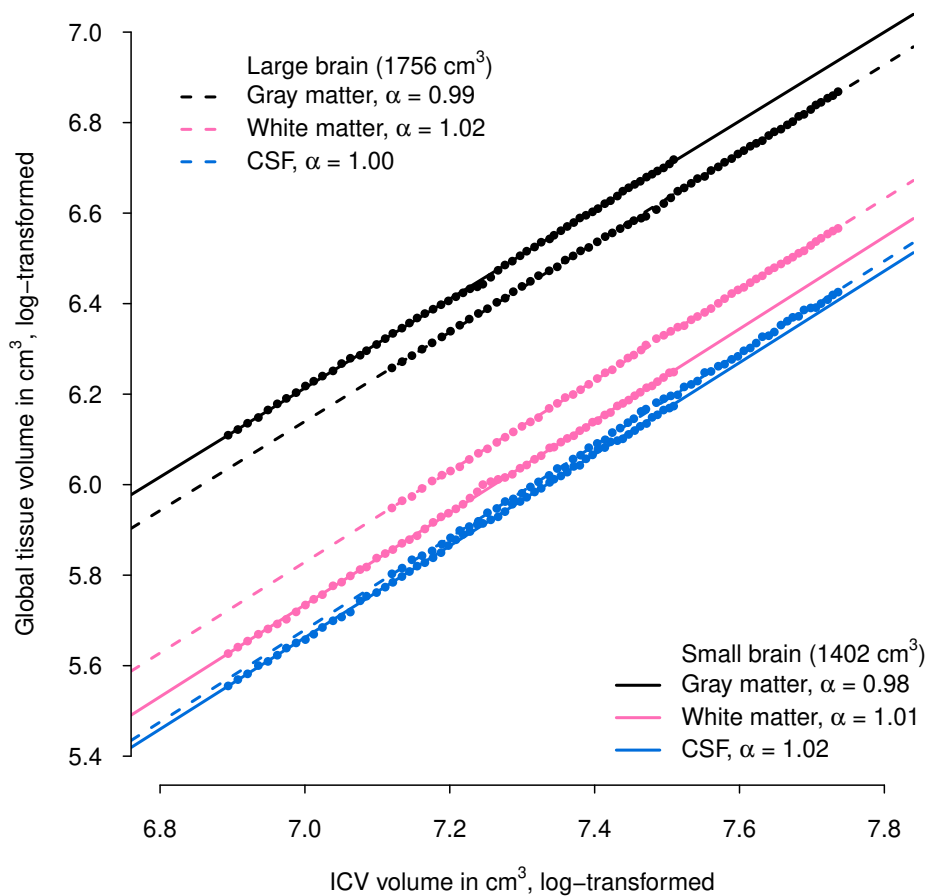
Bold figures represent non-significant p -values (> 0.00059) after Bonferroni correction.

Table 3: Comparison of α -coefficients of VOI to ICV of different quartiles of age

| Volume of interest | α -coefficients for quartile of age (95% CI) | | | | p^a |
|----------------------------------|-----------------------------------------------------|---------------------------|---------------------------|---------------------------|-------|
| | Quartile 1 66-71 years | Quartile 2 72-75 years | Quartile 3 76-79 years | Quartile 4 80-95 years | |
| Neocortical white matter | 1.05 (1.01-1.09) | 1.04 (1.00-1.08) | 1.09 (1.04-1.14) | 1.06 (1.02-1.11) | 0.40 |
| Frontal gray matter | 0.74 (0.70-0.79) | 0.71 (0.66-0.75) | 0.72 (0.67-0.77) | 0.66 (0.62-0.71) | 0.11 |
| Temporal gray matter | 0.77 (0.73-0.81) | 0.72 (0.68-0.76) | 0.73 (0.68-0.78) | 0.65 (0.61-0.70) | 0.004 |
| Parietal & occipital gray matter | 0.71 (0.66-0.76) | 0.66 (0.61-0.71) | 0.69 (0.63-0.75) | 0.66 (0.61-0.72) | 0.50 |
| Medial temporal lobe | 0.67 (0.62-0.72) | 0.66 (0.61-0.71) | 0.63 (0.57-0.69) | 0.60 (0.54-0.66) | 0.32 |
| Thalamus | 0.58 (0.53-0.62) | 0.55 (0.51-0.59) | 0.56 (0.51-0.61) | 0.55 (0.51-0.60) | 0.76 |
| Striatum | 0.56 (0.50-0.62) | 0.52 (0.46-0.57) | 0.53 (0.46-0.60) | 0.48 (0.42-0.55) | 0.38 |
| Cerebellum | 0.58 (0.53-0.63) | 0.57 (0.52-0.62) | 0.57 (0.51-0.62) | 0.55 (0.50-0.61) | 0.90 |

a linear regression with volume of interest as dependent variable and intracranial volume, quartile of age and their interaction term. p -value from the interaction term between ICV and quartile of age.

Figure 4: Accuracy of automated segmentation pipeline; scaling of artificially linearly scaled data



Little allometry introduced by segmentation pipeline

Figure 4 displays log of global tissue volumes plotted against log ICV obtained by the automated segmentation pipeline based on the artificially linearly scaled data set of a relatively large and small brain. The α -coefficients were 0.99 for GM, 1.02 for WM, and 1.00 for CSF for dataset based on the relatively large brain and 0.98 for GM, 1.01 for WM, and 10.2 for CSF for the dataset based on the relatively small brain. Because of the almost perfect fit of the points and the regression line these α -coefficients were significantly different from the isometric scaling law of 1.0 (all p -values < 0.0001), except for the CSF in the large brain.

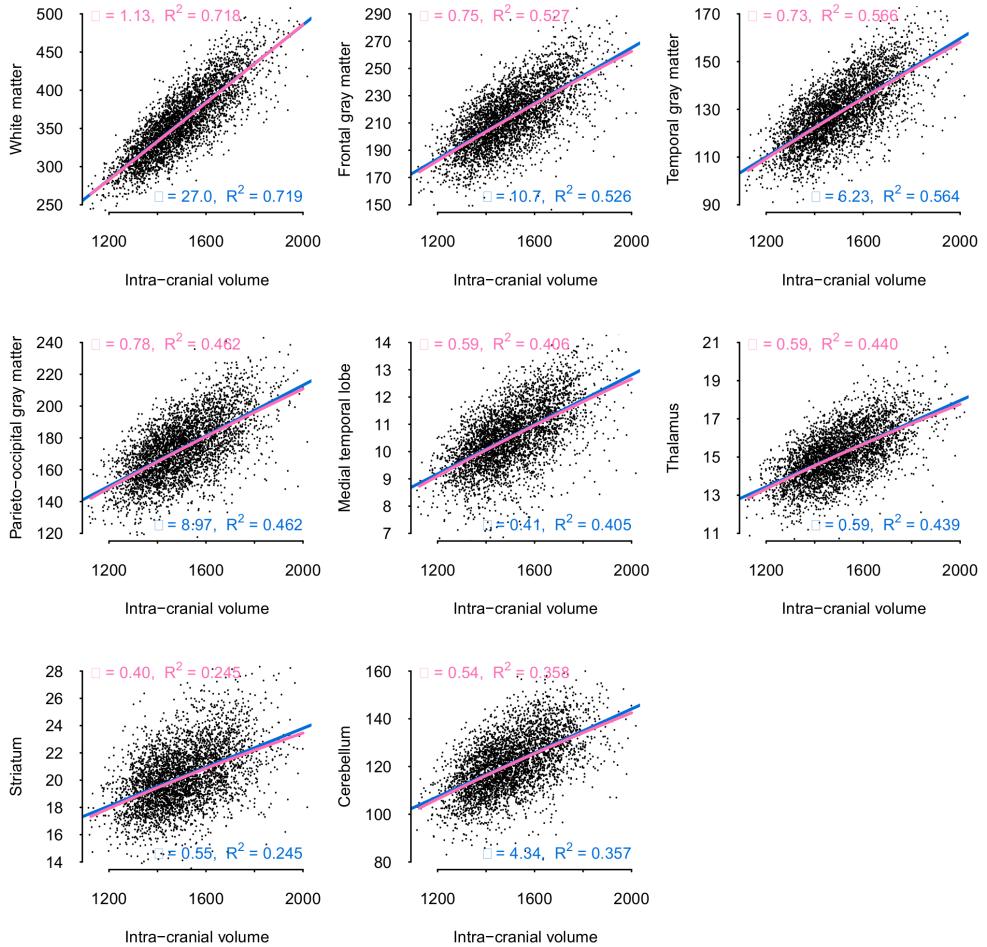
Comparable fit of allometric and linear regression models

Figure 5 superimposes the line of prediction of the allometric model (and associated α -coefficient and R^2) with line of prediction of the linear model (and associated β -coefficient and R^2). Compared to the R^2 of the linear model, the R^2 of the allometric model was a few per mill smaller for cerebellar, cortical and deep GM structures and a few per mill larger for WM. Thus, the models have a comparable fit and can substitute each other.

Allometric scaling in CARDIA and ADNI

The CARDIA sample consisted of individuals with a mean age of 50 (3.5) years, of which 52.9% were women. ICV in the CARDIA sample, including only supratentorial areas, varied from 999–1643 cm³. The ADNI sample consisted of individuals with a mean age of 76 (5.0) years, of which 49.4% were women. ICV in the ADNI sample varied from 1116–1985 cm³. We found the highest allometric coefficients for WM volume in both CARDIA ($\alpha = 1.05$) and ADNI ($\alpha = 1.00$). All GM areas had negative allometric coefficients with the lowest coefficients in the deep GM areas (table 4). Roughly, results suggest similar trends compared with those found in the AGES-Reykjavik data. However, important differences were 1) allometric coefficients of the neocortical GM areas to ICV in CARDIA with values between 0.90–0.94 were higher, compared with those in the AGES-Reykjavik and ADNI samples, and 2) WM volume in the ADNI data set seemed to increase isometrically with ICV.

Figure 5: Comparison of allometric log-log model to linear model of VOI to ICV



Red line, line of the allometric log-log model between the ICV and the VOI;

Blue line, line of the linear model between the ICV and the VOI.

Table 4: Comparison of α -coefficients in study populations of AGES-Reykjavik, ADNI, and CARDIA

| Volume of interest, M (SD) | AGES (N = 3883) | | ADNI (N = 180) | | CARDIA (N = 709) | |
|----------------------------|-----------------|----------------------------|----------------|----------------------------|-------------------------|----------------------------|
| | Vol, M (SD) | α (R ²) | Vol, M (SD) | α (R ²) | Vol, M (SD) | α (R ²) |
| Intracranial volume | 1503 (147) | NA | 1532 (156) | NA | 1208 (133) ^a | NA |
| Total brain volume | 1046 (98) | NA | 1000 (101) | NA | 983 (107) ^a | NA |
| Neocortical white matter | 360 (44) | 1.13 (0.72) | 443 (57) | 1.00 (0.67) | 462 (59) | 1.05 (0.84) |
| Frontal GM | 215 (22) | 0.75 (0.52) | 159 (16) | 0.72 (0.59) | 197 (22) | 0.90 (0.76) |
| Temporal GM | 129 (13) | 0.73 (0.56) | 122 (13) | 0.81 (0.67) | 156 (17) | 0.91 (0.73) |
| Parietal and occipital GM | 174 (19) | 0.78 (0.46) | 114 (12) | 0.81 (0.60) | 124 (14) | 0.94 (0.79) |
| Thalamus | 15.1 (1.4) | 0.59 (0.39) | 12 (1.4) | 0.76 (0.53) | 14 (1.5) | 0.50 (0.26) |
| Medial temporal lobe | 10.6 (1.1) | 0.59 (0.43) | 9.9 (1.2) | 0.49 (0.31) | 10 (1.1) | 0.61 (0.36) |
| Striatum | 20.3 (2.3) | 0.40 (0.24) | 20 (2.2) | 0.62 (0.30) | 20 (2.1) | 0.59 (0.48) |
| Cerebellum | 121 (12) | 0.54 (0.35) | 123 (12) | 0.50 (0.36) | NA | NA |

M (SD), mean (standard deviation); volumes are displayed in cm.³ AGES, Age, Gene, Environment/ Susceptibility - Reykjavik Study; ADNI, Alzheimer's Disease Neuroimaging Initiative; CARDIA, Coronary Artery Risk Development in Young Adults Study; Vol., volume; GM, gray matter.

α , allometric coefficient derived from $(\log(VOI) = intercept + \alpha \times \log(ICV) + \beta_{age} \times age + \beta_{sex} \times sex)$.

^a includes supratentorial areas only

DISCUSSION

Allometric scaling of WM, cortical and deep GM

One goal of the present study was to assess and compare scaling coefficients of different VOIs to ICV in the AGES-Reykjavik dataset. We found all VOI to scale allometrically with ICV. One could roughly discern three patterns of scaling, i.e., WM scaling, neocortical GM scaling and deep GM scaling. First, neocortical WM was the only structure to proportionally increase in larger ICV with a positive allometric coefficient of 1.14. Scaling of WM was found significantly different from all GM structures and cerebellum. Second, negative allometric coefficients were found for frontal (0.76), temporal (0.74), and parieto-occipital (0.79) cortical GM structures. Scaling of neocortical GM structures (frontal, temporal, and parieto-occipital) was not significantly different from each other, but was significantly larger than in deep GM structures when women and men were separately assessed. Also, scaling of MTL (0.60), thalamus (0.59), and the cerebellum (0.55) was not significantly different from each other in women and men separately. The scaling coefficient for striatal volume (0.41) was relatively most invariant over the range of ICV and was significantly different from all other structures, except the cerebellum.

Allometric scaling cannot solely be explained by age, sex, ethnicity or a systemic bias from segmentation pipeline. One important limitation of our study was that the sample consisted of older individuals, who have experienced various amounts of brain atrophy. Therefore, the observed scaling exponents cannot be extrapolated to younger samples. After stratifying the AGES-Reykjavik sample into quartiles of age, we found most structures to have similar scaling coefficients except for temporal GM (not including the MTL), which had lower α -coefficients in older individuals. We do not have an explanation for the significant difference in scaling found for temporal GM, but it prompted us not to rule out the possibility that allometric scaling of sub structures of the brain may vary with age in a way that we could not detect in the age span of our sample. Nonetheless, the findings of this analysis show that allometric scaling is a feature of the brain in the older population, which cannot be accounted for by adjusting for age when performing brain comparative studies.

A second important limitation was that all participants were Icelandic and the sample was genetically relatively homogeneous. Ancillary analyses in ADNI and CARDIA, with participants of younger age and different ethnicities, also showed that WM proportionally increased with increasing ICV, followed by proportionally decreases in GM, with greatest decreases in the deep GM structures, similar to our observations in the AGES-Reykjavik study. Still, there were also differences in the results between the studies. The allometric coefficients of the cortical GM areas to ICV in CARDIA seemed higher compared to

those in the AGES-Reykjavik and ADNI samples. A potential explanation could be that “ICV” in CARDIA was constructed from supratentorial structures only, and as a result allometric coefficients were higher. Another explanation could be that in the relatively young sample of the CARDIA allometric scaling is less pronounced. Further studies are needed to specifically examine this hypothesis. A second difference between the results of the additional analyses and our primary analyses in AGES-Reykjavik study was that WM volume in the ADNI data set seemed to increase isometrically with ICV. This may be explained by differences in tissue segmentation between GM and WM, as suggested by the higher mean volume of WM and lower mean volume of GM in ADNI compared with AGES-Reykjavik. Depending on how border voxels are assigned to the GM and WM tissue classes, the difference between allometric coefficients may differ. Because of these differences in scaling coefficients among the study samples, it is at the moment not possible to establish fixed reproducible allometric coefficients for the human brain and more studies are needed.

A third potential limitation of the study was the use of an automated MR segmentation technique. Systematic errors, such as improper skull stripping, incorrect intensity thresholds, difficulty in segmenting sulcal CSF, or imprecise template warping could all be possible sources of finding allometric correlations between VOI to ICV. However, when we fed artificially linearly scaled scans in the segmentation pipeline, the scaling coefficients of the output only showed small deviations from the isometric scaling law of 1, at maximum in the order of 2%. This could not explain the much larger deviations from 1 of the different scaling laws of VOI in the study sample. Therefore, we did not find evidence for a possible systematic error in the segmentation pipeline that could explain the allometry.

Allometric scaling as true feature of brain geometry

Differences in geometric or cytoarchitectural properties of different brain structures may underlie differences and similarities in scaling to ICV. We observed similar scaling coefficients of different neocortical GM areas, which suggest they preserve proportionality to one another regardless of ICV. However, cortical GM and WM had significantly different scaling coefficients, indicating they do not preserve proportionality with varying brain size. This can be explained by differences in topology, where GM can be regarded as a surface of neural tissue covering an associated volume of WM (Dale, Fischl, and Sereno 1999). The different lobes of the neocortex are similarly organized in repetitive cortical columns (Mountcastle 1997). Assuming a stable thickness of the neocortical GM “surface” across various brain sizes, as suggested by several studies (Hofman 1985; Hofman 1988; Mountcastle 1997), neocortical GM to WM should scale by an exponent of $2/3$

(square-cube). If we focus on the results based on the AGES-Reykjavik study sample, we can observe that scaling coefficients of neocortical white to gray matter range from 0.65 to 0.70 (0.76/1.14 for frontal GM, 0.74/1.14 for temporal GM, and 0.79/1.14 for parieto-occipital GM), which approximates the geometric square-cube scaling law. Nevertheless, we did not establish the same results in the younger sample of CARDIA or the smaller sample of the ADNI and caution should be taken to apply a purely square-cube scaling law to the architecture of neo cortex. In a previous study slight increases of neocortical thickness (scaling of 0.2) with increase in ICV were observed (Im et al. 2008). Another recent study showed the neocortical GM to have a more extensive gyrification, i.e., to be “twistier”, in larger brains compared to smaller ones (Germanaud et al. 2012). Also, for other parameters, such as cell soma size or amount of supporting glial cells, the extent to which they vary with increasing brain size is unclear. Some studies have also pointed to possible constraints in WM expansion, which should lead to scaling factors of white to gray that are higher than the square-cube law of $2/3$. It has been proposed that hemispheric specialization increases with increasing brain volume, which would lead to a decrease in interhemispheric connections and thus a decrease in WM volume (Ringo et al. 1994). However, the coefficients reported in the present study for the AGES-Reykjavik study provide no evidence for such a limitation on WM expansion

The disproportionately lower scaling coefficients of deep GM structures to ICV compared to the cortex are not readily explained. The cortex gives rise to connections with striatum and thalamus, thus these structures could be expected to expand with neocortical GM volume. However, we found no evidence for preserved proportionality of the striatum and thalamus with cortical GM with scaling. Possibly, the structures are more strongly influenced by other factors during brain development than neocortical growth. Brain structures grow in asynchronous patterns from birth through early adulthood and the striatum has been shown, together with frontal brain areas, to undergo more extensive developmental changes relatively late in early adulthood compared to other brain areas (Sowell et al. 1999). Also, genetic factors could influence variation in regional brain volumes and lead to disproportional neocortical and deep GM volume increases with ICV, especially for the striatum. One twin study showed that the volume of the striatum, thalamus, and cerebellum were significantly more influenced by genetic factors compared to neocortical structures that were influenced more by environmental factors (Yoon et al. 2011). And another twin-study concluded the phenotypic covariance of the striatal structures, hippocampus, and thalamus was primarily due to patterns of genetic covariance (Eyler et al. 2011).

Implications for methods of head/ brain size adjustment

Knowledge on allometric scaling of regional brain volumes is important for the discussion of adjustment methods for normal variation in comparative brain studies. Allometric scaling implies both nonproportionality and nonlinearity of scaling. Our results contribute to the understanding why certain methods should not be used. Ratios of brain structure volume over ICV or stereotaxic normalization by means of linear affine transformation assume isometric scaling of the brain, i.e., proportionate scaling, which may lead to over- or underestimation of results. Therefore the use of these methods should be avoided, except when studying disproportionality is the purpose. The erroneous effect of linear spatial normalization on groups with differences in ICV was illustrated in a study comparing neocortical thickness differences in stereotaxic and native space between men and women (Lüders, Narr, et al. 2006). The normalized data showed a disproportionately increased neocortical thickness in women compared to men, which was considerably attenuated in the unscaled data. Another important finding of our study was that allometric scaling was most apparent in deep GM structures. Unwanted effects of spatial registration therefore may be expected to be especially problematic in deep gray matter structures. Previously, a study reported that spatial-transformation based methods indeed produce significantly different proportions in smaller structures such as the hippocampus (Allen et al. 2008). Lastly, we compared the fit of the allometric model to a linear model in predicting the relation of VOI to ICV. We found very small differences in R^2 , which implies the allometric model and linear model could substitute each other in the range of total brain size variation among humans. Therefore, we conclude that it is important in brain comparative studies to adjust for nonproportionality, but not for nonlinearity.

CONCLUSION

In summary, our study found allometric scaling of WM, neocortical GM and deep GM structures to ICV in large samples of adult humans with different age, sex and ethnicity. A positive allometric coefficient was found for WM and negative allometric coefficients for neocortical and deep GM structures, with smallest scaling coefficients for deep GM. Furthermore, our analysis showed that the allometric scaling could not solely be explained by age, sex, ethnicity, or a possible systematic bias arising from the automated segmentation algorithm. We therefore conclude allometry is a true feature of the brain geometry.

BIBLIOGRAPHY

- Allen JS, Bruss J, Mehta S, Grabowski T, Brown CK, and Damasio H (2008). "Effects of spatial transformation on regional brain volume estimates". *Neuroimage* 42 (2): 535–547. DOI: [10.1016/j.neuroimage.2008.05.047](https://doi.org/10.1016/j.neuroimage.2008.05.047).
- Barnes J, Ridgway GR, Bartlett J, Henley SM, Lehmann M, et al. (2010). "Head size, age and gender adjustment in MRI studies: a necessary nuisance?" *Neuroimage* 53 (4): 1244–1255. DOI: [10.1016/j.neuroimage.2010.06.025](https://doi.org/10.1016/j.neuroimage.2010.06.025).
- Dale AM, Fischl B, and Sereno MI (1999). "Cortical surface-based analysis. I. Segmentation and surface reconstruction". *Neuroimage* 9 (2): 179–194. DOI: [10.1006/nimg.1998.0395](https://doi.org/10.1006/nimg.1998.0395).
- Davatzikos C, Tao X, and Shen D (2003). "Hierarchical active shape models, using the wavelet transform". *IEEE Trans. Med. Imaging* 22 (3): 414–423. DOI: [10.1109/TMI.2003.809688](https://doi.org/10.1109/TMI.2003.809688).
- Deacon TW (1990). "Fallacies of progression in theories of brain-size evolution". *Int. J. Primatol.* 11 (3): 193–236. DOI: [10.1007/BF02192869](https://doi.org/10.1007/BF02192869).
- Eyler LT, Prom-Wormley E, Fennema-Notestine C, Panizzon MS, Neale MC, et al. (2011). "Genetic patterns of correlation among subcortical volumes in humans: results from a magnetic resonance imaging twin study". *Hum. Brain Mapp.* 32 (4): 641–653. DOI: [10.1002/hbm.21054](https://doi.org/10.1002/hbm.21054).
- Friedman GD, Cutter GR, Donahue RP, Hughes GH, Hulley SB, et al. (1988). "CARDIA: study design, recruitment, and some characteristics of the examined subjects". *J. Clin. Epidemiol.* 41 (11): 1105–1116. DOI: [10.1016/0895-4356\(88\)90080-7](https://doi.org/10.1016/0895-4356(88)90080-7).
- Germanaud D, Lefevre J, Toro R, Fischer C, Dubois J, et al. (2012). "Larger is twistier: spectral analysis of gyrification (SPANGY) applied to adult brain size polymorphism". *Neuroimage* 63 (3): 1257–1272. DOI: [10.1016/j.neuroimage.2012.07.053](https://doi.org/10.1016/j.neuroimage.2012.07.053).
- Goldszal AF, Davatzikos C, Pham DL, Yan MXH, Bryan RN, and Resnick SM (1998). "An image-processing system for qualitative and quantitative volumetric analysis of brain images". *J. Comput. Assist. Tomogr.* 22 (5): 827–837. URL: http://journals.lww.com/jcat/Fulltext/1998/09000/An_Image_Processing_System_for_Qualitative_and_30.aspx (visited on 09/10/2018).
- Harris TB, Launer LJ, Eiriksdottir G, Kjartansson O, Jonsson PV, et al. (2007). "Age, Gene/Environment Susceptibility-Reykjavik Study: multidisciplinary applied phenomics". *Am. J. Epidemiol.* 165 (9): 1076–1087. DOI: [10.1093/aje/kwk115](https://doi.org/10.1093/aje/kwk115).
- Harvey PH (1982). "On rethinking allometry". *J. Theor. Biol.* 95 (1): 37–41. DOI: [10.1016/0022-5193\(82\)90285-5](https://doi.org/10.1016/0022-5193(82)90285-5).
- Hofman MA (1985). "Size and shape of the cerebral cortex in mammals. I. The cortical surface". *Brain Behav. Evol.* 27 (1): 28–40. DOI: [10.1159/000118718](https://doi.org/10.1159/000118718).
- Hofman MA (1988). "Size and shape of the cerebral cortex in mammals. II. The cortical volume". *Brain Behav. Evol.* 32 (1): 17–26. DOI: [10.1159/000116529](https://doi.org/10.1159/000116529).

- Im K, Lee JM, Lyttelton O, Kim SH, Evans AC, and Kim SI (2008). "Brain size and cortical structure in the adult human brain". *Cereb. Cortex* 18 (9): 2181–2191. DOI: [10.1093/cercor/bhm244](https://doi.org/10.1093/cercor/bhm244).
- Lao Z, Shen D, Liu D, Jawad AF, Melhem ER, et al. (2008). "Computer-assisted segmentation of white matter lesions in 3D MR images using support vector machine". *Acad. Radiol.* 15 (3): 300–313. DOI: [10.1016/j.acra.2007.10.012](https://doi.org/10.1016/j.acra.2007.10.012).
- Liu D, Johnson HJ, Long JD, Magnotta VA, and Paulsen JS (2014). "The power-proportion method for intracranial volume correction in volumetric imaging analysis". *Front. Neurosci.* 8: 356. DOI: [10.3389/fnins.2014.00356](https://doi.org/10.3389/fnins.2014.00356).
- Lüders E, Narr KL, Thompson PM, Rex DE, Woods RP, et al. (2006). "Gender effects on cortical thickness and the influence of scaling". *Hum. Brain Mapp.* 27 (4): 314–324. DOI: [10.1002/hbm.20187](https://doi.org/10.1002/hbm.20187).
- Lüders E, Steinmetz H, and Jancke L (2002). "Brain size and grey matter volume in the healthy human brain". *Neuroreport* 13 (17): 2371–2374. URL: http://journals.lww.com/neuroreport/Fulltext/2002/12030/Brain_size_and_grey_matter_volume_in_the_healthy.40.aspx (visited on 09/10/2018).
- Mountcastle VB (1997). "The columnar organization of the neocortex". *Brain* 120 (4): 701–722. DOI: [10.1093/brain/120.4.701](https://doi.org/10.1093/brain/120.4.701).
- O'Brien LM, Ziegler DA, Deutsch CK, Frazier JA, Herbert MR, and Locascio JJ (2011). "Statistical adjustments for brain size in volumetric neuroimaging studies: some practical implications in methods". *Psychiatry Res.* 193 (2): 113–122. DOI: [10.1016/j.psychres.2011.01.007](https://doi.org/10.1016/j.psychres.2011.01.007).
- R Core Team (2014). *R: A Language and Environment for Statistical Computing*. R Foundation for Statistical Computing. Vienna, Austria. URL: <http://www.R-project.org/>.
- Ringo JL, Doty RW, Demeter S, and Simard PY (1994). "Time is of the essence: a conjecture that hemispheric specialization arises from interhemispheric conduction delay". *Cereb. Cortex* 4 (4): 331–343. DOI: [10.1093/cercor/4.4.331](https://doi.org/10.1093/cercor/4.4.331).
- Shen D, Moffat S, Resnick SM, and Davatzikos C (2002). "Measuring size and shape of the hippocampus in MR images using a deformable shape model". *Neuroimage* 15 (2): 422–434. DOI: [10.1006/nimg.2001.0987](https://doi.org/10.1006/nimg.2001.0987).
- Sigurdsson S, Aspelund T, Forsberg L, Fredriksson J, Kjartansson O, et al. (2012). "Brain tissue volumes in the general population of the elderly: the AGES-Reykjavik study". *Neuroimage* 59 (4): 3862–3870. DOI: [10.1016/j.neuroimage.2011.11.024](https://doi.org/10.1016/j.neuroimage.2011.11.024).
- Sowell ER, Thompson PM, Holmes CJ, Jernigan TL, and Toga AW (1999). "In vivo evidence for post-adolescent brain maturation in frontal and striatal regions". *Nat. Neurosci.* 2 (10): 859–861. DOI: [10.1038/13154](https://doi.org/10.1038/13154).
- Voevodskaya O, Simmons A, Nordenskjold R, Kullberg J, Ahlstrom H, et al. (2014). "The effects of intracranial volume adjustment approaches on multiple regional MRI volumes in

- healthy aging and Alzheimer's disease". *Front. Aging Neurosci.* 6: 264. DOI: [10.3389/fnagi.2014.00264](https://doi.org/10.3389/fnagi.2014.00264).
- Yoon U, Perusse D, Lee JM, and Evans AC (2011). "Genetic and environmental influences on structural variability of the brain in pediatric twin: deformation based morphometry". *Neurosci. Lett.* 493 (1-2): 8–13. DOI: [10.1016/j.neulet.2011.01.070](https://doi.org/10.1016/j.neulet.2011.01.070).
- Zacharaki EI, Kanterakis S, Bryan RN, and Davatzikos C (2008). "Measuring brain lesion progression with a supervised tissue classification system". *Med. Image Comput. Comput. Assist. Interv.* 11 (1): 620–627. DOI: [10.1007/978-3-540-85988-8_74](https://doi.org/10.1007/978-3-540-85988-8_74).
- Zijdenbos AP, Dawant BM, and Margolin RA (1994). "Automatic detection of intracranial contours in MR images". *Comput. Med. Imaging Graph.* 18 (1): 11–23. DOI: [10.1016/0895-6111\(94\)90057-4](https://doi.org/10.1016/0895-6111(94)90057-4).
- Zijdenbos AP, Forghani R, and Evans AC (2002). "Automatic 'pipeline' analysis of 3-D MRI data for clinical trials: application to multiple sclerosis". *IEEE Trans. Med. Imaging* 21 (10): 1280–1291. DOI: [10.1109/TMI.2002.806283](https://doi.org/10.1109/TMI.2002.806283).

CHAPTER 7

Bigger brains atrophy faster in later life

Laura W de Jong
Jean-Sébastien Vidal
Alex P Zijdenbos
Lars E Forsberg
Sigurdur Sigurdsson
Vilmundur Gudnason
Mark A van Buchem
Lenore J Launer

Submitted

ABSTRACT

Previous literature suggests that in various clinical groups, those with larger ICV cope better facing the (relative) same amount of neurodegenerative changes when compared to those with smaller ICV. Therefore, ICV is often regarded as a proxy for brain reserve. However, whether larger ICV attenuates the amount of neurodegenerative changes or attenuates the effects of neurodegenerative changes has not been sufficiently studied. In the present study, we studied the relation of ICV to several MRI markers of neurodegeneration, i.e., brain atrophy, ventricular dilatation and white matter lesions (WML) load. Furthermore, we studied the relation of ICV to change in cognitive speed measured over 5 year. Our study population consisted of cross-sectional ($N = 4507$) and follow-up samples ($N = 1852$) from the well-described community-based Age, Gene, Environment, and Susceptibility - Reykjavik Study (AGES-RS) and included older adults spanning the spectrum from healthy cognition (HC) to mild cognitive impairment (MCI) and dementia. Automatically segmented brain MRI was used to estimate ICV and neurodegenerative markers. In HC, larger ICV was associated with lower fraction of total brain volume (TBV) and larger fractions of ventricular (vCSF) and WML volume. These relations were slightly more pronounced in MCI and dementia. Furthermore, after a five year follow-up, larger ICV was significantly associated with a larger yearly increase in vCSF and WML. In HC and MCI, larger ICV was also associated with a larger decrease in cognitive speed, which could partially be explained by the larger change in TBV, vCSF, and WML in larger ICV. Thus, contrarily to expectations, larger ICV was associated with higher levels of MRI markers for neurodegeneration and a larger decrease in cognitive speed.

INTRODUCTION

Previous epidemiological and clinical research suggests that those with a larger intracranial volume (ICV) cope better with neurodegenerative changes compared to those with a smaller ICV. Larger ICV and head circumference have been associated with better cognitive functioning in non-demented older adults (Farias et al. 2012; Gupta et al. 2015; Pernecky et al. 2012; Royle et al. 2013; Wolf et al. 2004). Larger ICV has also been associated with an attenuation of the negative impact of neurodegenerative changes, as represented by brain atrophy and having an APOE ϵ 4 allele, on clinical disease progression in persons with MCI (Guo et al. 2013; Pernecky et al. 2012). Additionally, smaller ICV and head circumference have been associated with an increased risk for mild cognitive impairment (MCI) and Alzheimer's disease (AD) (Schofield et al. 1997; Wolf et al. 2004).

These findings are theoretically encapsulated in the concept of brain reserve. Brain reserve has been defined by Barulli and Stern (2013) as differences in brain size and other quantitative aspects of the brain that explain differential susceptibility to functional impairment in the presence of pathology or other neurological insults (Barulli and Stern 2013). ICV is considered to reflect prior maximal brain size (Sgouros et al. 1999) and often regarded as a proxy for brain reserve. The larger the ICV, the larger the "reserve" is at the start of the neurodegenerative process. The concept of brain reserve has provided a theoretical basis to describe discrepancies in the relation of ICV and function in various clinical groups. For instance, brain reserve was proposed as an explanation of the association of larger ICV with a lower risk of progression in multiple sclerosis independent from disease burden (Sumowski et al. 2016). Or for example, Guo et al (2013) showed that older people with large ICV and severe atrophy (defined as a brain parenchymal fraction (PF) of ≤ 0.66) experienced slower cognitive deterioration when compared with older people with small ICV and mild atrophy. Furthermore, they found that the impact of brain atrophy and the presence of the APOE ϵ 4 allele on cognition was less in MCI cases with large ICV compared to small ICV. They proposed their findings supported the theory of a compensatory role of brain reserve.

Although the concept of brain reserve describes a similar phenomenon in various clinical groups, it is not well understood why larger ICV is beneficial to cognitive performance when facing neurodegeneration. Hypothetically, ICV may influence the amount of neurodegeneration and be associated with a resistance to neurodegenerative changes. The effect of ICV would then manifest itself as less neurodegenerative changes in those with larger ICV compared to peers with smaller ICV (Arenaza-Urquijo and Vemuri 2018). Among studies that propagate such an explanation are population cohorts studies that hypothesize that factors in early life favoring brain growth, contribute to enhanced re-

sistance to neurodegenerative changes and lead to a decreased incidence of dementia (Prince et al. 2011). However, most authors support the hypothesis that larger ICV is associated with an increased resilience (i.e., better than expected performance in face of neurodegenerative burden) to neurodegenerative changes, as in the examples given above. The nature of the compensatory mechanisms leading up to his effect is, however, not well understood. Larger brains are considered to have larger cell counts and/or larger amount of synaptic connections and therefore may withstand more neurodegenerative changes before clinical deficits appear because of a buffering effect. An important difference between the two theories of brain reserve is that the theory of resistance considers ICV to attenuate the amount of neurodegeneration, whereas the theory of resilience considers ICV to attenuate the effect of neurodegenerative changes. Whether or not a dependency exists between ICV and neurodegenerative burden and whether or not ICV attenuates the effect of neurodegenerative changes on cognition are verifiable scientific questions that have not been studied sufficiently.

As part of the efforts to further define the concept of brain reserve, here, we studied whether ICV was associated with an increased resistance or resilience to neurodegenerative changes in a large well-described population-based cohort of older people spanning the spectrum from normal cognition to dementia. Brain atrophy, ventricular dilatation, and WML load are considered markers of neurodegeneration that can be evaluated well by structural MRI. First, we studied the relation of ICV to these markers of neurodegeneration in HC, to determine whether ICV was associated with a resistance to neurodegenerative changes. Second, we studied the relation of ICV to the amount of brain atrophy, ventricular dilatation, and WML load in MCI and dementia and compared that to HC. And lastly, we studied whether ICV was related to the change in cognitive speed over five years and whether this relation was mediated by the change in the markers of neurodegeneration.

METHODS

Study design

Our study sample was extracted from the population-based cohort of the Age, Gene, Environment/Susceptibility – Reykjavik study (AGES-Reykjavik) consisting of 5764 men and women, born between 1907–1935. The general design and demographics of the AGES-Reykjavik have been described elsewhere (Harris et al. 2007). Participants underwent extensive clinical and cognitive evaluation and brain MRI between 2002–2006 and surviving participants were invited for a follow-up examination on after five years. All participants signed an informed consent. The AGES-Reykjavik study was approved

by the Intra-mural Research Program of the National Institute on Aging, the National Bioethics Committee in Iceland (VSN00-063), the Icelandic Data Protection Authority, and the institutional review board of the U.S. National Institute on Aging, National Institutes of Health.

Acquisition and automated segmentation of MRI

Brain MRI was performed on a 1.5-T GE Signa Twinspeed system MRI scanner at the Icelandic Heart Association. The image protocol included a 3D axial T1-weighted acquisition, a fluid-attenuated inversion recovery (FLAIR) sequence, and a fast spin echo proton density (PD)/T2-weighted (de Jong, Wang, et al. 2012; Sigurdsson et al. 2012; Sveinbjornsdottir et al. 2008). A fully automated segmentation pipeline was developed based on the Montreal Neurological Institute processing pipeline (Sigurdsson et al. 2012; Zijdenbos, Forghani, and Evans 2002). The pipeline used a multispectral approach to segment voxels into global tissue classes [cerebrospinal fluid (CSF), GM, WM and white matter hyperintensities (WMH)], of which the methods and validation were described previously (Sigurdsson et al. 2012). Cerebral spinal fluid (CSF), gray matter (GM), white matter (WM) and white matter lesions (WML) were separately segmented. WML included periventricular, deep and juxtacortical WMH. CSF was divided into ventricular CSF (lateral, third and fourth ventricle) and peripheral CSF (surrounding brain tissue in the sulci and basal cisterns), using the AGES atlas for regional segmentation (Forsberg et al. 2017). Total brain volume (TBV) was the sum of the GM, WM, and WML. ICV was the sum of TBV and CSF. Percentage TBV of ICV was considered a measure of global brain atrophy. Percentage vCSF of ICV was considered a marker for ventricular dilatation. Percentage WML of ICV was considered a measure for WML burden. Volume measurements of follow-up brain MRI were acquired the same way as measurements at baseline. Absolute change per year in TBV, vCSF, and WML, was calculated as (value at baseline – value at follow-up) / interval in years between scans. Yearly change per mill ICV in TBV, and per myriad vCSF and pCSF, were calculated as annualized absolute change \times 1000 or 10,000 / ICV.

Educational level, cognitive test score, and other covariates

Sample demographics and characteristics were chosen based on studies of their association with cognitive functioning in older age. Educational level (primary, secondary, college and university education), smoking history (never, ever), and alcohol intake history (never, ever) were assessed by questionnaire. Body mass index (BMI) was calculated as current weight divided by squared midlife height (taken from data of the Reykjavik

Study examination that occurred 25 (SD = 4.2) years earlier. Diabetes was defined as a history of physician diagnosed diabetes, use of glucose-modifying medication, or a fasting blood glucose ≥ 7.0 mmol/L. Hypertension was defined as measured systolic blood pressure ≥ 140 mmHg or diastolic blood pressure ≥ 90 mmHg, or self-reported doctor's diagnosis of hypertension, or use of antihypertensive medications. Speed of processing score was calculated as a composite of the following standardized tests: Figure Comparison Test (Salthouse and Babcock 1991), the Digit Symbol Substitution Test (Wechsler 1955), and the Stroop Test part 1 and 2 (Saczynski et al. 2008; Stroop 1935).

Diagnosis of dementia and MCI were ascertained in a three-step process, as described previously (Harris et al. 2007). In summary, every subject screened positive on the Mini-Mental State Examination and the Digit Symbol Substitution Test, were administered (underwent) extensive diagnostic neuropsychological test battery, a neurological examination, and one of their proxies was interviewed. A panel including a geriatrician, neurologist, neuropsychologist, and neuroradiologist reviewed all the data and made a consensus diagnosis of dementia and MCI. Dementia was classified according to Diagnostic and Statistical Manual of Mental Disorders, Fourth Edition, criteria (American Psychiatric Association 1994). MCI was defined as having a borderline score (< 1.5 standard deviations below a score determined according to the distribution of scores in a cohort subsample) in memory or two other domains, not severe enough to be classified as dementia.

Analytical sample

Brain MR scanning was performed on consenting MR eligible subjects. From the total AGES-RS sample of 5764 participants, 4726 underwent successful MRI. Tissue segmentation was successful in 4613 MR scans. Cases for whom cognitive status (either healthy cognition, MCI or dementia) was not determined ($N = 106$) were excluded. Our final study sample consisted of 4507 people with successful brain MRI and segmentation of the images, of whom 3883 had healthy cognition, 422 were diagnosed with MCI, and 202 with dementia.

The follow-up sample ($N = 3316$) consisted of all invited surviving participants from the baseline cohort. Part of this sample underwent successful follow-up brain scanning between 2007–2011, with an average interval of 5.19 (SD = 0.25) years from the first scan ($n = 2641$). From this sample, we excluded those with missing MRI at baseline ($N = 87$) and missing cognitive status assessment ($N = 20$). Our analysis was focused on the relation between ICV to change MRI based markers of neurodegeneration (i.e., brain atrophy, ventricular dilatation, and WML load), which constitute relatively small numbers over the course of 5 years. To ensure our results would not be distorted by

drift of the ICV measurements, for instance due to the update of the MRI scanner software, we excluded participants with more than 1% change in ICV between the two time points ($N = 682$). There were 40 individuals who had received MCI diagnosis at baseline, but who were scored HC at follow-up. In the follow-up sample they were considered HC. Our final follow-up sample consisted of 1586 non-demented participants, 176 participants with a diagnosis of MCI, and 90 with a diagnosis of dementia at time point 2, with successful brain MR segmentation at both time points.

Statistical analysis

All statistical analysis and graphs were computed with R v 3.4.3 (R Core Team 2014).

Comparison of study samples

Regarding the baseline sample, general characteristics and covariates were compared between groups of HC, MCI and dementia. Regarding the follow-up sample, general characteristics and covariates were compared between the group of participants who were included to those who were excluded based on a $\geq 1\%$ difference in ICV between baseline and follow-up measurements.

Analysis of the relation of ICV and markers of neurodegeneration

The relation of ICV to brain atrophy, ventricular dilatation, and WML load was first examined cross-sectionally in the baseline sample of HC. Quartiles of distribution of ICV were calculated in the HC sample among men and women separately. Threshold of the quartiles of ICV (in cm^3) were 1347, 1418, and 1486 for women, and 1536, 1615, and 1692 for men. Mean values of sample characteristics and fractions of TBV, vCSF, and WML over ICV were calculated per quartile of ICV. Associations of ICV to sample characteristics and fractions of TBV, vCSF, and WML were analyzed using a logistic regression model for categorical variables as dependent variable and a linear regression model for continuous variables as dependent variable. In both types of models, ICV was entered as independent continuous variable and adjustments were made for age and sex. Models for the relation of ICV to fractions of TBV, vCSF, and WML were further adjusted for educational level, smoking and drinking history, and diagnosis of diabetes and hypertension. A p -value < 0.05 was considered significant.

Second, the relation of ICV to brain atrophy, ventricular dilatation, and WML load, was visualized and analyzed in different age groups. Deciles of ICV were computed separately for each quartile of age with thresholds 66–71, 72–75, 76–79, and 80–95. The mean fractions of TBV, vCSF and WML over ICV were plotted for each decile of

ICV and for each quartile of age separately. For each quartile of age, a separate linear model was created with fraction of TBV, vCSF, or WML as dependent variable and ICV as independent variable, together with corrections for sex, educational level, smoking and drinking history, and diagnosis of diabetes and hypertension. The regression lines of each quartile of age were displayed in the same graph. The relation of ICV to fractions of TBV, vCSF, and WML was compared between the quartiles of age by testing the interaction term for ICV and quartile of age in the whole sample of baseline HC (also corrected for sex, educational level, smoking and drinking history, and diagnosis of diabetes and hypertension). A $p < 0.05$ was considered significant.

Third, the relation of ICV to the change in fractions of TBV, vCSF, and WML, over a period of on average five years was examined. Change in fraction of TBV was expressed as yearly change per mill of ICV and change in fractions of vCSF and WML were expressed as yearly change per myriad of ICV. The change in these markers was entered in a linear model as dependent variable, with baseline ICV measurement as independent continuous variable with adjustments for age, educational level, sex, smoking and drinking history, and diagnosis of diabetes and hypertension. The relation of ICV to change in fractions of TBV, vCSF, and WML after five-year follow-up was also visualized. Again, deciles of ICV were computed for the follow-up sample of HC. Mean values of annualized change per year in fractions of TBV, vCSF, and WML over ICV were plotted for each decile of ICV. The regression lines from the linear models were drawn in the same graph.

ICV and markers of neurodegeneration in MCI and dementia

The relation of ICV to fractions of TBV, vCSF, and WML was visualized and compared between groups of HC, MCI, and dementia. Deciles of ICV were computed separately for HC, MCI, and dementia. Mean values of fractions of TBV, vCSF and WML over ICV were plotted for each decile of ICV and for HC, MCI, and dementia groups separately. A linear model was created separately for HC, MCI, and dementia, with fraction of TBV, vCSF, or WML as the dependent variable and baseline ICV measurement as the independent variable. Corrections were made for age, sex, educational level, smoking and drinking history, and diagnosis of diabetes and hypertension. The relation of ICV to fractions of TBV, vCSF, and WML was compared among groups of HC, MCI, and dementia by testing the interaction term for ICV and group status (also corrected for sex, educational level, smoking and drinking history, and diagnosis of diabetes and hypertension). A $p < 0.05$ was considered significant.

Analysis of the relation of ICV and change in cognitive speed

Whether ICV was related to the change in cognitive speed over five years was assessed separately in HC, MCI, and dementia. First, mean cognitive speed scores at baseline and follow-up between the quartiles of ICV of HC were compared. Second, the relation was assessed in a linear model with change in cognitive speed entered as dependent variable and baseline ICV measurement entered as independent variable together with age, sex, and speed score at baseline. To assess whether the relation of ICV to change in cognitive speed was mediated through change in neurodegenerative markers, a second linear model was made with further addition of change in TBV, vCSF, and WML.

RESULTS

Sample characteristics

Mean age of our sample was 76.3 (5.4) years, and 58.1% ($N = 2619$) of the sample were women. ICV was on average 1502 (148) cm^3 and TBV was on average 1039 (99) cm^3 . Twenty four percent of the women ($N = 629$) and 32% of the men ($N = 605$) had a college or university education. Compared to HC, MCI and dementia groups were on average older, had a lower percentage of women, lower educational level, lower speed of processing, lower BMI, lower percentage of alcohol consumers and higher prevalence of hypertension (Table 1). There was no difference in mean ICV between the different cognitive status groups. Sample characteristics of the included participants versus the excluded participants of the follow-up sample did not differ (Table 2).

The relation of ICV and markers of neurodegeneration

In the baseline sample of HC, when ICV was taken as a continuous variable, those with larger ICV were on average younger, had a higher educational level, a faster speed of processing, smoked and drank more, and a lower prevalence of diabetes and hypertension (Table 3). Fraction of TBV over ICV was significantly lower in those with larger ICV and fractions of vCSF and WML over ICV were significantly larger in those with larger ICV. These relations did not change after correction for age, sex, educational level, smoking and drinking history, and diagnosis of diabetes or hypertension.

Figure 1 displays the relations of ICV with fractions of TBV, vCSF and WML per quartile of age. Mean fraction TBV declined with each consecutive older quartile of age. Yet, in all age groups, mean fraction TBV also declined with each consecutive larger decile of ICV. Also, mean fractions of vCSF and WML increased with each consecutive

Table 1: Sample characteristics of baseline study samples

| Sample characteristics, %(N) | HC <i>N</i> = 3883 | MCI <i>N</i> = 422 | Dementia <i>N</i> = 202 | <i>p</i> ^a |
|-----------------------------------|-----------------------|-----------------------|----------------------------|-----------------------|
| Age (years), M (SD) | 75.7 (5.2) | 79.7 (5.4) | 80.9 (4.9) | <.0001 |
| Women | 59.4 (2307) | 50.5 (213) | 49.0 (99) | <.0001 |
| ICV (in cm ³), M (SD) | 1502 (147) | 1494 (156) | 1510 (154) | 0.39 |
| Higher education | 29.9 (1160) | 10.9 (46) | 13.9 (28) | <.0001 |
| Speed of processing, M (SD) | 0.223 (0.634) | -0.888 (0.869) | -1.53 (1.20) | <.0001 |
| BMI (kg/m ²), M (SD) | 27.0 (4.3) | 26.8 (4.4) | 25.8 (4.2) | 0.0004 |
| Never smoked | 40.5 (1573) | 41.7 (176) | 41.1 (83) | 0.89 |
| Never drank alcohol | 21.4 (826) | 28.9 (121) | 28.6 (57) | 0.0003 |
| Diabetes | 11.1 (430) | 10.2 (43) | 11.5 (23) | 0.85 |
| Hypertension | 79.6 (3089) | 86.0 (363) | 84.7 (171) | 0.002 |

a *p*-value from ANOVA for continuous variables and χ^2 test for class variables.

% (N), percentage (number); M (SD), mean (standard deviation); HC, healthy cognition; MCI, mild cognitive impairment; ICV, intracranial volume; Higher education, college or university education; BMI, body mass index.

older quartile of age and in all age groups mean fractions of vCSF and WML increased with each consecutive larger decile of ICV. Thus, slopes of ICV fractions of TBV, vCSF, and WML in the different age groups had a different intercept but ran parallel. The interaction term ICV x quartile of age were non-significant, being 0.33 for TBV, 0.89 for vCSF, and 0.44 for WML.

Figure 2 and table 4 display the influence of ICV on change in neurodegenerative markers according to ICV. Measured over a 5 year period, yearly increase in vCSF and WML (expressed in per myriad ICV) was significantly larger in those with larger ICV, with 7.55 (4.88) in the lowest quartile of ICV compared to 9.49 (5.85) in the highest quartile of ICV for vCSF and with 6.80 (7.13) in the lowest quartile compared to 9.15 (10.14) in the highest quartile for WML (both $p < 0.001$). Figure 2 also shows the relation between ICV and change in TBV per mill ICV, and change in vCSF and WML per myriad ICV. Although, visually the change in per mill TBV was larger in those with larger ICV, this trend did not reach significance ($p = 0.34$).

ICV and markers of neurodegeneration in MCI and dementia

Figure 3 displays the relations of ICV and fractions of TBV, vCSF, and WML in groups of HC, MCI, and dementia. Mean fraction of TBV was lower in MCI and dementia

Figure 1: ICV and markers of neurodegeneration in different age groups

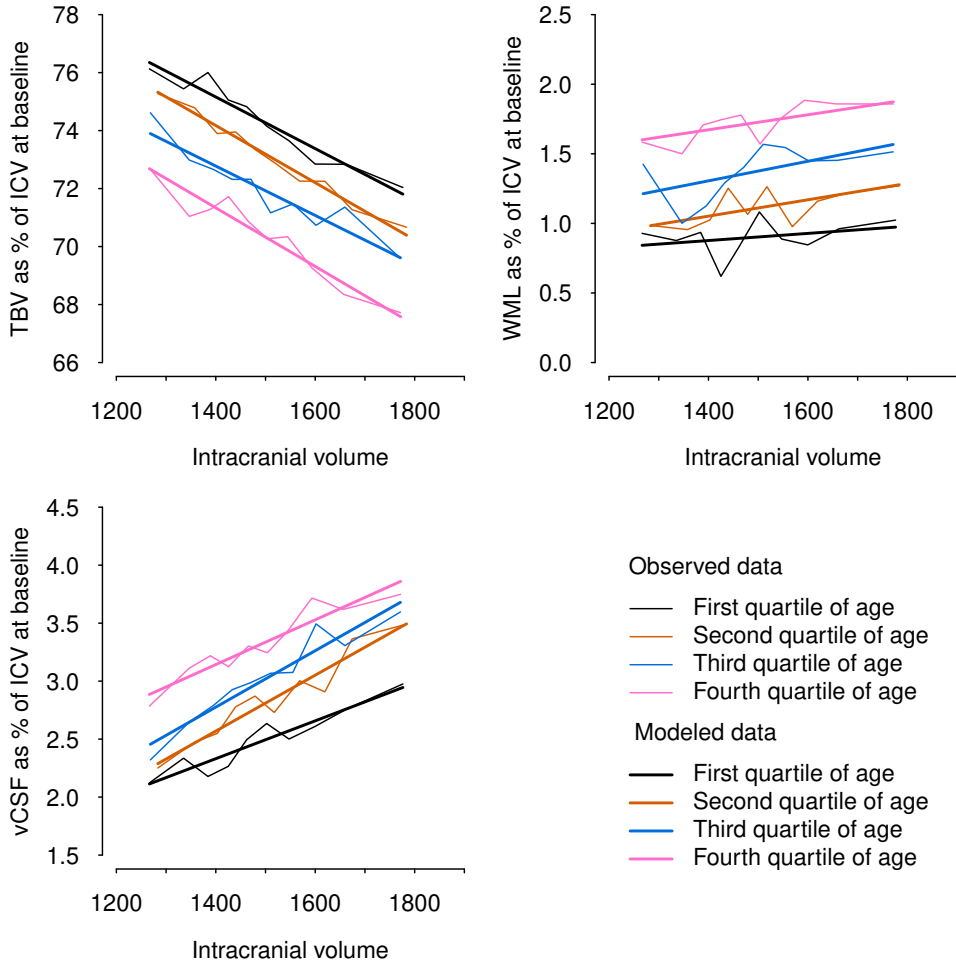


Figure 2: ICV and change in markers of neurodegeneration over 5 years in HC

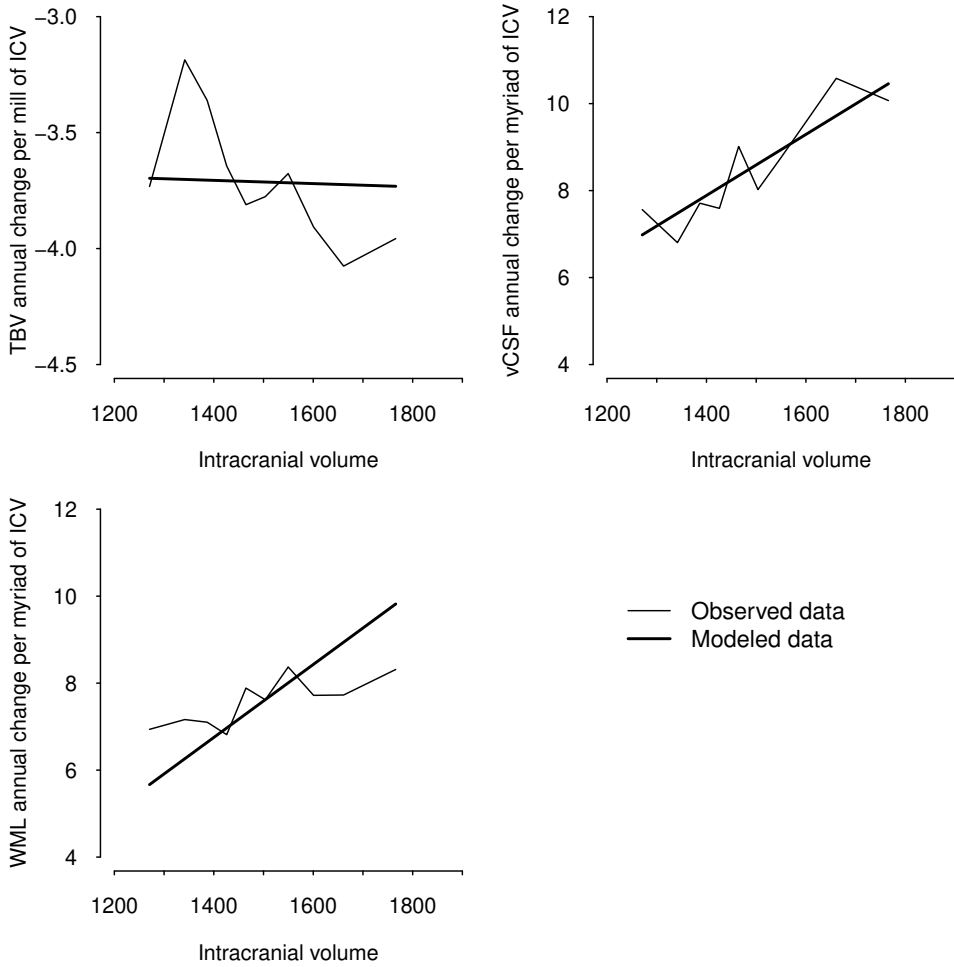


Figure 3: Association of ICV with neurodegeneration in HC, MCI and dementia

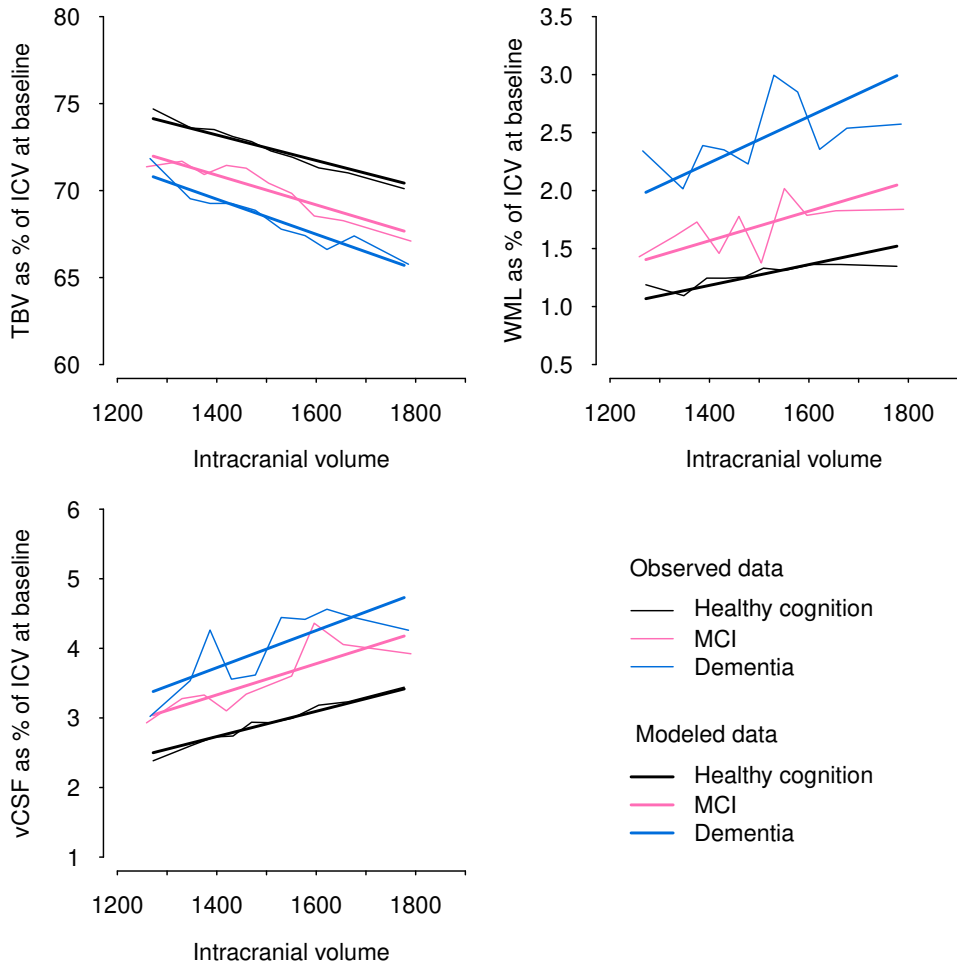


Table 2: Comparison of included versus excluded participants of the follow-up sample

| Sample characteristics, % (N) | Included subjects ICV change < 1% N = 1852 | Excluded subjects ICV change ≥ 1% N = 682 | <i>p</i> ^a |
|----------------------------------|--------------------------------------------------|-------------------------------------------------|-----------------------|
| Age (years), M (SD) | 74.6 (4.6) | 74.7 (5.2) | 0.69 |
| Women | 59.0 (1093) | 58.4 (398) | 0.80 |
| Higher education | 27.1 (502) | 30.2 (206) | 0.14 |
| Speed of processing | 0.070 (0.780) | 0.013 (0.776) | 0.11 |
| BMI (kg/m ²), M (SD) | 25.0 (3.3) | 24.9 (3.4) | 0.62 |
| Never smoked | 43.5 (806) | 43.8 (299) | 0.92 |
| Never drank alcohol | 20.6 (379) | 20.9 (140) | 0.92 |
| Diabetes | 9.62 (178) | 8.52 (58) | 0.44 |
| Hypertension | 77.6 (1438) | 77.6 (529) | 0.99 |

a *p*-value from *t*-test for continuous variables and χ^2 test for class variables.

ICV, intra cranial volume; M (SD), mean (standard deviation); Higher education, college or university education; BMI, body mass index

compared to HC, yet in all groups, fraction of TBV also declined in each consecutive larger decile of ICV. Also, mean fractions of vCSF and WML were higher in MCI and dementia compared to HC, yet in all groups, mean fractions of vCSF and WML increased in each consecutive larger decile of ICV. A subtle divergence of slopes of relation of ICV and fractions of TBV, vCSF and WML can be observed, with slopes in MCI and dementia being slightly steeper compared to the slopes in HC. The *p*-value for the interaction term with cognitive status did not reach significance but indicated a trend, being 0.12 for TBV, 0.18 for vCSF, and 0.16 for WML.

The relation of ICV and change in cognitive speed

In the follow-up sample, mean cognitive speed had decreased more in those with larger ICV. Cognitive speed had changed from 0.044 (0.71) to -0.17 (0.77) in quartile 1, from 0.22 (0.67) to 0.015 (0.74) in quartile 2, from 0.27 (0.65) to 0.046 (0.67) in quartile 3, and from 0.27 (0.62) to -0.010 (0.73) in quartile 4. Table 5 shows the relation of ICV to change in cognitive speed. ICV was significantly negatively associated with change in cognitive speed in HC ($p = 0.006$) and in MCI ($p < 0.001$) but not in dementia ($p = 0.12$). Thus, in HC and MCI, those with larger ICV had decreased more in cognitive speed compared to those with smaller ICV. After adding change in TBV, vCSF, and WML, to the model, the association of ICV to change in cognitive speed was attenuated, but continued to be significant in MCI ($p = 0.004$).

Table 3: Sample characteristics and neurodegeneration per quartile of ICV in HC at baseline

| Sample characteristics markers of neurodegeneration, % (N) | Quartile of ICV (sex specific) | | | | p^a | p^b |
|---------------------------------------------------------------|--------------------------------|----------------|----------------|----------------|--------|--------|
| | Q1 N = 1127 | Q2 N = 1127 | Q3 N = 1126 | Q4 N = 1127 | | |
| Age (years), M (SD) | 76.6 (5.6) | 76.5 (5.5) | 76.2 (5.3) | 75.8 (5.3) | <.0001 | |
| Women | 58.1 (655) | 58.1 (655) | 58.1 (654) | 58.1 (655) | - | |
| Higher education | 19.1 (215) | 25.7 (290) | 30.2 (340) | 34.5 (389) | <.0001 | |
| Speed of processing, M (SD) | -0.071 (0.814) | 0.029 (0.818) | 0.139 (0.779) | 0.120 (0.869) | <.0001 | |
| BMI (kg/m ²), M (SD) | 25.0 (3.5) | 24.9 (3.2) | 25.0 (3.3) | 24.9 (3.3) | 0.96 | |
| Never smoked | 46.4 (523) | 40.2 (453) | 38.6 (435) | 37.4 (421) | 0.002 | |
| Never drank alcohol | 46.4 (523) | 40.2 (453) | 38.6 (435) | 37.4 (421) | 0.0006 | |
| Diabetes | 12.7 (143) | 11.6 (130) | 8.36 (94) | 11.4 (129) | 0.01 | |
| Hypertension | 82.8 (933) | 81.5 (919) | 78.2 (880) | 79.1 (891) | 0.004 | |
| As % of ICV, M (SD) | | | | | | |
| TBV | 72.9 (3.7) | 72.3 (3.8) | 71.9 (3.8) | 71.1 (4.2) | <.0001 | <.0001 |
| vCSF | 2.76 (1.11) | 3.01 (1.30) | 3.09 (1.30) | 3.23 (1.32) | <.0001 | <.0001 |
| WML | 1.28 (1.35) | 1.30 (1.28) | 1.39 (1.35) | 1.50 (1.46) | <.0001 | <.0001 |

^a p -value from general linear model with ICV as continuous variable adjusted for age and sex.

^b model additionally adjusted for smoking history, drinking history, diagnosis of diabetes and diagnosis of hypertension. % (N), percentage (number); M (SD), mean (standard deviation); Higher education, college or university education; BMI, body mass index; ICV, intracranial volume; TBV, total brain volume; vCSF, ventricular cerebrospinal fluid volume; WML, white matter lesion volume.

Table 4: ICV and neurodegenerative markers over 5 years in HC

| Annualized change, M (SD) | Quartile of ICV (sex specific) | | | | p^a |
|---------------------------------|--------------------------------|-----------------|-----------------|-----------------|--------|
| | Q1 $N = 397$ | Q2 $N = 396$ | Q3 $N = 396$ | Q4 $N = 397$ | |
| TBV ‰ ICV | −3.79 (1.93) | −3.56 (2.00) | −3.76 (1.91) | −3.74 (1.97) | 0.43 |
| vCSF ‰ ICV | 7.55 (4.88) | 8.23 (5.17) | 9.00 (5.93) | 9.49 (5.85) | <.0001 |
| WML ‰ ICV | 6.80 (7.13) | 7.20 (7.77) | 7.11 (7.83) | 9.15 (10.1) | 0.02 |

a p -value from general linear model with change in TBV, vCSF or WML as dependent variable and ICV as continuous independent variable adjusted for age, sex, smoking history, drinking history, diagnosis of diabetes and diagnosis of hypertension.

M (SD), mean (standard deviation); ICV, intracranial volume; TBV, total brain volume; vCSF, ventricular cerebrospinal fluid volume, WML, white matter lesion volume.

DISCUSSION

Main findings

In a large sample of older individuals, larger ICV was associated with a lower fraction of TBV and larger fractions of vCSF and WML. These relations were similar in different age groups, slightly more pronounced in MCI and dementia, and independent from other sample characteristics associated with larger ICV (sex, educational level, smoking history, alcohol history, diagnosis of diabetes or hypertension). Furthermore, after a five year follow-up, larger ICV was significantly associated with a larger yearly increase in vCSF and WML. In HC and MCI, larger ICV was also associated with a larger decrease in cognitive speed, which could partially be explained by the larger increase in ventricular dilatation and WML in larger ICV.

General discussion

We investigated in a large sample of older people whether ICV was associated with either a higher resistance or higher resilience to neurodegenerative changes. ICV is often regarded as a proxy for brain reserve, because previously it was shown that in various clinical groups those with larger ICV seemed to cope better with the (relatively) same amount of neurodegenerative changes compared to those with smaller ICV (Hedges and Woon 2010; Kesler et al. 2003; Skoog et al. 2012; Sumowski et al. 2016; Tate et al. 2011). The notion of resistance implies that among people without overt neurodegenerative disease, those with larger ICV have fewer neurodegenerative changes, as measured by brain atrophy and WML load. However, our study showed that in a general popula-

Table 5: ICV and change in cognitive speed over 5 years

| Model 1 | HC N = 1586 | | MCI N = 176 | | Dementia N = 90 | |
|-----------------------------|----------------|--------|----------------|--------|--------------------|-------|
| | β (SD) | p^a | β (SD) | p^a | β (SD) | p^a |
| Age | -0.021 (0.002) | <.0001 | -0.010 (0.010) | 0.30 | 0.021 (0.029) | 0.47 |
| Sex | 0.004 (0.027) | 0.88 | -0.019 (0.116) | 0.87 | 0.23 (0.36) | 0.53 |
| Cognitive speed at baseline | -0.11 (0.02) | <.0001 | -0.37 (0.05) | <.0001 | -0.24 (0.17) | 0.17 |
| ICV at baseline | -0.026 (0.009) | 0.006 | -0.13 (0.04) | 0.0009 | -0.23 (0.14) | 0.10 |
| Model 2 | | | | | | |
| Age | -0.020 (0.002) | <.0001 | -0.011 (0.009) | 0.21 | 0.015 (0.030) | 0.63 |
| Sex | -0.013 (0.026) | 0.62 | -0.016 (0.109) | 0.88 | 0.12 (0.37) | 0.76 |
| Cognitive speed at baseline | -0.12 (0.01) | <.0001 | -0.33 (0.05) | <.0001 | -0.21 (0.17) | 0.23 |
| Change in TBV | 0.36 (0.05) | <.0001 | 0.19 (0.22) | 0.39 | 0.57 (0.66) | 0.39 |
| Change in vCSF | -0.56 (0.21) | 0.006 | -2.08 (0.82) | 0.01 | -1.36 (2.50) | 0.59 |
| Change in WML | -0.44 (0.12) | 0.0004 | -0.40 (0.48) | 0.40 | -0.44 (1.23) | 0.73 |
| ICV at baseline | -0.017 (0.009) | 0.05 | -0.11 (0.04) | 0.004 | -0.20 (0.14) | 0.17 |

a p -value from general linear model with change in cognitive speed score as dependent variable and independent variables listed in the 1st column.
 HC, healthy cognition; MCI, mild cognitive impairment; ICV, intracranial volume; TBV, total brain volume; vCSF, ventricular cerebrospinal fluid volume; WML, white matter lesion volume.

tion, larger ICV was associated with more neurodegenerative changes, both in terms of absolute and relative volumes. This finding was supported by the result of the follow-up analyses taken 5 years from baseline that showed a disproportionately faster increase in vCSF and WML in those with larger ICV. The relation between larger ICV and higher levels of markers of neurodegeneration is intriguing. Although, those with larger ICV had a higher prevalence of lifestyle traits unfavorable for health, i.e., they had smoked and drank more, these factors did not exert an influence on the relation of ICV and neurodegenerative markers and therefore could not explain the phenomenon. Why then would a brain that was favored to grow larger during early life, lose its volume quicker in later life and contain relatively more WML? The present study did not enable us to find an explanation, but we put forward two hypotheses. First, it may be that a larger brain is more difficult to maintain and therefore may be more vulnerable to neurodegenerative changes. Such a proposition could also explain for instance why those with larger ICV have been found to have an accelerated conversion to dementia (An et al. 2016). Our second hypothesis is that the brain atrophies in an allometric fashion, i.e., the larger the ICV, the proportionally larger the decrease in brain parenchymal volume per unit of time. Although, there is some familiarity with allometric geometrical scaling of brain structures to ICV (de Jong, Vidal, et al. 2017; Im et al. 2008), there are no reports on size-dependent non-linearity in age-related brain atrophy.

Furthermore, we investigated whether ICV was associated with an increased resilience to neurodegenerative changes. First, we compared the relation of ICV with neurodegenerative markers in HC to groups of MCI and dementia. In all groups larger ICV was associated with proportionately more neurodegenerative changes. A non-significant trend indicated that the effect of ICV on the amount of neurodegenerative changes was slightly more pronounced in MCI and dementia. Thus, finding more neurodegenerative changes in those with larger ICV in MCI or dementia seems not to be related to a later expression of a neurodegenerative disease due to a buffer effect in people with larger ICV. Rather, our study showed the relation of ICV to neurodegenerative markers was independent of the presence of a neurodegenerative disease. Second, we also studied whether ICV was related to change in cognitive speed in HC. At baseline those in quartile 4 had the fastest mean cognitive speed, but at follow-up the mean cognitive speed score of quartile 4 had dropped below the mean score of those in quartile 2. Also, after controlling for age, sex, and baseline speed score, cognitive speed had decreased significantly more in those with larger ICV. Since larger ICV was related to larger ventricular dilatation and larger increase in WML, it seems plausible that this could explain the faster decrease in cognitive speed. Indeed, when ICV together with change in TBV, vCSF, and WML were entered in the same model to explain change in cognitive speed, the effect of ICV on change in cognitive speed was largely attenuated, indicating that, in HC, the larger

decrease in cognitive speed in those with larger ICV was mediated through the presence of more brain atrophy and a higher increase in WML. In the MCI group, like in HC, larger ICV was also significantly associated with larger decrease in cognitive speed. However, this effect was only partially mediated through the change in vCSF. We do not have an explanation for the association of ICV with change in cognitive speed that seemed independent from the markers of neurodegeneration we controlled for. Possibly, brain atrophy and ventricular dilatation did not reflect the full extent of neurodegeneration in MCI. All together, regarding cognitive speed, we found no support for the notion that a larger ICV would be associated with a greater resilience in face of neurodegenerative changes.

The results of this study are important for our understanding of brain ageing in several ways. First, we found no supporting evidence that ICV was associated with either a raised resistance or resilience to neurodegenerative changes in older people. On the contrary, we found that larger ICV was associated with a higher degree of neurodegenerative changes and a larger decrease in cognitive speed. This can become clinically apparent as a faster conversion to dementia or as a faster clinical deterioration in those with a larger ICV, as previously described (An et al. 2016; Mungas et al. 2018). Second, if atrophy occurs in a non-linear fashion according to ICV, the interpretation of volumetric differences between groups will depend on the ICVs of the two groups. Furthermore, in our sample there was a substantial difference of 3.17% in mean fraction of TBV between the lowest and the highest decile of ICV. Whereas the difference in mean fraction of TBV between cognitively healthy and demented people was only 2.51%. Thus, the magnitude of the effect of ICV on fraction of TBV variation exceeded that of diagnosis of dementia, which indicates that the size-dependent non-linear brain atrophy could obscure pathological patterns of brain ageing.

Strengths and limitations

Strength of the current study was the availability of information on demographics, relevant risk factors, clinical parameters, and brain MRI for a large sample of older people spanning the range from HC, to MCI and dementia. We could therefore study the relation of ICV and markers of neurodegeneration not only in clinical groups but also in healthy cognitive ageing. Furthermore, the availability of follow-up data of a large part of the sample for further analysis supported and strengthened our findings in the cross-sectional data. However, the follow-up data did not show a faster decline in yearly change in TBV after 5 years and therefore we cannot be entirely certain whether the cross-sectional association of larger ICV with lower fraction TBV is based on faster atrophy of the brain in larger ICV. Theoretically, it is also possible that larger ICV is as-

sociated with smaller fraction TBV throughout the life span. A longer follow-up duration could make the relation between ICV and brain atrophy more clear. Another potential limitation of the current study was that all measures of neurodegenerative markers were based on estimations of the automated MRI segmentation pipeline. Automated segmentation of MRI into different tissue classes forms a very robust method compared to visual qualitative assessment scores. Even so, it is possible that the segmentation pipeline introduces errors into the tissue segmentation. However, we could not identify an error that could have affected all three different MRI markers of neurodegeneration in the same manner. Another potential problem may be a systematic error in estimation of ICV by the segmentation pipeline. A previous study compared the ICV estimation of Statistical Parametric Mapping (SPM, version 8) and Freesurfer (FS, version 5.1.0) to reference estimations of ICV based on manual segmentation and found that both automated methods overestimated ICV (Nordenskjold et al. 2013). Interestingly, they found that the overestimation of ICV by FS was related to the reference ICV estimation. FS did not explicitly segment ICV, but estimated it based on the determinant of the affine transform matrix used to align the image with an atlas. Affine transform only crudely approximates head shape. However, the automated segmentation pipeline used in the current study has two advantages over the segmentation software that was tested before. First, it made use of a probabilistic tissue atlas that was developed based on a sample of MRI from the AGES-RS cohort, and thus the atlas was age appropriate. And second, the tissue segmentation made use of non-linear transformation to warp the atlas from standard space to native space and therefore if present would be able to allow allometry in brain geometry.

CONCLUSION

In a large sample of older individuals spanning the range from normal cognition to dementia, larger ICV was associated with a relatively smaller brain volume and larger volumes of vCSF and WML. Larger ICV was also associated with a faster increase in vCSF and WML over five years. Moreover, larger ICV was significantly associated with a larger decline in cognitive speed, which was partially mediated through the change in TBV, vCSF, and WML. Thus, contrarily to what is often proposed in literature, we found no evidence for the notion that ICV is associated with a higher resistance or resilience to neurodegenerative changes. Rather, a larger ICV was associated with relatively more brain atrophy, a higher WML load, and a faster decline in cognitive speed.

BIBLIOGRAPHY

- American Psychiatric Association (1994). *Diagnostic and statistical manual of mental disorders DSM-IV (4th ed.)* Washington, DC: Authors.
- An H, Son SJ, Cho S, Cho EY, Choi B, and Kim SY (2016). "Large intracranial volume accelerates conversion to dementia in males and APOE4 non-carriers with mild cognitive impairment". *Int. Psychogeriatr.* 28 (5): 769–778. DOI: [10.1017/S104161021500229X](https://doi.org/10.1017/S104161021500229X).
- Arenaza-Urquijo EM and Vemuri P (2018). "Resistance vs resilience to Alzheimer disease: Clarifying terminology for preclinical studies". *Neurology* 90 (15): 695–703. DOI: [10.1212/WNL.0000000000005303](https://doi.org/10.1212/WNL.0000000000005303).
- Barulli D and Stern Y (2013). "Efficiency, capacity, compensation, maintenance, plasticity: emerging concepts in cognitive reserve". *Trends Cogn. Sci. (Regul. Ed.)* 17 (10): 502–509. DOI: [10.1016/j.tics.2013.08.012](https://doi.org/10.1016/j.tics.2013.08.012).
- de Jong LW, Vidal JS, Forsberg LE, Zijdenbos AP, Haight T, et al. (2017). "Allometric scaling of brain regions to intra-cranial volume: An epidemiological MRI study". *Hum. Brain Mapp.* 38 (1): 151–164. DOI: [10.1002/hbm.23351](https://doi.org/10.1002/hbm.23351).
- de Jong LW, Wang Y, White LR, Yu B, van Buchem MA, and Launer LJ (2012). "Ventral striatal volume is associated with cognitive decline in older people: a population based MR-study". *Neurobiol. Aging* 33 (2): 1–10. DOI: [10.1016/j.neurobiolaging.2010.09.027](https://doi.org/10.1016/j.neurobiolaging.2010.09.027).
- Farias ST, Mungas D, Reed B, Carmichael O, Beckett L, et al. (2012). "Maximal brain size remains an important predictor of cognition in old age, independent of current brain pathology". *Neurobiol. Aging* 33 (8): 1758–1768. DOI: [10.1016/j.neurobiolaging.2011.03.017](https://doi.org/10.1016/j.neurobiolaging.2011.03.017).
- Forsberg L, Sigurdsson S, Fredriksson J, Egilsdottir A, Oskarsdottir B, et al. (2017). "The AGES-Reykjavik study atlases: Non-linear multi-spectral template and atlases for studies of the ageing brain". *Med Image Anal* 39: 133–144. DOI: [10.1016/j.media.2017.04.009](https://doi.org/10.1016/j.media.2017.04.009).
- Guo LH, Alexopoulos P, Wagenpfeil S, Kurz A, and Perneczky R (2013). "Brain size and the compensation of Alzheimer's disease symptoms: a longitudinal cohort study". *Alzheimers Dement* 9 (5): 580–586. DOI: [10.1016/j.jalz.2012.10.002](https://doi.org/10.1016/j.jalz.2012.10.002).
- Gupta M, King KS, Srinivasa R, Weiner MF, Hulseley K, et al. (2015). "Association of 3.0-T brain magnetic resonance imaging biomarkers with cognitive function in the Dallas Heart Study". *JAMA Neurol.* 72 (2): 170–175. DOI: [10.1001/jamaneurol.2014.3418](https://doi.org/10.1001/jamaneurol.2014.3418).
- Harris TB, Launer LJ, Eiriksdottir G, Kjartansson O, Jonsson PV, et al. (2007). "Age, Gene/Environment Susceptibility-Reykjavik Study: multidisciplinary applied phenomics". *Am. J. Epidemiol.* 165 (9): 1076–1087. DOI: [10.1093/aje/kwk115](https://doi.org/10.1093/aje/kwk115).
- Hedges DW and Woon FL (2010). "Premorbid brain volume estimates and reduced total brain volume in adults exposed to trauma with or without posttraumatic stress disorder: a meta-analysis". *Cogn Behav Neurol* 23 (2): 124–129. DOI: [10.1097/WNN.0b013e3181e1cbe1](https://doi.org/10.1097/WNN.0b013e3181e1cbe1).

- Im K, Lee JM, Lyttelton O, Kim SH, Evans AC, and Kim SI (2008). "Brain size and cortical structure in the adult human brain". *Cereb. Cortex* 18 (9): 2181–2191. DOI: [10.1093/cercor/bhm244](https://doi.org/10.1093/cercor/bhm244).
- Kesler SR, Adams HF, Blasey CM, and Bigler ED (2003). "Premorbid intellectual functioning, education, and brain size in traumatic brain injury: an investigation of the cognitive reserve hypothesis". *Appl Neuropsychol* 10 (3): 153–162. DOI: [10.1207/S15324826AN1003_04](https://doi.org/10.1207/S15324826AN1003_04).
- Mungas D, Gavett B, Fletcher E, Farias ST, DeCarli C, and Reed B (2018). "Education amplifies brain atrophy effect on cognitive decline: implications for cognitive reserve". *Neurobiol. Aging* 68: 142–150. DOI: [10.1016/j.neurobiolaging.2018.04.002](https://doi.org/10.1016/j.neurobiolaging.2018.04.002).
- Nordenskjold R, Malmberg F, Larsson EM, Simmons A, Brooks SJ, et al. (2013). "Intracranial volume estimated with commonly used methods could introduce bias in studies including brain volume measurements". *Neuroimage* 83: 355–360. DOI: [10.1016/j.neuroimage.2013.06.068](https://doi.org/10.1016/j.neuroimage.2013.06.068).
- Pernecky R, Alexopoulos P, Wagenpfeil S, Bickel H, and Kurz A (2012). "Head circumference, apolipoprotein E genotype and cognition in the Bavarian School Sisters Study". *Eur. Psychiatry* 27 (3): 219–222. DOI: [10.1016/j.eurpsy.2011.01.008](https://doi.org/10.1016/j.eurpsy.2011.01.008).
- Prince M, Acosta D, Dangour AD, Uauy R, Guerra M, et al. (2011). "Leg length, skull circumference, and the prevalence of dementia in low and middle income countries: a 10/66 population-based cross sectional survey". *Int Psychogeriatr* 23 (2): 202–213. DOI: [10.1017/S1041610210001274](https://doi.org/10.1017/S1041610210001274).
- R Core Team (2014). *R: A Language and Environment for Statistical Computing*. R Foundation for Statistical Computing. Vienna, Austria. URL: <http://www.R-project.org/>.
- Royle NA, Booth T, Valdes Hernandez MC, Penke L, Murray C, et al. (2013). "Estimated maximal and current brain volume predict cognitive ability in old age". *Neurobiol. Aging* 34 (12): 2726–2733. DOI: [10.1016/j.neurobiolaging.2013.05.015](https://doi.org/10.1016/j.neurobiolaging.2013.05.015).
- Saczynski JS, Jonsdottir MK, Sigurdsson S, Eiriksdottir G, Jonsson PV, et al. (2008). "White matter lesions and cognitive performance: the role of cognitively complex leisure activity". *J. Gerontol. A Biol. Sci. Med. Sci.* 63 (8): 848–854. DOI: [10.1093/gerona/63.8.848](https://doi.org/10.1093/gerona/63.8.848).
- Salthouse TA and Babcock RL (1991). "Decomposing adult age differences in working memory". *Dev. psychol.* 27 (5): 763. DOI: [10.1037/0012-1649.27.5.763](https://doi.org/10.1037/0012-1649.27.5.763).
- Schofield PW, Logroscino G, Andrews HF, Albert S, and Stern Y (1997). "An association between head circumference and Alzheimer's disease in a population-based study of aging and dementia". *Neurology* 49 (1): 30–37. DOI: [10.1212/WNL.49.1.30](https://doi.org/10.1212/WNL.49.1.30).
- Sgouros S, Goldin JH, Hockley AD, Wake MJ, and Natarajan K (1999). "Intracranial volume change in childhood". *J. Neurosurg.* 91 (4): 610–616. DOI: [10.3171/jns.1999.91.4.0610](https://doi.org/10.3171/jns.1999.91.4.0610).
- Sigurdsson S, Aspelund T, Forsberg L, Fredriksson J, Kjartansson O, et al. (2012). "Brain tissue volumes in the general population of the elderly: the AGES-Reykjavik study". *Neuroimage* 59 (4): 3862–3870. DOI: [10.1016/j.neuroimage.2011.11.024](https://doi.org/10.1016/j.neuroimage.2011.11.024).

- Skoog I, Olesen PJ, Blennow K, Palmertz B, Johnson SC, and Bigler ED (2012). "Head size may modify the impact of white matter lesions on dementia". *Neurobiol. Aging* 33 (7): 1186–1193. DOI: [10.1016/j.neurobiolaging.2011.01.011](https://doi.org/10.1016/j.neurobiolaging.2011.01.011).
- Stroop JR (1935). "Studies of interference in serial verbal reactions". *J. Exp. Psychol.* 18 (6): 643. DOI: [10.1037/h0054651](https://doi.org/10.1037/h0054651).
- Sumowski JF, Rocca MA, Leavitt VM, Meani A, Mesaros S, et al. (2016). "Brain reserve against physical disability progression over 5 years in multiple sclerosis". *Neurology* 86 (21): 2006–2009. DOI: [10.1212/WNL.0000000000002702](https://doi.org/10.1212/WNL.0000000000002702).
- Sveinbjornsdottir S, Sigurdsson S, Aspelund T, Kjartansson O, Eiriksdottir G, et al. (2008). "Cerebral microbleeds in the population based AGES-Reykjavik study: prevalence and location". *J. Neurol. Neurosurg. Psychiatr.* 79 (9): 1002–1006. DOI: [10.1136/jnnp.2007.121913](https://doi.org/10.1136/jnnp.2007.121913).
- Tate DF, Neeley ES, Norton MC, Tschanz JT, Miller MJ, et al. (2011). "Intracranial volume and dementia: some evidence in support of the cerebral reserve hypothesis". *Brain Res.* 1385: 151–162. DOI: [10.1016/j.brainres.2010.12.038](https://doi.org/10.1016/j.brainres.2010.12.038).
- Wechsler D (1955). *Manual for the Wechsler adult intelligence scale*. Oxford, UK: Psychological Corp.
- Wolf H, Julin P, Gertz HJ, Winblad B, and Wahlund LO (2004). "Intracranial volume in mild cognitive impairment, Alzheimer's disease and vascular dementia: evidence for brain reserve?" *Int. J. Geriatr. Psychiatr.* 19 (10): 995–1007. DOI: [10.1002/gps.1205](https://doi.org/10.1002/gps.1205).
- Zijdenbos AP, Forghani R, and Evans AC (2002). "Automatic 'pipeline' analysis of 3-D MRI data for clinical trials: application to multiple sclerosis". *IEEE Trans. Med. Imaging* 21 (10): 1280–1291. DOI: [10.1109/TMI.2002.806283](https://doi.org/10.1109/TMI.2002.806283).

CHAPTER 8

Summary and general discussion

Importance of structural imaging markers of AD

Alzheimer's disease (AD) is a growing socio-economic concern for ageing populations and the search for a treatment or prevention of AD is pressing. Today, it is believed that the therapeutic window of AD may be during its preclinical phase (Sperling et al. 2011). Finding early imaging markers of AD is of interest because they may facilitate the selection of people at risk for developing AD in a noninvasive manner. Most prior imaging studies of AD have focused on cortical degeneration and in particular on allocortical degeneration. However, pathological studies have shown the involvement of deep gray matter structures in AD as well. The striatum plays a central role in the limbic system and the cholinergic system, which are both affected in AD. Therefore the striatum can be considered a key candidate structure to be affected early in the disease. Part one of this thesis bundled the results of several volumetric and morphometric structural MRI studies of the striatum in older people and especially in patients with AD. Identifying pathological (focal) brain atrophy is, however, complex and a simple estimation of brain structure volumes of an individual patient does not lead to a diagnosis but needs to be assessed relative to group volumes and premorbid brain size. Therefore, in part two of this thesis two large population studies were included that focused on improving our understanding of the physiologic variability of brain structure and degeneration.

Part 1 Ventral striatal atrophy in AD

Volume loss of the ventral striatum in AD

Like other brain structures, the striatum loses volume with ageing. However, as described in chapter 2 striatal volume loss is higher in patients diagnosed with probable AD compared with their peers with normal cognitive test scores. A study of 139 brain MRI from a memory clinic population showed that this striatal volume loss was not homogeneous, but more pronounced in the nucleus accumbens and the putamen. Since, there are no sharp anatomical borders between striatal substructures, the study of only striatal volumes with artificially drawn borders is limited. A study of the shape of the striatum provided more information on which parts are affected in AD. Especially the ventral surface of the putamen and medio-ventral head of the caudate nucleus in patients with AD showed an inward change compared to study participants with normal cognitive test scores. This indicates that striatal volume loss in AD can, for a large part, be attributed to atrophy in the ventral striatum. Theoretically, the finding of pronounced ventral striatal volume loss in AD fits well with already established knowledge on atrophy patterns of the brain in AD. The ventral striatum is an important part of the limbic sys-

tem (Olmos and Heimer 1999). Like in the rest of the brain where AD affects first and mostly the allocortical and limbic areas (Callen et al. 2001), the striatum also displays most severe losses of volume in the limbic part. The studies of striatal atrophy in AD presented in this thesis were among the first imaging studies that focused specifically on striatal atrophy in AD. Recent studies have confirmed the presence of striatal atrophy in AD with disproportionate loss of the ventral part (Pievani et al. 2013; Roh et al. 2011; Yi et al. 2016).

Ventral striatal volume loss predicts cognitive decline

In order to assess the implication for cognitive functioning of striatal atrophy in AD, the relation between striatal atrophy and change in cognitive function was examined in a large population based sample of older individuals including those with diagnosis of vascular dementia or AD. Furthermore, the relation of striatal atrophy and the trajectory in cognitive function was compared to the relation of hippocampal volume loss and change in cognitive function. Cognitive function was repeatedly assessed in 4 sessions spanning a decade. Brain, striatal, and hippocampal volume measurements were based on brain MRI performed at the second session. Thus, cognitive data were available for study participants diagnosed with dementia prior, at time of, and after volume measurements of the striatum and hippocampus. The volumes of the total striatum, nucleus accumbens, putamen, and hippocampus were all smaller in participants diagnosed with dementia. But, interestingly, the volume of the nucleus accumbens was also significantly smaller in those who were going to be diagnosed with dementia years after the brain scan. Nucleus accumbens volume predicted cognitive decline in people with dementia diagnosed 3 years prior to, at the time of, and up to 6 years after brain scanning. Moreover, nucleus accumbens volume also predicted cognitive decline in participants that did not receive the diagnosis of dementia throughout the entire follow-up duration. This predictive value of the nucleus accumbens volume for cognitive function was independent of the effect of the predictive value of hippocampal volume and was stronger than the predictive value of hippocampal volume for participants that never received the diagnosis of dementia during follow-up.

Vascular risk factors are not related to striatal volume loss

Although the striatum, particularly the ventral striatum, seems to be affected in an early stage of the dementia process, it is not clear what the histopathological basis for the volume loss of the striatum observed in AD as shown in chapters 2–4 is. One of the hypotheses was that striatal volume loss might be due to other disease processes that

often co-occur with AD, like large and/or small vessel disease. The striatum is known to be particularly prone to arteriolosclerosis with the frequent occurrence of lacunar infarcts and microbleeds in the striatum under hypertensive conditions (Shi and Wardlaw 2016). Perhaps the accumulation of small focal vascular damage eventually leads to atrophy of the overall volume of the striatum and thalamus. However, as described in chapter 5 the presence of cardiovascular risk factors, APOE ϵ 4 status, body mass index, cholesterol, smoking history, drinking history, diabetes, and hypertension were not related to a higher rate of striatal atrophy measured over 2.5 years. In contrast, the hippocampus atrophied faster in the presence of hypertension and APOE ϵ 4 status. Albeit this being a selective study on only cardiovascular risk factors, so far no alternative explanation was found for striatal volume loss in AD than the disease process itself.

Embedding ventral striatal atrophy in existing models of AD

How does ventral striatal atrophy fit into the existent knowledge on pathological brain changes in AD and what may be the responsible pathological mechanism for volume loss in this area? The best hypothetical explanation available today is based on older histopathological studies of the striatum in AD. First, some studies have shown that cell bodies of the cholinergic interneurons are almost entirely filled with neurofibrillary tangles and that there is a disproportionate loss of cholinergic interneurons in the ventral striatum (Lehéricy et al. 1989; Selden, MM Mesulam, and Geula 1994; H Braak and E Braak 1990; Oyanagi et al. 1987). Although, cholinergic interneurons constitute 1–2% of all striatal cells, their soma is large (up to 40 μ m), and their highest concentrations are found in the ventral striatum (Steiner and Tseng 2010). Thus, the volume loss of the ventral striatum in AD may be based on loss of cholinergic interneurons. The striatal cholinergic cells show the same pathological changes as magnocellular cholinergic forebrain complex. Loss of the cholinergic interneurons is a widespread phenomenon in the basal forebrain in AD, in particular the posterior part of the nucleus basalis of Meynert, and some studies found it to occur early in the process of AD (M Mesulam et al. 2004; Grothe, Heinsen, and Teipel 2013; Teipel et al. 2014). It is not known why cholinergic cells are lost in AD. The cholinergic cells are highly dependent for their existence on nerve growth factor. Some studies have shown the loss of nerve growth factor to precede cholinergic cell loss in the basal forebrain and striatum (Strada et al. 1992; Latina et al. 2017). And nerve growth factor signaling at cholinergic terminals on its turn has been shown to be sensitive to the toxic effect of A β (Triaca and Calissano 2016). But these relations need further confirmation. Another possible explanation for cholinergic cell loss in AD may be the more direct toxicity of A β in the striatum. The striatum of AD patients is heavily infiltrated by amyloid deposits (H Braak and E Braak

1990). In familial variants of AD cases and in Down syndrome, amyloid deposits have been shown to accumulate first in the striatum (Klunk et al. 2007; Annus et al. 2016; Villemagne et al. 2009). And in late onset AD the presence of striatal amyloid deposits together with cortical amyloid deposits on PiB/PET predicts Braak neurofibrillary stage and clinicopathologic stage of AD *in vivo* (Beach et al. 2012). However, it is not clear whether striatal A β depositions occur early in the disease process of late onset AD. Recently, a thorough florbetapir (¹⁸F) PET study to preclinical stages of AD, as defined by presence of number of biomarkers/ cognitive markers and NIA-AA criteria, found subcortical amyloid deposition to occur early in the disease process especially in the nucleus accumbens and putamen. The same study reported that the buildup of amyloid may be more complete in subcortical areas relative to cortical areas, even in the earliest phases of preclinical AD. These findings contrast the more dominant theoretical model that predicts a downward progression of A β from neocortex to subcortical regions (e.g., thalamus and striatum) (H Braak and Del Tredici 2015; Thal et al. 2002). In summary, the cause of ventral striatal atrophy in AD loss is unknown, but previous studies have shown important loss of cholinergic cells and dense amyloid deposition in the striatum in preclinical stages of the disease.

Can ventral striatal atrophy serve as a marker for early AD?

Many morphological and pathological processes occur in brains of AD patients, but not all of them are related to or crucial to the development of the eventual characteristic clinical presentation. For instance, the accumulation of amyloid in the cortex of older people is a well-known process in AD. Although the presence of amyloid plaques is a hallmark of AD, the presence of these plaques has a small effect on episodic memory but not on other cognitive domains (Hedden et al. 2013) and also does not exclusively occur in patients with AD but also in a considerable percentage of people that have died without cognitive decline (Wolf et al. 1999; Latimer et al. 2017). The challenge for studies on AD is therefore to unravel the temporal order of pathological events and to try to identify those key events in the pathological cascade that eventually lead to cognitive impairment. The findings of this thesis together with recently published data are promising indications that the ventral striatum may be one of the structures relatively early affected in the pathological cascade of AD and can predict cognitive decline. Especially supportive to this hypothesis are the observations described in chapter 4 that smaller ventral striatal volume is detectable in people before clinical diagnosis of dementia and predictive for cognitive decline up to 6 years before dementia diagnosis. Also, volume of the nucleus accumbens was independent from hippocampal volume in predicting cognitive decline. However, there are some limitations of the ventral striatal atrophy/volume

to function as a predictive structural imaging marker for AD. For instance, hippocampal atrophy can be easily approximated by visual assessment. A major advantage to this visual assessment is the anatomical proximity of the temporal horn of the lateral ventricle. Contrarily, the ventral striatum is surrounded by and part of the complex anatomical region encompassing the ventrostriatopallidal system and extended amygdala for which precise anatomy is still subject to debate (Olmos and Heimer 1999). Also, current MRI protocols in daily clinical practice use volumetric T1-weighted imaging with whole brain coverage and perhaps coronal T2 weighted imaging, but these are not optimized to show anatomical detail in the region of the striatum and basal forebrain. Therefore, ventral striatal atrophy at this stage cannot be used as a marker for AD in an individual patient.

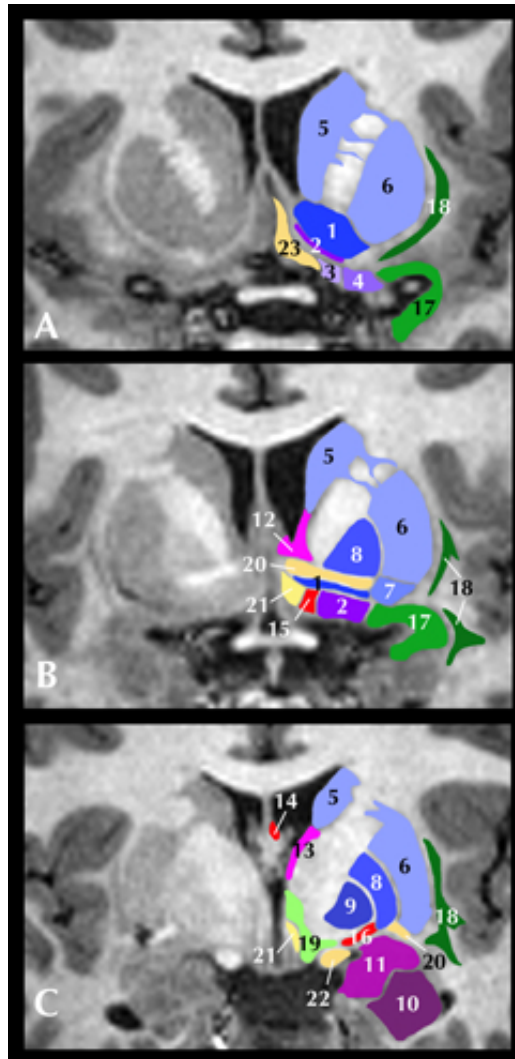
Limitations and future directions

There are two general limitations of the research presented in this thesis. The first limitation is related to the anatomical precision of the automated segmentation techniques used especially for segmenting the ventral striatum and nucleus accumbens. The nucleus accumbens is histologically well defined, being it the only structure in the striatum that is composed of a core and a shell. The ventral striatum includes besides the nucleus accumbens, also the ventral putaminal and caudate areas, olfactory tubercle, and anterior perforated substance (Heimer, Alheid, and Zahm 1993). The basal forebrain area surrounding the nucleus accumbens is packed with multiple white matter tracts and gray matter nuclei of the ventral striatopallidal system and extended amygdala, which are closely adjacent and in some areas continuous with each other. The extended amygdala is a concept that describes the phylogenetic continuity of the centromedial nuclei of the amygdala and the bed nucleus of the stria terminalis. The cortical-laterobasal part of the amygdala, provides important input to both the extended amygdala and to the ventral striatopallidal system (Olmos and Heimer 1999). Several studies have shown atrophy in the region of the basal forebrain in early AD, but the anatomical nomenclature used is not consistent. One study showed that atrophy in the basal nucleus of Meynert precedes atrophy of the entorhinal cortex (Schmitz et al. 2016). Others have pointed to disproportionately high degeneration of the gray matter in the basal forebrain in cholinergic magnocellular regions Ch1-4, corresponding to the medial septal nucleus (Ch1), vertical and horizontal limb of the diagonal band of Broca (Ch2-Ch3) and the basal nucleus of Meynert (Ch4) (MM Mesulam et al. 1983). This basal forebrain atrophy in the pre-dementia stage of AD first appeared in the posterior part, also known as the basal nucleus of Meynert (Grothe, Heinsen, and Teipel 2013). These studies used a probabilistic atlas based on superposition of several cytoarchitectonic maps on an MNI brain (Zaborszky et al. 2008) to segment the cholinergic basal forebrain nuclei. Another study manually

traced the substantia innominata by comparing the MR image to a Nissl-stained coronal section of the basal forebrain region and found the region to be atrophied in mild AD (George et al. 2011). Although the term substantia innominata has become obsolete, judging from the description in the latter study, the substantia innominata probably corresponded to area basal nucleus of Meynert. These studies highlight the importance of the basal nucleus of Meynert in early AD. However, they tend not to be critical towards segmenting different nuclei with sometimes a millimeter thickness (Mai, Majtanik, and Paxinos 2015) on MRI with insufficient resolution and contrast to discriminate these cholinergic cell clusters from the ventrostriatopallidal system or extended amygdala. A schematic representation of the anatomical structures of the basal forebrain area and striatum is given in figure 1. The automated segmentation methods used in the studies presented in previous chapters, may suffer as well from difficulties in discriminating atrophy of the ventral striatum from atrophy in the cholinergic cell clusters of the basal forebrain notably the basal nucleus of Meynert. However, the nucleus accumbens was segmented as the region anterior to the anterior commissure, both in the segmentation tool of FSL (chapters 2, 3, and 4) as in the segmentation pipeline of the AGES-Reykjavik study (chapter 5) (Patenaude et al. 2007). Thus, the volumetric estimations of the nucleus accumbens may be underestimated but at least do not include the basal nucleus of Meynert, which is located underneath/ventral to the ventral globus pallidus. Likewise the estimations regarding the putamen, in particular the morphological contraction in the ventral putamen in AD, should not be affected by the atrophy in the basal nucleus of Meynert. Future studies should be directed towards a finer grained segmentation of this intricate anatomical forebrain region requiring higher resolution MRI with a focused field-of-view.

The second limitation is related to the role of the ventral striatum in cognition and consequences of its volumetric decline for functioning of the patient. It has been postulated that the nucleus accumbens plays a pivotal role in memory and learning processes and selecting responses (Goldenberg et al. 1999; Gonzalez-Burgos and Feria-Velasco 2008; Graybiel 2008). In the studies described in this thesis the cognitive function of the study participants was tested by several cognitive tests but none of them was specifically directed to the function of the ventral striatum. Furthermore, since the function of the cholinergic cells in the striatum in particular is still not completely clarified (Apicella 2007), no test for function of these cells has yet been developed. The precise impact of ventral striatal atrophy on the clinical presentation of AD is therefore not known and perhaps underestimated. Interestingly, since the olfactory tubercle is an integrated part of the ventral striatum, perhaps olfaction tests form a good marker for ventral striatal degeneration. Indeed, olfaction is the only sense that is affected early in the disease process of AD (Naudin, Mondon, and Atanasova 2013).

Figure 1: Striatum and basal forebrain complex on coronal MRI



1 Nucleus accumbens; 2 Olfactory tubercle; 3 Anterior olfactory nucleus; 4 Olfactory area; 5 Caudate nucleus; 6 Putamen; 7 Fundus region of putamen; 8 External globus pallidus; 9 Internal globus pallidus; 10 Basolateral amygdaloid nucleus; 11 Basomedial amygdaloid nucleus; 12 Bed nucleus of the stria terminalis; 13 Stria terminalis; 14 Medial septal nucleus (Ch1); 15 Diagonal band of Broca (Ch2 and Ch3); 16 Basal nucleus of Meynert (Ch4); 17 Piriform cortex; 18 Claustrum; 19 Hypothalamic area; 20 Anterior commissure; 21 Medial forebrain bundle; 22 Optic tract; 23 Subcallosal area.

Part 2 Allometric scaling of brain structures

Allometric scaling of brain structures

The second part of the research presented in this thesis examined physiological variability in brain structure and degeneration depending on the size of the premorbid brain. To be able to differentiate pathological from normal atrophy pattern in the brain, it is essential to have a good understanding of the geometry of the brain. The human brain varies considerably in size. How can brains of different size be compared? The answer to this question is complex. Some adjustment methods rely on the preservation of isometry of substructures of the brain and use a ratio of region of interest to intracranial volume (ICV) or total brain volume (TBV) to adjust for overall brain size. However, as was shown in chapter 6, brain structures do not scale isometrically with ICV variation. A comprehensive study of three large datasets with together more than 4500 brain MRI proofed that people with larger ICV on average contained proportionally smaller volumes of cortical and deep gray matter and a proportionally larger volume of white matter. Although, allometric scaling was shown in previous studies for gray and white cortical matter volume and even for cortical thickness, the study described in chapter 6 is the largest such study ever to be conducted and was the first to thoroughly investigate the deep gray matter structures. Furthermore, allometric scaling of brain structures was found in three large different study samples and after extensive testing could not be attributed to age-associated atrophy, gender, ethnicity, or a systematic bias from study-specific segmentation algorithm. Larger brains have a smaller developmental outgrowth of deep gray matter structures compared to the cortex and a smaller outgrowth of gray matter compared to white matter. Structures that show the least variance are the striatum and the thalamus. These results show why methods of head size adjustment that rely on isometry of brain substructures lead to over- or underestimation of results, spark erroneous interpretations and should be avoided. Also, methods that rely solely on linear affine transformation of the brain should be handled with care.

Larger brains degenerate faster in later life

If the brain develops with allometric scaling of its substructures, do brains of different sizes involute differently with ageing? Previous literature suggests that in various clinical groups, those with larger ICV cope better facing the (relative) same amount of neurodegenerative changes when compared to those with smaller ICV. ICV is, therefore, by some regarded as a proxy for brain reserve. Why a larger ICV is beneficial in maintaining performance with ageing is, however, not understood. Hypothetically, a larger ICV could

be associated with a higher resistance to neurodegenerative changes and thus harbor less stigmata of neurodegeneration. Or, a larger ICV could be associated with an increased resilience (i.e., better than expected performance in face of neurodegenerative burden) to neurodegenerative changes. Whether or not larger ICV has a positive effect on the amount of neurodegenerative changes or whether or not ICV attenuates the effect of neurodegenerative changes on cognition are falsifiable scientific questions that have not been studied sufficiently. In chapter 7, the relation of ICV to three MRI markers of neurodegeneration, i.e., brain atrophy, ventricular dilatation, and white matter lesion load, was studied. Furthermore, the relation of ICV with change in cognitive speed was also examined. The study was conducted in a large sample of older people spanning the spectrum from normal cognition to dementia. Larger ICV was cross-sectionally associated with a proportionally smaller brain volume and larger ventricular and white matter lesion volumes. These relations were similar in different age groups, slightly more pronounced in MCI and dementia, and independent from other sample characteristics associated with larger ICV (among others sex and educational level). Furthermore, after a five year follow-up, larger ICV was significantly associated with a larger yearly increase in ventricular volume and white matter lesion load. In those with healthy cognition or MCI, larger ICV was also associated with a larger decrease in cognitive speed, which was partially mediated through the larger increase in ventricular dilatation and white matter lesions in larger ICV. Thus, contrarily to what is often proposed in literature, no evidence was found for the notion that ICV is associated with a higher resistance or resilience to neurodegenerative changes. Rather, a larger ICV was associated with relatively more brain atrophy, a higher WML load, and a faster decline in cognitive speed.

BIBLIOGRAPHY

- Annus T, Wilson LR, Hong YT, Acosta-Cabronero J, Fryer TD, et al. (2016). "The pattern of amyloid accumulation in the brains of adults with Down syndrome". *Alzheimers Dement.* 12 (5): 538–545. DOI: [10.1016/j.jalz.2015.07.490](https://doi.org/10.1016/j.jalz.2015.07.490).
- Apicella P (2007). "Leading tonically active neurons of the striatum from reward detection to context recognition". *Trends Neurosci.* 30 (6): 299–306. DOI: [10.1016/j.tins.2007.03.011](https://doi.org/10.1016/j.tins.2007.03.011).
- Beach TG, Sue LI, Walker DG, Sabbagh MN, Serrano G, et al. (2012). "Striatal amyloid plaque density predicts Braak neurofibrillary stage and clinicopathological Alzheimer's disease: implications for amyloid imaging". *J. Alzheimers Dis.* 28 (4): 869–876. DOI: [10.3233/JAD-2011-111340](https://doi.org/10.3233/JAD-2011-111340).

- Braak H and Braak E (1990). "Alzheimer's disease: striatal amyloid deposits and neurofibrillary changes". *J. Neuropathol. Exp. Neurol.* 49 (3): 215–224. DOI: [10.1097/00005072-199005000-00003](https://doi.org/10.1097/00005072-199005000-00003).
- Braak H and Del Tredici K (2015). "The preclinical phase of the pathological process underlying sporadic Alzheimer's disease". *Brain* 138 (Pt 10): 2814–2833. DOI: [10.1093/brain/awv236](https://doi.org/10.1093/brain/awv236).
- Callen DJ, Black SE, Gao F, Caldwell CB, and Szalai JP (2001). "Beyond the hippocampus: MRI volumetry confirms widespread limbic atrophy in AD". *Neurology* 57 (9): 1669–1674. DOI: [10.1212/WNL.57.9.1669](https://doi.org/10.1212/WNL.57.9.1669).
- George S, Mufson EJ, Leurgans S, Shah RC, Ferrari C, and deToledo-Morrell L (2011). "MRI-based volumetric measurement of the substantia innominata in amnesic MCI and mild AD". *Neurobiol. Aging* 32 (10): 1756–1764. DOI: [10.1016/j.neurobiolaging.2009.11.006](https://doi.org/10.1016/j.neurobiolaging.2009.11.006).
- Goldenberg G, Schuri U, Grömminger O, and Arnold U (1999). "Basal forebrain amnesia: does the nucleus accumbens contribute to human memory?" *J. Neurol. Neurosurg. Psychiatr.* 67 (2): 163–168. DOI: [10.1136/jnmp.67.2.163](https://doi.org/10.1136/jnmp.67.2.163).
- Gonzalez-Burgos I and Feria-Velasco A (2008). "Serotonin/dopamine interaction in memory formation". *Prog. Brain Res.* 172: 603–623. DOI: [10.1016/S0079-6123\(08\)00928-X](https://doi.org/10.1016/S0079-6123(08)00928-X).
- Graybiel AM (2008). "Habits, rituals, and the evaluative brain". *Annu. Rev. Neurosci.* 31: 359–387. DOI: [10.1146/annurev.neuro.29.051605.112851](https://doi.org/10.1146/annurev.neuro.29.051605.112851).
- Grothe M, Heinsen H, and Teipel S (2013). "Longitudinal measures of cholinergic forebrain atrophy in the transition from healthy aging to Alzheimer's disease". *Neurobiol. Aging* 34 (4): 1210–1220. DOI: [10.1016/j.neurobiolaging.2012.10.018](https://doi.org/10.1016/j.neurobiolaging.2012.10.018).
- Hedden T, Oh H, Younger AP, and Patel TA (2013). "Meta-analysis of amyloid-cognition relations in cognitively normal older adults". *Neurology* 80 (14): 1341–1348. DOI: [10.1212/WNL.0b013e31828ab35d](https://doi.org/10.1212/WNL.0b013e31828ab35d).
- Heimer L, Alheid G, and Zahm D (1993). *Basal forebrain organization: an anatomical framework for motor aspects of drive and motivation*. In: *Limbic motor circuits and neuropsychiatry*. Ed. by PW Kalivas and CD Barnes. Boca Raton, FL: CRC Press, 1–32.
- Klunk WE, Price JC, Mathis CA, Tsopelas ND, Lopresti BJ, et al. (2007). "Amyloid deposition begins in the striatum of presenilin-1 mutation carriers from two unrelated pedigrees". *J. Neurosci.* 27 (23): 6174–6184. DOI: [10.1523/JNEUROSCI.0730-07.2007](https://doi.org/10.1523/JNEUROSCI.0730-07.2007).
- Latimer CS, Keene CD, Flanagan ME, Hemmy LS, Lim KO, et al. (2017). "Resistance to Alzheimer disease neuropathologic changes and apparent cognitive resilience in the Nun and Honolulu-Asia Aging Studies". *J. Neuropathol. Exp. Neurol.* 76 (6): 458–466. DOI: [10.1093/jnen/nlx030](https://doi.org/10.1093/jnen/nlx030).
- Latina V, Caioli S, Zona C, Ciotti MT, Amadoro G, and Calissano P (2017). "Impaired NGF/TrkA Signaling Causes Early AD-Linked Presynaptic Dysfunction in Cholinergic Primary Neurons". *Front. Cell Neurosci.* 11: 68. DOI: [10.3389/fncel.2017.00068](https://doi.org/10.3389/fncel.2017.00068).

- Lehéricy S, Hirsch EC, Cervera P, Hersh LB, Hauw JJ, et al. (1989). "Selective loss of cholinergic neurons in the ventral striatum of patients with Alzheimer disease". *Proc. Natl. Acad. Sci. U.S.A.* 86 (21): 8580–8584. URL: <http://www.pnas.org/content/pnas/86/21/8580.full.pdf> (visited on 09/10/2018).
- Mai JK, Majtanik M, and Paxinos G (2015). *Atlas of the human brain*. London: Academic Press.
- Mesulam MM, Mufson EJ, Wainer BH, and Levey AI (1983). "Central cholinergic pathways in the rat: an overview based on an alternative nomenclature (Ch1-Ch6)". *Neuroscience* 10 (4): 1185–1201. DOI: [10.1016/0306-4522\(83\)90108-2](https://doi.org/10.1016/0306-4522(83)90108-2).
- Mesulam M, Shaw P, Mash D, and Weintraub S (2004). "Cholinergic nucleus basalis tauopathy emerges early in the aging-MCI-AD continuum". *Ann. Neurol.* 55 (6): 815–828. DOI: [10.1002/ana.20100](https://doi.org/10.1002/ana.20100).
- Naudin M, Mondon K, and Atanasova B (2013). "Maladie d'Alzheimer et olfaction". *Geriatr. Psychol. Neuropsychiatr. Vieil.* 11 (3): 287–293. DOI: [10.1684/pnv.2013.0418](https://doi.org/10.1684/pnv.2013.0418).
- Olmos JS de and Heimer L (1999). "The concepts of the ventral striatopallidal system and extended amygdala". *Ann. N. Y. Acad. Sci.* 877 (1): 1–32. DOI: [10.1111/j.1749-6632.1999.tb09258.x](https://doi.org/10.1111/j.1749-6632.1999.tb09258.x).
- Oyanagi K, Takahashi H, Wakabayashi K, and Ikuta F (1987). "Selective involvement of large neurons in the neostriatum of Alzheimer's disease and senile dementia: a morphometric investigation". *Brain Res.* 411 (2): 205–211. DOI: [10.1016/0006-8993\(87\)91071-7](https://doi.org/10.1016/0006-8993(87)91071-7).
- Patenaude B, Smith SM, Kennedy DN, and Jenkinson M (2007). "FIRST-FMRIB's integrated registration and segmentation tool". In: *Human Brain Mapping Conference*, 420–428.
- Pievani M, Bocchetta M, Boccardi M, Cavedo E, Bonetti M, et al. (2013). "Striatal morphology in early-onset and late-onset Alzheimer's disease: a preliminary study". *Neurobiol. Aging* 34 (7): 1728–1739. DOI: [10.1016/j.neurobiolaging.2013.01.016](https://doi.org/10.1016/j.neurobiolaging.2013.01.016).
- Roh JH, Qiu A, Seo SW, Soon HW, Kim JH, et al. (2011). "Volume reduction in subcortical regions according to severity of Alzheimer's disease". *J. Neurol.* 258 (6): 1013–1020. DOI: [10.1007/s00415-010-5872-1](https://doi.org/10.1007/s00415-010-5872-1).
- Schmitz TW, Nathan Spreng R, Weiner MW, Aisen P, Petersen R, et al. (2016). "Basal forebrain degeneration precedes and predicts the cortical spread of Alzheimer's pathology". *Nat. Commun.* 7: 13249. DOI: [10.1038/ncomms13249](https://doi.org/10.1038/ncomms13249).
- Selden N, Mesulam MM, and Geula C (1994). "Human striatum: the distribution of neurofibrillary tangles in Alzheimer's disease". *Brain Res.* 648 (2): 327–331. DOI: [10.1016/0006-8993\(94\)91136-3](https://doi.org/10.1016/0006-8993(94)91136-3).
- Shi Y and Wardlaw JM (2016). "Update on cerebral small vessel disease: a dynamic whole-brain disease". *Stroke and Vasc. Neurol.* DOI: [10.1136/svn-2016-000035](https://doi.org/10.1136/svn-2016-000035).
- Sperling RA, Aisen PS, Beckett LA, Bennett DA, Craft S, et al. (2011). "Toward defining the preclinical stages of Alzheimer's disease: recommendations from the National Institute on

- Aging-Alzheimer's Association workgroups on diagnostic guidelines for Alzheimer's disease". *Alzheimers Dement.* 7 (3): 280–292. DOI: [10.1016/j.jalz.2011.03.003](https://doi.org/10.1016/j.jalz.2011.03.003).
- Steiner H and Tseng KY (2010). *Handbook of Basal Ganglia Structure and function*. London: Academic Press.
- Strada O, Hirsch EC, Javoy-Agid F, Lehericy S, Ruberg M, et al. (1992). "Does loss of nerve growth factor receptors precede loss of cholinergic neurons in Alzheimer's disease? An autoradiographic study in the human striatum and basal forebrain". *J. Neurosci.* 12 (12): 4766–4774.
- Teipel S, Heinsen H, Amaro E, Grinberg LT, Krause B, and Grothe M (2014). "Cholinergic basal forebrain atrophy predicts amyloid burden in Alzheimer's disease". *Neurobiol. Aging* 35 (3): 482–491. DOI: [10.1016/j.neurobiolaging.2013.09.029](https://doi.org/10.1016/j.neurobiolaging.2013.09.029).
- Thal DR, Rub U, Orantes M, and Braak H (2002). "Phases of A β -deposition in the human brain and its relevance for the development of AD". *Neurology* 58 (12): 1791–1800. DOI: [10.1212/WNL.58.12.1791](https://doi.org/10.1212/WNL.58.12.1791).
- Triaca V and Calissano P (2016). "Impairment of the nerve growth factor pathway driving amyloid accumulation in cholinergic neurons: the incipit of the Alzheimer's disease story?" *Neural Regen. Res.* 11 (10): 1553–1556. DOI: [10.4103/1673-5374.193224](https://doi.org/10.4103/1673-5374.193224).
- Villemagne VL, Ataka S, Mizuno T, Brooks WS, Wada Y, et al. (2009). "High striatal amyloid β -peptide deposition across different autosomal Alzheimer disease mutation types". *Arch. Neurol.* 66 (12): 1537–1544. DOI: [10.1001/archneurol.2009.285](https://doi.org/10.1001/archneurol.2009.285).
- Wolf DS, Gearing M, Snowdon DA, Mori H, Markesbery WR, and Mirra SS (1999). "Progression of regional neuropathology in Alzheimer disease and normal elderly: findings from the Nun study". *Alzheimer Dis. Assoc. Disord.* 13 (4): 226–231. URL: http://journals.lww.com/alzheimerjournal/Fulltext/1999/10000/Progression_of_Regional_Neuropathology_in.9.aspx (visited on 09/10/2018).
- Yi HA, Moller C, Dieleman N, Bouwman FH, Barkhof F, et al. (2016). "Relation between subcortical grey matter atrophy and conversion from mild cognitive impairment to Alzheimer's disease". *J. Neurol. Neurosurg. Psychiatr.* 87 (4): 425–432. DOI: [10.1136/jnnp-2014-309105](https://doi.org/10.1136/jnnp-2014-309105).
- Zaborszky L, Hoemke L, Mohlberg H, Schleicher A, Amunts K, and Zilles K (2008). "Stereotaxic probabilistic maps of the magnocellular cell groups in human basal forebrain". *Neuroimage* 42 (3): 1127–1141. DOI: [10.1016/j.neuroimage.2008.05.055](https://doi.org/10.1016/j.neuroimage.2008.05.055).

APPENDIX A

Samenvatting

De ziekte van Alzheimer (ZvA) is de meest voorkomende vorm van dementie onder ouderen. In vergrijzende samenlevingen, zoals de Nederlandse, neemt de frequentie van de ziekte toe en zal de ZvA naar verwachting uitgroeien tot doodsoorzaak nummer 1 in 2040. Vanwege deze groeiende socio-economische zorg hebben de Nederlandse Organisatie voor Wetenschappelijk Onderzoek (NWO) en de Koninklijke Nederlandse Academie der Wetenschappen (KNAW) tussen 2000–2017 verscheidene initiatieven gelanceerd die het thema brein en cognitie tot één van de speerpunten van de Nederlandse wetenschapsagenda heeft gemaakt. De studies gebundeld in dit proefschrift zijn gedaan in het kader van deze grotere beweging om onze kennis over onder andere de ZvA te vergroten. Deze studies hebben in het bijzonder tot doel vroege markers van de ZvA op te sporen op structurele *magnetic resonance imaging* (MRI) en de onderzoeksmethoden in comparatieve volumetrische hersenstudies te verbeteren.

Deel 1 Atrofie van het ventrale striatum in de ZvA

De oorzaak van de ZvA is niet bekend, maar in de wetenschap worden twee theoretische modellen gebruikt om het ontstaan van de ZvA te verklaren. Het eerste model gaat ervan uit dat de ZvA het gevolg is van disfunctioneren van het cholinerge systeem. Het anatomische substraat voor dit systeem bevindt zich in de basale voorhersenen en het striatum. Het tweede model gaat ervan uit dat de ZvA het gevolg is van de toxische ophoping van seniele plaques met name in de cortex (hersenschors). Dit

tweede model heeft de laatste decennia een dominante positie ingenomen in de neuro-wetenschappelijke MRI studies naar de ZvA. Derhalve is veel onderzoek gedaan naar de atrofie van de cortex en in het bijzonder van de hippocampus, gelegen aan de mediale zijde van de temporale kwab. Atofie van de hippocampus is van voorspellende waarde voor de progressie van de ZvA. Dit treedt echter gedurende het ziekteproces relatief laat op, wanneer klinische symptomen al duidelijk aanwezig zijn. Tegenwoordig wordt ervan uitgegaan dat de ZvA een lange preklinische periode kent van ca. 10–20 jaar voordat de eerste klinische symptomen zich manifesteren. Ook gaat men ervan uit dat therapeutische interventies vooral zinvol zijn in deze preklinische fase. Opsporing van de ZvA in de preklinische fase is daarom essentieel.

In deel 1 van dit proefschrift staat onderzoek naar atrofie van het striatum op structurele MRI in de ZvA centraal. De keuze om MRI onderzoek te richten op het striatum werd onderbouwd met drie argumenten. Ten eerste is het ventrale gedeelte van het striatum een belangrijk onderdeel van het limbische systeem. Het is bekend dat de limbische corticale schors (ook wel de allocortex genoemd) disproportioneel atrofieert in de ZvA vergeleken met de neocortex. Over het optreden van atrofie in het subcorticale limbische systeem is echter weinig bekend. Ten tweede bevindt een grote concentratie cholinerge cellen zich in het striatum. Pathologische studies hebben aangetoond dat de cholinerge cellen in zowel de basale voorhersenen als het striatum in een vroeg stadium van de ZvA verloren gaan. Het is evenwel niet bekend of dit leidt tot atrofie van het striatum. Ten derde is in studies naar familiale of genetische varianten van de ZvA aangetoond dat de ophoping van seniele plaques begint in het striatum nog vóór de verschijning van seniele plaques in de cortex of de verschijning van klinische symptomen. Hoofdstukken 2 t/m 5 zijn gewijd aan volumetrische en morfologische studies van het striatum in de ZvA en in die hoofdstukken wordt de relatie van atrofie van het striatum met cognitieve achteruitgang onderzocht. In hoofdstuk 2 wordt aangetoond dat het volume van het striatum is afgenomen bij patiënten met de ZvA ten opzichte van een controle groep zonder aantoonbare cognitieve achteruitgang. Deze studie van 139 structurele MRI's van hersenen van patiënten van een geheugenpolikliniek laat zien dat het volume verlies in het striatum geen homogeen proces is maar dat voornamelijk de nucleus accumbens en het putamen zijn aangedaan. De studie naar enkel het volume van het striatum is echter relatief beperkt omdat er geen duidelijke anatomische grenzen tussen de verschillende structuren van het striatum bevinden. Hoofdstuk 3 beschrijft derhalve een studie naar veranderingen van de morfologie van het striatum in de ZvA. Met name de ventrale oppervlakte van het putamen toont een inwaartse contractie. Bovendien blijkt de mate van expansie en contractie van de gehele ventrale striatale oppervlakte en de oppervlakte van het laterale putamen gerelateerd te zijn aan het cognitief functioneren van de patiënt. Deze complementaire volumetrische en morfologische studies tonen aan dat

het verlies van het volume van het striatum in de ZvA vooral te wijten is aan het verlies van het ventrale striatum. In hoofdstuk 4 wordt verder onderzocht of de volumes van het striatum en zijn substructuren voorspellend zijn voor de achteruitgang in cognitie bij de oudere bevolking. In een op grote epidemiologische populatie gebaseerde studie blijkt het volume van de nucleus accumbens voorspellend te zijn voor cognitieve achteruitgang bij deelnemers gediagnosticeerd met dementie 3 jaar voor, tijdens, en tot 6 jaar na vervaardiging van een MRI van hersenen. Deze voorspellende waarde is onafhankelijk van de voorspellende waarde voor cognitieve achteruitgang van het volume van de hippocampus. Deze bevindingen geven aan dat het ventrale striatum mogelijk vroeg in het proces van dementie is aangedaan. Eén van de onzekerheden in de interpretatie van de bovenstaande resultaten is de vraag of het volume verlies van het striatum te wijten is aan de ZvA of aan andere ouderdoms-gerelateerde neurodegeneratieve processen die vaak gepaard gaan met de ZvA. Het striatum is bijvoorbeeld net als de thalamus gevoelig voor vasculaire schade in het kader van microangiopathie. In hoofdstuk 5 wordt in een follow up studie van 2.5 jaar onderzocht of de aanwezigheid van cardiovasculaire risicofactoren van invloed is op atrofie van het striatum en/of hippocampus. Geen van de onderzochte cardiovasculaire risicofactoren is geassocieerd met versneld verlies van volume van het striatum. Atofie van de hippocampus daarentegen blijkt geassocieerd te zijn met te hoge bloeddruk.

De beschreven onderzoeksresultaten maken aannemelijk dat het striatum is aangedaan in de ZvA en mogelijk in een vroeg stadium. Alvorens echter het volume van het ventrale striatum kan dienen als vroege marker voor de ZvA dient meer onderzoek te worden verricht naar de temporele relatie tussen atrofie van het ventrale striatum en het begin van de ZvA. Ook voor de klinische praktijk is een visuele inschatting van het volume van het ventrale striatum erg lastig vergeleken met bijvoorbeeld de beoordeling van atrofie van de hippocampus, welke wordt vergemakkelijkt door de aangrenzende temporale hoorn van de laterale ventrikel. Het ventrale striatum wordt omgeven door en is onderdeel van de complexe anatomie van de basale voorhersenen. De huidige klinische MRI protocollen zijn niet geoptimaliseerd voor de beoordeling van de ingewikkelde en minutieuze anatomie in deze regio.

Deel 2 Allometrie van de hersenstructuren

Atofie van de hersenstructuur op MRI kan zowel globaal als focaal voorkomen en wordt gezien als een maat voor verlies aan neuronen en als substraat voor functionele achteruitgang van de structuur. Op groepsniveau, hebben metingen van volumes van hersenstructuren gebaseerd op structurele MRI hun waarde bewezen in het verstrekken van inzicht in de veranderingen die optreden in de hersenen in veroudering en in neurodegeneratieve

aandoeningen zoals de ZvA. Op individueel niveau, echter, bestaat geen gestandaardiseerde metriek voor de fysiologische variatie in hersenstructuur volumes. Een individuele meting van hersenstructuur volume leidt niet tot een diagnose en de voorspellende waarde voor een neurodegeneratieve aandoening is matig. De oorzaak hiervoor is de aanzienlijke fysiologische variatie in hersenvolumes in de bevolking. Om de ruis van fysiologische variatie van hersenvolumes in analyses te verminderen is het gangbaar in comparatieve hersenstudies te corrigeren voor hoofdgrootte of intracranieel volume (ICV). Eén van de aspecten in de methodologie van humane comparatieve hersenstudies welke weinig aandacht heeft gekregen is dat in sommige van deze correctiemethoden ten onrechte wordt uitgegaan van een isometrische geometrie van hersenen van verschillende grootte. Voorbeelden van dergelijke methoden zijn registratie van MRI beelden van verschillende onderzoeksdeelnemers naar een gestandaardiseerde ruimte middels affine transformatie of door gebruik te maken van ratio's van hersenstructuur volume ten opzichte van ICV. Ondanks het feit dat deze methodes veel worden toegepast zijn er tal van aanwijzingen dat de hersenen van verschillende mensen zich niet isometrisch tot elkaar verhouden. Deel 2 van dit proefschrift wordt gewijd aan de studie van allometrie in de ontwikkeling en degeneratie van de hersenstructuur. Hoofdstuk 6 onderzoekt de allometrische coëfficiënt van verschillende hersenstructuren in een grote dataset van meer dan 4500 MRI scans en toont aan dat grotere hersenen relatief kleinere volumes corticale en subcorticale grijze stof bevatten en relatief meer witte stof. Hoewel, allometrie in de hersenen eerder werd aangetoond, behoort deze studie tot de grootste studies ooit verricht naar allometrie in de menselijke hersenen en werd voor het eerst speciaal aandacht geschonken aan de allometrische coëfficiënt van de diepe grijze stof. In hoofdstuk 7 wordt de fysiologische variatie in degeneratie van de hersenen onderzocht. Ook wat betreft degeneratie van de hersenen in veroudering blijken grotere hersenen te verschillen van kleinere hersenen. Grotere hersenen lijken sneller volume te verliezen en proportioneel meer witte stof afwijkingen te bevatten. De resultaten van deze twee studies tonen aan dat zowel de fysiologische ontwikkeling als degeneratie van het brein door allometrische wetten gecontroleerde processen zijn. Allometrie leidt tot aanzienlijke proportionele verschillen tussen hersenen van verschillende grootte. Bewustwording van deze fysiologische proportionele verschillen zou moeten leiden tot 1) een betere interpretatie van resultaten van comparatieve hersenstudies en 2) een beter begrip van waarom correctiemethoden voor ICV gebaseerd op een isometrische hersengeometrie leiden tot over- en wel onderschatting van volumetrische verschillen.

Toekomst perspectief

De onderzoeksresultaten gepresenteerd in dit proefschrift leiden tot enkele aanbevelingen voor toekomstig onderzoek. Op basis van de gevonden atrofie van het striatum in de ZvA met name het ventrale deel is het aan te bevelen om de subcorticale signatuur van de ZvA nauwkeuriger te onderzoeken. Dit proefschrift en ook andere recente studies suggereren dat het striatum mogelijk vrij vroeg in het ziekteproces van de ZvA is betrokken en derhalve vormen veranderingen in het ventrale striatum een belangrijke kandidaat-marker voor de preklinische fase van ZvA. De temporele relatie tussen atrofie van het ventrale striatum en de ZvA dient nader te worden onderzocht. Ook dient atrofie van het ventrale striatum in de ZvA te worden onderzocht ten opzichte van degeneratieve veranderingen in de andere systemen van de basale voorhersenen.

APPENDIX B

List of publications

- de Jong LW, Vidal JS, Forsberg LE, Zijdenbos AP, Haight T, et al. (2017). "Allometric scaling of brain regions to intra-cranial volume: An epidemiological MRI study". *Hum. Brain Mapp.* 38 (1): 151–164. DOI: [10.1002/hbm.23351](https://doi.org/10.1002/hbm.23351).
- Lilamand M, Vidal JS, Plichart M, de Jong LW, Duron E, and Hanon O (2016). "Arterial stiffness and medial temporal lobe atrophy in elders with memory disorders". *J. Hypertens.* 34 (7): 1331–1337. DOI: [10.1097/HJH.0000000000000954](https://doi.org/10.1097/HJH.0000000000000954).
- de Jong LW, Forsberg LE, Vidal JS, Sigurdsson S, Zijdenbos AP, et al. (2014). "Different susceptibility of medial temporal lobe and basal ganglia atrophy rates to vascular risk factors". *Neurobiol. Aging* 35 (1): 72–78. DOI: [10.1016/j.neurobiolaging.2013.07.009](https://doi.org/10.1016/j.neurobiolaging.2013.07.009).
- de Rotrou J, Wu YH, Mabire JB, Moulin F, de Jong LW, et al. (2013). "Does cognitive function increase over time in the healthy elderly?" *PLoS ONE* 8 (11): e78646. DOI: [10.1371/journal.pone.0078646](https://doi.org/10.1371/journal.pone.0078646).
- de Jong LW, Wang Y, White LR, Yu B, van Buchem MA, and Launer LJ (2012). "Ventral striatal volume is associated with cognitive decline in older people: a population based MR-study". *Neurobiol. Aging* 33 (2): 1–10. DOI: [10.1016/j.neurobiolaging.2010.09.027](https://doi.org/10.1016/j.neurobiolaging.2010.09.027).
- de Jong LW, Ferrarini L, van der Grond J, Milles JR, Reiber JH, et al. (2011). "Shape abnormalities of the striatum in Alzheimer's disease". *J. Alzheimers Dis.* 23 (1): 49–59. DOI: [10.3233/JAD-2010-101026](https://doi.org/10.3233/JAD-2010-101026).
- de Jong LW, van der Hiele K, Veer IM, Houwing JJ, Westendorp RG, et al. (2008). "Strongly reduced volumes of putamen and thalamus in Alzheimer's disease: an MRI study". *Brain* 131 (12): 3277–3285. DOI: [10.1093/brain/awn278](https://doi.org/10.1093/brain/awn278).

- de Kroon CD and de Jong LW (2007). “De standaard ‘Pelvic inflammatory disease’ (eerste herziening) van het Nederlands Huisartsen Genootschap; reactie vanuit de gynaecologie”. *Ned. Tijdschr. Geneeskd.* 151 (13): 732–734. URL: <https://www.ntvg.nl/system/files/publications/2007107320001a.pdf> (visited on 09/10/2018).
- Monraats PS, de Vries F, de Jong LW, Pons D, Sewgobind VD, et al. (2006). “Inflammation and apoptosis genes and the risk of restenosis after percutaneous coronary intervention”. *Pharmacogenet. Genomics* 16 (10): 747–754. DOI: [10.1097/01.fpc.0000220572.28585.5e](https://doi.org/10.1097/01.fpc.0000220572.28585.5e).

APPENDIX C

Dankwoord

Hierbij wil ik iedereen bedanken die heeft bijgedragen aan de totstandkoming van dit proefschrift, en in het bijzonder:

Mark, dank voor je open blik en positieve feedback tijdens het gehele traject van mijn onderzoek, maar bovenal het vertrouwen en de ruimte die je me hebt gegeven voor het volgen van mijn eigen pad in de wetenschap.

Lenore, thank you for your guidance and feedback over the years. Your critical and thorough approach in science have shaped and sharpened my work and me as a scientist.

Alex, Lars, Jeroen, Ilja, Paul, Luca, Pauline en Elmi dank ik voor de goede samenwerking. Many thanks to all colleagues of the Laboratory of Epidemiology Biometry and Demography for the pleasant collaboration and good memories, with a special thank to Paolo, Sonia, Julia, Salka, Saskia, Patrick, Annemarie, and Kushang.

Siggi, Villi and Gudny, Kærar þakkir fyrir hlýjar móttökur á stofnun þinni. Ég hef lært mikið af sérfræðipækkingu þinni.

Jean, Marie-Françoise, Rébecca, Alexandre et Clémentine, je vous remercie, grâce à vous j'ai pu me sentir chez moi en France.

Opa, bedankt voor alle inspirerende gesprekken.

Ilse en Jasmijn mijn steun en toeverlaten. Jullie zijn onmisbaar voor mij.

Pap en Mam, bedankt voor jullie onvoorwaardelijke steun en belangstelling.

Jean-Sébastien, l'amour ne connaît pas de limites ou de distance. Je t'aime.

Oskar en Louise, lieverds, bedankt voor alle blijdschap en liefde iedere dag weer.

APPENDIX D

Curriculum vitae

Laura de Jong was born in Gouda, on May 27, 1981.

After finishing high school at the Coenecoop College in Waddinxveen, she started her medical studies at the Leiden University Medical Center (LUMC) in 1999 and her study in history at the University of Leiden in 2001. In 2005 she graduated in history of science and obtained her bachelor's degree in history. In 2008 she obtained her medical degree and started the PhD research project under supervision of Professor Mark van Buchem (LUMC) and Dr. Lenore Launer (National Institute on Aging, National Institute of Health (NIA/NIH)). For the execution of the research she received an AGIKO-grant from the Dutch Organisation for Health Research and Development (Zon Mw). In the following years until October 2011, she performed research at the NIA/NIH in Bethesda, MD/US, and the Icelandic Heart Institute in Kópavogur/IS. Upon her return to the Netherlands, she entered the radiology residency program of the LUMC and subspecialized in neuroradiology. During her training she worked 12 months as a resident in radiology at Sainte-Anne hospital in Paris/FR under supervision of professors Catherine Oppenheim and Jean-François Meder. In 2017 she obtained the *Diplôme Inter-Universitaire Imagerie neurovasculaire diagnostique et thérapeutique* at the *Université René Descartes* and in 2018 the European Diploma in Neuroradiology (EBNR). In 2018 she was registered as a radiologist in the Netherlands and in France. The same year she was awarded a grant from the European Society of Neuroradiology for a 12-month research fellowship in diagnostic neuroradiology at Sainte-Anne hospital in Paris. Laura currently lives in Paris with her partner Jean-Sébastien and their two children Oskar and Louise.

